

國立交通大學

電信工程學系

博士論文

用於多輸入多輸出無線通訊系統之空-時信號處理：空-時信號模式與干擾抑制

Space-Time Signal Processing for MIMO  
Wireless Communications: Space-Time  
Signaling and Interference Suppression

研究生：何從廉

指導教授：李大嵩博士

中華民國九十四年五月

用於多輸入多輸出無線通訊系統之空-時信號處理：空-時信號模式與干擾抑制

Space-Time Signal Processing for MIMO  
Wireless Communications: Space-Time  
Signaling and Interference Suppression

研究生：何從廉

Student: Chung-Lien Ho

指導教授：李大嵩 博士

Advisor: Dr. Ta-Sung Lee



國立交通大學  
電信工程學系  
博士論文

A Dissertation  
Submitted to Institute of Communication Engineering  
College of Electrical Engineering and Computer Science  
National Chiao Tung University  
in Partial Fulfillment of the Requirements  
for the Degree of Doctor of Philosophy  
in  
Communication Engineering  
Hsinchu, Taiwan, Republic of China

中華民國九十四年五月

# 用於多輸入多輸出無線通訊系統之空-時信號處理：空-時信號模式與干擾抑制

研究生：何從廉

指導教授：李大嵩博士

國立交通大學  
電信工程學系

## 摘要

近年來，許多研究組織均積極投入於多輸入多輸出(Multi-Input Multi-Output, MIMO)技術的研發，以提升無線行動網際網路服務及下世代細胞式無線行動通訊系統之性能。這些新技術必須能夠有效克服無線通訊環境中嚴苛的挑戰，而基於適應性天線陣列或智慧型天線形式之天線系統恰可提供一套有效且良好的解決方案，以達到『高可靠度』及『高資料率』的傳輸品質。在此一研究範疇裡，已有許多研發成果大量產出，而許多用於無線通訊系統的商業化產品也已相繼問世。

本論文即在探討於無線通訊系統中，同時在傳輸端及接收端使用多根天線情況下的相關研究。吾人試圖提供無線通訊天線系統一個完整的綜合評述及概要說明，並介紹一些環繞在此一系統周圍的重要議題。其關鍵點為所探討的系統必須是具有適應性且於收發端使用多根天線。吾人亦將討論用於多輸入多輸出無線通訊架構下，有關空-時(Space-Time, ST)信號模式及干擾抑制之空-時信號處理的相關議題。在本論文中，吾人首先將研究重點放在發展一種基於空-時接收機架構之干擾消除技術上；具體而言，為研究一個適用於頻率選擇式多路徑通道下，基於排序式漸次干擾消除(Ordered Successive Interference Cancellation, OSIC)技術的多輸入多輸出等化器

(Equalizer)。此一多輸入多輸出等化器將基於傳統最小均方誤差 (Minimum Mean Square Error, MMSE) 決策迴授等化器 (Decision Feedback Equalizer, DFE) 的形式以降維 (Reduced Rank, RR) 技術方式實現之。其中，在排序式漸次干擾消除架構下每一個階段中之最小均方誤差的權值將以廣義旁波瓣干擾消除器 (Generalized Sidelobe Canceller, GSC) 技術求得，而降維處理則以共軛梯度 (Conjugate Gradient, CG) 法則實現，以降低計算量。隨後，吾人將探討在頻率平坦式通道下之多輸入多輸出收發機的研究設計。在此一部份，吾人將首先研究一種通用多用戶雙模信號 (Dual-Signaling) 傳輸系統。在此一雙模信號傳輸系統中，每個用戶終端的資料可基於其當時通道狀況，以正交空-時編碼 (Orthogonal Space-Time Block Code, O-STBC) 方式傳輸以獲取傳輸多樣 (Transmit Diversity, TD) 亦或是以空間多工 (Spatial Multiplexing, SM) 方式進行傳輸以獲取高頻譜效益 (Spectral Efficiency, SE)。接下來，吾人將發展一種具有微量回傳資訊之高效率多輸入多輸出收發機架構 (主要針對空-時編碼/空-時解碼設計)。此一收發機架構在群組式空-時區塊編碼 (Grouped Space-Time Block Code, G-STBC) 系統，於位元錯誤率 (BER) 性能之考量下可使空-時傳輸字碼最佳化，以同時達到高頻譜效益與高鏈結品質 (Link Quality, LQ) 的通訊。在上述二種多輸入多輸出系統架構下之接收機亦可基於排序式漸次干擾消除技術發展設計。藉由利用正交空-時編碼所具有的強大代數性質，經驗證後，上述二系統所考量基於次序式連續干擾消除技術的偵測器可以群組 (Group-Wise) 偵測方式實現。此一群組式偵測性質為使用正交碼情況下的一種獨特結果，它可大大地改善信號分離的能力。此外，吾人更進一步利用潛藏於通道矩陣中豐富且特殊的結構，發展出一套具有計算量效益的遞迴式偵測器。

綜言之，本論文所提出之接收機與既存之接收架構比較，其主要的優點為具備較低實現複雜度、較快的收斂速率及較低的位元錯誤率。此外，本論文對於多輸入多輸出無線通訊收發機的設計也提供一種具智慧及強健性能的解決方案以適當地配合其通道狀況及系統需求。藉由數學分析與模擬評估，吾人證實所提出之新型收發機架構可有效提升系統之傳輸鏈結品質及獲取高頻譜效益，並有效抑制干擾及雜訊。

# Space-Time Signal Processing for MIMO Wireless Communications: Space-Time Signaling and Interference Suppression

Student : Chung-Lien Ho

Advisor : Dr. Ta-Sung Lee

Department of Communication Engineering, National Chiao Tung  
University, Hsinchu, Taiwan, Republic of China

## Abstract

Recently, there has been a substantial increase in the development of multi-input multi-output (MIMO) technologies for evolving wireless mobile Internet services and next-generation cellular systems. These technologies must be able to cope with the challenging wireless environment, and antenna systems in the form of adaptive array or smart antennas can provide an effective and promising solution while achieving *reliable* and *high data-rate* transmission. Research and development in this area have significantly increased, and many commercial products are now readily available for wireless communication systems.

This thesis is concerned with the use of multiple antennas at the transmitter and receiver in wireless communication systems. We attempt to provide an overview of all these antenna systems for wireless communications and introduce some of the important issues surrounding them. The key points are that the system must be adaptive and consist of multiple antennas. Several aspects of space-time (ST) processing related to the **ST signaling and interference suppression for MIMO based wireless communications** will be discussed. In this thesis, we first focus on developing the interference suppression scheme based on an ST receiver. We study an ordered successive interference cancellation (OSIC) based MIMO equalizer over the frequency selective multipath channels. The MIMO

equalizer is developed as a reduced-rank (RR) realization of the conventional minimum mean square error (MMSE) decision feedback equalizer (DFE). The MMSE weight vectors at each stage of the OSIC are computed based on the “generalized sidelobe canceller (GSC)” technique and RR processing is incorporated by using the “conjugate gradient (CG)” algorithm for reduced complexity implementation. After that, we then work on the design of MIMO transceiver over the frequency flat channels. In this part, we first study a general MU dual-signaling system, in which each user’s data stream is either orthogonal ST block encoded for transmit diversity (TD) or spatially multiplexed for high spectral efficiency (SE) based on its own channel condition. Second we develop an efficient MIMO transceiver architecture (ST encoding/decoding design) with a slight amount of feedback information that optimizes the ST codeword with respect to the BER performance for a grouped orthogonal ST block coded system to achieve both the high SE and link quality (LQ). In particular, the receiver in the two MIMO systems is also designed based on the OSIC scheme. By exploiting the algebraic structure of orthogonal codes, it is shown that the OSIC based detector in the above considered two systems allows for an attractive “group-wise” implementation. The group-wise detection property, resulting uniquely from the use of orthogonal codes, potentially improves the signal separation efficiency. Moreover, the imbedded structure of the channel matrix is also exploited for deriving a computationally efficient “recursive based” detector implementation.

In summary, the main advantages of the proposed ST receivers over the popular existing ones lie in its lower implementation complexity, much faster convergence behavior and better BER performance. On the other hand, we provide a smart and robust solution for transmitter and receiver designs better matched to the channel condition and system requirement in MIMO wireless communications. Mathematical analysis and computer simulations show that the proposed methods can achieve high LQ and high SE and offer excellent immunity to interference and noise.

# Acknowledgement

I would like to express the deepest gratitude to my advisor, Professor Ta-Sung Lee, for his enthusiastic guidance and great patience during my student career. He brought me to the field of wireless communication and MIMO signal processing. His knowledge, experience and commitment have benefited me tremendously over these years. Besides, I thank Professor Chong-Yung Chi in the Institute of Communication Engineering in NTHU for providing me with two courses in multi-user detection and statistical signal processing. All his lecture materials are very well organized and his clear ways of presentation indeed made learning enjoyable. I also thank the members of my committee for their valuable comments and feedback.

I would also like to thank my former and present student colleagues of Communication Signal Processing Laboratory (CSP Lab.) for their inspiring discussions and constant encouragement. Finally, I deeply appreciate the encouragement and love of my family and friends. Without their support, this work would never have come into existence. I dedicate this thesis to my family who spent so many lonely moments due to my work during these years, as well as to my beloved fiancée.

# Contents

<b>Chinese Abstract</b>		<b>i</b>
<b>English Abstract</b>		<b>iii</b>
<b>Acknowledgement</b>		<b>v</b>
<b>Contents</b>		<b>vi</b>
<b>List of Figures</b>		<b>xi</b>
<b>List of Tables</b>		<b>xiv</b>
<b>Notations</b>		<b>xv</b>
<b>1 Introduction</b>		<b>1</b>
1.1 Overview of Multiple Antenna Systems . . . . .		2
1.2 Overview of MIMO Techniques . . . . .		7
1.2.1 Beamforming/Equalization Techniques . . . . .		7
1.2.2 Spatial Diversity Techniques . . . . .		10
1.2.3 Spatial Multiplexing Techniques . . . . .		13
1.2.4 Tradeoffs Between TD and SM . . . . .		14
1.3 Background and Literature Review . . . . .		15
1.4 Outline of Thesis . . . . .		19





<b>2</b>	<b>Basic Concepts of MIMO Wireless Communications</b>	<b>26</b>
2.1	Introduction . . . . .	26
2.2	MIMO System Model . . . . .	27
2.2.1	Continuous-Time MIMO Systems Model . . . . .	27
2.2.2	MIMO Channel Model . . . . .	28
2.2.3	MIMO Sampled Signal Model . . . . .	31
2.2.4	MU MIMO Sampled Signal Model . . . . .	34
2.3	Channel Capacity . . . . .	34
2.3.1	Channel Unknown to The Transmitter . . . . .	35
2.3.2	Channel Known to The Transmitter . . . . .	39
2.3.3	Outage Capacity . . . . .	40
2.4	Space-Time Block Coding . . . . .	41
2.4.1	General Framework for Linear STBC . . . . .	41
2.4.2	Orthogonal STBC: Encoding and Decoding . . . . .	47
2.4.3	Performance Analysis of O-STBC Systems . . . . .	51
2.5	Vertical Bell Laboratories Layered Space-Time . . . . .	53
2.5.1	Spatial Multiplexing Techniques . . . . .	54
2.5.2	Detection Algorithm for V-BLAST Systems . . . . .	54
2.5.3	Performance Analysis of V-BLAST Systems . . . . .	58
<b>3</b>	<b>An OSIC Based Reduced-Rank MIMO Equalizer Using Conjugate Gradient Algorithm</b>	<b>68</b>
3.1	Introduction . . . . .	68
3.2	MIMO Channel and Signal Model . . . . .	69
3.3	OSIC Based MIMO MMSE Equalizer . . . . .	70
3.4	New Ordering Strategy and GSC Equalizer . . . . .	72
3.4.1	SIR Based Ordering Strategy . . . . .	72
3.4.2	GSC Realization of MMSE DFE . . . . .	73

3.5	OSIC Based Reduced-Rank GSC DFE Using CG Algorithm . . . . .	74
3.5.1	Realization of Reduced-Rank GSC by CG Algorithm . . . . .	75
3.5.2	Finite Termination Property of CG . . . . .	77
3.5.3	Computational Complexity . . . . .	78
3.5.4	Iterative Equalization with Soft Decoding . . . . .	79
3.6	Computer Simulations . . . . .	79
3.7	Summary . . . . .	82
<b>4</b>	<b>Group-Wise OSIC Detection in Multiuser Space-Time Dual-Signaling Wire-</b>	
	<b>less Systems</b>	<b>89</b>
4.1	Introduction . . . . .	89
4.2	System Model . . . . .	92
4.2.1	System Description and Basic Assumptions . . . . .	92
4.2.2	Vectorized Signal Model . . . . .	94
4.3	Matched-Filtered Channel Matrix . . . . .	94
4.4	Group-Wise OSIC Detection . . . . .	97
4.4.1	OSIC Ordering . . . . .	97
4.4.2	Algorithm Outline and Related Discussions . . . . .	101
4.4.3	Conservation of Spatial Resource: CDMA Based Implementation . . . . .	102
4.5	Low-Complexity Algorithm Implementation . . . . .	103
4.5.1	Computation of $\mathbf{F}^{-1}$ . . . . .	104
4.5.2	Recursive Computation of $\mathbf{F}_i^{-1}$ . . . . .	106
4.5.3	Complexity Comparisons with Other Multiuser Detection Schemes . . . . .	109
4.6	Two-Stage Processing of Dual-Mode Signals . . . . .	111
4.7	Simulation Results . . . . .	112
4.8	Summary . . . . .	115
<b>5</b>	<b>Efficient Transmitter and Receiver Design for Grouped Space-Time Block</b>	

<b>Coded Systems with Feedback Information</b>	<b>123</b>
5.1 Introduction . . . . .	123
5.2 System Model . . . . .	125
5.2.1 System Description and Basic Assumptions . . . . .	125
5.2.2 Real-Valued Vectorized Signal Model . . . . .	126
5.3 OSIC Detection: Real-Valued Constellations . . . . .	127
5.3.1 Matched-Filtered Channel Matrix . . . . .	128
5.3.2 Antenna Group-Wise OSIC Detection . . . . .	129
5.4 OSIC Detection: Complex-Valued Constellations . . . . .	131
5.4.1 Matched-Filtered Channel Matrix . . . . .	131
5.4.2 Semi-Antenna Group-Wise OSIC Detection . . . . .	133
5.5 Implementation Issues of OSIC Detection . . . . .	137
5.5.1 Antenna Group-Wise Detection Strategy . . . . .	137
5.5.2 Two-Stage Detection Strategy . . . . .	138
5.5.3 Recursive Implementation . . . . .	139
5.6 Grouped Space-Time Block Codes . . . . .	142
5.6.1 Codeword Construction and Property . . . . .	142
5.6.2 Codeword Selection Criterion . . . . .	145
5.7 Computer Simulations . . . . .	147
5.8 Summary . . . . .	151
<b>6 Conclusions</b>	<b>160</b>
6.1 Summary of Thesis . . . . .	160
6.2 Future Work . . . . .	162
<b>A Proof of Lemma 4.3.1</b>	<b>165</b>
<b>B Matched-Filtered Channel Matrix: Complex-Valued Constellation Case</b>	<b>170</b>

C Proof of Lemma 4.4.1	172
D Group-Wise OSIC Detection: Complex-Valued Constellation Case	175
E Group-Wise OSIC Detection in CDMA Based Implementation	179
F Proof of Lemma 5.3.1	182
G Proof of Lemma 5.4.1	185
H Proof of Theorem 5.4.1	187
Bibliography	191



# List of Figures

1.1	Four basic configurations in wireless systems. . . . .	22
1.2	Leverages of ST processing. . . . .	22
1.3	Illustration of SO filtering/processing (beamforming). . . . .	23
1.4	Illustration of TO filtering/processing (equalization). . . . .	23
1.5	Illustration of joint ST filtering/processing (ST beamforming/equalization). . . . .	24
1.6	Block diagram of STC systems. . . . .	25
1.7	Block diagram of SM systems. . . . .	25
2.1	Illustration of decomposing a MIMO channel $\mathbf{H}$ into parallel SISO channels when the channel is known to the transmitter and receiver. . . . .	61
2.2	Illustration of water filling algorithm. . . . .	61
2.3	Channel capacity of several antenna configurations as a function of SNR $\rho$ . (a) Ergodic Capacity. (b) 10% outage capacity. . . . .	62
2.4	ccdf of several antenna configurations at SNR $\rho = 10$ dB. . . . .	63
2.5	Block diagram of STBC systems. . . . .	64
2.6	BER performance of STBCs as a function of SNR $\rho$ for different number of transmit antennas over a frequency flat MISO channel. (a) 1 bps/Hz. (b) 2 bps/Hz. . . . .	65
2.7	ST encoding of SM techniques. (a) V-BLAST scheme. (b) D-BLAST scheme. . . . .	66
2.8	Schematic of V-BLAST detection. . . . .	66

2.9	BER performance of different detection algorithms for SM systems as a function of SNR $\rho$ with $N = M = 4$ over a frequency flat MIMO channel. . . . .	67
3.1	Architecture of proposed MIMO equalizer with OSIC. . . . .	83
3.2	Structure of proposed RR realization of FFF using CG algorithm. . . . .	84
3.3	<b>A</b> -norm error of proposed CG-GSC DFE as a function of $D$ (iteration number) at different stages of OSIC. . . . .	85
3.4	BER performance of proposed CG-GSC DFE as a function of $D$ (iteration number), with SNR as a control parameter. . . . .	86
3.5	BER performance of proposed CG-GSC DFE as a function of SNR, with OSIC “on” or “off” as a control parameter. . . . .	86
3.6	BER performance of proposed CG-GSC DFE as a function of SNR, with DFE length $(K_F, K_B)$ as a control parameter. . . . .	87
3.7	BER performance of proposed CG-GSC DFE as a function of SNR, with fading variance $\sigma_n^2$ as a control parameter. $\kappa$ is a normalizing scalar such that $\sum_{n=1}^N \kappa n^2 = \frac{N}{L+1}$ . . . . .	87
4.1	The schematic diagram of the transceiver. . . . .	116
4.2	Structure of MFCM <b>F</b> . . . . .	116
4.3	Flop counts of the proposed group-wise OSIC detection as a function of $Q_D$ for an MU dual-signaling system, with $Q = 16$ , $Q_M = Q - Q_D$ and $N = 2$ . . . . .	117
4.4	Average BER performances of various detection schemes as a function of SNR for a four-user MU STBC system, with $N = 2$ and $M = 4$ . The Alamouti’s code with 8-PSK modulation is used for each user. . . . .	117

4.5	BER performance of various detection schemes as a function of SNR for a four-user dual-signaling system, with $Q_D = Q_M = 2$ , $N = 2$ , $M = 6$ and $\mathcal{K} = 10$ . 16-QAM and QPSK modulations are used for O-STBC signaling and SM signaling, respectively. (a) Average BER of the two detected O-STBC users. (b) Average BER of the two detected SM users. . . . .	118
4.6	BER performance of three detection schemes in a four-user dual-signaling system for different Ricean $\mathcal{K}$ -factors, with $Q_D = Q_M = 2$ , $N = 2$ and $M = 6$ . 16-QAM and QPSK modulations are used for O-STBC signaling and SM signaling, respectively. (a) Average BER of the two detected O-STBC users. (b) Average BER of the two detected SM users. . . . .	119
5.1	Proposed transmitter and receiver architectures for G-STBC system. . . . .	153
5.2	Five possible $N \times K$ G-STBC structures with $N = 10$ . (a) $K = 8$ , $Q = 3$ , $\mathcal{S}^N = (3, 3, 4)$ , $R^N = 1.5$ and $\bar{L}^N = 3$ . (b) $K = 8$ , $Q = 3$ , $\mathcal{S}^N = (2, 4, 4)$ , $R^N = 2$ and $\bar{L}^N = 6$ . (c) $K = 8$ , $Q = 4$ , $\mathcal{S}^N = (2, 2, 3, 3)$ , $R^N = 3$ and $\bar{L}^N = 8$ . (d) $K = 8$ , $Q = 4$ , $\mathcal{S}^N = (2, 2, 2, 4)$ , $R^N = 3.5$ and $\bar{L}^N = 8$ . (e) $K = 2$ , $Q = 5$ , $\mathcal{S}^N = (2, 2, 2, 2, 2)$ , $R^N = 5$ and $\bar{L}^N = 5$ . . . . .	154
5.3	BER performance of different detection methods as a function of SNR with $M = 3$ and $Q = 3$ . (a) $N = 6$ and $\mathcal{S}^N = (2, 2, 2)$ . (b) $N = 7$ and $\mathcal{S}^N = (2, 2, 3)$ .	155
5.4	BER performance of different detection strategies of proposed OSIC detector as a function of SNR with $N = 8$ , $M = 3$ , $Q = 3$ and $\mathcal{S}^N = (2, 2, 4)$ . . . . .	156
5.5	BER performance of different transmission techniques as a function of SNR with $N = 4$ and $M = 4$ . . . . .	156
5.6	BER performance of different proposed ST codewords as a function of SNR. (a) $N = 6$ and $M = 3$ . (b) $N = 8$ and $M = 4$ . . . . .	157

# List of Tables

3.1	Conjugate Gradient Algorithm . . . . .	88
3.2	Computational Complexity . . . . .	88
4.1	Algorithm summary of the proposed group-wise OSIC detector. . . . .	120
4.2	Flop counts of different detection methods ( $D$ : constellation size). . . . .	121
4.3	Summary of structures of the MFCM $\mathbf{F}_{p,q}$ for complex-valued constellations. . . . .	122
5.1	Summary of structures of the MFCM $\mathbf{F}_{p,q}$ for real-valued constellations. . . . .	158
5.2	Summary of structures of the MFCM $\mathbf{F}_{p,q}$ for complex-valued constellations. . . . .	158
5.3	Possible sets of antenna configuration and corresponding code rate and maximum required number of stages for OSIC based detection. . . . .	159



## Acronyms

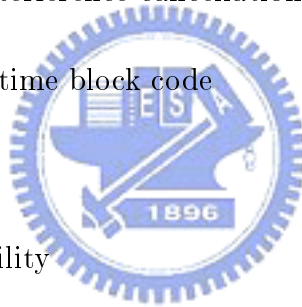
- AOA: angle-of-arrival
- AOD: angle-of-departure
- AWGN: additive white Gaussian noise
- BER: bit error rate
- BLAST: Bell laboratories layered space-time
- BPSK: binary phase shift keying
- BS: base station
- ccdf: complementary cumulative distribution function
- CCI: cochannel interference
- CDMA: code division multiple access
- CG: conjugate gradient
- CIR: channel impulse response
- D-BLAST: diagonal Bell laboratories layered space-time
- DFE: decision feedback equalizer
- EVD: eigenvalue decomposition
- FA: fully adaptive



- FB: feedback
- FBF: feedback filter
- FDMA: frequency division multiple access
- FF: feedforward
- FFF: feedforward filter
- FIR: finite impulse response
- FR: full-rank
- GSC: generalized sidelobe canceller
- GSM: global system for mobile communications
- G-STBC: grouped space-time block code
- IMVDR: iterative minimum variance distortionless response
- ISI: intersymbol interference
- LDC: linear dispersion code
- LOS: line-of-sight
- LSTC: layered space-time code
- MF: matched filter
- MFCM: matched-filtered channel matrix
- MIMO: multi-input multi-output
- MISO: multi-input single-output
- ML: maximum likelihood



- MMSE: minimum mean square error
- MRC: maximal ratio combining
- MS: mobile station
- MSE: mean square error
- MU: multiuser
- NLOS: non-line-of-sight
- OFDM: orthogonal frequency division multiplexing
- OTD: orthogonal transmit diversity
- OSIC: ordered successive interference cancellation
- O-STBC: orthogonal space-time block code
- PA: partially adaptive
- PEP: pairwise error probability
- PIC: parallel interference cancellation
- PSK: phase shift keying
- QAM: quadrature amplitude modulation
- QPSK: quadrature phase shift keying
- RR: reduced-rank
- SD: spatial diversity
- SE: spectral efficiency
- SIR: signal-to-interference ratio



- SIC: successive interference cancellation
- SINR: signal-to-interference-plus-noise ratio
- SISO: single-input single-output
- SIMO: single-input multi-output
- ST: space-time
- STBC: space time block code
- STC: space-time code
- STTC: space-time trellis code
- SM: spatial multiplexing
- SNR: signal-to-noise ratio
- SO: space only
- SU: single-user
- SVD: singular value decomposition
- TD: transmit diversity
- TDMA: time division multiple access
- TO: time only
- V-BLAST: vertical Bell laboratories layered space-time
- ZF: zero-forcing



## Symbols and Variables

- $\beta_{i,l}$ : the  $l$ th diagonal entry of  $\mathbf{F}_i$  at the  $i$ th stage of OSIC
- $\eta(\mathcal{M}_j^N)$ : SE of the  $j$ th selection mode over  $N$  transmit antennas
- $\lambda_i$ : the  $i$ th eigenvalue of a matrix
- $\rho$ : input SNR
- $\sigma_v^2$ : additive white noise power
- $\tau_{max}$ : maximum delay spread of physical channel
- $\theta_j^T$ : AOD of the  $j$ th path
- $\theta_j^R$ : AOA of the  $j$ th path
- $\mathbf{a}(\theta)$ : array manifold (steering) vector
- $\mathbf{A}_l$ : the  $l$ th ST modulation matrix
- $\mathbf{A}_{q,l}$ : the  $l$ th ST modulation matrix of the  $q$ th user terminal/antenna group
- $B_q$ : number of input symbols of data stream to ST encoder for the  $q$ th antenna group
- $\mathbf{B}$ : codeword different matrix
- $\tilde{\mathbf{B}}_n$ : reduced size block matrix of the  $n$ th data stream
- $c(\tau)$ : continuous-time impulse response of physical SISO propagation channel
- $C$ : channel capacity
- $C_{out,q}$ :  $q\%$  outage channel capacity
- $\mathbf{C}(\tau)$ : continuous-time impulse response of physical MIMO propagation channel



- $d^2(x_l(k), \hat{x}_l(k))$ : Euclidean distance between  $x_l(k)$  and  $\hat{x}_l(k)$
- $D^{(j)}$ : number of iteration in CG algorithm at the  $j$ th stage of OSIC
- $D_i(G_i)$ : number of different levels of those diagonal entries of  $\mathbf{F}_i$  which has  $G_i$  decision groups at the  $i$ th stage of OSIC
- $E_b$ : transmit bit energy
- $E_s$ : transmit symbol energy
- $\mathbf{e}_l$ : the  $l$ th standard vector
- $\mathbf{e}_{n,i}$ : error of the  $n$ th data stream in the  $i$ th iteration in CG algorithm
- $f_{p,q}^{(i,j)}$ : the  $(i, j)$ th entry of  $\mathbf{F}_{p,q}$
- $\mathbf{F}$ : MFCM
- $\mathbf{F}_i$ : deflated MFCM at the  $i$ th stage of OSIC
- $\mathbf{F}_{p,q}$ : the  $(p, q)$ th block submatrix of  $\mathbf{F}$
- $\bar{\mathbf{F}}_{i-1}$ :  $(L_T - iP) \times (L_T - iP)$  principle submatrix of  $\mathbf{F}_{i-1}^{-1}$
- $g(t)$ : pulse shaping waveform
- $G_c$ : coding gain of STC
- $G_d$  diversity gain of STC
- $G_i$ : cardinality of  $\mathcal{I}_i$
- $G_{i,1}$ : cardinality of  $\mathcal{I}_{i,1}$
- $G_{i,2}$ : cardinality of  $\mathcal{I}_{i,1/2}$
- $G^{(j)}$ : signal-plus-interference rank at the  $j$ th stage of OSIC



- $h(t)$ : continuous-time CIR
- $h_{m,n}(t)$ : continuous-time CIR from the  $n$ th transmit antenna to the  $m$ th receive antenna
- $h$ : SISO CIR
- $h_{m,n}$ : the  $(m, n)$ th entry of  $\mathbf{H}$
- $\mathbf{h}$ : channel vector
- $\mathbf{h}_{c,pr,n}$ : desired channel vector which is the  $(d + 1)$ th column of  $\mathbf{H}_{c,n}$
- $\mathbf{H}$ : MIMO channel matrix
- $\mathbf{H}_{c,n}$ : ST block Toeplitz channel matrix of the  $n$ th data stream
- $\mathbf{H}_{c,fu,n}$ : channel matrix of future part which consists of the first  $d$  columns of  $\mathbf{H}_{c,n}$
- $\mathbf{H}_{c,F,n}$ : channel matrix of FFF part which consists of the first  $(d + 1)$  columns of  $\mathbf{H}_{c,n}$
- $\mathbf{H}_{c,pa,n}$ : channel matrix of past part which consists of the  $(d + 2)$ th to  $(d + 1 + K_B)$ th columns of  $\mathbf{H}_{c,n}$
- $\mathbf{H}_{sc}$ : scattered component of MIMO channel matrix
- $\mathbf{H}_{sp}$ : specular component of MIMO channel matrix
- $\mathbf{H}_w$ : spatially white (i.i.d.) MIMO channel matrix
- $\mathcal{H}(Y)$ : differential entropy of  $Y$
- $\mathcal{H}(Y|X)$ : differential conditional entropy of  $Y$  with knowledge of  $X$  given
- $\mathcal{I}(X;Y)$ : mutual information between  $X$  and  $Y$
- $\mathcal{I}_i$ : index set of total decision groups

- $\mathcal{I}_i(g)$ : the  $g$ th entry of  $\mathcal{I}_i$
- $\mathcal{I}_{i,1}$ : index set of decision group for unit-rate codes
- $\mathcal{I}_{i,1/2}$ : index set of decision group for half-rate codes
- $J^N$ : cardinality of  $\mathcal{S}^N$
- $K_B$ : number of taps of FBF
- $K_F$ : number of taps of FFF
- $K_q$ : ST encoding symbol period of the  $q$ th antenna group
- $\mathcal{K}$ : Ricean  $\mathcal{K}$ -factor
- $\bar{l}_i$ : optimal detection order at the  $i$ th stage of OSIC
- $L_q$ : number of transmitted independent symbols from each antenna group over  $K$  symbol periods
- $L_q$ : number of transmitted independent symbols from each antenna group over  $K$  symbol periods
- $L_T$ : number of total transmitted independent symbols
- $\mathbf{L}$ : lower triangular matrix of Cholesky factorization
- $\bar{L}^N$ : maximum required number of stages over  $N$  transmit antennas in OSIC detection
- $M$ : number of receive antennas
- $\mathcal{M}_j^N$ : the  $j$ th mode of all the possible mode candidates over  $N$  transmit antennas
- $N$ : number of transmit antennas
- $N_0$ : noise spectral power density



- $N_q$ : number of transmit antennas of the  $q$ th antenna group
- $\mathcal{O}(P)$ : the set of all  $P \times P$  real orthogonal designs with  $P$  independent inputs
- $\mathcal{O}(K, L)$ : the set of all  $K \times K$  real orthogonal designs with  $L$  independent inputs
- $P$ : number of transmitted independent symbols of O-STBC user
- $P_e$ : average error probability
- $P_{e,q}$ : error probability of the  $q$ th antenna group
- $P_i^o$ : optimal power allocation of the  $i$ th sub-channel
- $P_q$ : transmit power of the  $q$ th user terminal/antenna group
- $P_T$ : total average transmit power
- $Q$ : number of total user terminals/antenna groups
- $Q_D$ : number of O-STBC user terminals
- $Q_M$ : number of SM user terminals
- $Q_j^N$ : number of antenna groups of the  $j$ th possible set over  $N$  transmit antennas
- $Q_{\max}^N$ : maximum number of antenna groups over  $\mathcal{S}^N$
- $Q_{\min}^N$ : minimum number of antenna groups over  $\mathcal{S}^N$
- $\mathbf{q}_{B,n}$ : FBF weight vector of the  $n$ th data stream
- $\mathbf{q}_{F,n}$ : FFF weight vector of the  $n$ th data stream
- $r$ : rank of a matrix
- $R$ : code rate of O-STBC
- $R_b$ : transmission bit rate

- $R_b(j)$ : transmission bit rate of the  $j$ th mode
- $R_{b,q}$ : transmission bit rate of the  $q$ th antenna group
- $R^N$ : code rate of G-STBC over  $N$  transmit antennas
- $R^N(j)$ : code rate of G-STBC of the  $j$ th mode over  $N$  transmit antennas
- $R_q^N$ : code rate of the  $q$ th antenna group code over  $N$  transmit antennas
- $\mathbf{R}_{c,F,n}$ : autocorrelation matrix of signal vector of FFF part  $\mathbf{x}_{c,F,n}(k)$
- $\mathbf{R}_{xx}$ : autocorrelation matrix of signal vector  $\mathbf{x}(k)$
- $s(k)$ : input symbol to the ST encoder
- $s_l(k)$ : the  $l$ th input symbol to the ST encoder
- $\tilde{s}_l(k)$ : split real-valued symbol of  $s_l(k)$
- $\mathbf{s}(k)$ : input symbol vector to the ST encoder
- $\hat{\mathbf{s}}(k)$ : estimate of  $\mathbf{s}(k)$
- $\mathcal{S}_D$ : index set of O-STBC user terminal
- $\mathcal{S}_M$ : index set of SM user terminal
- $\mathcal{S}^N$ : the set of all possible antenna architectures over  $N$  transmit antennas
- $T$ : symbol period
- $\mathbf{t}_{n,l}$ : the  $l$ th column of  $\mathbf{T}_n$
- $\mathbf{T}_n$ : transformation matrix of the  $n$ th data stream
- $\tilde{\mathbf{u}}_n$ : RR adaptive vector of GSC of the  $n$ th data stream
- $v(t)$ : continuous-time noise

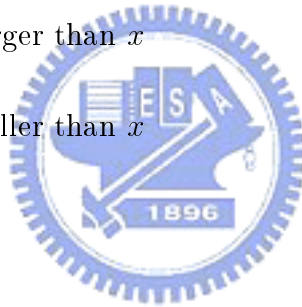
- $v(k)$ : discrete-time noise
- $v_m(t)$ : continuous-time noise at the  $m$ th antenna
- $v_m(k)$ : discrete-time noise at the  $m$ th antenna
- $\mathbf{v}(t)$  continuous-time noise vector
- $\mathbf{v}(k)$  discrete-time noise vector
- $\mathbf{V}(k)$  discrete-time noise matrix
- $\mathbf{w}_l$ : weight vector of the  $l$ th data stream at the  $i$ th stage of OSIC
- $\mathbf{W}_i$ : weight matrix at the  $i$ th stage of OSIC
- $x(t)$ : continuous-time transmitted symbol
- $x(k)$ : discrete-time transmitted symbol
- $x_n(t)$ : continuous-time transmitted symbol at the  $n$ th antenna
- $x_n(k)$ : discrete-time transmitted symbol at the  $n$ th antenna
- $\mathbf{x}(t)$  continuous-time transmitted symbol vector
- $\mathbf{x}(k)$  discrete-time transmitted symbol vector
- $\mathbf{X}(k)$  discrete-time transmitted symbol matrix (ST codeword)
- $\hat{\mathbf{X}}(k)$  estimate of  $\mathbf{X}(k)$
- $y(t)$ : continuous-time received signal
- $y(k)$ : discrete-time received signal
- $y_m(t)$ : continuous-time received signal at the  $m$ th antenna
- $y_m(k)$ : discrete-time received signal at the  $m$ th antenna

- $\mathbf{y}(t)$  continuous-time received signal vector
- $\mathbf{y}(k)$  discrete-time received signal vector
- $\mathbf{Y}(k)$  discrete-time received signal matrix
- $\mathbf{z}(k)$ : MF signal vector

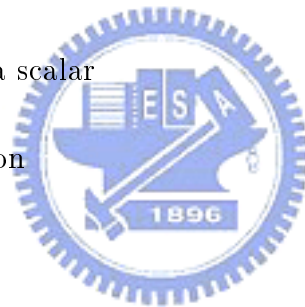


# Mathematical Notations

- $\otimes$ : convolution operator
- $\odot$ : Hadamard product
- $\otimes$ : Kronecker product
- $|\cdot|$ : magnitude of a scalar, determinant of a matrix, or cardinality of a set
- $\|\cdot\|$ : Euclidean norm
- $\|\cdot\|_F$ : Frobenius norm
- $\|\cdot\|_{\mathbf{A}}$ :  $\mathbf{A}$ -norm
- $\lceil x \rceil$ : the smallest integer larger than  $x$
- $\lfloor x \rfloor$ : the largest integer smaller than  $x$
- $a$ : scalar  $a$
- $\mathbf{a}$ : vector  $\mathbf{a}$
- $\mathbf{A}$ : matrix  $\mathbf{A}$
- $[\mathbf{A}]_{i,j}$ : the  $(i, j)$ th entry of matrix  $\mathbf{A}$
- $\mathbf{0}_M$ :  $M \times 1$  zero vector
- $\mathbf{O}_{M \times N}$ :  $M \times N$  zero matrix
- $\mathbf{I}_M$ :  $M \times M$  identity matrix
- $(\cdot)^*$ : complex conjugate
- $(\cdot)^T$ : transpose



- $(\cdot)^H$ : complex conjugate transpose
- $(\cdot)^+$ : Moore-Penrose inverse (pseudoinverse)
- $\ln(\cdot)$ : natural logarithm
- $\log_2(\cdot)$ : base-2 logarithm
- $\det(\cdot)$ : determinant of a matrix
- $\text{diag}(\cdot)$ : diagonal operator of a matrix
- $\text{rank}(\cdot)$ : rank operator of a matrix
- $\text{vec}(\cdot)$ : vectorization operator of a matrix
- $\text{mod}(x, y)$ : remainder after  $y$  dividing  $x$
- $\mathcal{Q}(\cdot)$ : quantize operator of a scalar
- $\delta[\cdot]$ : Kronecker delta function
- $E\{\cdot\}$ : expectation operator
- $\text{tr}(\cdot)$ : trace of a matrix
- $\text{rank}(\cdot)$ : rank of a matrix
- $\text{Re}\{\cdot\}, \text{Im}\{\cdot\}$ : real and imaginary parts
- $\mathbf{P}^\perp$ : orthogonal projection
- $Q(x)$ : Gaussian  $Q$ -function
- $\text{erfc}(x)$ : complementary error function
- $\mathbb{R}$ : real field
- $\mathbb{C}$ : complex field



# Chapter 1

## Introduction

In the past two decades, wireless communication has grown with unprecedented speed from early radio paging, cordless telephone and cellular telephony to today's personal communication and computing devices. These commercial wireless applications have had a great impact on today's business world and people's daily lives. The growth and demand for wireless services will play a significant role in the evolution of Internet service from wireline systems to wireless systems.

With the increasing demand of communication service for subscribers, e.g., the need of multi-media message, the frequency spectrum has become more and more a precious resource. Hence, the major challenge for future wireless communications will be to effectively enhance the capability of radio access, under a limited bandwidth requirement, so as to achieve *high transmission rate* and *high link quality (LQ)*. Also, the power requirements are that devices should use as little power as possible to conserve battery life and keep the products small. Wireless system designers are thus faced with a two-part challenge: improve performance and increase data rates while incurring little or no increase in bandwidth or power. In particular, the wireless channel is characterized by its random and unpredictable nature, and in general the channel error rates are poorer over a wireless channel than over a wired channel. Therefore, the major problem in wireless channel is the signal distortion due to

the complex multipath fading and time-varying effects. The intersymbol interference (ISI) caused by long delay multipaths and the cochannel interference (CCI) due to the frequency reuse in cellular communications will also result in an increased error rate.

To combat these problems and meet such diverse requirements mentioned above simultaneously, different technologies including advanced multiple-access schemes, bandwidth-efficient source coding and sophisticated signal processing technologies have been used. Among these technologies, “signal processing” has always played a critical role in the research and development of wireless communications. While the conventional temporal-domain or frequency-domain only signal processing technique would suffer from the need of additional bandwidth, the spatial-domain approaches (i.e., the smart antenna or multi-input multi-output (MIMO) techniques) are known to be capable of enhancing signal quality and system capacity through exploiting spatial resource without extra bandwidth expansion. With multiple antennas, transmitted and received signals can be effectively separated using the conventional temporal-domain processing combined with the spatial-domain processing, that is, the space-time (ST) signal processing. Therefore, the scheme that employs multiple antennas at the transmitter and receiver, or the so called MIMO technique, will become a promising technology in future wireless communications that is ideal for high *spectral efficiency (SE)* requirement.

## 1.1 Overview of Multiple Antenna Systems

Wireless channels are characterized by large attenuation and vagaries in the channel termed as fading. It is well known that “diversity” in signal processing is very effective in countering the effects of fading [1]-[5]. Diversity techniques are based on the notion that if the receiver can be provided with several replicas of the same information signal (redundancy of signal) transmitted over independently fading channels, then the probability that all the signal components will fade simultaneously is reduced considerably. The three basic forms



of diversity can be applied in the frequency, temporal and spatial domains [1]-[3].

- **Frequency Diversity:** Replicas of the information bearing signal are transmitted in different frequency bands, where the separation between the frequency bands is greater than the *coherent bandwidth* of the channel. For example, the *equalization*, *RAKE* and *orthogonal frequency division multiplexing (OFDM)* are the common used techniques for achieving the frequency diversity.
- **Temporal Diversity:** In this case, replicas of the information bearing signal are transmitted in different time slots, where the separation between the time slots is greater than the *coherent time* of the channel. A more well-known technique for temporal diversity is the *channel coding with interleaving*.
- **Spatial Diversity:** Spatial diversity (SD) is also called antenna diversity. It has been observed that antennas with a spacing of more than a number of wavelengths (*coherent distance*) lead to spatially uncorrelated channels. The transmission of replicas of the information bearing signal over these uncorrelated spatial channels leads to SD. Polarization diversity and angle diversity are two special examples of SD. On the other hand, *selection combining*, *switch combining*, *equal gain combining* and *maximum ratio combining (MRC)* are the examples of efficient combining schemes for SD. Depending on whether multiple antennas are used for transmission or reception, SD can be classified into two categories: receive diversity and transmit diversity.

Note that not all kinds of diversity are always feasible. For example, a slowly fading channel (with a long coherent time) cannot support the temporal diversity with practical interleaving depths. Similarly, frequency diversity is not feasible when the coherent bandwidth of the channel is comparable to the bandwidth of the signal employed. However, irrespective of the channel characteristics, SD can always be exploited as long as there is sufficient spacing between the antennas. It becomes very important to utilize SD at both the transmitter and the receiver especially when other forms of diversity are not feasible due to the nature

of the channel available as well as the nature of the signaling used in the system. It is also noticed that, in above forms of diversity, only the *SD* can be applied without any system bandwidth expansion. These inspire the use of multiple antennas at the transmitter and/or receiver, leading to the MIMO schemes.

### **Leverages of Space-Time Processing (Smart Antenna)**

ST processing, or the so called smart antenna, is a tool for improving the overall economy and efficiency of the wireless communication systems by exploiting multiple antennas at the transmitter and/or receiver. Most conventional wireless modems do not, however, efficiently exploit the spatial dimension offered by multiple antennas. The use of multiple antennas in wireless links with appropriate ST coding/modulation and demodulation/decoding is rapidly becoming the new frontier of wireless communications. Recent years have seen the field mature substantially, both in theory and practice. Recent advances in theory include the solid understanding of capacity and other performance limits of ST wireless links, ST propagation and channel models, and also ST modulation/coding and receiver design. A growing awareness of the huge performance gains possible with ST techniques has spent efforts to integrate this technology into practical systems.

Based on the antenna architecture perspective, wireless system links can be classified into four basic configurations: single-input single-output (SISO), single-input multi-output (SIMO), multi-input single-output (MISO) and MIMO, as depicted in Figure 1.1. Multiple antenna systems incorporating ST processing have a number of advantages over SISO channels such as *antenna array gain*, *interference reduction gain*, *SD gain* and *spatial multiplexing (SM) gain*. Except for SM gain, the three gains are not exclusive in MIMO channels and also exist in SIMO and MISO channels. The SM gain, however, is a unique characteristic of MIMO channels. These leverages can translate into improving the system performance in terms of coverage, LQ, capacity and data rate. Typically, Some of the leverages and advantages are conflicting depending on the algorithms used, but some of them can be si-

multaneously achieved. They are summarized as follows and illustrated in Figure 1.2. An excellent overview of the leverage of ST processing (smart antenna) can be found in [5], [6].

- **Antenna Array Gain:** Multiple antennas at the receiver or transmitter or both can coherently combine the signal energy to improve the average signal-to-noise ratio (SNR) at the receiver. The average increase in signal power at the receiver is proportional to the number of antennas. In channel with multiple antennas at the transmitter (MISO or MIMO case), array gain exploitation requires channel information at the transmitter. With the array gain obtained at the receiver, the signal *range/coverage* can be enlarged (or the transmit power can be reduced) and the  $LQ$  can be increased. For example, *beamforming* is an efficient technique to realize the antenna array gain [5], [6].
- **Interference Reduction Gain:** When multiple antennas are used, the differentiation between the spatial signatures of the desired signal and interfering signals can be exploited by forming a null in the direction of interference to reduce its strength. Interference reduction requires channel knowledge of the desired signal. However, exact knowledge of the interferer's channel may not be necessary. Interference reduction can improve the signal-to-interference ratio (SIR). This improvement will directly enhance the  $LQ$  and allow the introduction of reuse factors to increase network *capacity*. A well-known example for achieving the interference reduction gain is the *beamforming or smart antenna* technique [5], [6].
- **Spatial Diversity Gain:** When the antenna spacing is large enough (larger than coherent distance), the receiver or transmitter will see independently faded versions of the same signal. The use of high-order modulation and low BER targets make the system very sensitive to fading. Using multiple antennas to combine the independently faded versions of signal causes that the resultant signal exhibits considerably reduced amplitude fluctuation in comparison with the signal at any single antenna.

Receive/transmit diversity is characterized by the number of independently fading branches, a.k.a., the diversity order, and is equal to the number of receive/transmit antennas in SIMO/MISO channels. Diversity is capable of improving the *LQ*, *capacity and transmission data rate*. SD gain can be accomplished through the receive diversity and/or TD techniques. *MRC* [2] is a good example for receive diversity and *ST coding (STC)* [7], [8] is an excellent example for TD.

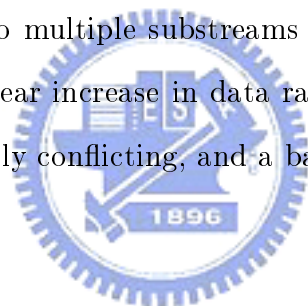
- **Spatial Multiplexing Gain:** Multipath propagation has long been regarded as an *impairment* because it causes signal fading. To mitigate this problem, diversity techniques described above were developed. Recently, information theory [9], [10] has shown that with multipath propagation, multiple antennas at both the transmitter and receiver can establish essentially multiple parallel channels that operate simultaneously, on the same frequency band at the same total radiated power. Spatial multiplexing (SM) means that independent data streams are transmitted from different antennas to improve the SE. SM requires multiple antennas at both ends of the wireless link, i.e., the MIMO channels so that the spatial signatures of the transmitted signals induced at the receive antennas are well separated. Under favorable (rich scattering) channel conditions, SM offers increased *capacity or data rate* linearly, proportional to the minimum number of transmit and receive antennas. A popular example to the SM systems is the *layered ST coding (LSTC)*, a.k.a., *Bell Laboratories layered ST (BLAST)* [11].

Based on the degrees of scattering richness, a wireless channel can be characterized by the “specular” and “scattering” components [12]. In the limit of rich scattering (uncorrelated) environment, the deterministic component vanishes while, in the limit of a pure specular (correlated) environment, it constitutes the entire channel response. Hence, a wireless channel comprises rich scattering and specular as extreme cases. In particular, *indoor* environment has high degrees of scattering richness and thus is a scattering channel. However, *outdoor* environment is highly dominated by the specular component and thus is a specular channel. In summary, for the leverages of ST processing described above, the antenna array gain is

very substantial in specular scenarios, but negligible in highly scattering environments. On the other hand, the advantages of SM is significant in rich scattering case, but vanishes in highly specular case [12]-[14].

## 1.2 Overview of MIMO Techniques

Multiple antennas can be used in wireless systems to improve the communication performance. *Beamforming/Equalization* [2], [14]-[16], *SD* [2], [7], [8], and *SM* [11], [17], are three very popular and different signal processing techniques in multiple-antenna systems. By coherently combining the signals at different antennas, beamforming can efficiently cancel the interference and provide an improved coverage [18]. SD attempts to spread information across antennas to enable robust transmission in the presence of fading [19]. SM, on the other hand, divides data into multiple substreams and transmit each substream on a different antenna leading to a linear increase in data rate [11]. The goals of the aforementioned techniques may be mutually conflicting, and a balance is needed to optimize system performance [20].



### 1.2.1 Beamforming/Equalization Techniques

#### Beamforming Techniques

Spatial filtering or beamforming [15], [21]-[24] can be applied to benefit from the angular spread and commonly different spatial signatures of the desired and interfering signals. Beamforming is achieved by adjusting the complex coefficient weights and combining (summing) the signals induced at different spatially correlated antennas to form a single output of an array as illustrated in Figure 1.3. For the given set of complex antenna weights, the direction in which the array has the maximum gain is typically called the beam pointing direction. The main advantage of applying beamforming in reception comes from CCI reduction (filtering the desired signal from interfering signals), ISI suppression (nulling the

delayed versions of signals arriving from directions), and angular diversity (forming multiple beams and coherently combining the spatially filtered multipath components from different dominant scatters). Angular diversity gain becomes rather limited in the case of small angular spread. For accurate spatial filtering in reception, angle-of-arrival (AOA) estimation are required for calculating the set of complex antenna weights. The weights of beamformer can be determined by an adaptive process using temporal information (reference signal) or spatial information (AOA of the signal) [21]-[23]. A overview of beamforming (smart antenna) techniques for wireless communication systems is presented in [15], [22]-[24].

Three main schemes of beamforming may be defined as follows [25]-[27].

- **Switched Beam Scheme:** It comprises only a switching function between separate predefined beams of an array, offering maximized received power [26]. This is the simplest method and is easier to implement in existing systems than other beamforming schemes. However, it offers a limited interference reduction.
- **Direction Finding Scheme:** In this case, AOAs from the signals are first estimated and then the weights of beamformer are calculated in accordance with the specified directions. In this scheme, the received power is maximized [22], [24]. No reference signal is required. However, it is not applicable to non-line-of-sight (NLOS) environments.
- **Adaptive Array Scheme:** In this scheme, the beam pattern is adapted to the received signal using a reference signal or a spatial signature. The beam pattern can be adjusted to null the interferers. This approach optimizes the signal-to-interference ratio (SIR), and is applicable to NLOS environments. Since the weights are updated according to the environment by some criteria, such as the minimum mean square error (MMSE), minimum variance distortionless response (MVDR) and linearly constrained minimum variance (LCMV), not only is the interference reduced, but the multipath fading is also mitigated. The nice references on how to determine the beamforming weights can be found in [21]-[23].

## Equalization Techniques

Adaptive beamforming and AOA estimation are commonly regarded as conventional array or space only (SO) (see Figure 1.3) processing techniques. Temporal or time only (TO) filtering/processing techniques as shown in Figure 1.4 employ adaptive equalizers to offer time domain ISI suppression (and possible CCI reduction) by complex coefficient weighting and combining of the temporally sampled signals [1], [2], [28]. ST beamforming (also called the ST filtering/processing technique) is loosely defined as any combination of SO and TO filtering/processing. Figure 1.5 depicts the joint ST processing. It allows the advantages to be simultaneously exploited in both dimensions improving the different aspects in the performance of a wireless communication system. For a comprehensive overview of the ST processing area see [15], [28]. A popular optimality criterion in ST processing is the maximum likelihood (ML) criterion based on the Viterbi algorithm. It is usually referred to as the ML sequence estimation (MLSE) [1]. Other frequently used criteria are the MMSE and zero-forcing (ZF) [1], [28]. In theory, ST MLSE outperforms ST MMSE in the presence of significant ISI. However, for strong CCI scenarios, ST MMSE is superior to ST MLSE. An efficient approach to combating the CCI and ISI problems is to combine the strengths of MMSE and MLSE in a two-stage hybrid structure [29].

## Transmit Beamforming/Equalization Techniques

One possible approach for antenna array transmit processing is transmit beamforming [30], [31], which provides antenna array gain and interference reduction gain at the subscriber unit. In this scheme, the transmitter typically operates in a “closed-loop” manner, which means that it uses the channel information fed back by the receiver through the uplink link in order to shape the beams so that the subscriber unit can receive the desired signal without interference in the downlink. This scheme can significantly reduce the computational load at the subscriber unit. However, the success of transmit beamforming depends on the quality of the channel estimates, feedback channel, mapping between the two links, and dynamics of the

signal and interference. Closed-loop techniques typically suffer from reduced uplink capacity because of the extra channel information that is transmitted. It is not applicable to situation when the uplink and downlink use different frequency bands. With a large multipath channel delay, the ST processing can be exploited at the transmitter to pre-combat the ISI effects, called the ST pre-equalization techniques [32].

## 1.2.2 Spatial Diversity Techniques

### Receive Diversity Techniques

Traditionally, SD is referred to receive diversity [33]. The receive diversity can be used in SIMO channels. Multiple antennas at the base station (BS) have been exploited in various communication systems, such as microwave relay stations and cellular based mobile stations (MSs), to obtain receive diversity and improve uplink performance. However, in many wireless systems, additional antennas may be expensive or impractical at the remote station (i.e., MS), since the remote unit is supposed to be with small volume and simple structure. The small size of the MS limits both the spatial resolution of the array (because of the small number of antenna elements) and the diversity gain (because the antenna elements are close to one another). In these cases, multiple transmit antenna array is considered.

### Transmit Diversity Techniques

Most recently, TD technique, which provides diversity benefit at a receiver with multiple transmit antennas, has received much attention, especially for wireless cellular application. TD is applicable to MISO channels. Some interesting approaches for TD have been suggested. The TD that is a delay diversity scheme was first inspired by Wittneben [34] in 1991. After that, the time-switched TD (or the so called antenna hopping) and the phase-switched TD (or the so called frequency weighting) were proposed by Hiroike in 1992 [35]. In delay TD scheme, the BS transmits a delayed version of the original signal, hence creating an artificial multipath distortion [36]. Then, Seshardi and Winters in 1994 first attempted to develop it



as an STC [37]. After that, in 1996, the delay TD combined the signal design with linear modulation was proposed by Guey et al [38]. However, due to the degrading orthogonality and increasing interference level seen at the mobile receiver, the delay TD has a limited link performance gain over the non-transmit diversity [39].

Another approach in [40] recommended that each user can be assigned a different orthogonal code for each transmit antenna. This scheme can provide arbitrary-fold diversity and have very simple demodulation scheme, but the diversity gain and simplicity of this scheme come with the penalty of requiring more than one spreading codes per user. One open-loop approach that offers some diversity gains without requiring extra resource is the orthogonal transmit diversity (OTD) scheme [41], which was an early inclusion as an option in the IS-2000 standard. According to this technique, each user's data stream is extended by one spreading code and transmitted through each transmit antenna in a scanning way. However, OTD provides unbalanced diversity to each of the user's data substreams, and usually OTD cannot provide full SD gain. Without interleaving or channel coding, OTD does not improve the transmission performance.

Another very important approach for TD is STC technique as shown in Figure 1.6. STC techniques are first put forward under the assumption of narrow band wireless fading environment. But these techniques can be easily applied to wideband communications by combining with other wideband communication techniques such as code division multiple access (CDMA) [42], [43] or OFDM [44], [45]. Generally, STC can be classified into two broad categories, the ST trellis coding (STTC) and ST block coding (STBC).

- **STBC Scheme:** The first STBC was proposed by Alamouti for two transmit antennas, the so called Alamouti's code [46], in 1998. Then it was further developed and put into a theoretical framework by Tarokh, Jafarkhani and Calderbank [47]. STBC operates on a block of input symbols and produces a matrix output whose columns represent times and rows represent antennas. Unlike traditional single antenna block codes for the additive white Gaussian noise (AWGN) channel, STBC may not provide

error correction ability. The key feature of STBC is the provision of full diversity with extremely low encoder and decoder complexity. The STBCs first studied in [46] and [47] are the orthogonal STBCs (O-STBCs). Due to their inherent orthogonality, these STBCs benefit from full diversity gain with low complexity receiver since the corresponding ML decoding scheme is based on linear processing only, e.g., MRC. However, except for the system with two transmit antennas, there is no rate one complex orthogonal code design for systems with multiple transmit (beyond two) antennas [47].

- **STTC Scheme:** The other kind of STC is STTC. STTC proposed by Tarokh, Seshardi and Calderbank in 1998 [49] combines signal processing at the receiver with coding techniques appropriate to multiple transmit antennas. Such a technique operates on one input symbol at a time producing a sequence of vector symbols whose length equals to the number of transmit antennas. Like conventional trellis coding technique for the single antenna channel, STTC provides the coding gain. Since it also provides full diversity gain the key advantage over STBC is the provision of coding gain. However, when the number of transmit antennas is fixed, the decoding complexity of STTC increases exponentially with transmission rate. The disadvantages of STTC are that it is extremely difficult to design and requires a computationally intensive encoder/decoder.

By trading the code orthogonality for higher coding rates, a full-rate, partial diversity codes, named the “quasi-orthogonal” codes, was proposed in [50]. It has been pointed out that the decoding of quasi-orthogonal codes can be done by searching symbols pair by pair, but the decoding method reported is trivial and the symbol pair exhaustive searching is used for ML decoding. Another coding approach preserving the full-rate and full diversity, named the “non-orthogonal” codes, was proposed in [51] at the cost of a small loss in BER performance and some extra decoding complexity relative to truly orthogonal schemes.

### 1.2.3 Spatial Multiplexing Techniques

In 1987, Winters first hinted that the capacity can be increased significantly by using multiple antennas at the transmitter and/or receiver [52]. After some years, a ground breaking result of the SM concepts was exploited by Paulraj and Kailath in 1994 for broadcast digital television systems [53]. Figure 1.7 illustrates the SM concepts in a MIMO system. In 1995, recent advances in information theory opened by Telatar [9], Foschini and Gans [10] revealed an important fact that the rich scattering multipath wireless channel can lift enormous SE (capacity) if the multipath propagation is properly exploited using multiple antennas at the transmitter and receiver. The communication system architecture of the LSTCs, which are first developed by Foschini in 1996 [54], provides an experimental demonstration. The LSTCs can be categorized into two large types, the vertical-BLAST (V-BLAST) and diagonal-BLAST (D-BLAST).

- **V-BLAST Scheme:** In V-BLAST systems, independently encoded data streams are transmitted from each transmit antenna simultaneously, and detected at the receiver by nulling and ordered successive interference cancellation (OSIC) schemes [17], [54]-[56], or sphere decoding scheme [57].
- **D-BLAST Scheme:** In D-BLASTs, each data stream switches transmit antenna after each symbol duration time slot and the completing of each data stream transmission is contributed by all transmit antennas. With the channel coding scheme, a more momentous advantage possessed by the D-BLAST is that it can effectively provide additional time diversity [54], [58]. Like V-BLASTs, D-BLASTs also use the nulling and OSIC schemes for data detection at the receiver. However, due to the encoding structure, the detection framework of D-BLAST is more complex than that of V-BLAST [54], [58].

With BLAST systems, very high data transmission rate can be achieved. However, BLAST cannot be used when the number of receive antennas is smaller than the number

of transmit antennas [11], [17], [54]-[56]. On the other hand, because that the data streams transmitted on the different antennas are independent to each other in BLAST system, V/D-BLAST structure cannot provide TD gain leading to a low reliability in LQ. To increase the link performance, V/D-BLAST usually combines some reliable channel coding schemes [58]. Note that BLAST can also be easily applied to the wideband channels. In this case, an ST processing (equalization) is needed at the receiver [59]-[61].

### 1.2.4 Tradeoffs Between TD and SM

Traditionally, the design of systems has been focused on either extracting maximum TD gain or maximum SM gain. Recently, however, it has been shown that diversity and multiplexing have complementary properties [20]. The maximum performance needs *tradeoffs between diversity and multiplexing*. Nevertheless, both gains can in fact be simultaneously achieved, but there is a fundamental tradeoff between how much of each type of gain any communication technique can extract as was shown in the excellent groundbreaking paper investigated by Zheng and Tse [20]. Note that, since the diversity gain is related to the BER (it is the slope of the BER curve in the high signal-to-interference-plus-noise ratio (SINR) region [20], [47], [49]) and the multiplexing gain is related to the achieved rate, the diversity-multiplexing tradeoff is essentially the tradeoff between the error probability and the data rate of a system.

To achieve high data rates as well as diversity gain, Hassibi and Hochwald proposed a new scheme, named the “linear dispersion code (LDC)” [62], in which transmitter sends substreams of data in linear combinations over space and time. This new scheme allows any number of transmit and receive antennas, provides diversity and maximizes the *mutual information* between transmitter and receiver based on the O-STBC and V-BLAST techniques. This approach generally outperforms both O-STBC and V-BLAST in terms of capacity and/or error probability. Alternative code designs, at the same time, for the framework of LDCs in [62] have also appeared in [63] based on the criterion of minimizing

instantaneous *probability of error*. Other various transmission scheme combined with the O-STBC and V-BLAST techniques have also been proposed for simultaneously achieving the two demands [7], [64], [65]. On the other hand, the observation on such tradeoffs motivates the design of switched diversity and multiplexing systems which use spatial adaptation to improve link performance based on the euclidean distance between the received signal and transmitted data streams [66], [67].

### 1.3 Background and Literature Review

Future wireless applications create the insatiability in the demand for *high data rate* and *high LQ* wireless access [3]-[8], [14], [68], [69]. Spectrum has thus become a scarce and very expensive resource so that a good spectrum management is very important for achieving high SE. Intuitively, the simplest technique to tackle this is to increase the transmit power. However, since system capacity is interference limited in most of the wireless communication systems, SE cannot be directly increased by this way [70]. On the other hand, the popular time and frequency domain processing techniques may also sacrifice the spectrum resource and thus are limited for use. Only the *space* domain processing technique is not [14], [15]. The adoption of multiple antennas at the transmitter and receiver, i.e., MIMO technique [10], [17], [47], [49], [54], [55] promises a significant increase in data rate and LQ without bandwidth expansion and is thus capable of meeting the formidable service requirements in the next-generation wireless communications.

The core scheme of MIMO systems is the STC [3]-[8], [14], [68], [69]. The two main functions of STC are the SM and TD. High SE can be achieved through SM by simultaneously transmitting independent data streams from different antennas, e.g., LSTCs or a.k.a., BLAST techniques [54]-[56]. High LQ, on the other hand, is guaranteed if redundant signals are made and sent from different antennas through independent channels to the receiver. STBCs [46], [47] and STTCs [49] are the two well-know TD techniques for MIMO systems.

In particular, these goals may be mutually conflicting, and a balance is needed to maximize the system performance [14], [20].

To achieve the potential advantages in MIMO systems, several layered ST (BLAST) structures are proposed [17], [59], [60]. The BLAST systems transmit equal-rate independent data streams simultaneously and use an OSIC technique at the receiver to perform multi-stage detection in order to improve the system performance. In BLAST systems, the transmitter does not require any channel information or preprocessing; only the receiver needs to estimate the channel information and realize multiuser (MU) detection. Most researches on BLAST systems have been focused on flat-fading channel scenarios [17].

For wideband systems, the BLAST receiver will suffer from performance degradation due to the presence of ISI. On the other hand, increasing transmit antennas to improve the SE leads to large CCI and therefore further degrades the system performance. To combat these problems, ST processing techniques are required to perform CCI/ISI cancellation via spatial-temporal filtering/equalization [15], [71], typically in the form of a DFE architecture [59]. In MIMO DFE based BLAST, some form of interference cancellation, such as OSIC, can be incorporated for enhanced multi-stage signal detection [59]. However, the complexity of the multi-stage MIMO DFE may be too high if the ST dimension is large. A modified DFE based BLAST receiver has been proposed in which multiple data streams are selected at the same time for detection and interference cancellation such that fewer stages are required, leading to reduced total computational load [60]. In spite of that, a large matrix manipulation is still required at each stage as described in [59]. Therefore, a MIMO equalizer suitable for practical use should work with as small an ST dimension as possible, while offering reliable CCI/ISI suppression.

Reduced-rank (RR) adaptive filtering is a computationally efficient scheme which has been proposed for various signal processing applications [72]-[76]. The goal of RR filtering is to find a lower dimension filter which can achieve nearly the same performance as the full-rank (FR) one. A popular technique of reduced-rank filtering by subspace selection is

the principle components (PC) technique [72], whose performance degrades as the dimension of the adaptive weights is lower than that of the signal-plus-interference subspace [74]. An alternative to the PC technique is the cross spectral (CS) technique [73]. Unfortunately, these two techniques require either the eigenvalue decomposition (EVD) or matrix inversion, which is computationally expensive. A relatively simple RR technique which requires no EVD or matrix inversion is the iterative based MVDR (IMVDR) technique [76]. It can iteratively solve for the optimal MVDR weight vector and corresponding bases (auxiliary vectors) for the best representation of the solution, simultaneously. The main disadvantage of the iterative MVDR technique, however, is the need of a large number of iterations for convergence. RR processing is very suitable for the equalization problem considered herein. This is seen by the observation that the signal-plus-ISI channel matrix has a special band Toeplitz structure in which the leading and trailing columns corresponding to “distant” pre- and post-cursor ISI, respectively, have a sparse structure with many zero entries. These columns are “insignificant” relative to the middle ones, which suggests that using an equalizer with an effective rank smaller than that of the signal-plus-interference subspace (i.e., rank of the channel matrix) should be sufficient to achieve the optimal FR performance. On the other hand, in [77], an RR (partially adaptive (PA)) MIMO MMSE DFE has been proposed based on the generalized sidelobe canceller (GSC) technique [23] and a simple algebraic criterion for determining the blocking matrix of the GSC. In spite of its simplicity, the DFE in [77] requires a matrix inversion for detecting each user signal, and suffers a certain performance degradation at high SNR due to a limited diversity order [59].

MU ST block coded systems [4], [7], [61], [70] can provide multiple fading resistant links but the cochannel user interference then becomes a crucial factor for system performance. In stead of resorting to the computationally-intensive joint ML decoding for signal recovery, there are various proposals exploiting the algebraic structures of the orthogonal ST block codes for facilitating interference mitigation, e.g., the Naguib’s parallel interference cancellation (PIC) scheme [78], and the Stamoulis’s decoupled-based method [79]. Recently it is

suggested in [80] and [81] to tackle the problem alternatively via OSIC approach, which is also known as the V-BLAST algorithm [56]. This is because the OSIC mechanism shows a different approach as compared with [78], [79], and it is believed to maintain a reasonable tradeoff between performance and complexity with respect to the joint ML decoding [6], [68]. In [81], the usage of the orthogonal codes is shown to have an attractive impact on the OSIC detector: it allows a user-wise group detection property. Such an OSIC based detection is also considered in [82]-[84] to resolve multi-antenna ST coded streams; the presented frameworks therein, however, are mainly for STTCs, and do not explicitly exploit the codeword's algebraic structures whenever block codes are considered.

Specifically, the SM and TD are two extreme and complementary transmission strategies in MIMO systems. In a rich-scattering environment, SM technique is the most effective solution for achieving the high data rate transmission. However, in such an environment, the receive SNR's for certain links may be low due to deep channel fades or large path-loss [14]. The high-rate benefit of the SM can thus be largely annihilated by extremely poor detection performance. On the other hand, one important issues for SM techniques is that the number of receive antennas must be greater than that of transmit antennas, which is an unfavorable factor for the mobile terminal. On the contrary, TD scheme is an effective solution, in general suitable for small transmit antenna array (less than four antenna elements), for maintaining link robustness over the severe fading environment. Identically, the good link quality guarantee can allow the high data rate transmission through the use of high order modulation techniques. However, power requirement becomes excessive and hardware realization becomes more complex for it leading to a limit in performance [1]. A feasible solution without leveraging the power resource is to combine these two types of transmission technique for promoting the data rate and compensating the link loss.

To promote a high-speed transmission with an utmost data transmission efficiency, a prospective approach, therefore, is to look for a certain transmission strategy that can boost as much as possible the data rate for good link channels and, on the other hand, switch



to other securing mechanisms for guarding the data from channel impairments if any [85]. To build up such a high-throughput link platform, a reasonable method is to endow the transmitter with the flexibility in choosing a flexible and robust signal transmission scheme better suited for the system requirements and/or the channel conditions. Therefore, a more general class combined with the two concepts of SM and TD techniques should be considered simultaneously at the transmitter. Specifically, decoupling a large transmit antenna array into several small groups with each group using a number of antennas from two to four and being encoded via O-STBCs [47] yields a “grouped STBC (G-STBC)”. Such a transmit antenna configuration can be regarded as a variety of SM signaling strategy by treating one antenna group as a particular data stream unit. Essentially, since the multiple various coding rates can be provided by this encoding strategy over a block of symbols at the transmitter, it can also be referred to as a “variable-rate” STBC scheme. This coding strategy is different to the scheme proposed independently by Kim and Tarokh [86] and [87], which mainly focuses on the small transmit antenna array (for total two, three or four antennas).

## 1.4 Outline of Thesis

This thesis discusses the MIMO techniques for wireless communications. First, the main objective of the thesis is a detailed investigation into the performance of low-complexity, RR ST receiver in the MIMO based environment over the frequency-selective multipath channels. The new receiver architectures are proved to be robust and capable of interference suppression. Furthermore, the RR schemes are incorporated at the receiver for reduced complexity processing, and achieving the faster convergence. Then we mainly work on the efficient design of MIMO transmitter and receiver over the frequency-flat fading channels. In this part, a computationally efficient group-wise OSIC detector is first proposed in an MU ST dual-signaling wireless systems for better matching to each user’s own channel condition. Such a low-complexity group-wise OSIC detector is then properly exploited for a more general

STBC system. With a relatively small feedback overhead, the ST codeword structure is constructed and an optimal codeword selection is proposed to effectively achieve the high LQ and high SE at the same time. The thesis is organized as follows.

In **Chapter 1**, we first introduce the multiple antenna systems, MIMO techniques, background and literatures review of the thesis. **Chapter 2** establishes the basic system model, theoretical background of the research and several MIMO techniques.

In **Chapter 3**, a reduced complexity MIMO equalizer with OSIC is proposed for combating the ISI and CCI over frequency selective multipath channels. It is developed as an RR realization of the conventional MMSE DFE. In particular, the MMSE weights at each stage of OSIC are computed based on the GSC technique and RR processing is incorporated by using the conjugate gradient (CG) algorithm for reduced complexity implementation. The CG algorithm leads to a best low-rank representation of the GSC blocking matrix via an iterative procedure, which in turn gives an RR equalizer weight vector achieving the best compromise between ISI and CCI suppression. With the dominating interference successfully cancelled at each stage of OSIC, the number of iterations required for the convergence of CG algorithm decreases accordingly for the desired signal. Computer simulations demonstrate the proposed RR MIMO DFE can achieve nearly the same performance as the FR MIMO MMSE DFE with an effective rank much lower than the dimension of the signal-plus-interference subspace. *The results in this chapter have been published in [77] and [88].*

**Chapter 4** studies the OSIC detection in a general MU ST wireless system, in which each user's data stream is either orthogonal ST block coded for TD or spatially multiplexed for high SE. The motivation behind this work is that each user adopting a signaling scheme better matched to his own channel condition proves to improve the individual link performance but the resultant CCI mitigation problem is scarcely addressed thus far. By exploiting the algebraic structure of orthogonal code, it is shown that the OSIC detector in the dual-signaling environment allows for an attractive "group-wise" implementation: at each stage, a group of symbols, transmitted either from an O-STBC station or from an antenna of an

SM terminal, is jointly detected. The group detection property, resulting uniquely from the use of orthogonal codes, potentially improves the dual-mode signal separation efficiency, especially when the O-STBC terminals are dense in the cell. The embedded structure of channel matrix is also exploited for deriving a computationally efficient detector. Flop count evaluations and numerical examples are used for illustrating the performance of the proposed OSIC solution. *Parts of the material in this chapter have been published in [80], [89] and further results submitted as the journal papers [81] and [90].*

**Chapter 5** extends an STBC system to a more general case: G-STBC systems. In this chapter, an efficient design of the transmitter and receiver is studied for the G-STBC system with feedback information in the downlink over the Rayleigh flat-fading channels. At the transmitter, all the antenna elements are partitioned into several small groups, each of which places two, three or four antennas and is encoded via the orthogonal based STBC. Again, by exploiting the algebraic structure of orthogonal codes, it is shown that the OSIC based detector in such a G-STBC system will allow for an “group-wise” implementation. The group-wise detection property, resulting uniquely from the use of orthogonal codes, also potentially improves the signal separation efficiency. Moreover, the low-complexity detector implementation developed in Chapter 4 is then modified and used for signal separation. Finally, the code structures are built up based on the group-wise OSIC detection strategy and a code selection criterion that minimizes the BER performance under the constraints of total transmit power and SE is then proposed. Numerical examples are used for illustrating the performance of the proposed G-STBCs and OSIC based solution. *The results in this chapter will be submitted as the journal paper [91].*

Finally, **Chapter 6** concludes this thesis and discusses future extension of this research.

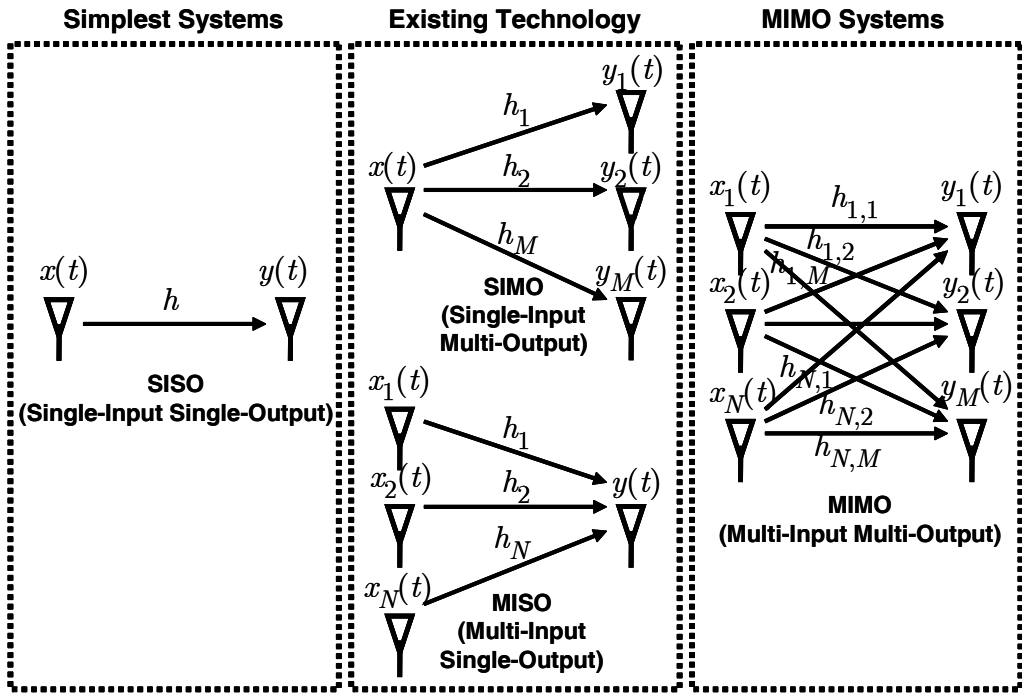


Figure 1.1: Four basic configurations in wireless systems.

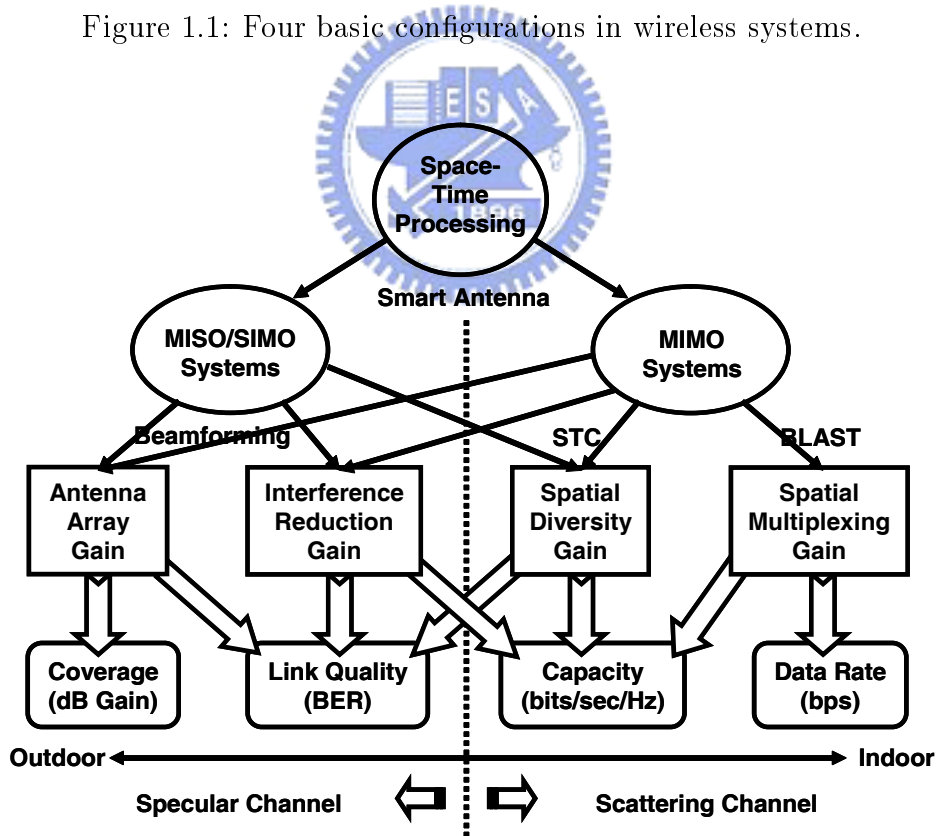


Figure 1.2: Leverages of ST processing.

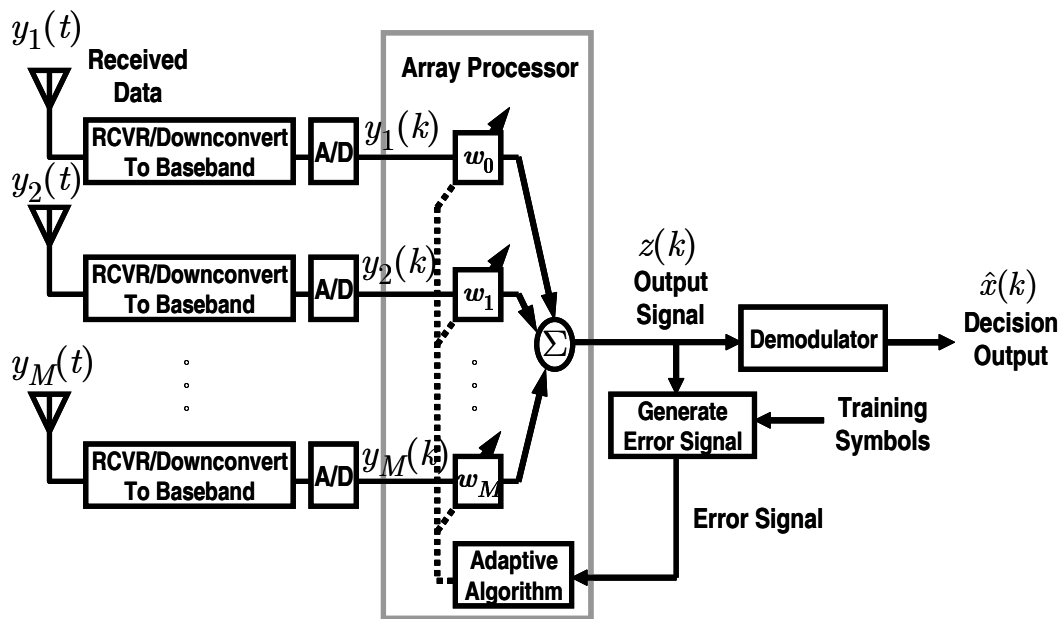


Figure 1.3: Illustration of SO filtering/processing (beamforming).

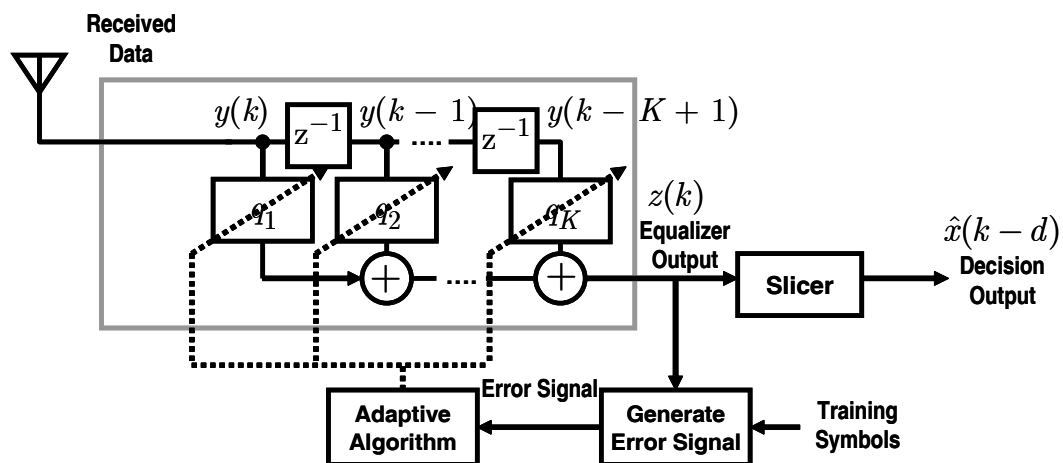


Figure 1.4: Illustration of TO filtering/processing (equalization).

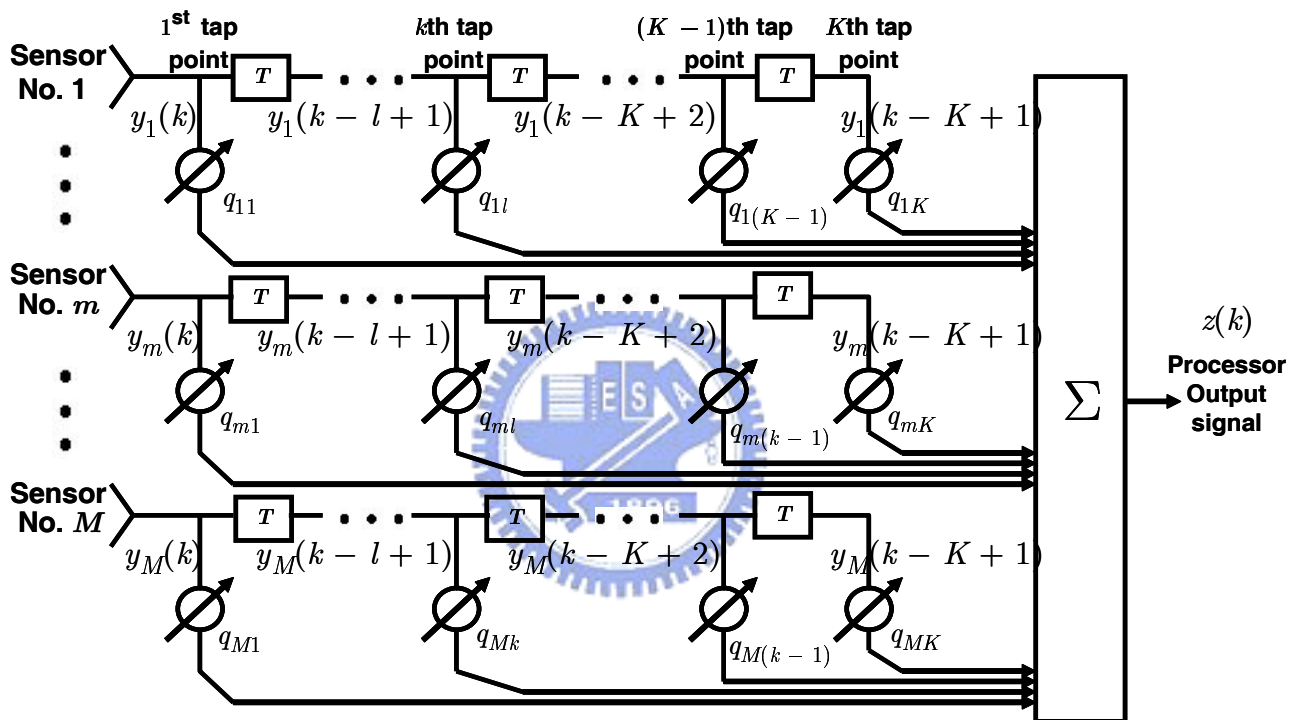


Figure 1.5: Illustration of joint ST filtering/processing (ST beamforming/equalization).

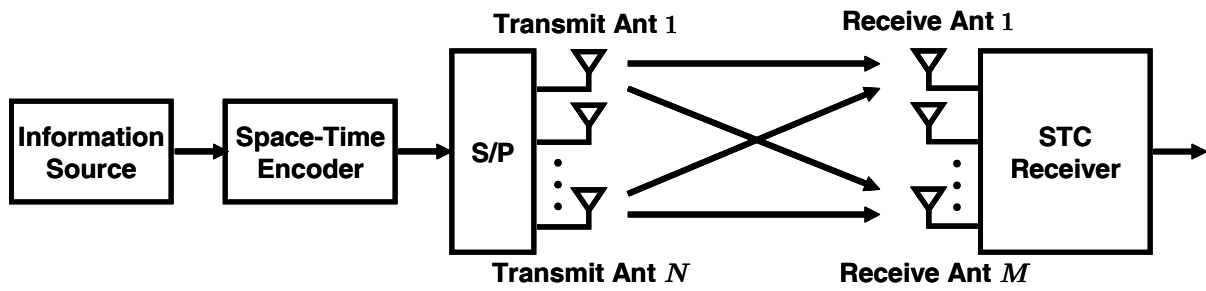


Figure 1.6: Block diagram of STC systems.

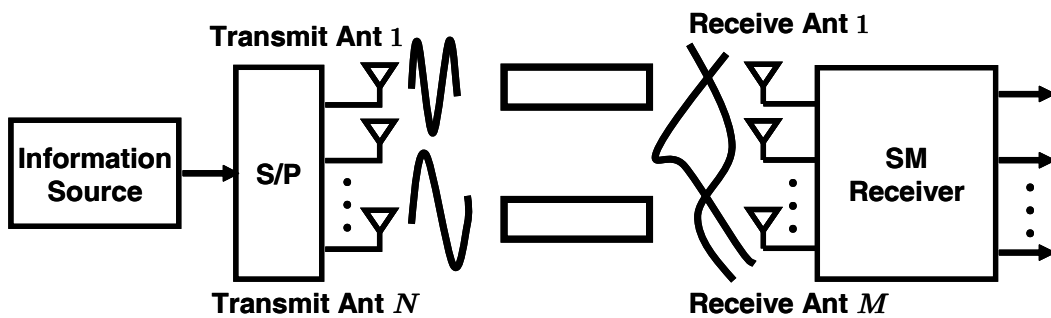


Figure 1.7: Block diagram of SM systems.

# Chapter 2

## Basic Concepts of MIMO Wireless Communications

### 2.1 Introduction

In this chapter, we give an overview of MIMO wireless communications. Section 2.2 introduces the MIMO system model, derives the channels from statistical ST channel descriptions in physical and non-physical propagation environments and discuss the sampled signal models over the frequency flat and frequency selective channels. Section 2.3 studies channel capacity of several channels under a variety of conditions: channel unknown and known to the transmitter. We also discuss the ergodic capacity and outage capacity of random channels. Then the STC techniques for providing SD and the SM techniques for achieving high SE are developed in Section 2.4 and 2.5, respectively. In particular, in this two techniques we mainly address the STBC schemes and V-BLAST techniques. The detection algorithm and performance analysis of both the schemes will also be studied.



## 2.2 MIMO System Model

In this section, we define the MIMO system model with  $N$  transmit antennas and  $M$  receive antennas for the time division multiple access (TDMA) systems. Several commonly used MIMO channel models are also discussed and the received sampled signal models are derived.

### 2.2.1 Continuous-Time MIMO Systems Model

For the MIMO channels, the received signal, in based form, at the  $m$ th antenna can be expressed as

$$y_m(t) := \sqrt{\frac{P_T}{N}} \sum_{n=1}^N h_{m,n}(t) \otimes x_n(t) + v_m(t), \quad m = 1, 2, \dots, M, \quad (2.1)$$

where  $P_T$  is the total transmit power,  $h_{m,n}(t)$  is the overall channel impulse response (CIR) from the  $n$ th transmit antenna to the  $m$ th receive antenna, which includes the effects of pulse shaping  $g(t)$  and propagation channel  $c(t)$ ;  $x_n(t)$  is the transmitted symbol from the  $n$ th antenna, and  $v_m(t)$  is the AWGN at the  $m$ th receive antenna with power  $\sigma_v^2$ . Concatenating  $y_m(t)$ ,  $m = 1, 2, \dots, M$ , into a vector, we obtain an  $M \times 1$  received signal vector

$$\mathbf{y}(t) := [y_1(t), y_2(t), \dots, y_M(t)]^T = \sqrt{\frac{P_T}{N}} \mathbf{H}(t) \otimes \mathbf{x}(t) + \mathbf{v}(t), \quad (2.2)$$

where

$$\mathbf{H}(t) := \begin{bmatrix} h_{1,1}(t) & h_{1,2}(t) & \dots & h_{1,N}(t) \\ h_{2,1}(t) & h_{2,2}(t) & \dots & h_{2,N}(t) \\ \vdots & \vdots & \ddots & \vdots \\ h_{M,1}(t) & h_{M,2}(t) & \dots & h_{M,N}(t) \end{bmatrix} \in \mathbb{C}^{M \times N}, \quad (2.3)$$

is the MIMO channel vector and

$$\mathbf{x}(t) := [x_1(t), x_2(t), \dots, x_N(t)]^T \in \mathbb{C}^N \quad (2.4)$$

is the transmitted symbol vector.  $\mathbf{v}(t)$  is the noise vector whose components are assumed temporally and spatially white with the same power  $\sigma_v^2$ . Note that the “row” and “column” of  $\mathbf{H}(t)$  in (2.3) represent the MISO CIR and SIMO CIR, respectively.

## 2.2.2 MIMO Channel Model

In this section, we introduce the MIMO channel models in the physical and non-physical environments. Specifically, the physical model is described based on some crucial physical parameters of the multipath propagation paths, and the non-physical model is based on the channel statistical characteristics using non-physical parameters.

### Physical Channel Model

Consider a SISO model. Assume that the transmitted signal is scattered and arrives at the receiver at different  $J$  multipaths with the complex path amplitudes  $\alpha_j$ ,  $j = 1, 2, \dots, J$  and propagation delays  $\tau_j$ ,  $j = 1, 2, \dots, J$ . We also assume that  $\alpha_j$ 's are i.i.d. complex Gaussian random variables with unit-variance and treated as constant over the processing period of interest due to the slow fading assumption. As a result, the characteristic of CIR  $c(\tau)$  can thus be described by the summation of  $J$  path responses [1]

$$c(\tau) := \sum_{j=1}^J \alpha_j \delta(\tau - \tau_j). \quad (2.5)$$

The overall SISO CIR can thus be written as

$$h(\tau) = \sum_{j=1}^J \alpha_j g(\tau - \tau_j). \quad (2.6)$$

Note that, in (2.6), we assume that  $\tau_1 = 0$  and  $\tau_J = \tau_{max}$ , where  $\tau_{max}$  is the maximum delay spread of the physical channel.

For a MIMO system with  $N$  transmit antennas and  $M$  receive antennas, the physical MIMO channel is thus given by [14]

$$\mathbf{C}(\tau, \theta) := \sum_{j=1}^J \alpha_j \mathbf{a}_R(\theta_j^R) \mathbf{a}_T(\theta_j^T) \delta(\tau - \tau_j), \quad (2.7)$$

and

$$\mathbf{H}(\tau) := \sum_{j=1}^J \alpha_j \mathbf{a}_R(\theta_j^R) \mathbf{a}_T(\theta_j^T) g(\tau - \tau_j). \quad (2.8)$$

where  $\mathbf{a}(\theta)$  is the array manifold vector and  $\theta_j^R$  and  $\theta_j^T$  are the angle-of-arrival (AOA) and angle-of-departure (AOD) of the  $j$ th path.

## Non-Physical Channel Model

The scatter location, antenna element patterns and geometry and the scattering model together determine the correlation between elements of  $\mathbf{H}(\tau)$ , the channel between the transmit and receive antennas. With suitable choices of the above, including a double scattering model, it can be shown in [14] that the elements of  $\mathbf{H}(\tau)$  are independent zero-mean circularly symmetric complex Gaussian random variables.

We assume that the delay spread in the channel is negligible, i.e.,  $\tau_{max} \approx 0$ . Therefore, the MIMO channel  $\mathbf{H}(\tau)$  in (2.8) can be rewritten as

$$\mathbf{H}(\tau) = \left( \sum_{j=1}^J \alpha_j \mathbf{a}_R(\theta_j^R) \mathbf{a}_T(\theta_j^T) \right) g(\tau) = \mathbf{H}g(\tau), \quad (2.9)$$

where

$$\mathbf{H} := \sum_{j=1}^J \alpha_j \mathbf{a}_R(\theta_j^R) \mathbf{a}_T(\theta_j^T) \in \mathbb{C}^{M \times N}. \quad (2.10)$$

We drop  $g(\tau)$  and under assumptions discussed above, with “rich scatters” in the propagation environment, that is  $J \approx \infty$ , the elements of  $\mathbf{H}(\tau) = \mathbf{H}$  can be modeled to be circularly symmetric complex Gaussian with zero-mean and unit-variance [14]. We then get

$$\mathbf{H} = \mathbf{H}_{J=\infty} := \mathbf{H}_w, \quad (2.11)$$

which is the i.i.d. (spatially white) channel.

The non-physical MIMO channel  $\mathbf{H}_w$  can be restricted to SIMO and MISO channels by dropping either columns or rows respectively. The respectively resulting vector channels are  $\mathbf{h}_w$  with dimension  $M \times 1$  for SIMO and  $\mathbf{h}_w^T$  with dimension  $1 \times N$  for MISO.

So far we have considered only Rayleigh fading in describing the wireless channels. In order to simulate a wireless channel with different degrees of scattering richness, we introduce the well-known *Ricean* model. In such the mode, there are an LOS component between the transmitter and receiver. The MIMO channel may be modeled approximately as the sum of a “deterministic (or specular)” component and a “variable (or scattered)” component:

- **Specular Component:** Illuminates the entire array and is thus spatially deterministic from antenna to antenna.
- **Scattered Component:** It is Rayleigh distributed and varies randomly from antenna to antenna.

Notice that the Ricean model implicitly assumes that the scattering terms on different antennas are fully uncorrelated and that, therefore, the only source of correlation among the array antenna is the deterministic component. With the Ricean  $\mathcal{K}$ -factor defined as the ratio of deterministic-to-scattered power, the channel response is given by [12]

$$\mathbf{H} := \sqrt{\frac{\mathcal{K}}{\mathcal{K} + 1}} \mathbf{H}_{sp} + \sqrt{\frac{1}{\mathcal{K} + 1}} \mathbf{H}_{sc} \in \mathbb{C}^{M \times N}, \quad (2.12)$$

where

$$\mathbf{H}_{sp} := \mathbf{a}_R(\theta^R) \mathbf{a}_T(\theta^T) \in \mathbb{C}^{M \times N}, \quad (2.13)$$

is the specular component, which can be obtained from (2.10) by setting “ $J = 1$ ” and  $\alpha_1 = 1$  as  $\mathbf{H}_{J=1}$ , and  $\mathbf{H}_{sc} := \mathbf{H}_w$  is the scattered component given in (2.11), i.e., “ $J \approx \infty$ ” in (2.10). Note that in (2.12), the Ricean  $\mathcal{K}$ -factor “ $\mathcal{K} = 0$ ” corresponds to a pure scattering channel (Rayleigh fading), while “ $\mathcal{K} = \infty$ ” corresponds to a pure specular channel (non-fading). Again, the MISO and SIMO channels can be easily obtained from (2.12) by dropping either columns or rows, respectively. Specifically, the specular channel response can be rewritten in a general form as

$$\mathbf{H} := \mathbf{h}_R \mathbf{h}_T^T = \alpha_R \mathbf{a}_R(\theta^R) \cdot \alpha_T \mathbf{a}_T^T(\theta^T) \in \mathbb{C}^{M \times N}, \quad (2.14)$$

which is a “keyhole” channel [13], where  $\mathbf{h}_R := \alpha_R \mathbf{a}_R(\theta^R) \in \mathbb{C}^M$  and  $\mathbf{h}_T := \alpha_T \mathbf{a}_T(\theta^T) \in \mathbb{C}^N$  are the channel vector from the keyhole to the receive antenna array and the channel vector from the transmit antenna array to the keyhole, with  $\alpha_R$  and  $\alpha_T$  being the fading gains assumed to be i.i.d. complex Gaussian with zero-mean and unit-variance. The envelope of each element of  $\mathbf{H}$  in (2.14) is double Rayleigh distributed and  $\text{rank}(\mathbf{H}) = 1$  [13].

### 2.2.3 MIMO Sampled Signal Model

This section presents the MIMO sampled (discrete time) signal model in conjunction with TDMA systems over the frequency selective and frequency flat fading channels. We directly express the discrete time received signal model, in baseband form, from the continuous time relation described in Section 2.2.1.

**Remark:** For TDMA systems, we assume that the channel bandwidth is  $B_c = 1$  Hz and the symbol period is  $T = 1$  second. We also assume in the SISO and SIMO cases that the average transmit symbol energy is  $E_s$ . Since  $T = 1$  second,  $E_s$  is thus also the transmit power  $P_T$ . As a result, we shall refer to  $P_T$  in conjunction with TDMA systems interchangeably as energy or power throughout this thesis. For MISO or MIMO channels, we assume that the average total transmit power per symbol period is constant and therefore the symbol power per antenna is reduced by the number of transmit antennas  $N$ , i.e., the average total transmit power per symbol per antenna is  $P_T/N$ . On the other hand, assume that the AWGN is modeled as independent circularly symmetric complex Gaussian random variable with zero-mean and variance  $\sigma_v^2$ . Due to  $B_c = 1$  Hz, the noise power  $\sigma_v^2$  in the band is the same as spectral power density  $N_0$ . As a result, we interchangeably refer to  $\sigma_v^2$  as noise power or noise spectral density.

Consider a MIMO system with  $N$  transmit antennas and  $M$  receive antennas. In to order to facilitate discrete time processing, the received signal of dimension  $M \times 1$  (discrete time version of (2.2)) is sampled with symbol rate at  $t = t_0 + kT$ ,  $k = 0, 1, \dots$ , to yield

$$\begin{aligned} \mathbf{y}(k) &= \sqrt{\frac{P_T}{N}} \sum_{n=1}^N \mathbf{H}_n \mathbf{x}_n(k) + \mathbf{v}(k) \\ &= \sqrt{\frac{P_T}{N}} \mathbf{H} \mathbf{x}(k) + \mathbf{v}(k), \end{aligned} \quad (2.15)$$

where

$$\begin{aligned} \mathbf{H} &:= [\mathbf{H}_1, \mathbf{H}_2, \dots, \mathbf{H}_N] \\ &:= [\mathbf{H}(0), \mathbf{H}(1), \dots, \mathbf{H}(L)] \in \mathbb{C}^{M \times N(L+1)}, \end{aligned} \quad (2.16)$$

is the discrete time MIMO space-only (SO) channel matrix with

$$\mathbf{H}_n := [\mathbf{h}_n(0), \mathbf{h}_n(1), \dots, \mathbf{h}_n(L)] \in \mathbb{C}^{M \times (L+1)}, \quad n = 1, 2, \dots, N, \quad (2.17)$$

being the SO channel matrix associated with the  $n$ th transmit antenna, and

$$\mathbf{H}(l) := \begin{bmatrix} h_{1,1}(l) & h_{1,2}(l) & \dots & h_{1,N}(l) \\ h_{2,1}(l) & h_{2,2}(l) & \dots & h_{2,N}(l) \\ \vdots & \vdots & \ddots & \vdots \\ h_{M,1}(l) & h_{M,2}(l) & \dots & h_{M,N}(l) \end{bmatrix} \in \mathbb{C}^{M \times N}, \quad l = 0, 1, \dots, L, \quad (2.18)$$

being the  $l$ th symbol sampled MIMO channel matrix.  $L$  is the channel order (in symbols) assumed to be the same for all  $n$ , and  $\mathbf{h}_n(l) \in \mathbb{C}^M$ ,  $l = 0, 1, \dots, L$ , is the SO symbol response channel vectors. In (2.15),

$$\mathbf{x}_n(k) := [x_n(k), x_n(k-1), \dots, x_n(k-L)]^T \in \mathbb{C}^{(L+1)}, \quad (2.19)$$

is the symbol sequence vector from the  $n$ th transmit antenna, and

$$\mathbf{x}(k) := [x_1(k), x_2(k), \dots, x_N(k), x_1(k-1), x_2(k-1), \dots, x_N(k-1), \dots, x_1(k-L+1), x_2(k-L+1), \dots, x_N(k-L+1)]^T \in \mathbb{C}^{N(L+1)}, \quad (2.20)$$

is the transmitted symbol vector over  $N$  antennas. Finally,  $\mathbf{v}(k)$  is the noise vector having the same structure as  $\mathbf{y}(k)$ .

The  $K$  contiguous samples of the received signal can be stacked and written as an  $MK \times 1$  ST signal vector

$$\begin{aligned} \mathbf{y}_c(k) &:= [\mathbf{y}^T(k), \mathbf{y}^T(k-1), \dots, \mathbf{y}^T(k-K+1)]^T \\ &= \sqrt{\frac{P_T}{N}} \sum_{n=1}^N \mathbf{H}_{c,n} \mathbf{x}_{c,n}(k) + \mathbf{v}_c(k) \\ &= \sqrt{\frac{P_T}{N}} \mathbf{H}_c \mathbf{x}_c(k) + \mathbf{v}_c(k), \end{aligned} \quad (2.21)$$

where  $\mathbf{v}_c(k)$  is the noise vector having the same structure as  $\mathbf{y}_c(k)$ ,

$$\mathbf{H}_{c,n} := \begin{bmatrix} \mathbf{h}_n(0) & \mathbf{h}_n(1) & \cdots & \mathbf{h}_n(L) & \mathbf{0} & \cdots & \mathbf{0} \\ \mathbf{0} & \mathbf{h}_n(0) & \mathbf{h}_n(1) & \cdots & \mathbf{h}_n(L) & \cdots & \vdots \\ \vdots & \vdots & \ddots & \ddots & \ddots & \ddots & \mathbf{0} \\ \mathbf{0} & \cdots & \mathbf{0} & \mathbf{h}_n(0) & \mathbf{h}_n(1) & \cdots & \mathbf{h}_n(L) \end{bmatrix} \in \mathbb{C}^{MK \times (L+K)}, \quad (2.22)$$

is the ST block Toeplitz channel matrix associated with the  $n$ th transmit antenna, for  $n = 1, 2, \dots, N$ ,

$$\mathbf{H}_c := \begin{bmatrix} \mathbf{H}(0) & \mathbf{H}(1) & \cdots & \mathbf{H}(L) & \mathbf{O} & \cdots & \mathbf{O} \\ \mathbf{O} & \mathbf{H}(0) & \mathbf{H}(1) & \cdots & \mathbf{H}(L) & \cdots & \mathbf{O} \\ \vdots & \vdots & \ddots & \ddots & \ddots & \ddots & \vdots \\ \mathbf{O} & \cdots & \mathbf{O} & \mathbf{H}(0) & \mathbf{H}(1) & \cdots & \mathbf{H}(L) \end{bmatrix} \in \mathbb{C}^{MK \times N(L+K)}, \quad (2.23)$$

is the discrete time (MIMO) ST block Toeplitz channel matrix over  $N$  transmit antennas and

$$\mathbf{x}_{c,n}(k) := [x_n(k), x_n(k-1), \dots, x_n(k-L-K+1)]^T \in \mathbb{C}^{L+K}, \quad (2.24)$$

$$\mathbf{x}_c(k) := [\mathbf{x}(k), \mathbf{x}(k-1), \dots, \mathbf{x}(k-L-K+1)]^T \in \mathbb{C}^{N(L+K)}. \quad (2.25)$$

with  $\mathbf{x}(k)$  being defined as (2.20).

For a frequency flat channel,  $\mathbf{H}(l) = \mathbf{0}$  for  $l \neq 0$  and denoting  $\mathbf{H}(0)$  by

$$\mathbf{H} := \begin{bmatrix} h_{1,1} & h_{1,2} & \cdots & h_{1,N} \\ h_{2,1} & h_{2,2} & \cdots & h_{2,N} \\ \vdots & \vdots & \ddots & \vdots \\ h_{M,1} & h_{M,2} & \cdots & h_{M,N} \end{bmatrix} \in \mathbb{C}^{M \times N}, \quad (2.26)$$

the MIMO (SO) sampled signal model can be simplified to an  $M \times 1$  vector

$$\mathbf{y}(k) = \sqrt{\frac{P_T}{N}} \mathbf{H} \mathbf{x}(k) + \mathbf{v}(k), \quad (2.27)$$

where

$$\mathbf{x}(k) := [x_1(k), x_2(k), \dots, x_N(k)]^T \in \mathbb{C}^N. \quad (2.28)$$

## 2.2.4 MU MIMO Sampled Signal Model

So far we have only considered MIMO systems for a single user model (one transmitter and one receiver) with multiple antennas at either or both ends. These models can be extended to MU MIMO channels. In the multiple access channel, assume that  $N$  transmit antennas are located at each of  $Q$  active users and  $M$  receive antennas are placed at the base station. Here we only show the frequency flat channels. Extensions to frequency selective channels are readily possible. In such a system, the  $M \times 1$  received signal vector can be expressed as

$$\begin{aligned} \mathbf{y}(k) &= \sum_{q=1}^Q \sqrt{\frac{P_q}{N}} \mathbf{H}_q \mathbf{x}_q(k) + \mathbf{v}(k) \\ &= \mathbf{H} \mathbf{x}(k) + \mathbf{v}(k), \end{aligned} \quad (2.29)$$

where  $P_q$  is the transmit power of the  $q$ th user,

$$\mathbf{H} := \left[ \sqrt{\frac{P_1}{N}} \mathbf{H}_1, \sqrt{\frac{P_2}{N}} \mathbf{H}_2, \dots, \sqrt{\frac{P_Q}{N}} \mathbf{H}_Q \right] \in \mathbb{C}^{M \times QN}, \quad (2.30)$$

is the MU SO MIMO channel matrix with  $\mathbf{H}_q$  having the same structure as (2.26) and

$$\mathbf{x}(k) := [\mathbf{x}_1^T(k), \mathbf{x}_2^T(k), \dots, \mathbf{x}_Q^T(k)]^T \in \mathbb{C}^{QN}. \quad (2.31)$$

with  $\mathbf{x}_q(k)$  having the same structure as (2.28).

## 2.3 Channel Capacity

This section studies the fundamental limit on the SE that can be supported reliably in ST wireless channels. We discuss the capacity of ST channels for the cases: channel unknown and channel known to the transmitter (perfect channel knowledge at the receiver is always assumed), both over the frequency flat channels. We first introduce the SISO channel capacity and then study the capacity of a MIMO channel and note that SIMO and MISO channels are sub-sets of the MIMO case.



The maximum information rate that can be used causing negligible probability of errors at the channel output is called the “channel capacity”. The channel capacity for AWGN channels was first derived by C. Shannon in 1948 [92]. With a band-limited channel, the capacity is measured in information bits per second. It is common to represent the channel capacity within a unit bandwidth of the channel. The channel capacity is then measured in bits/sec/Hz (or bps/Hz).

It is desirable to design transmission schemes that exploit the channel capacity as much as possible. Representing the input and output of a memoryless (frequency flat) channel with the random variables  $X$  and  $Y$  respectively, the channel capacity is defined as [93]

$$C := \max_{p(x)} \mathcal{I}(X;Y), \quad (2.32)$$

where

$$\mathcal{I}(X;Y) := \mathcal{H}(Y) - \mathcal{H}(Y|X), \quad (2.33)$$

is the *mutual information* between  $X$  and  $Y$ , with  $\mathcal{H}(Y)$  and  $\mathcal{H}(Y|X)$  being the differential entropy of  $Y$  and differential conditional entropy of  $Y$  with knowledge of  $X$  given, respectively [93]. The entropy of a random variable can be described as a measure of the uncertainty of the random variable. In (2.32), it states that the mutual information is maximized with respect to all possible transmitter statistical distributions  $p(x)$ .

### 2.3.1 Channel Unknown to The Transmitter

#### SISO Channel Capacity

For a SISO system, the *ergodic (mean) capacity* of a random channel can be expressed as [93]

$$C := E \left\{ \max_{p(x):P=1} \mathcal{I}(X;Y) \right\}, \quad (2.34)$$

where  $P := E \{|x(k)|^2\}$  is the power of a symbol transmitted over the channel and  $E\{\cdot\}$  denotes the expectation over all channel realizations. The capacity defined in (2.34) is

the maximum of the mutual information between the input and output over all statistical distributions on the input symbol that satisfy the power constraint. From (2.34), the ergodic capacity of a SISO system with a random complex channel gain  $h$  is given by [9], [10]

$$C = E \left\{ \log_2 \left( 1 + \frac{P_T}{\sigma_v^2} |h|^2 \right) \right\} = E \left\{ \log_2 (1 + \rho |h|^2) \right\}, \quad (2.35)$$

where  $\rho := \frac{P_T}{\sigma_v^2}$  is the average SNR at the receiver branch [6], [62], [65], [68]. Assuming that the channel gain is one, i.e.,  $h = 1$  yields

$$C = \log_2 (1 + \rho). \quad (2.36)$$

### MIMO Channel Capacity

Consider a MIMO system with  $N$  transmit antennas and  $M$  receive antennas (see (2.27)).

The capacity of random MIMO channel can be expressed as [9]

$$C := E \left\{ \max_{p(\mathbf{x}): \text{tr}(\mathbf{R}_{xx})=N} \mathcal{I}(\mathbf{x}; \mathbf{y}) \right\}, \quad (2.37)$$

where  $\mathbf{R}_{xx} := E \left\{ \mathbf{x}(k) \mathbf{x}^H(k) \right\}$  is the covariance matrix of the transmitted symbol vector  $\mathbf{x}(k)$  given in (2.28). With a MIMO channel used, the mutual information between  $\mathbf{x}(k)$  and  $\mathbf{y}(k)$  in (2.37) can be given as [9]

$$\mathcal{I}(\mathbf{x}; \mathbf{y}) := E \left\{ \log_2 \left[ \det \left( \mathbf{I}_M + \frac{P_T}{\sigma_v^2 N} \mathbf{H} \mathbf{R}_{xx} \mathbf{H}^H \right) \right] \right\}. \quad (2.38)$$

Substituting (2.38) into (2.37), we have

$$C = \max_{\text{tr}(\mathbf{R}_{xx}) \leq N} E \left\{ \log_2 \left[ \det \left( \mathbf{I}_M + \frac{P_T}{\sigma_v^2 N} \mathbf{H} \mathbf{R}_{xx} \mathbf{H}^H \right) \right] \right\}. \quad (2.39)$$

Note that the total transmit power is limited to  $P_T$ , irrespective of the number of transmit antennas. Assume that the transmitted symbol vector  $\mathbf{x}(k)$  is independent of noise  $\mathbf{v}(k)$  and the noise is uncorrelated in each receive branch (spatially white). When the channel knowledge is unknown to the transmitter, it is optimal to use a “uniform” power distribution [9]. The covariance matrix of  $\mathbf{x}(k)$  is then given by  $\mathbf{R}_{xx} = \mathbf{I}_N$ , which implies that the

transmitted symbol  $x(k)$  is an *i.i.d.* random variable with zero-mean and unit-variance. As a result, the ergodic capacity for a spatially white MIMO channel can be written as [9], [10]

$$C = E \left\{ \log_2 \left[ \det \left( \mathbf{I}_M + \frac{P_T}{\sigma_v^2 N} \mathbf{H} \mathbf{H}^H \right) \right] \right\} = E \left\{ \log_2 \left[ \det \left( \mathbf{I}_M + \frac{\rho}{N} \mathbf{H} \mathbf{H}^H \right) \right] \right\}, \quad (2.40)$$

where  $\mathbf{H}$  is the MIMO channel matrix given in (2.26) and  $\rho := \frac{P_T}{\sigma_v^2}$  is the average SNR at each receiver branch. Consider a MIMO channel with  $M = N$  and  $\mathbf{H} = \mathbf{H}_w$ . Using the strong law of large numbers, we have the result

$$\frac{1}{N} \mathbf{H} \mathbf{H}^H \xrightarrow{N \rightarrow \infty} \mathbf{I}_N, \quad (2.41)$$

Therefore, the capacity of this channel in the absence of channel knowledge at the transmitter approaches

$$C \rightarrow M \cdot \log_2(1 + \rho). \quad (2.42)$$

Asymptotically (in  $N$ ), the capacity of a spatially white MIMO channel thus becomes deterministic and increases “linearly” with  $N$  for a fixed SNR. From (2.42), we can also see that for every 3 dB increase in SNR we get  $N$  bps/Hz increase in capacity for a MIMO channel (compared with 1 bps/Hz for a SISO channel (see (2.36))).

By using the eigenvalue decomposition, the matrix product of  $\mathbf{H} \mathbf{H}^H$  can be decomposed as  $\mathbf{H} \mathbf{H}^H = \mathbf{E} \mathbf{\Lambda} \mathbf{E}^H$ , where  $\mathbf{E}$  is an  $M \times M$  matrix which consists of the eigenvectors satisfying  $\mathbf{E} \mathbf{E}^H = \mathbf{E}^H \mathbf{E} = \mathbf{I}_M$  and  $\mathbf{\Lambda} = \text{diag}\{\lambda_1, \lambda_2, \dots, \lambda_M\}$  is a diagonal matrix with the eigenvalues  $\lambda_i \geq 0$  on the main diagonal. Assuming that the eigenvalues  $\lambda_i$ 's are ordered so that  $\lambda_i \geq \lambda_{i+1}$ , then we have  $\lambda_i = 0$  if  $r + 1 \leq i \leq M$ , where

$$r := \text{rank}(\mathbf{H}) \leq \min\{N, M\}. \quad (2.43)$$

Then the capacity of a MIMO channel can hence be rewritten as

$$\begin{aligned} C &= E \left\{ \log_2 \left[ \det \left( \mathbf{I}_M + \frac{\rho}{N} \mathbf{E} \mathbf{\Lambda} \mathbf{E}^H \right) \right] \right\} = E \left\{ \log_2 \left[ \det \left( \mathbf{I}_M + \frac{\rho}{N} \mathbf{\Lambda} \right) \right] \right\} \\ &= \sum_{i=1}^r E \left\{ \log_2 \left( 1 + \frac{\rho}{N} \lambda_i \right) \right\}. \end{aligned} \quad (2.44)$$

In (2.44), the second equation holds due to the fact  $\det(\mathbf{I}_m + \mathbf{A}\mathbf{B}) = \det(\mathbf{I}_n + \mathbf{B}\mathbf{A})$  for matrices  $\mathbf{A} \in \mathbb{C}^{m \times n}$  and  $\mathbf{B} \in \mathbb{C}^{n \times m}$  and  $\mathbf{E}^H \mathbf{E} = \mathbf{I}_m$ . Equation (2.44) shows that the capacity of a MIMO channel is made up by sum of capacities of  $r$  parallel SISO sub-channels with power gains  $\lambda_i$ ,  $i = 1, 2, \dots, r$ , and transmit power  $P_T/N$  individually as shown in Figure 2.1.

The capacities of SIMO and MISO channels, which are special cases of a MIMO channel, can be evaluated using (2.44). For a SIMO channel, the channel matrix can be simplified to an  $M \times 1$  vector  $\mathbf{h} = [h_1, h_2, \dots, h_M]^T$  such that  $r = 1$  and  $\lambda_1 = \|\mathbf{h}\|^2$ . As a result, the capacity of the SIMO channel is given by

$$C = E \left\{ \log_2 \left( 1 + \rho \|\mathbf{h}\|^2 \right) \right\}. \quad (2.45)$$

Assume that the channel gain is one, i.e.,  $|h_m|^2 = 1$ ,  $m = 1, 2, \dots, M$ , so that  $\|\mathbf{h}\|^2 = M$ . The channel capacity in (2.45) can be reduced to

$$C = \log_2 (1 + M \cdot \gamma). \quad (2.46)$$

This implies that an increment of receive antennas yields only “logarithmic” increment in capacity over SIMO channels.

For a MISO channel, similarly to the SIMO case, in the absence of channel knowledge at the transmitter, the capacity of MISO channel is given by

$$C = E \left\{ \log_2 \left( 1 + \frac{\rho}{N} \|\mathbf{h}\|^2 \right) \right\}, \quad (2.47)$$

where  $\mathbf{h} = [h_1, h_2, \dots, h_N]^T$  is the  $N \times 1$  channel vector. Again, if the channel gain is one, then we have

$$C = \log_2 (1 + \rho). \quad (2.48)$$

This shows that there is “no improvement” in capacity over a SISO channel. Making a comparison between (2.45) and (2.47) obviously shows that the capacities of MISO channels are less than those of SIMO channels when the channel is unknown to the transmitter for the same value  $\|\mathbf{h}\|^2$ . This is because that the transmitter in MISO channels fails to exploit transmitter array gain when the channel is unknown previously.

### 2.3.2 Channel Known to The Transmitter

In absence of channel knowledge, the individual channel modes are not accessible and that equal transmit power is allocated to each spatial data pipe. Furthermore, if the channel knowledge is known to the transmitter, from (2.44), the capacity of a MIMO channel is the sum of the capacities associated with the parallel SISO channels and is given by

$$C = \sum_{i=1}^r E \left\{ \log_2 \left( 1 + P_i \frac{\rho}{N} \lambda_i \right) \right\}, \quad (2.49)$$

where  $P_i := E \{|x_i|^2\}$ ,  $i = 1, 2, \dots, r$ , is the transmit power in the  $i$ th sub-channel and satisfies that

$$\sum_{i=1}^r P_i = N. \quad (2.50)$$

Because that the transmitter can access the spatial sub-channels, it can allocate variable power across the sub-channels to maximize the mutual information. The mutual information maximization problem now becomes [9]

$$C := \max_{\sum_{i=1}^r P_i = N} \sum_{i=1}^r E \left\{ \log_2 \left( 1 + P_i \frac{\rho}{N} \lambda_i \right) \right\}, \quad (2.51)$$

whose solution can be obtained by using the Lagrangian methods [93]. The optimal power allocation of the  $i$ th sub-channel,  $P_i^o$ , is given by [9], [93]

$$P_i^o := \left( \mu - \frac{N}{\rho \lambda_i} \right)_+, \quad i = 1, 2, \dots, r, \quad (2.52)$$

where  $\mu$  is a constant chosen to satisfy the power constraint (2.50) and  $(x)_+$  denotes

$$(x)_+ := \begin{cases} x & x \geq 0 \\ 0 & x < 0 \end{cases}. \quad (2.53)$$

The optimal power allocation in (2.52) is found iteratively through the “waterfilling” algorithm [9], [14], [93], and this is shown in Figure 2.2.

For a MISO channel, when the transmitter knows the channel information, all power can be directly imposed into the single spatial mode (i.e., use the waterfilling algorithm). As a result, from (2.47), the capacity of the MISO channel in this case can be expressed as

$$C = E \left\{ \log_2 \left( 1 + \rho \|\mathbf{h}\|^2 \right) \right\}. \quad (2.54)$$

This indicates that the capacity of a MISO channel is the same as that of a SIMO channel for the same value  $\|\mathbf{h}\|^2$ . As in SIMO channels, MISO channels offer only a logarithmic increment in capacity with the number of antennas.

### 2.3.3 Outage Capacity

The ergodic (mean) capacity described in Section 2.3.1 and Section 2.3.2 defined is defined as the average of the maximal value of the mutual information between the transmitted symbol and received signal, where the maximization was carried out with respect to all possible transmitter statistical distributions. Another measure of channel capacity that is frequently used is the *outage capacity*. With outage capacity, the channel capacity is associated to an outage probability. If the channel capacity falls below the outage capacity, there is no possibility that the transmitted symbol can be decoded with no errors.

Outage analysis quantifies the level of performance (i.e., capacity) that is guaranteed with a certain level of reliability. Define the  $q\%$  outage capacity  $C_{out,q}$  as the information rate that is guaranteed for  $(100 - q)\%$  of the channel realizations [9], that is,

$$Prob(C \leq C_{out,q}) = q\%. \quad (2.55)$$

In this case, (2.55) represents an upper bound due to the fact that there is a finite probability  $q$  that the channel capacity is *less* than the outage capacity.

**Example 2.3.1:** Figure 2.3 (a) and (b) respectively show the ergodic capacity and 10% outage capacity of several antenna configurations as a function of SNR  $\rho$ . As expected, the ergodic/outage capacity increases with increasing  $\rho$  and also with  $N$  and  $M$ . From Figure 2.3 (a) and (b), we can see that the ergodic/outage capacity of a MIMO channel is much greater than the others. Note that the ergodic capacity of a SIMO channel is larger than that of a MISO channel as the channel is unknown to the transmitter, which follows from (2.45) and (2.47) for the capacity of SIMO and MISO channels respectively, where SIMO outperforms MISO.

**Example 2.3.2:** Figure 2.4 shows the complementary cumulative distribution function (ccdf) capacity of several antenna configurations at SNR  $\rho = 10$  dB. Again, as observed, the capacity of a MIMO channel is much larger than the others, and the capacity of a SIMO channel is greater than that of MISO channel as the channel knowledge is not available at the transmitter, which consists with the results in Figure 2.3. However, as the channel knowledge is available at the transmitter, the capacity of a SIMO channel can equal to that of a SIMO channel. This shows that under the same antenna configuration, the capacity of that has the channel knowledge at the transmitter can larger than that without channel knowledge at the transmitter. Moreover, compared with Figure 2.3 (a), we find that the ergodic capacity is the mean information rate and may equal to the median information rate (50 percentile). On the other hand, the 90 percentile ccdf capacity will be the 10% outage capacity shown in Figure 2.3(b).

## 2.4 Space-Time Block Coding

As mentioned in Section 1.2.2, when the number of antennas is fixed, the decoding complexity of STTCs increases exponentially as a function of the diversity level and transmission rate [49]. In addressing the issue of decoding complexity, we will mainly focus on the STBC techniques due to its very simple coding structure and linear processing for ML decoding at the receiver. In what follows, we first give a general framework for linear STBCs over a frequency flat fading channels. Then we introduce the orthogonal designs of the STBCs and ML detection of such the orthogonal based STBCs (O-STBCs). Finally we discuss the performance of the O-STBCs.

### 2.4.1 General Framework for Linear STBC

Consider the MIMO sampled signal model (2.27). The data stream  $s(k)$ , in general complex-valued, is divided into blocks of  $L$  consecutive symbols to obtain  $s_l(k) := s(Lk +$

$l - 1)$ ,  $l = 1, 2, \dots, L$ , is encoded over successive  $K$  symbol periods to form the  $N \times K$  ST codeword [4], [62], [65]. The  $L \times 1$  input symbol vector to ST encoder is thus given by

$$\mathbf{s}(k) := [s_1(k), s_2(k), \dots, s_L(k)]^T \in \mathbb{C}^L, \quad (2.56)$$

and the  $N \times K$  output matrix of ST encoder (or called the codeword matrix) is given by

$$\begin{aligned} \mathbf{X}(k) &:= \begin{bmatrix} x_1(k) & x_1(k+1) & \dots & x_1(k+K-1) \\ x_2(k) & x_2(k+1) & \dots & x_2(k+K-1) \\ \vdots & \vdots & \ddots & \vdots \\ x_N(k) & x_N(k+1) & \dots & x_N(k+K-1) \end{bmatrix} \\ &= \sum_{l=1}^{2L} \mathbf{A}_l \tilde{s}_l(k), \end{aligned} \quad (2.57)$$

where  $\mathbf{A}_l \in \mathbb{C}^{N \times K}$  is the ST “modulation matrix” [65],  $\tilde{s}_l(k) := \text{Re}\{s_l(k)\}$  for  $l = 1, 2, \dots, L$  and  $\tilde{s}_l(k) := \text{Im}\{s_{l-L}(k)\}$  for  $l = L+1, L+2, \dots, 2L$ , i.e.,  $s_l(k) := \tilde{s}_l(k) + j\tilde{s}_{l+L}(k)$ . Therefore,  $\mathbf{s}(k)$  is used to construct the ST codeword  $\mathbf{X}(k)$  according to some specific designs. Since the total  $L$  symbols are transmitted over  $K$  symbol periods, the code rate of linear STBC is

$$\mathbf{s}(k) \mapsto \mathbf{X}(k) : \quad R := \frac{L}{K} \leq 1. \quad (2.58)$$

Note that the variance of  $\tilde{s}_l(k)$  is  $E\{|\tilde{s}_l(k)|^2\} = 1/2$  regardless of symbol constellations. Also notice that the complex-valued modulation matrices  $\{\mathbf{A}_l\}_{l=1}^L$  are used to spread the input information symbol over  $NK$  spatial-temporal dimensions. The real and imaginary part of each input symbol  $s_l(k)$  is modulated separately with the matrices  $\mathbf{A}_l$  and  $\mathbf{A}_{l+L}$ . In particular, splitting the source symbols into the real and imaginary parts will also *unify both the problem formulation and the underlying analysis, regardless of the symbol constellations*. Collecting  $\mathbf{y}(k)$  over  $K$  symbol periods at the receiver yields the  $M \times K$  ST signal model

$$\mathbf{Y}(k) := [\mathbf{y}(k), \mathbf{y}(k+1), \dots, \mathbf{y}(k+K-1)] = \sqrt{\frac{P_T}{N}} \mathbf{H} \mathbf{X}(k) + \mathbf{V}(k), \quad (2.59)$$

where  $\mathbf{H}$  is the  $M \times N$  MIMO channel matrix defined in (2.26), and  $\mathbf{V}$  is the noise matrix having the same structure of  $\mathbf{Y}(k)$ .



To meet the total transmit power constraint, the ST modulation matrix must satisfy [62], [65]

$$\|\mathbf{A}_l\|_F^2 := \text{tr}(\mathbf{A}_l \mathbf{A}_l^H) = \frac{NK}{L}, \quad l = 1, 2, \dots, 2L, \quad (2.60)$$

such that

$$E \{ \text{tr}(\mathbf{X}(k) \mathbf{X}^H(k)) \} = NK. \quad (2.61)$$

To facilitate the detection process and further analysis, it is common to rely on an associated equivalent “vectorized” linear model [62], [65]. Specifically, let us split each received signal vector  $\mathbf{y}(k+i)$ ,  $i = 0, 1, \dots, K-1$ , and the transmitted symbol block  $\mathbf{s}(k)$  into the respective real and imaginary parts to obtain

$$\tilde{\mathbf{y}}(k+i) := [\text{Re}\{\mathbf{y}^T(k+i)\} \text{Im}\{\mathbf{y}^T(k+i)\}]^T \in \mathbb{R}^{2M}, \quad (2.62)$$

and

$$\tilde{\mathbf{s}}(k) := [\text{Re}\{\mathbf{s}^T(k)\} \text{Im}\{\mathbf{s}^T(k)\}]^T \in \mathbb{R}^{2L}. \quad (2.63)$$

Associate with the MIMO channel matrix  $\mathbf{H}$ , we form the following augmented matrix

$$\tilde{\mathbf{H}} := \mathbf{I}_K \otimes \tilde{\mathbf{H}} \in \mathbb{R}^{2KM \times 2KN}, \quad (2.64)$$

where

$$\tilde{\mathbf{H}} := \begin{bmatrix} \text{Re}\{\mathbf{H}\} & -\text{Im}\{\mathbf{H}\} \\ \text{Im}\{\mathbf{H}\} & \text{Re}\{\mathbf{H}\} \end{bmatrix} \in \mathbb{R}^{2M \times 2N}, \quad (2.65)$$

and the notation  $\otimes$  stands for the Kronecker product. Also, define the matrix

$$\bar{\mathbf{A}} := \begin{bmatrix} \tilde{\mathbf{a}}_1^{(1)} & \tilde{\mathbf{a}}_2^{(1)} & \dots & \tilde{\mathbf{a}}_{2L}^{(1)} \\ \tilde{\mathbf{a}}_1^{(2)} & \tilde{\mathbf{a}}_2^{(2)} & \dots & \tilde{\mathbf{a}}_{2L}^{(2)} \\ \vdots & \vdots & \ddots & \vdots \\ \tilde{\mathbf{a}}_1^{(K)} & \tilde{\mathbf{a}}_2^{(K)} & \dots & \tilde{\mathbf{a}}_{2L}^{(K)} \end{bmatrix} \in \mathbb{R}^{2KN \times 2L}, \quad (2.66)$$

where

$$\tilde{\mathbf{a}}_l^{(k)} := \left[ \operatorname{Re} \left\{ \mathbf{a}_l^{(k)} \right\}^T \operatorname{Im} \left\{ \mathbf{a}_l^{(k)} \right\}^T \right]^T \in \mathbb{R}^{2N}, \quad k = 1, 2, \dots, K, \quad (2.67)$$

with  $\mathbf{a}_l^{(k)} \in \mathbb{C}^N$  denoting the  $k$ th column of the matrix  $\mathbf{A}_l$ . Then the “complex-valued matrix” signal model (2.59) can be rewritten, after some manipulations, as the following  $2KM \times 1$  “real-valued vectorized” signal model

$$\mathbf{y}_c(k) := \left[ \tilde{\mathbf{y}}^T(k), \tilde{\mathbf{y}}^T(k+1), \dots, \tilde{\mathbf{y}}^T(k+K-1) \right]^T = \sqrt{\frac{P_T}{N}} \mathbf{H}_c \tilde{\mathbf{s}}(k) + \mathbf{v}_c(k), \quad (2.68)$$

where

$$\mathbf{H}_c := \bar{\mathbf{H}} \bar{\mathbf{A}} \in \mathbb{R}^{2KM \times 2L}, \quad (2.69)$$

is the equivalent concatenated MIMO channel matrix induced by the ST codeword  $\mathbf{X}(k)$  (essentially, the modulation matrices  $\{\mathbf{A}_l\}$ ), and  $\mathbf{v}_c(k)$  is the corresponding noise vector having the structure of  $\mathbf{y}_c(k)$ .

To detect all transmitted symbols based on (2.68), it is typical to further reduce the dimension of the observed signal vector  $\mathbf{y}_c(k)$  through proper linear combination of its entries (ST linear combining). More precisely, this is done by multiplying both sides of (2.68) from the left by  $\mathbf{H}_c^T$  to yield the  $2L \times 1$  “matched-filter (MF)” signal vector

$$\mathbf{z}(k) := \mathbf{H}_c^T \mathbf{y}_c(k) = \sqrt{\frac{P_T}{N}} \mathbf{F} \tilde{\mathbf{s}}(k) + \mathbf{v}(k), \quad (2.70)$$

where

$$\mathbf{F} := \mathbf{H}_c^T \mathbf{H}_c \in \mathbb{R}^{2L \times 2L}, \quad (2.71)$$

is the matched-filtered channel matrix (MFCM) and  $\mathbf{v}(k) := \mathbf{H}_c^T \mathbf{v}_c(k)$ . Based on the MF signal vector  $\mathbf{z}(k)$ , we can detect the unknown symbols over an observation space of a relatively small dimension. We will hereafter rely on the filtered model (2.70) for detection.

## MU Framework

Consider a  $Q$ -user STBC system with each user terminal comprising  $N$  transmit antennas. Collecting  $\mathbf{y}(k)$  over  $K$  successive symbol periods, we have the following ST signal model (assuming that the  $Q$  users are symbol synchronized<sup>1</sup>)

$$\mathbf{Y}(k) := [\mathbf{y}(k), \mathbf{y}(k+1), \dots, \mathbf{y}(k+K-1)] = \sum_{q=1}^Q \sqrt{\frac{P_q}{N}} \mathbf{H}_q \mathbf{X}_q(k) + \mathbf{V}(k), \quad (2.72)$$

where  $P_q$  is the total transmit power of the  $q$ th user terminal,  $\mathbf{H}_q \in \mathbb{C}^{M \times N}$  is the channel matrix from the  $q$ th user terminal to the receiver, which is assumed to be static during the  $K$  signaling periods,  $\mathbf{X}_q(k)$  is the ST codeword matrix of the  $q$ th user having the same structure as (2.57), and  $\mathbf{V}(k) \in \mathbb{C}^{M \times K}$  is the channel noise.

### • Equivalent Vectorized Signal Model

We note that in the MU scenario the signal part in the matrix signal model (2.72) is a linear mixture of the  $Q$  codeword matrices. Toward a compatible MU detection framework, it is common to work with an associated equivalent vectorized linear model that will “restore” each user’s symbol block. Specifically, let  $\mathbf{s}_q(k) := [s_{q,1}(k), s_{q,2}(k), \dots, s_{q,L_q}(k)]^T$  be the transmitted symbol block of the  $q$ th user. Define  $\tilde{\mathbf{s}}_q(k) := [\text{Re}\{\mathbf{s}_q^T(k)\} \ \text{Im}\{\mathbf{s}_q^T(k)\}]^T \in \mathbb{R}^{2L_q}$  and  $\tilde{\mathbf{y}}(k) := [\text{Re}\{\mathbf{y}^T(k)\} \ \text{Im}\{\mathbf{y}^T(k)\}]^T \in \mathbb{R}^{2M}$  to be the split real-valued symbol block of the  $q$ th user and the received vector. Associated with the  $q$ th user’s channel matrix  $\mathbf{H}_q$ , we form the following augmented matrix

$$\tilde{\mathbf{H}}_q := \mathbf{I}_K \otimes \tilde{\mathbf{H}}_q \in \mathbb{R}^{2KM \times 2KN}, \quad (2.73)$$

where

$$\tilde{\mathbf{H}}_q := \begin{bmatrix} \text{Re}\{\mathbf{H}_q\} & -\text{Im}\{\mathbf{H}_q\} \\ \text{Im}\{\mathbf{H}_q\} & \text{Re}\{\mathbf{H}_q\} \end{bmatrix} \in \mathbb{R}^{2M \times 2N}. \quad (2.74)$$

---

<sup>1</sup>Symbol synchronization is necessary in TDMA based cellular implementations, e.g., IS-136 and GSM, and 3G TDD CDMA systems such as time division synchronous CDMA (TD-SCDMA). In the literature, this assumption is commonly made when dealing with uplink interference cancellation in MU MIMO systems [78], [79], [104], [105], [106]

Also, with  $\mathbf{a}_{q,l}^{(j)}$  denoting the  $j$ th column of the matrix  $\mathbf{A}_{q,l}$  and

$$\tilde{\mathbf{a}}_{q,l}^{(j)} := \begin{bmatrix} \operatorname{Re} \left\{ \mathbf{a}_{q,l}^{(j)} \right\} \\ \operatorname{Im} \left\{ \mathbf{a}_{q,l}^{(j)} \right\} \end{bmatrix} \in \mathbb{R}^{2N}, \quad (2.75)$$

we define the  $2KN \times 2L_q$  real-valued ST modulation matrix

$$\bar{\mathbf{A}}_q := \begin{bmatrix} \tilde{\mathbf{a}}_{q,1}^{(1)} & \tilde{\mathbf{a}}_{q,2}^{(1)} & \cdots & \tilde{\mathbf{a}}_{q,2L_q}^{(1)} \\ \tilde{\mathbf{a}}_{q,1}^{(2)} & \tilde{\mathbf{a}}_{q,2}^{(2)} & \cdots & \tilde{\mathbf{a}}_{q,2L_q}^{(2)} \\ \vdots & \vdots & \ddots & \vdots \\ \tilde{\mathbf{a}}_{q,1}^{(K)} & \tilde{\mathbf{a}}_{q,2}^{(K)} & \cdots & \tilde{\mathbf{a}}_{q,2L_q}^{(K)} \end{bmatrix} \in \mathbb{R}^{2KN \times 2L_q}. \quad (2.76)$$

Then the matrix signal model (2.72) can be rewritten, after some manipulations, as the following equivalent vectorized linear model

$$\mathbf{y}_c(k) := [\tilde{\mathbf{y}}^T(k), \tilde{\mathbf{y}}^T(k+1), \dots, \tilde{\mathbf{y}}^T(k+K-1)]^T = \mathbf{H}_c \mathbf{s}_c(k) + \mathbf{v}_c(k), \quad (2.77)$$

where

$$\mathbf{H}_c := \left[ \sqrt{\frac{P_1}{N}} \bar{\mathbf{H}}_1 \bar{\mathbf{A}}_1, \sqrt{\frac{P_2}{N}} \bar{\mathbf{H}}_2 \bar{\mathbf{A}}_2, \dots, \sqrt{\frac{P_Q}{N}} \bar{\mathbf{H}}_Q \bar{\mathbf{A}}_Q \right] \in \mathbb{R}^{2KM \times 2L_T}, \quad (2.78)$$

is the effective channel matrix,

$$\mathbf{s}_c(k) := [\tilde{\mathbf{s}}_1^T(k), \tilde{\mathbf{s}}_2^T(k), \dots, \tilde{\mathbf{s}}_Q^T(k)]^T \in \mathbb{R}^{2L_T}, \quad (2.79)$$

and  $\mathbf{v}_c(k) \in \mathbb{R}^{2KM}$  is the corresponding noise component. Through linearly combining the received signal  $\mathbf{y}_c(k)$  with  $\mathbf{H}_c$ , we can obtain the MF signal vector

$$\mathbf{z}(k) := \mathbf{H}_c^T \mathbf{y}_c(k) = \mathbf{F} \mathbf{s}_c(k) + \mathbf{v}(k), \quad (2.80)$$

where  $\mathbf{F} := \mathbf{H}_c^T \mathbf{H}_c \in \mathbb{R}^{2L_T \times 2L_T}$  is the MFCM and given by

$$\mathbf{F} = \begin{bmatrix} \mathbf{F}_{1,1} & \cdots & \mathbf{F}_{1,Q} \\ \vdots & \ddots & \vdots \\ \mathbf{F}_{Q,1} & \cdots & \mathbf{F}_{Q,Q} \end{bmatrix} = \begin{bmatrix} \frac{P_1}{N} \bar{\mathbf{A}}_1^T \bar{\mathbf{H}}_1^T \bar{\mathbf{H}}_1 \bar{\mathbf{A}}_1 & \cdots & \sqrt{\frac{P_1 P_Q}{N^2}} \bar{\mathbf{A}}_1^T \bar{\mathbf{H}}_1^T \bar{\mathbf{H}}_Q \bar{\mathbf{A}}_Q \\ \vdots & \ddots & \vdots \\ \sqrt{\frac{P_1 P_Q}{N^2}} \bar{\mathbf{A}}_Q^T \bar{\mathbf{H}}_Q^T \bar{\mathbf{H}}_1 \bar{\mathbf{A}}_1 & \cdots & \frac{P_Q}{N} \bar{\mathbf{A}}_Q^T \bar{\mathbf{H}}_Q^T \bar{\mathbf{H}}_Q \bar{\mathbf{A}}_Q \end{bmatrix}, \quad (2.81)$$

with

$$\mathbf{F}_{p,q} := \sqrt{\frac{P_p P_q}{N^2}} \bar{\mathbf{A}}_p^T \bar{\mathbf{H}}_p^T \bar{\mathbf{H}}_q \bar{\mathbf{A}}_q \in \mathbb{R}^{2L_p \times 2L_q}, \quad (2.82)$$

and  $\mathbf{v}(k) := \mathbf{H}_c^T \mathbf{v}_c(k)$ . It can be easily shown that

$$\mathbf{F}_{q,q} = \frac{P_q}{N} \|\mathbf{H}_q\|_F^2 \mathbf{I}_{2L_q}, \quad (2.83)$$

with  $E\{\|\mathbf{H}_q\|_F^2\} = NM$  being the diversity order achieved by the  $q$ th user terminal. We will hereafter rely on the MF model (2.80) for detection.

## 2.4.2 Orthogonal STBC: Encoding and Decoding

### Code Construction of O-STBC

Consider the O-STBC systems as depicted in Figure 2.5. In particular, O-STBCs are a special example of linear codes, where the codeword  $\mathbf{X}(k)$  is design to be a unitary matrix, which has the following “unitary property” [47].

**Theorem 2.4.1.** *Let  $\mathbf{X}(k)$  be an  $N \times K$  ST codeword matrix as defined in (2.57). The ST codewords that satisfy the unitary property*

$$\mathbf{X}(k)\mathbf{X}^H(k) = K\mathbf{I}_N, \quad (2.84)$$

are called the O-STBC. More specifically, (2.84) holds for all complex  $\{s_l(k)\}$  if and only if

$$\begin{aligned} \mathbf{A}_p \mathbf{A}_p^H &= \frac{K}{L} \mathbf{I}_N & p = 1, 2, \dots, 2L \\ \mathbf{A}_p \mathbf{A}_q^H &= -\mathbf{A}_q \mathbf{A}_p^H, & p \neq q; \quad p, q = 1, 2, \dots, 2L \end{aligned} \quad (2.85)$$

in which  $\{\mathbf{A}_l\}$  is also an orthogonal design. ■

*Proof:* Based on (2.57) and using (2.85) and the fact  $|\tilde{s}_l(k)|^2 = 1/2$ , we have

$$\begin{aligned} \mathbf{X}(k)\mathbf{X}^H(k) &= \sum_{p=1}^{2L} \sum_{q=1}^{2L} (\mathbf{A}_p \mathbf{A}_q^H \tilde{s}_p(k) \tilde{s}_q(k)) \\ &= \sum_{p=1}^{2L} \mathbf{A}_p \mathbf{A}_p^H \tilde{s}_p(k) \tilde{s}_p(k) + \sum_{p=1}^{2L} \sum_{q=1, q>p}^{2L} \mathbf{A}_p \mathbf{A}_q^H \tilde{s}_p(k) \tilde{s}_q(k) \end{aligned}$$

$$\begin{aligned}
& + \sum_{q=1}^{2L} \sum_{p=1, p>q}^{2L} \mathbf{A}_p \mathbf{A}_q^H \tilde{s}_p(k) \tilde{s}_q(k) \\
& = \sum_{p=1}^{2L} \mathbf{A}_p \mathbf{A}_p^H \tilde{s}_p(k) \tilde{s}_p(k) + \sum_{p=1}^{2L} \sum_{q=1, q>p}^{2L} (\mathbf{A}_p \mathbf{A}_q^H - \mathbf{A}_q \mathbf{A}_p^H) \tilde{s}_p(k) \tilde{s}_q(k) \\
& = \frac{K}{L} \sum_{p=1}^{2L} |\tilde{s}_p(k)|^2 \mathbf{I}_N = \frac{K}{L} \left( \frac{1}{2} \right) \cdot (2L) \mathbf{I}_N = K \mathbf{I}_N. \tag{2.86}
\end{aligned}$$

The converse is shown in [4] for a complete proof. This thus proves the results.  $\square$

Therefore, Theorem 2.4.1 establishes an important link between the theory of orthogonal designs and O-STBC. For example, the ‘‘Alamouti code’’ [46] is an O-STBC

$$\begin{aligned}
\underbrace{\begin{bmatrix} s_1(k) \\ s_2(k) \end{bmatrix}}_{:=\mathbf{s}(k)} & \mapsto \underbrace{\begin{bmatrix} s_1(k) & s_2^*(k) \\ s_2(k) & -s_1^*(k) \end{bmatrix}}_{:=\mathbf{X}(k)} = \underbrace{\begin{bmatrix} 1 & 0 \\ 0 & 1 \end{bmatrix}}_{\mathbf{A}_1} \tilde{s}_1(k) + \underbrace{\begin{bmatrix} 0 & -1 \\ 1 & 0 \end{bmatrix}}_{\mathbf{A}_2} \tilde{s}_2(k) \\
& + \underbrace{\begin{bmatrix} j & 0 \\ 0 & -j \end{bmatrix}}_{\mathbf{A}_3} \tilde{s}_3(k) + \underbrace{\begin{bmatrix} 0 & j \\ j & 0 \end{bmatrix}}_{\mathbf{A}_4} \tilde{s}_4(k). \tag{2.87}
\end{aligned}$$

in which

$$\mathbf{X}(k) \mathbf{X}^H(k) = 2 \mathbf{I}_N, \tag{2.88}$$

and the modulation matrices  $\{\mathbf{A}_l\}_{l=1}^4$  satisfy the properties (2.85). This shows that Alamouti code is an O-STBC for  $N = 2$ . A consequence of this observation is that the Alamouti code achieves *full rate, full diversity as well as simple (decoupled) ML decoding*. Another O-STBCs for different number of transmit antennas  $N$  and code rate  $R$  have been derived in [47], [62], [94]. Here we only give some important results of STBC with orthogonal designs. The detail derivation of constructing the O-STBCs can be found in [47]. In particular, for real-valued constellations, square codewords ( $N \times N$ ) offering a full rate of  $R = 1$  exist only for  $N = 2, 4, 8$ . For complex-valued constellations, full rate is achievable only with  $N = 2$ . For  $N > 2$ , we always have a codeword with the code rate lower than one, i.e.,  $R < 1$ . Using the complex number theory, the ‘‘Hurwitz-Radon’’ problem, it is known that [47], [62], [94]:

- Rate 1 codes with simple linear processing is achievable for  $N \leq 8$  for real constellations.
- Rate 1/2 codes with simple linear processing is achievable for  $N \geq 2$  for complex constellations.
- Rate 3/4 codes with simple linear processing is achievable for  $N = 3$  and  $N = 4$  for complex constellations.

Finally, the ST modulation matrices of O-STBCs that satisfy the properties (2.85) will also meet the total transmit power constraint, i.e.,

$$\begin{aligned}
E \{ \text{tr} (\mathbf{X}(k)\mathbf{X}^H(k)) \} &= E \left\{ \text{tr} \left( \sum_{p=1}^{2L} \sum_{q=1}^{2L} \mathbf{A}_p \mathbf{A}_q^H \tilde{s}_p(k) \tilde{s}_q(k) \right) \right\} \\
&= \text{tr} \left( \sum_{p=1}^{2L} \sum_{q=1}^{2L} \mathbf{A}_p \mathbf{A}_q^H E \{ \tilde{s}_p(k) \tilde{s}_q(k) \} \right) \\
&= \frac{1}{2} \text{tr} \left( \sum_{p=1}^{2L} \mathbf{A}_p \mathbf{A}_p^H \right) \\
&= \frac{1}{2} \text{tr} \left( \sum_{p=1}^{2L} \frac{K}{L} \mathbf{I}_N \right), \\
&= NK.
\end{aligned} \tag{2.89}$$

which ensures the constraint (2.61).

### ML Decoding of O-STBC

To realize a simple (decoupled) ML decoding of O-STBC, we need the following lemma.

**Lemma 2.4.1.** *Let  $\mathbf{F} = \mathbf{H}_c^T \mathbf{H}_c \in R^{2L \times 2L}$  be the MFCM of O-STBC as defined in (2.71), where  $\mathbf{H}_c \in R^{2KM \times 2L}$  is given by (2.69). If  $\{\mathbf{A}_i\}$  satisfy the orthogonal properties (2.85), then we have*

$$\mathbf{F} = \alpha \mathbf{I}_{2L}, \tag{2.90}$$

where  $\alpha := \frac{K}{L} \|\mathbf{H}\|_F^2$  and  $\|\mathbf{A}\|_F$  denotes the Frobenius norm of matrix  $\mathbf{A}$ . ■

*Proof:* From (2.68) that the effective signature (priori to matched filtering) is  $\mathbf{H}_c = \bar{\mathbf{H}}\bar{\mathbf{A}}$ . Accordingly, the MFCM signature is thus  $\mathbf{H}_c^T \mathbf{H}_c = \bar{\mathbf{A}}^T \bar{\mathbf{H}} \bar{\mathbf{H}} \bar{\mathbf{A}}$ , whose  $(i, j)$ th entry,  $i, j = 1, 2, \dots, 2L$ , can be directly computed as

$$\begin{aligned}
f_{i,j} &= \sum_{k=1}^K \left( \tilde{\mathbf{a}}_i^{(k)} \right)^T \tilde{\mathbf{H}}^T \tilde{\mathbf{H}} \tilde{\mathbf{a}}_j^{(k)} = \sum_{k=1}^K \operatorname{Re} \left\{ \left( \mathbf{a}_i^{(k)} \right)^H \mathbf{H}^H \mathbf{H} \mathbf{a}_j^{(k)} \right\} \\
&= \sum_{k=1}^K \operatorname{Re} \left\{ \sum_{m=1}^M \mathbf{h}_m^H \mathbf{a}_i^{(k)} \left( \mathbf{a}_j^{(k)} \right)^H \mathbf{h}_m \right\} \\
&= \operatorname{Re} \left\{ \sum_{m=1}^M \mathbf{h}_m^H \left[ \sum_{k=1}^K \mathbf{a}_i^{(k)} \left( \mathbf{a}_j^{(k)} \right)^H \right] \mathbf{h}_m \right\} \\
&= \operatorname{Re} \left\{ \sum_{m=1}^M \mathbf{h}_m^H \mathbf{A}_i \mathbf{A}_j^H \mathbf{h}_m \right\}, \quad i, j = 1, 2, \dots, 2L,
\end{aligned} \tag{2.91}$$

where  $\mathbf{h}_m^T$  is the  $m$ th row of  $\mathbf{H}$ . Equation (2.91) gives an important observation that the  $(i, j)$ th element of  $\mathbf{F}$  fully describing the structure of  $\mathbf{F}$  is completely characterized by  $\{\mathbf{A}_l\}$ . The proof of lemma is thus based on (2.91). We first note that the first property in (2.85) implies that  $f_{i,j} = \frac{K}{L} \sum_{m=1}^M \|\mathbf{h}_m\|^2 = \frac{K}{L} \|\mathbf{H}\|_F^2$ ; the second property in (2.85), namely, the matrix  $\mathbf{A}_i \mathbf{A}_j^H$  is skew-symmetric for  $i \neq j$ , guarantees that  $f_{i,j} = 0$ . As a result,  $\mathbf{F}$  is always a scalar multiple of the identity matrix.  $\square$

From Lemma 2.4.1, it follows that for O-STBCs the ML decoding metric can be written

$$\begin{aligned}
E \left\{ \left\| \mathbf{z}(k) - \sqrt{\frac{P_T}{N}} \mathbf{F} \hat{\mathbf{s}}(k) \right\|^2 \right\} &= E \left\{ \left\| \mathbf{z}(k) - \alpha \sqrt{\frac{P_T}{N}} \hat{\mathbf{s}}(k) \right\|^2 \right\} \\
&= E \{ \|\mathbf{z}(k)\|^2 \} - 2\alpha \sqrt{\frac{P_T}{N}} E \{ \operatorname{Re} \{ \mathbf{z}^T(k) \hat{\mathbf{s}}(k) \} \} \\
&\quad + \alpha^2 \frac{P_T}{N} E \{ \|\hat{\mathbf{s}}(k)\|^2 \} \\
&= \alpha^2 \frac{P_T}{N} E \{ \|\tilde{\mathbf{s}}(k) - \hat{\mathbf{s}}(k)\|^2 \} + \text{const.}
\end{aligned} \tag{2.92}$$

This shows that the ML decoding of  $\{\tilde{s}_l(k)\}$  is equivalent to directly solving  $2L$  scalar decoding problems, one for each  $\tilde{s}_l(k)$  based on  $\mathbf{z}(k)$  through the ST matched filtering (2.70). Therefore,  $\{\tilde{s}_l(k)\}$  can be decoded “independently”, leading to a lower decoding complexity due to that the noise term is  $\mathbf{v}(k)$  still white.



### 2.4.3 Performance Analysis of O-STBC Systems

Assume that ML decoding is used at the receiver with perfect channel knowledge based on the received signal  $\mathbf{Y}(k)$  (see (2.59)). The estimated codeword is

$$\hat{\mathbf{X}}(k) := \arg \min_{\mathbf{X}(k)} \left\| \mathbf{Y}(k) - \sqrt{\frac{P_T}{N}} \mathbf{H} \mathbf{X}(k) \right\|_F^2, \quad (2.93)$$

where the minimization is performed over all admissible codewords  $\mathbf{X}(k)$ . An error occurs when the receiver mistakes a transmitted codeword for another codeword from the set of possible codewords.

Assume that a codeword  $\mathbf{X}$  is transmitted. If the receiver uses the ML decoding to estimate the transmitted codeword according to (2.93), the probability that the receiver decides in favor of another codeword  $\hat{\mathbf{X}}(k)$ , given the knowledge of the channel realization at the receiver, is (also called the pairwise error probability (PEP)) [1]

$$\begin{aligned} P \left( \mathbf{X}(k) \rightarrow \hat{\mathbf{X}}(k) \mid \mathbf{H} \right) &= Q \left( \sqrt{\frac{P_T \left\| \mathbf{H} \left( \mathbf{X}(k) - \hat{\mathbf{X}}(k) \right) \right\|_F^2}{2N\sigma_v^2}} \right) \\ &= Q \left( \sqrt{\frac{\rho \left\| \mathbf{H} \mathbf{B} \right\|_F^2}{2N}} \right), \end{aligned} \quad (2.94)$$

where

$$\mathbf{B} := \mathbf{X}(k) - \hat{\mathbf{X}}(k) \in \mathbb{C}^{N \times K}, \quad (2.95)$$

is the codeword difference matrix. Applying the Chernoff bound [1] we have

$$P \left( \mathbf{X}(k) \rightarrow \hat{\mathbf{X}}(k) \mid \mathbf{H} \right) \leq \exp \left( -\frac{\rho \left\| \mathbf{H} \mathbf{B} \right\|_F^2}{4N} \right). \quad (2.96)$$

Assuming that  $\mathbf{H} = \mathbf{H}_w$ , the PEP averaged, after some manipulations, over all channel realizations can be upper-bounded as

$$\begin{aligned} P \left( \mathbf{X}(k) \rightarrow \hat{\mathbf{X}}(k) \right) &\leq \left( \frac{1}{\det \left( \mathbf{I}_N + \frac{\rho}{4N} \mathbf{A} \right)} \right)^M \\ &= \prod_{i=1}^r \left( \frac{1}{1 + \frac{\rho \lambda_i}{4N}} \right)^M, \end{aligned} \quad (2.97)$$

where  $\mathbf{A} := \mathbf{B}\mathbf{B}^H$ ,  $\lambda_i$ ,  $i = 1, 2, \dots, r$  are the non-zero eigenvalues of  $\mathbf{A}$  and  $r$  is the rank of  $\mathbf{A}$ . When the SNR is high ( $\rho \gg 1$ ), (2.97) can be further simplified as [47]

$$P(\mathbf{X}(k) \rightarrow \hat{\mathbf{X}}(k)) \leq \left( \prod_{i=1}^r \lambda_i \right)^{-M} \cdot \left( \frac{\rho}{4N} \right)^{-rM}. \quad (2.98)$$

Equation (2.98) shows that the STC gives two types of advantages, namely the “diversity gain” and the “coding gain” [47]. We have following some discussions.

- **Diversity Advantage:**  $G_d := rM$ . Diversity gain is an approximate measure of power gain of system with space diversity over system without diversity at the same error probability. This type of advantage determines “slop” of error rate curve.
- **Coding Advantage:**  $G_c := (\prod_{i=1}^r \lambda_i)^{1/r}$ . Coding gain measures power gain of coded system over uncoded system with the same diversity, at the same error probability. This type of advantage determines “horizontal shift” of uncoded system error rate curve to ST coded one for the same diversity order.

Equation (2.98) also leads us to the two well-known criteria for ST codeword construction, namely the “rank criterion” and the “determinant criterion” [47]. Some discussions about the ST code design criteria are given as follows.

- **Rank Criterion:** To maximize “diversity advantage”, it has to maximize the minimum rank  $r$  of  $\mathbf{A}$  over all pairs of distinct codewords. In particular, the maximum rank  $r$  means that  $\mathbf{A}$  has a full rank of  $r = N$ .
- **Determinant Criterion:** To maximize “coding advantage”, it has to maximize minimum product  $\prod_{i=1}^r \lambda_i$  of  $\mathbf{A}$ , which is the non-zero part of determinant of  $\mathbf{A}$ , over all pairs of distinct codewords.

It is easily to show that the codeword difference matrix  $\mathbf{B}$  of O-STBCs is also a orthogonal design, which means that  $\mathbf{A}$  has a full rank of  $r = N$ . From (2.98), the average PEP in the

high SNR regime for O-STBCs is thus given by [14]

$$P(\mathbf{X}(k) \rightarrow \hat{\mathbf{X}}(k)) \leq \left( \frac{N}{\|\mathbf{B}\|_F^2} \right)^{-MN} \cdot \left( \frac{\rho}{4N} \right)^{-MN}. \quad (2.99)$$

Clearly, from (2.99), we can see that O-STBCs extract the full diversity gain of  $MN$ .

**Example 2.4.1:** Figure 2.6 shows the BER performance of STBCs as a function of SNR  $\rho$  for different number of transmit antennas over a frequency flat MISO channel. Assume that BPSK modulation is used for Figure 2.6 (a). In this case, the SE of all STBCs are the same and equals to 1 bps/Hz. We further examine the STBC performance with the SE being 2 bps/Hz and show it in Figure 2.6 (b). In this case, the STBC with  $N = 2$  is the unit-rate code with QPSK modulation<sup>2</sup>. But the STBC with  $N = 3$  and  $N = 4$  are the half-rate code with 16-QAM modulation. As expected, the all BER curves of Figure 2.6 decrease as  $\rho$  and  $M$  increase, showing the diversity advantage provided by STBC schemes. As shown in the two figures, the STBC with  $N = 2$  provides a better performance as SNR is small. However, when the SNR is large, the STBC with  $N = 4$  will outperform the others.

## 2.5 Vertical Bell Laboratories Layered Space-Time

SM scheme exploits the rich scattering wireless channel allowing the receiver to detect the different data streams simultaneously transmitted by the different antennas. That is, SM technique uses multiple antennas at the transmitter and receiver in conjunction with rich scattering environment within the same frequency band to provide a “linearly” increasing capacity gain in the number of antennas [13], [53], [54]. Therefore, the concept of SM techniques is different from that of STC techniques, which permit to efficiently introduce an *ST correlation* among transmitted data streams to improve information protection and increase diversity gain.

---

<sup>2</sup>For a fair comparison, the most used approach for evaluating the performance is to examine the BER performance under a given SE constraint [3], [82]

### 2.5.1 Spatial Multiplexing Techniques

As mentioned in Section 1.2.3, the SM techniques can be classified into two types, namely the D-BLAST and V-BLAST. D-BLAST is one of the SM schemes to approach the theoretical capacity limit of MIMO systems [54]. However, due to its complex coding procedure and complicated decoding processing, V-BLAST has been proposed as a simplified version [55]. In V-BLAST system, channel coding may be applied to individual antennas (layers), corresponding to the data stream transmitted from each antenna, while in D-BLAST system, coding processing is applied not only across the “time” but also to each “layer”, which implies higher ST encoding complexity. These are depicted in Figure 2.7. From Figure 2.7, we can see that the essential difference between D-BLAST and V-BLAST is the vector encoding process. In D-BLAST system, redundancy between the sub-streams is introduced by using specialized inter-substream block coding, and code blocks organized along diagonals in space and time domains leads to higher SEs. On the other hand, in V-BLAST system, demultiplexing followed by independent bit-to-symbol mapping of each substream, so no coding is required [10], [11], [54]. From the implementation advantages of V-BLAST [55], [56], in what follows we will thus focus on the aspect of V-BLAST techniques.

### 2.5.2 Detection Algorithm for V-BLAST Systems

The transmitted data stream  $s(k)$ , in general complex-valued, of V-BLAST systems is first demultiplexed into  $N$  lower rate substreams, say,  $s_n(k) := s(Nk+n-1)$ ,  $n = 1, 2, \dots, N$ . After coding and modulation processing, each demultiplexed substream is transmitted simultaneously from the  $N$  transmit antennas. The substreams are co-channel signals, that is, they have the same frequency band. Specifically, V-BLAST [54], [55] can be regarded as a special class of STBCs where the independent data streams are transmitted over different antennas. Since no any redundancy (correlation) is introduced into the temporal domain of ST codeword; only encoded in spatial domain by independent streams, the input to the ST

encoder can be expressed by following  $N \times 1$  symbol vector

$$\mathbf{s}(k) := [s_1(k), s_2(k), \dots, s_N(k)]^T \in \mathbb{C}^N, \quad (2.100)$$

and the output of ST encoder is thus given by the  $N \times 1$  vector

$$\mathbf{x}(k) := [x_1(k), x_2(k), \dots, x_N(k)]^T = [s_1(k), s_2(k), \dots, s_N(k)]^T = \sum_{l=1}^{2N} \mathbf{a}_l \tilde{s}_l(k), \quad (2.101)$$

where the ST modulation matrix  $\mathbf{A}_l$  presented in (2.57) is simplified to an  $N \times 1$  vector  $\mathbf{a}_l$  since  $K = 1$  in SM systems. In (2.101), we can see that  $\mathbf{x}(k) = \mathbf{s}(k)$ , which means that the output of ST encoder is just the input to ST encoder. Considering the MIMO systems, the received signal model can be intuitively written as (2.27)

$$\mathbf{y}(k) = \sqrt{\frac{P_T}{N}} \mathbf{H} \mathbf{x}(k) + \mathbf{v}(k). \quad (2.102)$$

Since  $N$  data streams are transmitted simultaneously from different antennas at the same time, the code rate of SM systems is thus given by

$$\mathbf{s}(k) \mapsto \mathbf{x}(k) : \quad R = N > 1. \quad (2.103)$$

On the other hand, to meet the total transmit power constraint,  $\mathbf{a}_l$  must be normalized as

$$\|\mathbf{a}_l\|^2 := 1, \quad l = 1, 2, \dots, 2L, \quad (2.104)$$

such that [62], [65]

$$E \{ \text{tr} (\mathbf{x}(k) \mathbf{x}^H(k)) \} = N. \quad (2.105)$$

According to (2.101) and (2.104) and assuming  $N = 2$ , we have

$$\begin{aligned} \underbrace{\begin{bmatrix} s_1(k) \\ s_2(k) \end{bmatrix}}_{:=\mathbf{s}(k)} &\mapsto \underbrace{\begin{bmatrix} s_1(k) \\ s_2(k) \end{bmatrix}}_{:=\mathbf{x}(k)} = \begin{bmatrix} \tilde{s}_1(k) + j\tilde{s}_3(k) \\ \tilde{s}_2(k) + j\tilde{s}_4(k) \end{bmatrix} \\ &= \underbrace{\begin{bmatrix} 1 \\ 0 \end{bmatrix}}_{\mathbf{a}_1} \tilde{s}_1(k) + \underbrace{\begin{bmatrix} 0 \\ 1 \end{bmatrix}}_{\mathbf{a}_2} \tilde{s}_2(k) + \underbrace{\begin{bmatrix} j \\ 0 \end{bmatrix}}_{\mathbf{a}_3} \tilde{s}_3(k) + \underbrace{\begin{bmatrix} 0 \\ j \end{bmatrix}}_{\mathbf{a}_4} \tilde{s}_4(k). \end{aligned} \quad (2.106)$$

Note that the modulation vectors  $\{\mathbf{a}_l\}_{l=1}^4$  also satisfy the properties (2.85).

At the receiver, each antenna observes a superposition of the transmitted signals, separates them into constituent data streams, and demultiplexes them in order to recover the original data stream [55], [56]. Receivers for V-BLAST systems can be divided into three classes: the ML receiver, linear receiver and SIC receiver.

**ML Receiver:** It is well known that theoretically, the optimal method of recovering the transmitted signal at the receiver is ML detection algorithm, where the receiver compares all possible combinations of symbols which could have been transmitted with what is observed via the following criterion

$$\hat{\mathbf{x}}(k) := \arg \min_{\mathbf{x}(k)} \left\| \mathbf{y}(k) - \sqrt{\frac{P_T}{N}} \mathbf{H} \mathbf{x}(k) \right\|^2. \quad (2.107)$$

Since the comparison complexity increases exponentially with the number of transmit antennas and the modulation order, it is very difficult to be used at the receiver in practice, which is the main disadvantage of this method.

**Linear ZF/MMSE Receiver:** The principle of detection processing for ZF/MMSE receiver is the same as that of beamformer with multiple sources [15].

**SIC Receiver:** The SIC algorithm is in general combined with V-BLAST receiver. Therefore, the SIC receiver is called just as V-BLAST receiver, which is an attractive alternative to ZF and MMSE receivers. The SIC receiver provides improved performance at the cost of increased computational complexity. Rather than just jointly decoding the transmitted signals, this nonlinear detection scheme first detects the strongest transmitted signal, cancels the effect of this strongest signal from the received signal, and then proceeds to detect the strongest of the remaining transmitted signals, and so on. Under the assumption that the channel matrix  $\mathbf{H}$  is known, the basic steps of the SIC algorithm is summarized as follows [17], [55], [56] and illustrated in Figure 2.8

- *Ordering:* Determine the optimal detection order in accordance with some criteria such as the ZF and MMSE.

- *Nulling*: Nulling out all weaker signals to estimate the strongest signal.
- *Slicing*: Detect the strongest signal.
- *Cancellation*: Cancel the effect of the detected strongest signal from the received signal.

Since the SIC algorithm can be combined with ZF receiver or MMSE receiver, it can accordingly be classified into the ZF V-BLAST receiver and MMSE V-BLAST receiver. The main difference between the two receiver is the ordering criterion and nulling processing. We summarize the detection algorithms of ZF V-BLAST receiver and MMSE V-BLAST receiver.

- **ZF V-BLAST Detection Algorithm:** [55], [56]

$$\textbf{Initialization : } \quad \mathbf{y}_1(k) := \mathbf{y}(k), \quad \mathbf{G}_1 := \sqrt{\frac{N}{P_T}} \mathbf{H}^+, \quad i := 1 \quad (2.108)$$

$$\textbf{Recursion : } \quad l_i := \arg \min_{j \neq \{l_1, \dots, l_{i-1}\}} \left\| (\mathbf{G}_i)_j \right\|_F^2 \quad (2.109)$$

$$\mathbf{w}_{l_i} := (\mathbf{G}_i)_{l_i} \quad (2.110)$$

$$z_{l_i}(k) := \mathbf{w}_{l_i}^H \mathbf{y}_i(k) \quad (2.111)$$

$$\hat{x}_{l_i}(k) := \mathcal{Q}(z_{l_i}(k)) \quad (2.112)$$

$$\mathbf{y}_{i+1} := \mathbf{y}_i - \sqrt{\frac{P_T}{N}} (\mathbf{H})_{l_i} \hat{x}_{l_i}(k) \quad (2.113)$$

$$\mathbf{G}_{i+1} := \sqrt{\frac{N}{P_T}} \bar{\mathbf{H}}_{l_i}^+ \quad (2.114)$$

$$i := i + 1 \quad (2.115)$$

- **MMSE V-BLAST Detection Algorithm:** [95], [96]

$$\textbf{Initialization : } \quad \mathbf{y}_1(k) := \mathbf{y}(k), \quad \mathbf{H}_1 := \mathbf{H}, \quad i := 1 \quad (2.116)$$

$$\textbf{Recursion : } \quad \mathbf{Q}_i := \mathbf{I} - \frac{P_T}{N} \mathbf{H}_i \mathbf{H}_i^H \left( \frac{P_T}{N} \mathbf{H}_i \mathbf{H}_i^H + \sigma_v^2 \mathbf{I} \right)^{-1} \mathbf{H}_i \quad (2.117)$$

$$l_i := \arg \min_{j \neq \{l_1, \dots, l_{i-1}\}} (\text{diag}(\mathbf{Q}_i))_j \quad (2.118)$$

$$\mathbf{w}_{l_i} := \sqrt{\frac{P_T}{N}} \left( \frac{P_T}{N} \mathbf{H}_i \mathbf{H}_i^H + \sigma_v^2 \mathbf{I} \right)^{-1} (\mathbf{H}_i)_{l_i} \quad (2.119)$$

$$z_{l_i}(k) := \mathbf{w}_{l_i}^H \mathbf{y}_i(k) \quad (2.120)$$

$$\hat{x}_{l_i}(k) := \mathcal{Q}(z_{l_i}(k)) \quad (2.121)$$

$$\mathbf{y}_{i+1} := \mathbf{y}_i - \sqrt{\frac{P_T}{N}} (\mathbf{H})_{l_i} \hat{x}_{l_i}(k) \quad (2.122)$$

$$\mathbf{H}_{i+1} := \bar{\mathbf{H}}_{l_i} \quad (2.123)$$

$$i := i + 1 \quad (2.124)$$

where  $(\mathbf{A})_j$  denotes the  $j$ th column of matrix  $\mathbf{A}$ ,  $\mathcal{Q}(\cdot)$  denotes the quantize operator,  $\bar{\mathbf{A}}_{l_i}$  denotes the matrix obtained by zeroing columns  $l_1, \dots, l_i$  of  $\mathbf{A}_{l_i}$ , and  $(\text{diag}(\mathbf{A}))_j$  denotes the  $j$ th element of the diagonal entries of matrix  $\mathbf{A}$ .

### 2.5.3 Performance Analysis of V-BLAST Systems

We analysis the BER performance of V-BLAST systems over the slow Rayleigh flat fading channels based on the QR decomposition method [97]. The  $M \times N$  MIMO channel matrix (given in (2.26)) can be expressed as follows through the QR decomposition

$$\mathbf{H} := \mathbf{Q}\mathbf{R}, \quad (2.125)$$

where  $\mathbf{Q}$  is an  $M \times M$  unitary matrix so that  $\mathbf{Q}^H \mathbf{Q} = \mathbf{I}_M$  and  $\mathbf{R}$  is an  $M \times N$  upper triangular matrix

$$\mathbf{R} = \begin{bmatrix} r_{1,1} & r_{1,2} & \cdots & r_{1,N} \\ 0 & r_{2,2} & \cdots & r_{2,N} \\ \vdots & \vdots & \ddots & \vdots \\ 0 & \cdots & 0 & r_{M,N} \end{bmatrix} \in \mathbb{C}^{M \times N} \quad (2.126)$$

At the receiver, the  $M \times 1$  modified received signal after an  $M \times M$  partially decorrelated nulling weight matrix  $\mathbf{W} = \mathbf{Q}$  is given by

$$\begin{aligned} \mathbf{z}(k) &:= \mathbf{W}^H \mathbf{y}(k) = \sqrt{\frac{P_T}{N}} \mathbf{Q}^H \mathbf{Q} \mathbf{R} \mathbf{x}(k) + \mathbf{Q}^H \mathbf{v}(k) \\ &= \sqrt{\frac{P_T}{N}} \mathbf{R} \mathbf{x}(k) + \tilde{\mathbf{v}}(k), \end{aligned} \quad (2.127)$$



where  $\tilde{\mathbf{v}}(k) := \mathbf{Q}^H \mathbf{v}(k)$  is the AWGN which has the same statistical distribution as that of  $\mathbf{v}(k)$ . From (2.127), the modified received signal at the  $l$ th layer can thus be written as

$$z_l(k) = \sqrt{\frac{P_T}{N}} r_{l,l} x_l(k) + \tilde{v}_l(k) + \text{interference from } x_{l+1}(k), x_{l+2}(k), \dots, x_N(k). \quad (2.128)$$

Assuming that the decisions of  $\{x_i(k)\}_{i=l+1}^N$  are correct, so that the effects of them can be perfectly removed from the  $l$ th layer  $z_l(k)$ , yields the decision variable of the  $l$ th layer

$$\tilde{x}_l(k) = \sqrt{\frac{P_T}{N}} r_{l,l} x_l(k) + \tilde{v}_l(k). \quad (2.129)$$

Since there is no any correlation is introduced in temporal domain of ST codeword for V-BLAST systems, the PEP of the  $l$ th layer  $P(x_l(k) \rightarrow \hat{x}_l(k))$  is the probability that the decoder decides as its output  $\hat{x}_l(k)$ , when the transmitted symbol of the  $l$ th layer was in fact  $x_l(k)$ . This scenario occurs if

$$\left| \tilde{x}_l(k) - \sqrt{\frac{P_T}{N}} r_{l,l} x_l(k) \right|^2 \geq \left| \tilde{x}_l(k) - \sqrt{\frac{P_T}{N}} r_{l,l} \hat{x}_l(k) \right|^2, \quad (2.130)$$

or equivalently, it can be rewritten as

$$\begin{aligned} 2\text{Re} \left\{ \sqrt{\frac{P_T}{N}} \tilde{v}_l(k) r_{l,l} (x_l(k) - \hat{x}_l(k)) \right\} &\geq \left| \sqrt{\frac{P_T}{N}} r_{l,l} (x_l(k) - \hat{x}_l(k)) \right|^2 \\ &:= \frac{P_T}{N} d^2(x_l(k), \hat{x}_l(k)), \end{aligned} \quad (2.131)$$

where

$$d^2(x_l(k), \hat{x}_l(k)) := |r_{l,l} (x_l(k) - \hat{x}_l(k))|^2. \quad (2.132)$$

For a given  $\mathbf{H}$  (or equivalently the matrix  $\mathbf{R}$ ), the left hand side of (2.131) is a Gaussian random variable with zero-mean and variance  $\left(\frac{4N\sigma_v^2}{P_T}\right) d^2(x_l(k), \hat{x}_l(k))$ . As a result, applying the Chernoff bound, the conditional PEP for a given  $\mathbf{H}$  is upper-bounded by

$$\begin{aligned} P(x_l(k) \rightarrow \hat{x}_l(k) | \mathbf{H}) &\leq \exp\left(-\frac{P_T d^2(x_l(k), \hat{x}_l(k))}{8N\sigma_v^2}\right) \\ &\leq \exp\left(\frac{-\rho |r_{l,l}|^2 |x_l(k) - \hat{x}_l(k)|^2}{8N}\right), \end{aligned} \quad (2.133)$$

where  $|r_{l,l}|^2$  is a sum of  $2(M-l)$  Gaussian random variable with zero-mean and variance 0.5, that is,  $|r_{l,l}|^2$  is chi-square distribution with  $2(M-l)$  degrees of freedom. Assuming that  $\mathbf{H} = \mathbf{H}_w$ , the PEP averaged, after some manipulations, over all channel realizations can be upper-bounded by

$$\begin{aligned}
P(x_l(k) \rightarrow \hat{x}_l(k)) &:= E\{P(x_l(k) \rightarrow \hat{x}_l(k) | \mathbf{H})\} \\
&\leq E\left\{\exp\left(-\frac{\rho d^2(x_l(k), \hat{x}_l(k))}{8N}\right)\right\} \\
&= \left\{1 + \frac{\rho d^2(x_l(k), \hat{x}_l(k))}{8N}\right\}^{-(M-l)}. \tag{2.134}
\end{aligned}$$

Equation (2.134) shows that the average PEP of the first (worst) layer of V-BLAST is inversely proportional to the  $(M-N+1)$ th power of SNR, and the  $M$ th power SNR for last layer. This implies that in V-BLAST system different layer has different diversity order, ranging from  $M-N+1$  to  $M$  (from the first layer to the last layer), which mean that a diversity order for a later detection stage is more than that for an earlier one.

**Example 2.5.1:** Figure 2.9 shows the BER performance of ZF V-BLAST detection as a function of SNR  $\rho$  with  $N = M = 4$  over a frequency flat MIMO channel. For comparison, we also consider the linear ZF receiver and ML receiver. Assume that BPSK modulation is used. As shown in Figure 2.9 V-BLAST receiver provides a reasonable tradeoff between the BER performance and computational complexity.

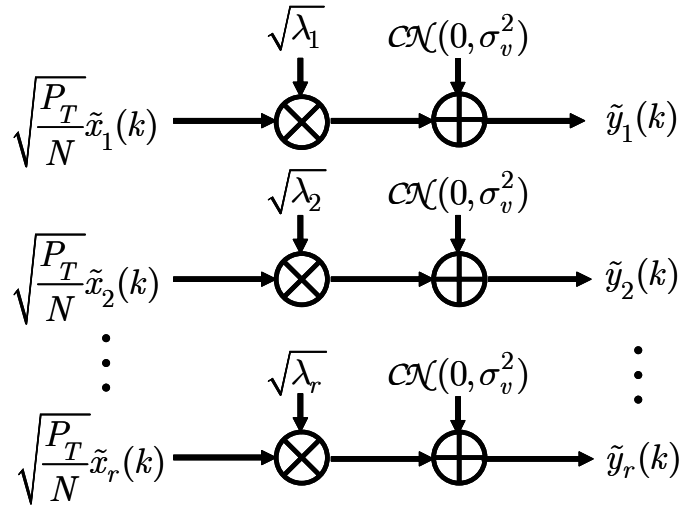


Figure 2.1: Illustration of decomposing a MIMO channel  $\mathbf{H}$  into parallel SISO channels when the channel is known to the transmitter and receiver.

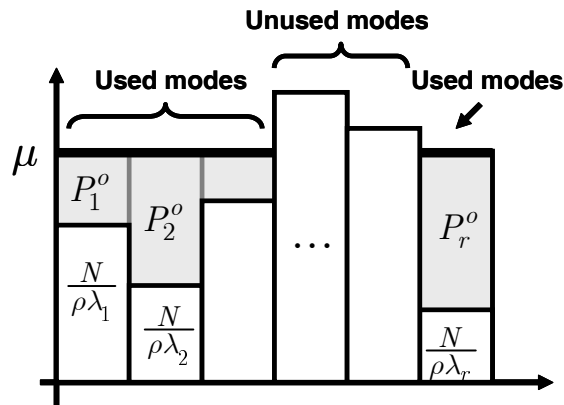


Figure 2.2: Illustration of water filling algorithm.

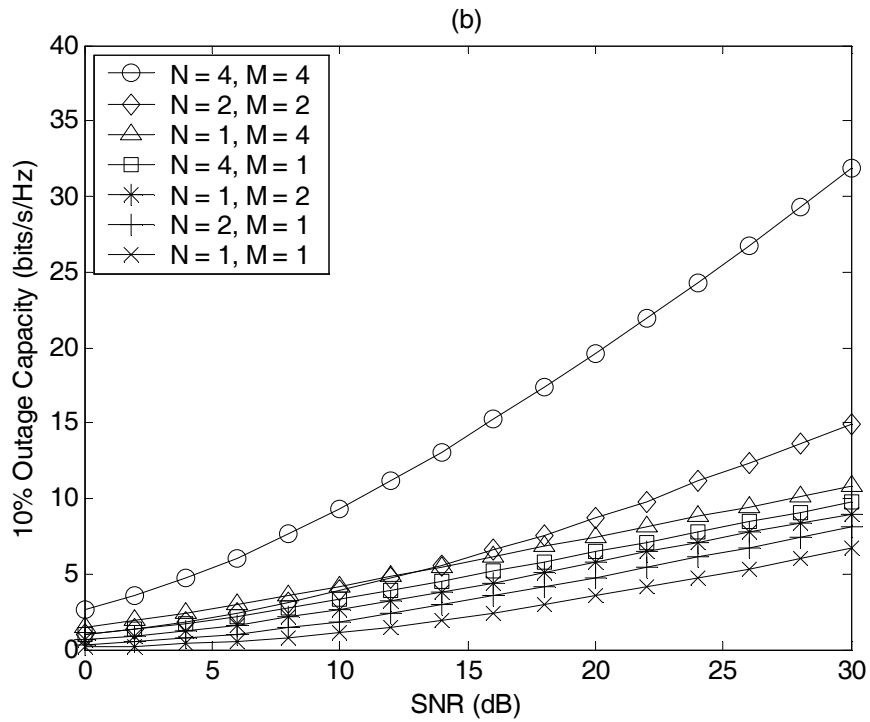
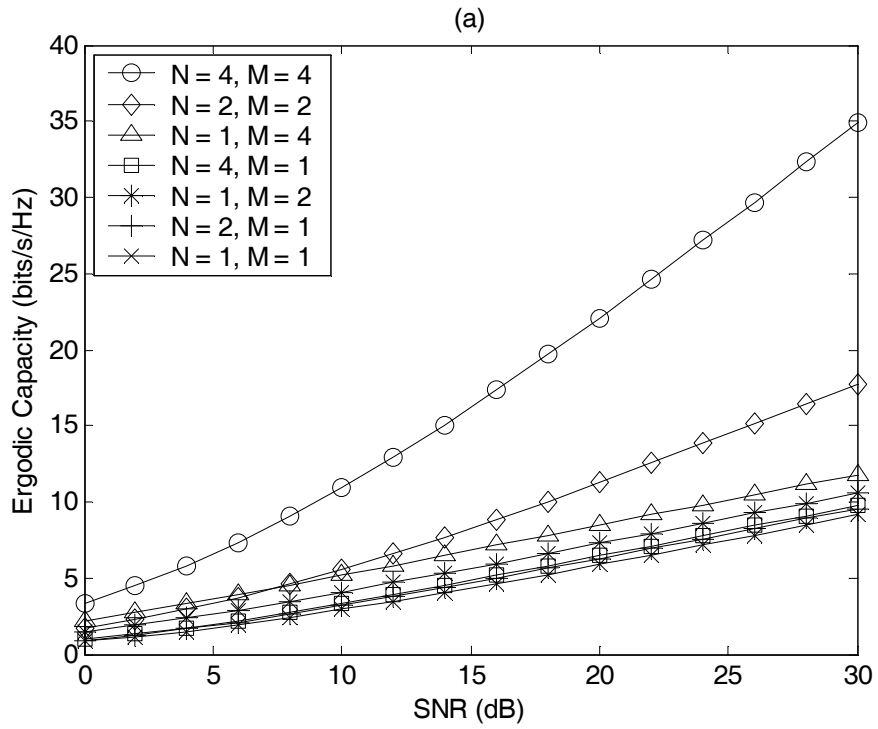


Figure 2.3: Channel capacity of several antenna configurations as a function of SNR  $\rho$ . (a) Ergodic Capacity. (b) 10% outage capacity.

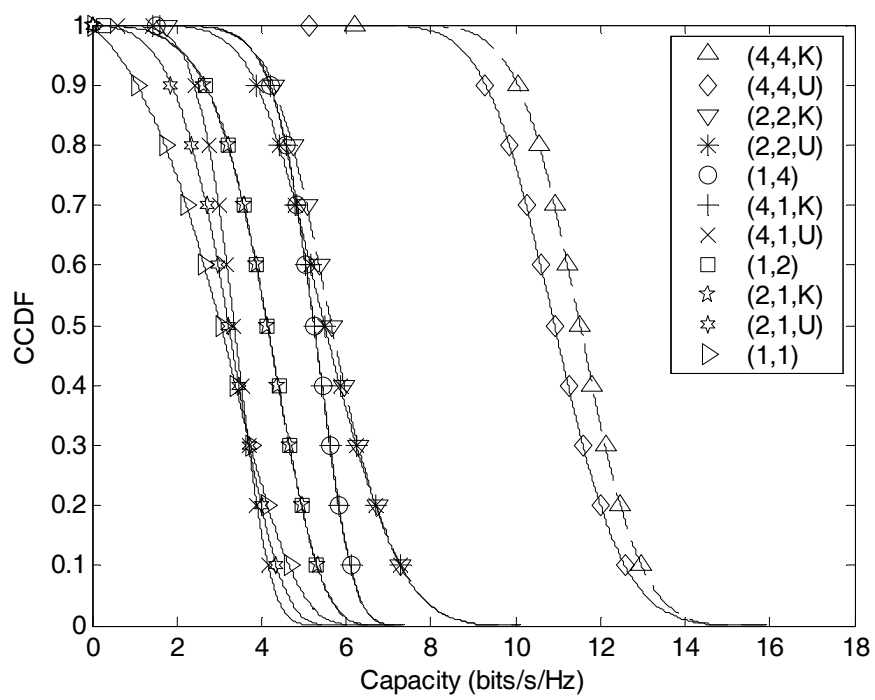


Figure 2.4: ccdf of several antenna configurations at SNR  $\rho = 10$  dB.

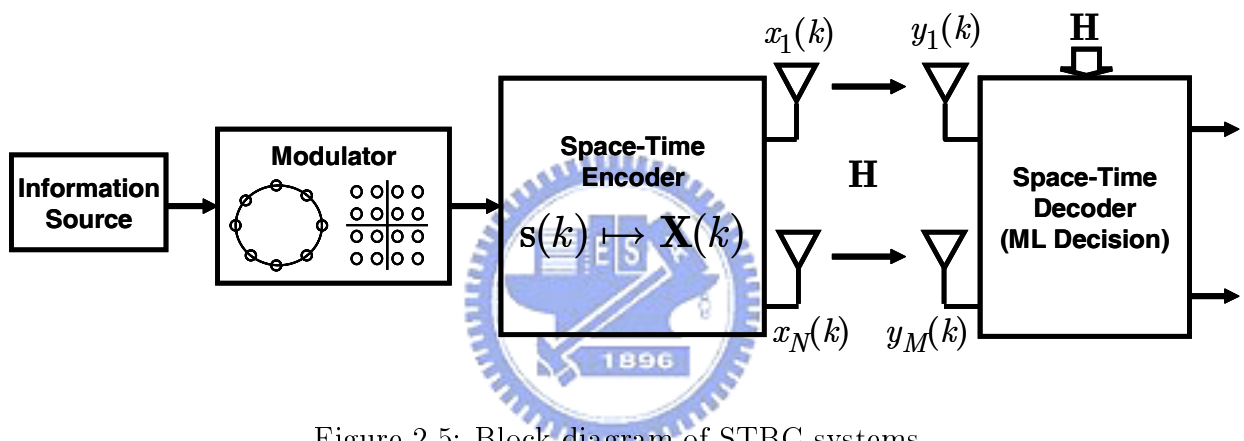


Figure 2.5: Block diagram of STBC systems.

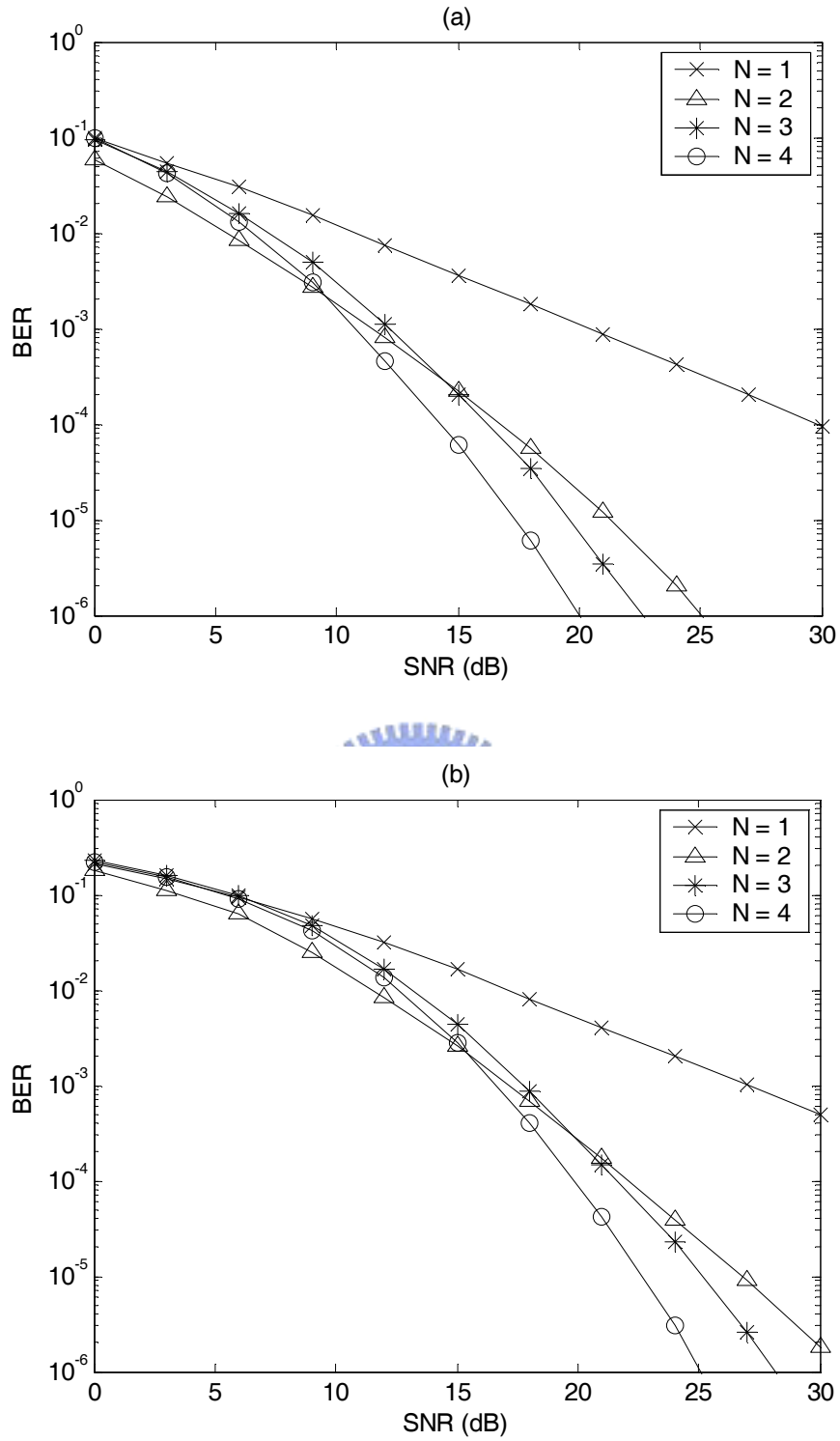
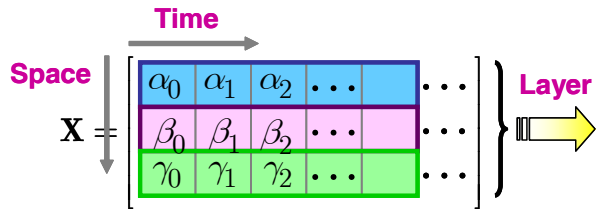
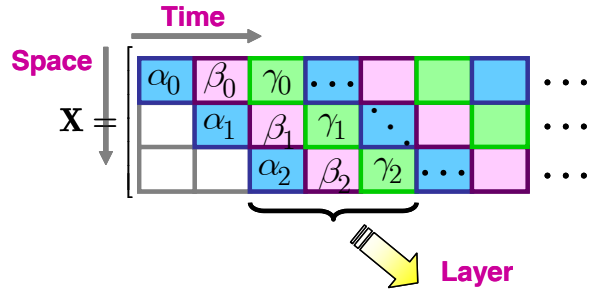


Figure 2.6: BER performance of STBCs as a function of SNR  $\rho$  for different number of transmit antennas over a frequency flat MISO channel. (a) 1 bps/Hz. (b) 2 bps/Hz.



(a)



(b)

Figure 2.7: ST encoding of SM techniques. (a) V-BLAST scheme. (b) D-BLAST scheme.

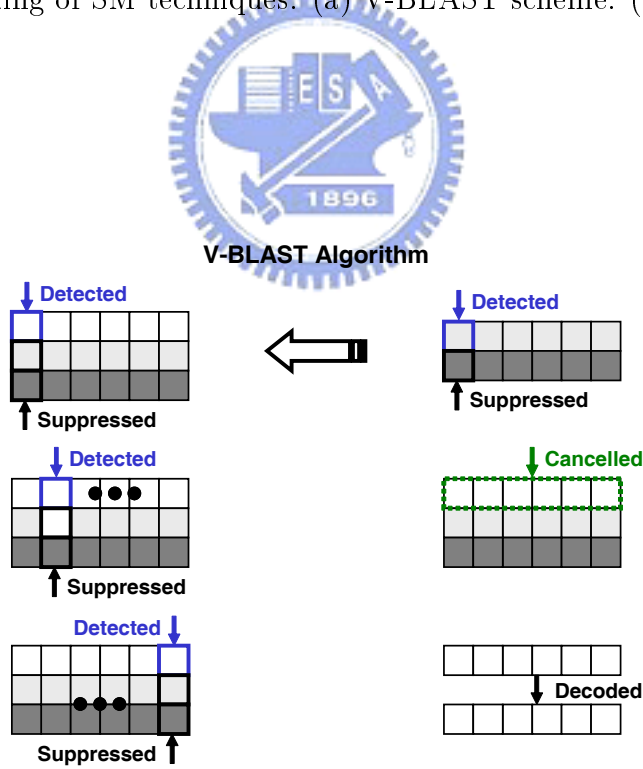


Figure 2.8: Schematic of V-BLAST detection.



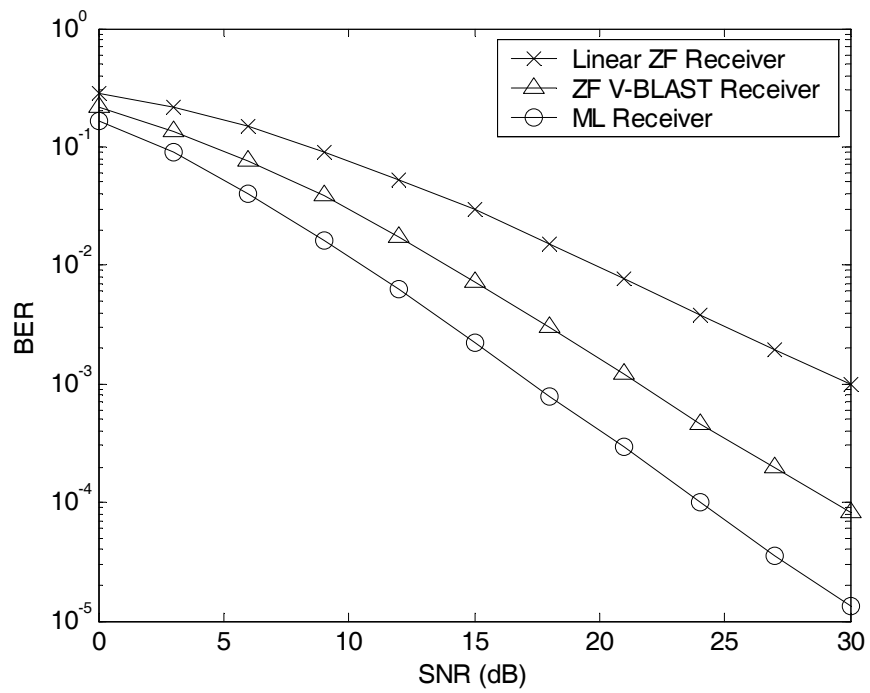


Figure 2.9: BER performance of different detection algorithms for SM systems as a function of SNR  $\rho$  with  $N = M = 4$  over a frequency flat MIMO channel.

# Chapter 3

## An OSIC Based Reduced-Rank MIMO Equalizer Using Conjugate Gradient Algorithm

### 3.1 Introduction



This chapter presents a reduced-rank (RR) (partially adaptive) MIMO MMSE DFE based on the generalized sidelobe canceller (GSC) technique [23] and a simple algebraic criterion for determining the blocking matrix of the GSC. First, the DFE is developed using the direct matrix inversion method for detecting each user signal, and suffers a certain performance degradation at high SNR due to a limited diversity order [59]. The work is then extended with significant improvements in system architecture, computational complexity, and performance. In particular, the multi-stage OSIC is introduced, and RR processing is incorporated with the aid of channel information in which a reduced size blocking matrix is chosen judiciously via the conjugate gradient (CG) algorithm [97], [98]. The CG algorithm is an iterative method for solving a system of equations and employed to obtain a set of basis

vectors for best representing the solution. The RR adaptive FF weight vector is obtained by working with a partial set of basis vectors representing a reduced size blocking matrix of the GSC. In general, the number of basis vectors required is approximately equal to the effective rank of interference subspace (i.e., number of effective interferers). With successful interference cancellation at each stage of OSIC, the number of iterations required for the convergence of the CG algorithm can be reduced stage-by-stage due to the progressively smaller interference subspace. Since the optimal weight vector is given as a by-product of the CG algorithm, computationally intensive matrix inversion due to a large data dimension can be avoided entirely, leading to a low complexity implementation. In summary, the contributions of the proposed method are two-fold: (1) The incorporation of the OSIC and CG algorithms leads to an efficient new implementation of the high dimensional MIMO DFE (2) The incorporation of the GSC and CG algorithms offers an effective new strategy for RR realization of DFE. It is ascertained by computer simulations that the proposed RR MIMO DFE can indeed achieve nearly the same performance as the full-rank MMSE equalizer under moderate conditions.

The rest of this chapter is organized as follows. Section 3.2 describes the MIMO channel and signal model. Section 3.3 explains the OSIC based MIMO MMSE equalizer. Next, a new ordering strategy and GSC equalizer for ISI suppression is proposed in Section 3.4. In Section 3.5, an OSIC based RR GSC DFE is developed using the CG algorithm. Finally, Section 3.6 shows simulation examples, and Section 3.7 concludes the chapter.

## 3.2 MIMO Channel and Signal Model

Consider an MIMO wireless communication system with  $N$  inputs (i.e.,  $N$  transmit antennas) and  $M$  outputs (i.e.,  $M$  receive antennas) over the frequency selective multipath channels.  $N$  substreams  $x_n(k)$ ,  $n = 1, 2, \dots, N$ , from the transmit antennas are passed through the MIMO channel, which is assumed to be frequency selective, to produce  $M$

received signal  $y_m(t)$  (in baseband format),  $m = 1, 2, \dots, M$ . Sampling  $y_m(t)$ 's at  $t = kT$ , where  $T$  is the symbol period, and putting them together yields an  $M \times 1$  space-only (SO) signal vector (2.15). In (2.15), the entries of  $\mathbf{h}_n(l)$ 's are assumed to be i.i.d. zero-mean complex Gaussian and are stationary over the processing period of interest, and  $x_n(k)$  is i.i.d. with zero-mean and unit-variance. Finally,  $\mathbf{v}(k)$  is the noise vector whose entries are assumed to be temporally and spatially white with the same power  $\sigma_v^2$ .

### 3.3 OSIC Based MIMO MMSE Equalizer

An OSIC based MIMO equalizer for the scenario considered consists of  $N$  successive stages, the first two of which are illustrated in Figure 3.1. The structure at each stage is a multi-dimensional single-user DFE that consists of a set of  $K_F$ -tap  $T$ -spaced feedforward filters (FFF's) and a  $K_B$ -tap  $T$ -spaced feedback filter (FBF). At the first stage, the input to the FFF bank is  $\mathbf{y}(k)$  and the input to the FBF is the detected symbol of a specific substream  $\hat{x}_n(k-d)$ , with an optimally chosen delay of  $d$  symbol periods. The choosing of  $d$  depends on  $K_F$  and  $K_B$ , and is typically  $d = K_F - 1$  for  $K_B = L$  [99]. For ST processing,  $K_F$  successive signal samples are collected and concatenated into an  $MK_F \times 1$  ST signal vector (2.21).

At a certain stage  $j$ , the detection algorithm of the OSIC based MMSE DFE can be summarized as follows [59] (with stage index  $j$  omitted for brevity):

- Ordering: Select the best substream  $n$  from all of undetected ones in the MMSE sense:

$$\varepsilon_n := 1 - \frac{P_T}{N} \mathbf{h}_{c,pr,n}^H \mathbf{R}_{c,F,n}^{-1} \mathbf{h}_{c,pr,n}, \quad (3.1)$$

where

$$\mathbf{R}_{c,F,n} := \frac{P_T}{N} \left( \mathbf{H}_{c,F,n} \mathbf{H}_{c,F,n}^H + \sum_{q \neq n} \mathbf{H}_{c,q} \mathbf{H}_{c,q}^H \right) + \sigma_v^2 \mathbf{I} \in \mathbb{C}^{MK_F \times MK_F}, \quad (3.2)$$

is the correlation matrix of  $\mathbf{y}_{c,F,n}(k)$ , which is the signal vector of the FFF part,  $\mathbf{H}_{c,F,n}$  consists of the first  $d + 1$  columns of  $\mathbf{H}_{c,n}$ , and  $\mathbf{h}_{c,pr,n}$  is the  $(d + 1)$ th column of  $\mathbf{H}_{c,n}$ . Note that, in (3.2), the summation is over the “yet-to-be-detected” substreams.

- Weight calculation: Determine the FFF weight  $\mathbf{q}_{F,n} \in \mathbb{C}^{MK_F}$  and FBF weight  $\mathbf{q}_{B,n} \in \mathbb{C}^{K_B}$  of the  $n$ th substream:

$$\begin{aligned}\mathbf{q}_{F,n} &= \sqrt{\frac{P_T}{N}} \mathbf{R}_{c,F,n}^{-1} \mathbf{h}_{c,pr,n} \\ &= \sqrt{\frac{P_T}{N}} \left[ \left( \frac{P_T}{N} \mathbf{H}_{c,F,n} \mathbf{H}_{c,F,n}^H + \sum_{q \neq n} \mathbf{H}_{c,q} \mathbf{H}_{c,q}^H \right) + \sigma_v^2 \mathbf{I} \right]^{-1} \mathbf{h}_{c,pr,n},\end{aligned}\quad (3.3)$$

$$\begin{aligned}\mathbf{q}_{B,n} &= \sqrt{\frac{P_T}{N}} \mathbf{H}_{c,pa,n}^H \mathbf{q}_{F,n} \\ &= \frac{P_T}{N} \mathbf{H}_{c,pa,n}^H \left[ \left( \frac{P_T}{N} \mathbf{H}_{c,F,n} \mathbf{H}_{c,F,n}^H + \sum_{q \neq n} \mathbf{H}_{c,q} \mathbf{H}_{c,q}^H \right) + \sigma_v^2 \mathbf{I} \right]^{-1} \mathbf{h}_{c,pr,n}\end{aligned}\quad (3.4)$$

where  $\mathbf{H}_{c,pa,n}$  consists of the  $(d + 2)$ th to  $(d + 1 + K_B)$ th columns of  $\mathbf{H}_{c,n}$ .

- Extraction: Extract the  $n$ th substream:  $z_n(k) := \mathbf{q}_{F,n}^H \mathbf{y}_{c,n}(k) - \mathbf{q}_{B,n}^H \hat{\mathbf{x}}_{B,n}(k)$ , where  $\hat{\mathbf{x}}_{B,n}(k) := [\hat{x}_n(k - d - 1), x_n(k - d - 2), \dots, \hat{x}_n(k - d - K_B)]^T \in \mathbb{C}^{K_B}$ .
- Detection: Make a decision  $\hat{x}_n(k - d)$  on  $z_n(k)$ :  $\hat{x}_n(k - d) = \mathcal{Q}(z_n(k))$ .
- Interference cancellation: Remove the contribution of the  $n$ th substream  $\hat{x}_n(k)$  (including its ISI) from the received signal:  $\mathbf{y}_{c,n}(k) - \mathbf{H}_{c,n} \hat{\mathbf{x}}_{c,n}(k)$ , where  $\mathbf{y}_{c,n}(k)$  is the input signal vector to the current stage.

In practice, at a certain stage, the SO channel matrix  $\mathbf{H}_n$  can be estimated as  $\hat{\mathbf{H}}_n$  with the aid of training symbols by using the direct sample average or least-squares method [15]. With  $\hat{\mathbf{H}}_n$  obtained, the ST block Toeplitz channel matrix  $\hat{\mathbf{H}}_{c,n}$  can then be obtained directly from  $\hat{\mathbf{H}}_n$  according to (2.22).

## 3.4 New Ordering Strategy and GSC Equalizer

The main computational complexity of the OSIC based MIMO MMSE DFE described in Section 3 involves the determination of the ordering of substream indices, and computation of the corresponding weight vectors [59]. These steps require a computational complexity of order  $O(N^2 M^3 K_F^3)$  [59], which may be too high if the FFF dimension  $MK_F$  and/or the number of transmit antennas  $N$  is large. To reduce the complexity, a simplified ordering strategy is presented, and an RR implementation of the MMSE DFE is proposed based on the generalized sidelobe canceller (GSC) technique [23], [100].

### 3.4.1 SIR Based Ordering Strategy

In the OSIC procedure, data streams are detected according to a specific ordering metric. With interference cancellation successfully performed, the system performance is affected mainly by the order in which the substreams are detected. The ordering metric as described in (3.1) is developed based on the MMSE criterion, and is computationally intensive if the ST dimension is large due to the repeated matrix inversions required at each stage. A simple alternative ordering metric without needing any matrix inversion is here suggested based on the signal-to-interference ratio (SIR) measurement:

$$\gamma_n := \frac{\|\mathbf{h}_{c,pr,n}\|^2}{\text{tr}(\mathbf{H}_{c,fu,n}^H \mathbf{H}_{c,fu,n}) + \sum_{q \neq n} \text{tr}(\mathbf{H}_{c,q}^H \mathbf{H}_{c,q})}, \quad (3.5)$$

where  $\mathbf{H}_{c,fu,n}$  consists of the first  $d$  columns of  $\mathbf{H}_{c,n}$ , and  $\text{tr}(\cdot)$  represents the trace operation of a matrix. Again, the summation in (3.5) is over the yet-to-be-detected substreams. The substream (assumed to be the  $n$ th) to be detected can then be chosen at each stage with the largest SIR measurement. Note that the proposed SIR based ordering can be determined entirely by the channel information. The proposed SIR based ordering strategy can be shown to provide better performance (lower BER at the same SNR) for a large fading variation among different transmit antennas. This will be demonstrated in the simulation section.

### 3.4.2 GSC Realization of MMSE DFE

The GSC is essentially an indirect but simpler implementation of the MVDR receiver [23]. It is a widely used structure that allows a constrained adaptive algorithm to be implemented in an unconstrained fashion. Under the GSC formulation, the FFF weight vector  $\mathbf{q}_{F,n} = \sqrt{\frac{P_T}{N}} \mathbf{R}_{c,F,n}^{-1} \mathbf{h}_{c,pr,n}$  for the selected substream at a certain stage  $j$  can be represented as

$$\mathbf{q}_{F,n} = \sqrt{\frac{P_T}{N}} (\mathbf{h}_{c,pr,n} - \mathbf{B}_n \mathbf{u}_n), \quad (3.6)$$

where  $\mathbf{B}_n \in \mathbb{C}^{MK_F \times (MK_F - 1)}$  is the blocking matrix satisfying

$$\mathbf{B}_n^H \mathbf{h}_{c,pr,n} = \mathbf{0}. \quad (3.7)$$

The goal is to choose the adaptive weight vector  $\mathbf{u}_n$  to cancel the “precursor” ISI (with the FBF  $\mathbf{q}_{B,n}$  canceling the postcursor ISI as generally assumed) and CCI. This means that the adaptive weight vector  $\mathbf{u}_n \in \mathbb{C}^{MK_F - 1}$  is designed in accordance with the following MMSE problem [23]:

$$\min_{\mathbf{u}_n} E \left\{ \left| \mathbf{h}_{c,pr,n}^H \mathbf{y}_{c,F,n}(k) - \mathbf{u}_n^H \mathbf{B}_n^H \mathbf{y}_{c,F,n}(k) \right|^2 \right\}, \quad (3.8)$$

where

$$\mathbf{y}_{c,F,n}(k) := \mathbf{H}_{c,F,n} \mathbf{x}_{F,n}(k) + \sum_q \mathbf{H}_{c,q} \mathbf{x}_{c,q}(k) + \mathbf{v}_c(k), \quad (3.9)$$

is the  $MK_F \times 1$  signal vector of the FFF part whose correlation matrix is  $\mathbf{R}_{c,F,n}$  and

$$\mathbf{x}_{F,n}(k) := [x_n(k), x_n(k-1), \dots, x_n(k-d)]^T \in \mathbb{C}^{d+1}. \quad (3.10)$$

Note that, in (3.9), the summation is over the “yet-to-be-detected” substreams. Since  $\mathbf{h}_{c,pr,n}^H \mathbf{y}_{c,F,n}(k)$  contains both the signal and interference and  $\mathbf{u}_n^H \mathbf{B}_n^H \mathbf{y}_{c,F,n}(k)$  contains the interference only, the resulting  $\mathbf{u}_n$  will cancel the interference in order to minimize the MSE. Solving (3.8) leads to:

$$\mathbf{u}_n = \sqrt{\frac{P_T}{N}} (\mathbf{B}_n^H \mathbf{R}_{c,F,n} \mathbf{B}_n)^{-1} \mathbf{B}_n^H \mathbf{R}_{c,F,n} \mathbf{h}_{c,pr,n}, \quad (3.11)$$

and thus

$$\mathbf{q}_{F,n} = \sqrt{\frac{P_T}{N}} \left[ \mathbf{I} - \mathbf{B}_n (\mathbf{B}_n^H \mathbf{R}_{c,F,n} \mathbf{B}_n)^{-1} \mathbf{B}_n^H \mathbf{R}_{c,F,n} \right] \mathbf{h}_{c,pr,n}. \quad (3.12)$$

This is called the direct-matrix-inversion (DMI) implementation of the full-rank GSC DFE. The above development represents an alternative realization of the FFF part, and do not make any change to the structure of the FBF part of the MMSE DFE. In fact, straightforward mathematical manipulation can show that the GSC DFE is equivalent to the MMSE DFE up to a scalar multiple.

In the DMI implementation, the computation of the adaptive weight vector in (3.12) involves the inversion of  $\mathbf{B}_n^H \mathbf{R}_{c,F,n} \mathbf{B}_n$ , which is  $(MK_F - 1) \times (MK_F - 1)$ . To alleviate the high computational load due to a large  $MK_F$ , an RR GSC is proposed which uses only a portion of the available degrees of freedom offered by the adaptive weights. Specifically, the RR techniques can be employed to reduce the size of  $\mathbf{B}_n$  or dimension of  $\mathbf{u}_n$  [23]. In the following, a simple and effective RR technique is proposed which is suitable for the MIMO DFE.



### 3.5 OSIC Based Reduced-Rank GSC DFE Using CG Algorithm

An OSIC based RR GSC working with a  $D^{(j)}$ -dimensional ( $D^{(j)} < MK_F$  for all  $j$ ) adaptive weight vector  $\tilde{\mathbf{u}}_n \in \mathbb{C}^{D^{(j)}}$  at the  $j$ th stage can be obtained through the use of a transformation matrix  $\mathbf{T}_n \in \mathbb{C}^{(MK_F-1) \times D^{(j)}}$  [72]-[74]. This leads to a reduced size blocking matrix

$$\tilde{\mathbf{B}}_n := \mathbf{B}_n \mathbf{T}_n \in \mathbb{C}^{MK_F \times D^{(j)}}, \quad (3.13)$$

as illustrated in Figure 3.2. The criteria for the selection of  $\mathbf{T}_n$  include: (i)  $\tilde{\mathbf{B}}_n$  should have as few columns as possible (ii) ISI and CCI should be retained as much as possible in the lower branch of the GSC. Criterion (i) is for complexity reduction and (ii) is for optimal



mutual cancellation of ISI and CCI in the upper and lower branches [75]. Criterion (ii) is equivalent to saying that a reduced size blocking matrix should be chosen such that the upper and lower branch outputs of the GSC have a large cross-correlation [75]. Since the lower branch contains no signal, the only way to maximize the cross-correlation is to retain as much ISI and CCI as possible in the lower branch. By doing so, a maximum mutual cancellation of interference can be achieved between the upper and lower branches. In the following, an efficient method for finding  $\mathbf{T}_n$  is developed based on the “conjugate gradient (CG)” algorithm, which can also avoid the inversion of  $\mathbf{B}_n^H \mathbf{R}_{c,F,n} \mathbf{B}_n \in \mathbb{C}^{(MK_F-1) \times (MK_F-1)}$  by giving  $\tilde{\mathbf{u}}_n$  as a “by-product”.

### 3.5.1 Realization of Reduced-Rank GSC by CG Algorithm

It is observed from (3.11) that  $\mathbf{u}_n$  can be considered as the solution to the following system of equations:

$$\mathbf{B}_n^H \mathbf{R}_{c,F,n} \mathbf{B}_n \mathbf{u}_n = \mathbf{B}_n^H \mathbf{R}_{c,F,n} \mathbf{h}_{c,pr,n}, \quad (3.14)$$

based on which a method is proposed in which the CG algorithm [97], [98] is employed to obtain an  $(MK_F - 1) \times D^{(j)}$  transformation matrix  $\mathbf{T}_n$  and a  $D^{(j)}$ -dimensional RR weight vector  $\tilde{\mathbf{u}}_n$  simultaneously. The CG algorithm is an iterative algorithm for solving the system  $\mathbf{A}\mathbf{x} = \mathbf{b}$ , where  $\mathbf{A}$  is a Hermitian and positive definite matrix. In particular,  $\mathbf{x}$  is obtained as a linear combination of a set of solution basis vectors generated at different iterations. An RR solution can thus be easily constructed by terminating the iterations at some stage, and working with a partial set of basis vectors [97]. Along this line, consider executing the CG algorithm for  $D^{(j)}$  iterations, as delineated in Table 1, in which:

$$\begin{aligned} \mathbf{A} &:= \mathbf{B}_n^H \mathbf{R}_{c,F,n} \mathbf{B}_n, \\ \mathbf{b} &:= \mathbf{B}_n^H \mathbf{R}_{c,F,n} \mathbf{h}_{c,pr,n}. \end{aligned} \quad (3.15)$$

After  $D^{(j)}$  iterations, the solution is approximated as

$$\mathbf{u}_n \approx \mathbf{u}_{n,D^{(j)}} = \sum_{i=1}^{D^{(j)}} \alpha_{n,i} \mathbf{t}_{n,i} := \mathbf{T}_n \mathbf{a}_n, \quad (3.16)$$

where  $\alpha_{n,i}$  and  $\mathbf{t}_{n,i}$  are the step-size and search direction, respectively, at the  $i$ th iteration.

It is easily seen from Figure 3.2 that

$$\mathbf{T}_n := [\mathbf{t}_{n,1}, \mathbf{t}_{n,2}, \dots, \mathbf{t}_{n,D^{(j)}}] \in \mathbb{C}^{(MK_F-1) \times D^{(j)}}, \quad (3.17)$$

is the transformation matrix, and

$$\tilde{\mathbf{u}}_n = \mathbf{a}_n := [\alpha_{n,1}, \alpha_{n,2}, \dots, \alpha_{n,D^{(j)}}]^T \in \mathbb{C}^{D^{(j)}}, \quad (3.18)$$

is the desired RR solution.

According to the CG algorithm, the range space of  $\mathbf{T}_n$  is equal to the ‘‘Krylov’’ subspace described by [97]

$$\text{range}\{\mathbf{T}_n\} = \text{span}\{\mathbf{b}, \mathbf{A}\mathbf{b}, \mathbf{A}^2\mathbf{b}, \dots, \mathbf{A}^{(D^{(j)}-1)}\mathbf{b}\}, \quad (3.19)$$

which is the best  $D^{(j)}$ -dimensional representation of the Wiener solution [74]. Since  $\mathbf{A}$  and  $\mathbf{b}$  represent the ISI/CCI correlation matrix and cross-correlation vector after signal blocking, we can conclude that  $\tilde{\mathbf{B}}_n = \mathbf{B}_n \mathbf{T}_n$  somehow represents a best reduced size approximation to  $\mathbf{B}_n$  in the sense that the ISI/CCI can be sufficiently retained at the lower branch of the GSC. This is also confirmed in [75] that  $\mathbf{T}_n$  can maximize the cross-correlation between the upper and lower branch outputs of the GSC, as dictated by RR processing. Another interesting property derived from the CG algorithm is that the columns of  $\mathbf{T}_n$  satisfy the  $\mathbf{A}$ -conjugacy property [97]:

$$\mathbf{t}_{n,l}^H \mathbf{A} \mathbf{t}_{n,i} = 0, \quad l \neq i, \quad i, l = 1, 2, \dots, D^{(j)}, \quad (3.20)$$

which implies that the  $D^{(j)}$  outputs from  $\tilde{\mathbf{B}}_n = \mathbf{B}_n \mathbf{T}_n$  in Figure 3.2 are mutually uncorrelated.

Replacing  $\mathbf{B}_n$  by  $\tilde{\mathbf{B}}_n$  in (3.8)-(3.11), and solving for  $\tilde{\mathbf{u}}_n$ , we have

$$\tilde{\mathbf{u}}_n = \sqrt{\frac{P_T}{N}} (\mathbf{T}_n^H \mathbf{B}_n^H \mathbf{R}_{c,F,n} \mathbf{B}_n \mathbf{T}_n)^{-1} \mathbf{T}_n^H \mathbf{B}_n^H \mathbf{R}_{c,F,n} \mathbf{h}_{c,pr,n}, \quad (3.21)$$

which, from (3.20), involves the inversion of a diagonal matrix such that

$$\tilde{u}_{n,i} = \sqrt{\frac{P_T}{N}} \frac{\mathbf{t}_{n,i}^H \mathbf{B}_n^H \mathbf{R}_{c,F,n} \mathbf{h}_{c,pr,n}}{\mathbf{t}_{n,i}^H \mathbf{B}_n^H \mathbf{R}_{c,F,n} \mathbf{B}_n \mathbf{t}_{n,i}}, \quad i = 1, 2, \dots, D^{(j)}, \quad (3.22)$$

where  $\tilde{u}_{n,i}$  is the  $i$ th element of  $\tilde{\mathbf{u}}_n$ . It can be shown, after some manipulation, that  $\tilde{u}_{n,i} = \alpha_{n,i}$  in Table 1, which confirm the earlier assertion of  $\tilde{\mathbf{u}}_n = \mathbf{a}_n$  in (3.18).

Recall that  $D^{(j)}$  is the number of iterations in the CG algorithm and represents the “dimension” for RR processing at the  $j$ th stage. According to GSC,  $D^{(j)}$  should be chosen to be the smallest number that ensures effective interference suppression. In other words,  $D^{(j)}$  should be approximately equal to the effective rank of  $\mathbf{R}_{c,F,n}$ , which contains mainly the pre-cursor ISI and CCI. At the  $j$ th stage of OSIC, there are  $N - j$  interfering substreams left, each having a rank of  $L + K_F$  due to the channel and FFF orders, and the pre-cursor ISI of the signal of rank  $d$ . This leads to the following signal-plus-interference rank at the  $j$ th stage:

$$G^{(j)} := (N - j)(L + K_F) + d + 1. \quad (3.23)$$

With successful interference cancellation at each stage of OSIC, the signal-plus-interference rank is decreased progressively such that  $G^{(N)} < G^{(N-1)} < \dots < G^{(1)}$ . Moreover, since the channel matrix in (2.22) is band Toeplitz with many zeros at the leading and trailing columns corresponding to “distant” pre- and post-cursor ISI for each substreams, the effective interference rank will be actually smaller than  $G^{(j)}$ , leading to a further reduction of processing dimension. A general criterion which works well for most scenarios is  $D^{(j)} = \lceil G^{(j)}/2 \rceil$ . Note that all the information for estimating  $G^{(j)}$  are available so  $D^{(j)}$  can be determined beforehand.

### 3.5.2 Finite Termination Property of CG

The CG algorithm converges to the exact solution  $\mathbf{u}_n$  in at most  $MK_F - 1$  iterations [97]. The following inequality is commonly used to describe its convergence during the iterations

[97], [98]:

$$\|\mathbf{e}_{n,i}\|_{\mathbf{A}} \leq 2 \left( \frac{\sqrt{\kappa_n} - 1}{\sqrt{\kappa_n} + 1} \right)^i \|\mathbf{e}_{n,0}\|_{\mathbf{A}}, \quad (3.24)$$

where

$$\|\mathbf{e}_{n,i}\|_{\mathbf{A}} := \sqrt{\mathbf{e}_{n,i}^H \mathbf{A} \mathbf{e}_{n,i}}, \quad (3.25)$$

is the  $\mathbf{A}$ -norm of the error  $\mathbf{e}_{n,i} := \mathbf{u}_n - \mathbf{u}_{n,i}$  at the  $i$ th iteration, and  $\kappa_n$  is the condition number of  $\mathbf{A}$  [98]. Assuming that it is desired to reduce the  $\mathbf{A}$ -norm error with a given factor of  $\epsilon_n$  such that  $\|\mathbf{e}_{n,D^{(j)}}\|_{\mathbf{A}} \leq \epsilon_n \|\mathbf{e}_{n,0}\|_{\mathbf{A}}$ , the number of iterations can be bounded in according with [97]:

$$D^{(j)} \leq \left\lceil \frac{1}{2} \sqrt{\kappa_n} \ln \left( \frac{2}{\epsilon_n} \right) \right\rceil, \quad (3.26)$$

where  $\lceil x \rceil$  denotes the smallest integer larger than  $x$ .

### 3.5.3 Computational Complexity

The tradeoff between system performance and computational complexity is an issue depending on the number of transmit and receive antennas  $N$ ,  $M$ , and number of FFF taps  $K_F$  of the MIMO DFE. For batch processing, the major computations in the full-rank GSC DFE at each stage of OSIC involve the inversion of  $\mathbf{B}_n^H \mathbf{R}_{c,F,n} \mathbf{B}_n$  of size  $(MK_F - 1) \times (MK_F - 1)$  as described in (3.12). The CG algorithm assisted RR GSC DFE, on the other hand, requires no matrix inversion whatsoever. In fact, the dominant operation during one iteration of the CG-GSC DFE is the  $(MK_F - 1)$ -dimensional matrix-vector product of  $\mathbf{A} \mathbf{t}_{n,i}$ . For the OSIC based MIMO MMSE DFE, the major computations at each stage involve the computation of MSE for all undetected substreams, and FFF weight vector. It requires the inversion of  $\mathbf{R}_{c,F,n}$  of size  $MK_F \times MK_F$ . For comparison, the approximate complexity (in number of complex multiplications) of the MMSE, CS, IMVDR and proposed full-rank GSC and CG-GSC equalizers are given in Table 2 (for a complete cycle of OSIC) [73], [76]. As an example, choosing  $N = 4$ ,  $M = 6$ ,  $K_F = 4$ ,  $L = 2$ ,  $d = 3$  and  $D^{(j)} = \lceil G^{(j)}/2 \rceil$ , yields the

approximate ratio of complexity of 8 : 4 : 1 : 4 : 1 for MMSE, CS, IMVDR, full-rank GSC and CG-GSC, respectively. The major advantage of CG-GSC over IMVDR is the better performance as seen later in the simulations.

### 3.5.4 Iterative Equalization with Soft Decoding

As known, a critical factor injuring the performance of DFE with hard decision is the error propagation. To remedy this, recently, Reynolds and Wang proposed a low-complexity “turbo-based” equalizer for the ISI channels [101] in accordance with the iterative MU detector in CDMA systems [102]. The basic idea is that it first replicates the ISI components by incorporating the log-likelihood ratio (LLR) information of the interference coded bits fed back from their channel decoder and then subtracts the *soft* replica from the received signal. An adaptive linear filter is considered for nulling the interference residuals based on the MMSE criterion to calculate the LLR of the filter output. After de-interleaving, the LLR values of the filter output are provided as an extrinsic information to the channel decoder. Finally, the channel decoder performs the soft-input-soft-output decoding to decode the transmitted data streams. The process is repeated in an iterative manner. Then this approach is applied in the MIMO channels. Abe and Matsumoto derived an ST turbo equalization for mitigating both the ISI and CCI [103] based on the Reynolds and Wang’s method. It is shown in [103] that the proposed detector indeed can substantially increase BER performance. However, we do not consider such an approach because that it goes beyond the objective of this chapter. It may be included in the future works for further discussion.

## 3.6 Computer Simulations

Computer simulations were conducted in this section to evaluate the performance of the proposed CG-GSC RR DFE in a packet data system. The scenario involves  $N = 4$  transmit antennas and  $M = 6$  receive antennas, and a quasi-static fading channel in which the fading

gains were i.i.d. complex Gaussian random variables. By quasi-static fading channel, it is meant that the channel is time invariant over the period of a data packet. The variance of the entries of  $\mathbf{h}_n(l)$ 's were the same and equal to  $\sigma_n^2$ . The channel order was  $L = 2$  (in symbols), and perfect channel estimation was assumed. All  $N$  data substreams were assumed QPSK modulated. Finally, the following “standard” parameters will be used throughout the section unless otherwise mentioned:

$$D^{(j)} = \left\lceil \frac{G^{(j)}}{2} \right\rceil; \quad d = 3; \quad \text{SNR} = 10 \text{ dB};$$

$$K_F = 4; \quad K_B = 2; \quad \sigma_n^2 = \frac{1}{L+1}, \quad n = 1, 2, \dots, N.$$

The average receive signal-to-noise ratio (SNR) was defined as [59]

$$\text{SNR} := \frac{P_T}{N\sigma_v^2} \sum_{n=1}^N (L+1)\sigma_n^2 = \frac{\rho}{N} \sum_{n=1}^N (L+1)\sigma_n^2,$$

which is the average SNR measured at a single receive antenna, where  $\rho := P_T/\sigma_v^2$  is the input SNR. The average BER was calculated with 25000 packets from the  $N$  substreams, with each packet composed of 50 data symbols and using a different set of complex multipath fading gains, random QPSK sequences, and white noise sequences, but with fixed multipath delays. For comparison, the MIMO MMSE DFE [59] (by direct matrix inversion), CS RR DFE [73] and IMVDR RR DFE [76] were also examined. For MMSE DFE, the ordering metric given in (3.1) was used, and for the others, the metric in (3.5) was used.

The first simulation investigates the termination property of the proposed DFE by observing the number of iterations  $D$  (RR dimension) required for the convergence of the CG algorithm at different stages of OSIC. Figure 3.3 plots the  $\mathbf{A}$ -norm error defined in (3.24) as a function of  $D$ , for  $j = 1, 2, 3, 4$ . As shown, the number of iterations required for the  $\mathbf{A}$ -norm error to reach the bottom progressively decreases as the stage index increases. This is because that the effective interference rank decreases as more and more dominating interference has been removed as stages proceed. Note that the dimensions of signal-plus-interference subspace are  $G^{(1)} = 22$ ,  $G^{(2)} = 16$ ,  $G^{(3)} = 10$ ,  $G^{(4)} = 4$ . The second set of simulations compares the convergence behavior of the CS, IMVDR and proposed RR DFE at the first stage

of OSIC as a function of iteration number  $D$ , with SNR being a control parameter. The MMSE DFE is also included for reference. The resulting BER curves are shown in Figure 3.4. As expected, the BER decreases as  $D$  increases for all three RR DFEs. The proposed DFE can achieve nearly the same performance of the MMSE DFE in ten iterations, and converges much faster than the other two for both SNR values. The numbers of iterations for convergence are about  $D \approx 5$  and  $D \approx 10$  for SNR = 10 dB and SNR = 15 dB, respectively, which are much smaller than  $G^{(1)} = 22$ . In particular, the advantage of the proposed DFE over CS and IMVDR DFEs becomes more significant at higher SNR.

In the third set of simulations, the BER performance of the proposed DFE is examined as a function of SNR, with OSIC “on” or “off” as a control parameter. With OSIC off, an MIMO DFE is used for detecting each substream individually without any ordering and interference cancellation. The results in Figure 3.5 show that the BER decreases as the input SNR increases for all equalizers. As expected, all DFEs achieve better performance with OSIC on. Again, the proposed DFE offers nearly the same performance of the MMSE DFE, but the CS and IMVDR DFEs exhibit performance saturation at high SNR, due to their limited efficiency in using the degrees-of-freedom for interference nulling. Next, the BER performance of the proposed DFE is evaluated and compared with MMSE DFE as a function of SNR, with different values of  $K_F$  and  $K_B$  as a control parameter. The results shown in Figure 3.6 indicate that the performance of both DFEs can be improved by increasing  $K_F$  and  $K_B$ . However, the improvement seems to be less significant as  $K_F$  and  $K_B$  become large. Note that for  $K_F = 2$  and  $K_B = 1$ , the number of iterations is not large enough to allow for full convergence to the optimal solution. This explains why the MMSE DFE gains the advantage in this case. Finally, the BER performance of the proposed DFE is examined as a function of SNR, with the fading gain variance  $\sigma_n^2$  being a control parameter. For the two different sets of fading gains, the total variance  $\sum_{n=1}^N \sigma_n^2$  is the same so that the same SNR is measured at each receive antenna. The resulting BER curves shown in Figure 3.7 indicate that with a larger distinction of fading gain variance

among different data substreams, both DFEs suffer from performance degradation. This is more significant for the MMSE DFE as the ordering metric it used cannot reflect the true order of the substream power.

### 3.7 Summary

An OSIC based RR MIMO MMSE DFE is proposed for combating CCI/ISI in a frequency-selective multipath fading environment. By working with the GSC technique and conjugate gradient (CG) algorithm, a reduced-dimension feedforward filter weight vector can be determined at each stage of OSIC, leading to a partially adaptive realization of the DFE. With the dominating interference successfully cancelled at each stage of OSIC, the number of iterations required for the convergence of the CG algorithm decreases accordingly for the desired signal. In particular, the optimal number of iterations can be estimated beforehand from the readily available channel information, making the CG-GSC DFE easy to use in practice. The proposed RR processing scheme is particularly suitable for equalizers for which the channel matrix is sparse in nature such that the effective interference rank is smaller than what appears in the mathematical structure. Simulations confirmed that the proposed CG-GSC DFE significantly outperforms other RR methods, and offers nearly the same performance of the full-rank MMSE DFE with a much lower computational complexity. Summarizing the above, the major contributions of the proposed new method would include a very low complexity implementation, and a new strategy of RR realization of the MIMO DFE, without sacrificing its performance.



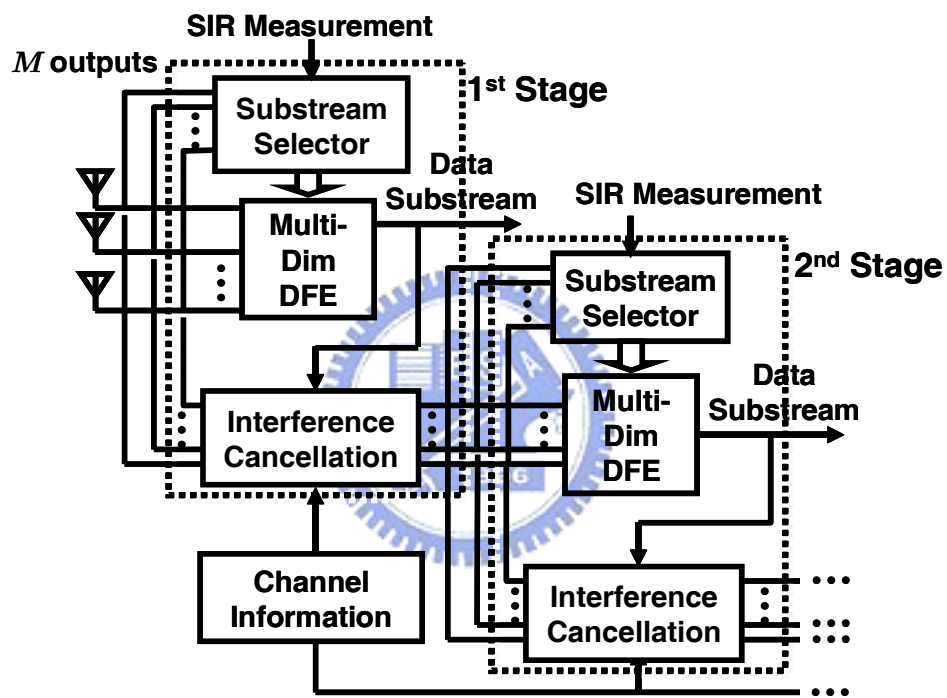


Figure 3.1: Architecture of proposed MIMO equalizer with OSIC.

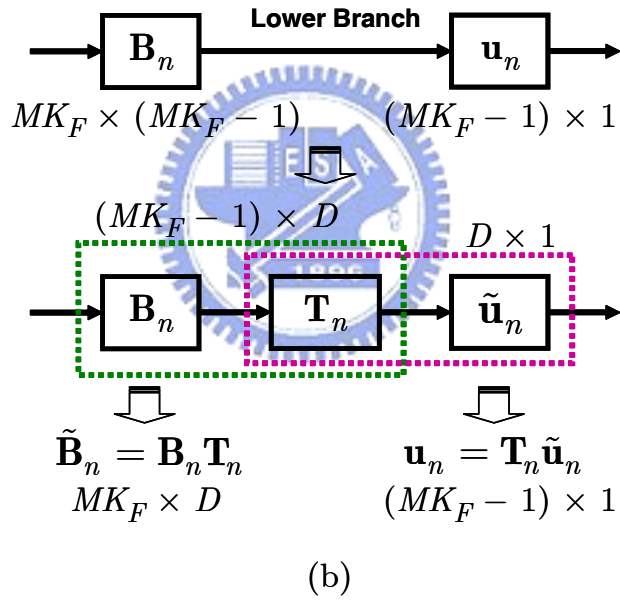
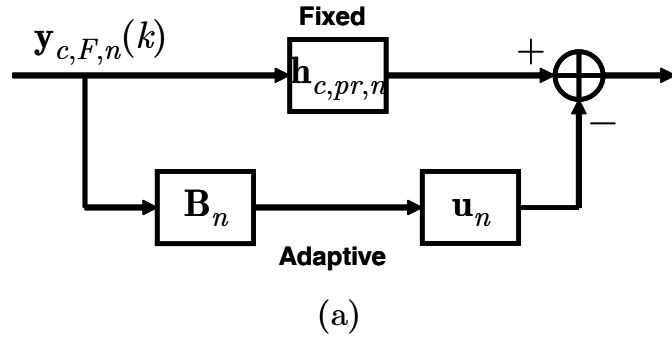


Figure 3.2: Structure of proposed RR realization of FFF using CG algorithm.

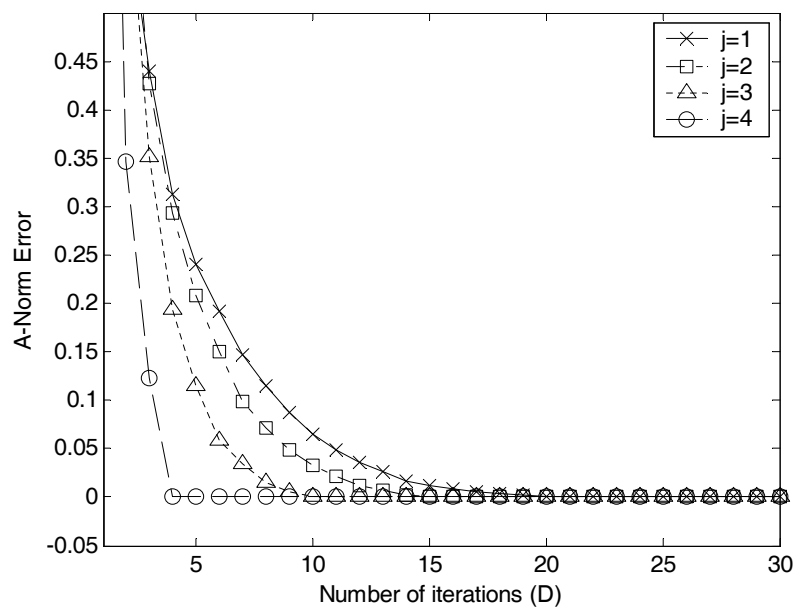


Figure 3.3: **A**-norm error of proposed CG-GSC DFE as a function of  $D$  (iteration number) at different stages of OSIC.

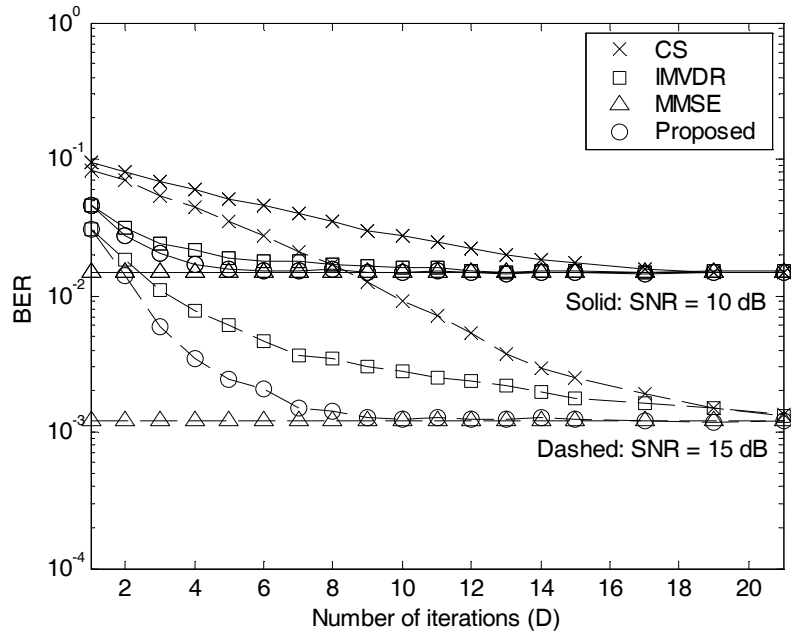


Figure 3.4: BER performance of proposed CG-GSC DFE as a function of  $D$  (iteration number), with SNR as a control parameter.

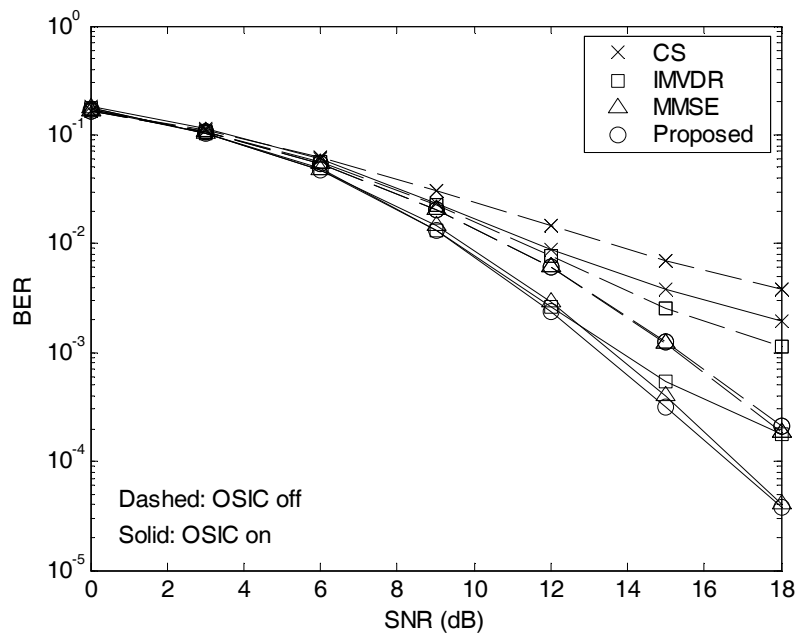


Figure 3.5: BER performance of proposed CG-GSC DFE as a function of SNR, with OSIC “on” or “off” as a control parameter.

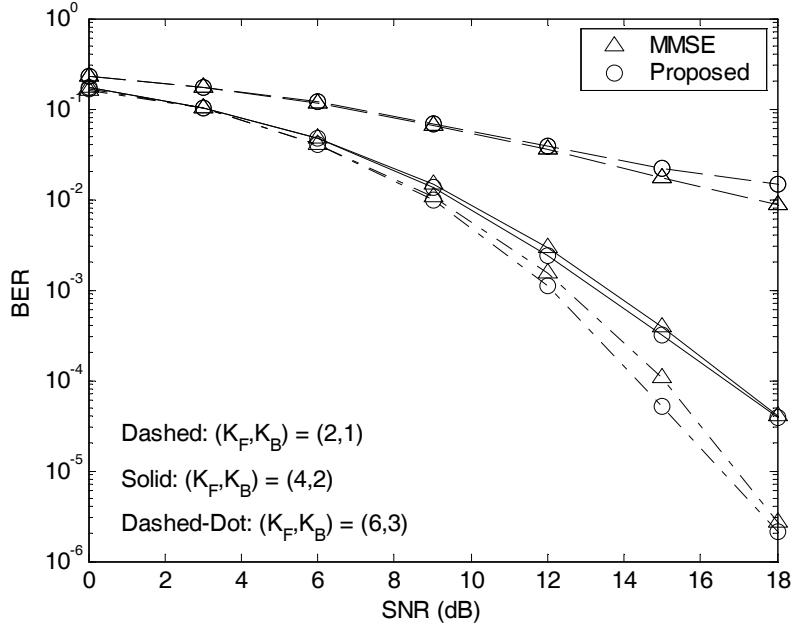


Figure 3.6: BER performance of proposed CG-GSC DFE as a function of SNR, with DFE length  $(K_F, K_B)$  as a control parameter.

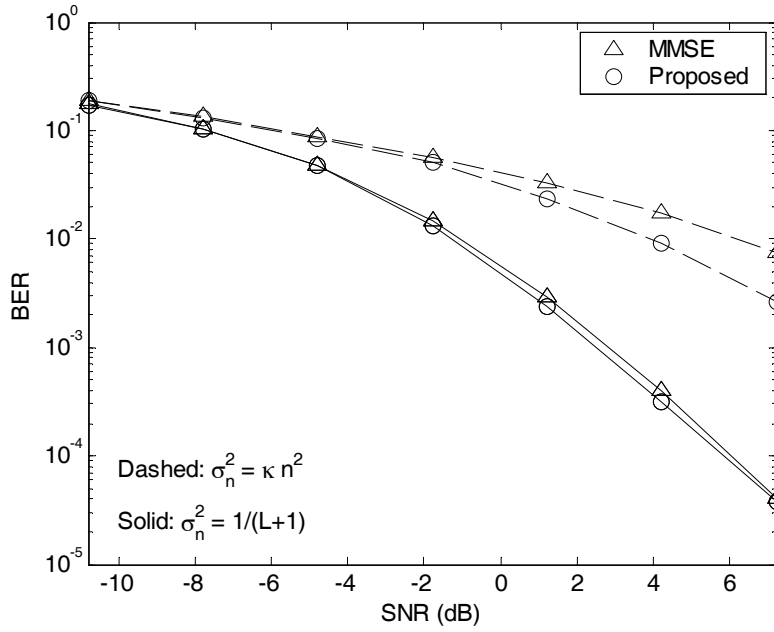


Figure 3.7: BER performance of proposed CG-GSC DFE as a function of SNR, with fading variance  $\sigma_n^2$  as a control parameter.  $\kappa$  is a normalizing scalar such that  $\sum_{n=1}^N \kappa n^2 = \frac{N}{L+1}$

Table 3.1: Conjugate Gradient Algorithm

1. Initialization:

$$\mathbf{u}_{n,0} = \mathbf{0}, \mathbf{r}_{n,0} = \mathbf{b} \text{ and } \mathbf{t}_{n,1} = \mathbf{r}_{n,0} = \mathbf{b}$$

2. Iteration:

for  $i = 1$  to  $D^{(j)}$  do

$$\alpha_{n,i} = \frac{\mathbf{r}_{n,i-1}^H \mathbf{r}_{n,i-1}}{\mathbf{t}_{n,i}^H \mathbf{A} \mathbf{t}_{n,i}}$$

$$\mathbf{u}_{n,i} = \mathbf{u}_{n,i-1} + \alpha_{n,i} \mathbf{t}_{n,i}$$

$$\mathbf{r}_{n,i} = \mathbf{r}_{n,i-1} - \alpha_{n,i} \mathbf{A} \mathbf{t}_{n,i}$$

$$\beta_{n,i} = \frac{\mathbf{r}_{n,i}^H \mathbf{r}_{n,i}}{\mathbf{r}_{n,i-1}^H \mathbf{r}_{n,i-1}}$$

$$\mathbf{t}_{n,i+1} = \mathbf{r}_{n,i} + \beta_{n,i} \mathbf{t}_{n,i}$$

end for

3. Approximate solution after  $D^{(j)}$  iterations:

$$\mathbf{u}_n = \mathbf{u}_{n,D^{(j)}}$$

Table 3.2: Computational Complexity

Method	Complexity
1. MMSE	$O\left(\frac{N^2}{2} M^3 K_F^3\right)$
2. CS	$O\left(NM^3 K_F^3 + \sum_{j=1}^N (D^{(j)})^3\right)$
3. IMVDR	$O\left(\left(\sum_{j=1}^N D^{(j)}\right) M^2 K_F^2\right)$
4. Full-rank GSC	$O(NM^3 K_F^3)$
5. CG-GSC	$O\left(\left(\sum_{j=1}^N D^{(j)}\right) M^2 K_F^2\right)$

# Chapter 4

## Group-Wise OSIC Detection in Multiuser Space-Time Dual-Signaling Wireless Systems

### 4.1 Introduction



#### *A. Motivations*

In this chapter we consider a more general class of MU ST wireless systems, in which each user's data stream is either orthogonal ST block coded (O-STBC) for transmit diversity or spatially multiplexed (SM) for high spectral efficiency. Such a system configuration has been suggested for future MIMO uplink transmission: users nearby the base station could usually send high-rate data due to relatively reliable channel conditions, whereas the far-end users might sacrifice data rate for transmit diversity in order to guard against the channel impairments like large path-loss or the near-far effect [85]. As reported in [66], [85], different signaling types can also be adopted for improving individual user's link throughput against channel spatial correlations: spatial multiplexing in general fits with independently fading channels, but transmit diversity would be alternatively preferred for correlated low-rank

channels. The overall MU link performance in all cases, however, crucially depends on effective interference rejection mechanisms. To the authors' best knowledge, there seems to be yet no related discussions aiming for a dual-signaling system; in particular, an investigation of how the orthogonal codes can facilitate the dual-mode signal separation. In this chapter, this problem will be addressed based on the OSIC detection approach.

### ***B. Design Challenge and Technical Contributions***

For the dual-signaling environment, there is a unique receiver design challenge to be addressed. Observe that, since some link users will send data via the O-STBC mode, the base station will have to suffer a certain time latency for data collection/detection so as to exploit the diversity benefit for those O-STBC terminals. For example, if the Alamouti's code [46] is used, two symbol periods are the temporal latent cost for realizing a diversity gain of order two. The inherent time latency produces link robustness for the O-STBC users at the expense of a reduced cell-wide data processing efficiency. This is because, during the processing time required for diversity, the base station will receive extra independent source symbols from other high-rate SM terminals: this can enlarge the overall data processing dimension up to a factor equal to the latent cost. As a result, there will be an unavoidable increase in the detector complexity; the computational overload could be significant, especially for the in general one symbol per-layer detection strategy of the OSIC algorithm.

This chapter proposes a group-wise OSIC detection scheme that can effectively tackle such a design challenge. Specifically, it is shown that, even though some users may send the data via the SM mode, the usage of orthogonal codes can induce a distinctive structure on the matched-filtered channel matrix (MFCM): it consists of orthogonal design [47] block submatrices. This fact is then exploited for developing a group-wise OSIC detector: at each processing step a group of symbols, transmitted either from a particular O-STBC station or from an antenna of an SM terminal during the latent time, can jointly be detected. This result is a generalization of the work for MU STBC systems to the more general dual-signaling



scenario. Note that the proposed group-wise detection is different from the method proposed in [104]. In [104], the authors consider a CDMA system with each user using single antenna and receiver locating multiple antennas. All users in this system are partitioned into several groups, each of which is assigned a unique spreading code. Therefore, the different groups can be separated by the spreading code at the receiver, leaving the multiuser interference mitigation problem between the users within a group for further process using the V-BLAST algorithm. However, the established detection property of our proposed group-wise detection, which reduces the number of stages, tends to restore the algorithm complexity back, and hence prompts an efficient receiver implementation, despite of the system model expansion for dual-mode data processing. The imbedded structure of the MFCM is moreover exploited for deriving a low-complexity algorithm realization. It can further reduce computations from the following two aspects. First, it is shown that inverting the “big” channel matrix at the initial stage, which would often dominate the overall cost, reduces to solving a set of linear equations of relatively small dimensions. Second, the computation of the initial channel matrix inverse turns out to be the only “direct” inversion operations required; there is an elegant recursive formula for computing the inverse matrix needed at each stage. Flop cost evaluations and numerical simulations are given, showing the advantages of the proposed solution over existing MU detection schemes applicable to the considered systems.

The rest of this chapter is organized as follows. Section 4.2 describes the system model. Section 4.3 specifies the MFCM. The result is then used for developing a group-wise OSIC detector in Section 4.4. Section 4.5 proposes a computationally efficient detector implementation and Section 4.6 a simple two-stage processing for dual-mode signals. Section 4.7 shows the simulation results. Finally, Section 4.8 is the conclusion. Most of the mathematical details required in our discussions are relegated to the appendix.

## 4.2 System Model

### 4.2.1 System Description and Basic Assumptions

Consider the uplink MU ST wireless system over the flat fading channels as shown in Figure 4.1, in which  $N$  transmit antennas are placed at each of the  $Q$  user terminals. The data stream of the  $q$ th user  $s_q(k)$  ( $q = 1, 2, \dots, Q$ ) can be either O-STBC [47] for transmit diversity or SM [56] for achieving high data rate. Let  $\mathcal{S}_D$  and  $\mathcal{S}_M$  be respectively the index sets of the O-STBC and SM users, with  $Q_D := |\mathcal{S}_D|$  and  $Q_M := |\mathcal{S}_M|$  denoting the respective cardinalities. Specifically,  $Q_D$  and  $Q_M$  are respectively the numbers of the O-STBC users and SM users so that  $Q = Q_D + Q_M$ . At each O-STBC terminal, consecutive  $P$  symbols of the data stream are spatially and temporally encoded according to [47], and are then transmitted across  $N$  antenna elements over  $K$  time periods. During the same signaling epochs each SM user then sends  $NK$  independent symbols; there are thus in total

$$L_T := PQ_D + NKQ_M \quad (4.1)$$

data symbols transmitted from the  $Q$  users every  $K$  symbol periods. The two ST signaling schemes in the considered system can be completely described by the associated  $N \times K$  ST codeword matrices. A commonly used codeword description is the linear matrix modulation representation [4]. Let us divide the data stream of the  $q$ th user  $s_q(k)$  into groups of substreams as  $s_{q,l}(k) := s_q(L_q k + l - 1)$ ,  $l = 1, 2, \dots, L_q$ , where the number of substreams  $L_q$  depends on the signaling mode chosen for the  $q$ th user so that  $L_q = P$  if  $q \in \mathcal{S}_D$  and  $L_q = NK$  if  $q \in \mathcal{S}_M$ . Then the codeword matrix of the  $q$ th user can be written as

$$\mathbf{X}_q(k) := \sum_{l=1}^{2L_q} \mathbf{A}_{q,l} \tilde{s}_{q,l}(k), \quad (4.2)$$

in which  $\mathbf{A}_{q,l} \in \mathbb{C}^{N \times K}$  is the ST modulation matrix, the split real-valued symbols  $\tilde{s}_{q,l}(k) := \text{Re}\{s_{q,l}(k)\}$  for  $l = 1, 2, \dots, L_q$  and  $\tilde{s}_{q,l}(k) := \text{Im}\{s_{q,l-L_q}(k)\}$  for  $l = L_q + 1, L_q + 2, \dots, 2L_q$ .

We note that, for  $q \in \mathcal{S}_D$ ,  $\mathbf{X}_q(k)$  is an orthogonal design [47] with [4]

$$\begin{cases} \mathbf{A}_{q,k}\mathbf{A}_{q,l}^H = \frac{K}{L_q}\mathbf{I}_N & k = l \\ \mathbf{A}_{q,k}\mathbf{A}_{q,l}^H + \mathbf{A}_{q,l}\mathbf{A}_{q,k}^H = \mathbf{O}_N & k \neq l. \end{cases} \quad (4.3)$$

For  $q \in \mathcal{S}_M$ , there is no imbedded coding structure in  $\mathbf{X}_q(k)$ , leaving each  $\mathbf{A}_{q,l}$  an  $N \times K$  matrix with only single nonzero entry equal to 1 or  $\sqrt{-1}$ . Although the O-STBC and SM schemes are quite different in nature, the linear matrix modulation representation (4.2) does provide a consistent description of the respective codeword matrices. Moreover, the splitting of the source symbols into the real and imaginary parts will also unify both the problem formulation and the underlying analysis, *regardless of the constellations*.

We assume that  $M$  ( $\geq Q_D + NQ_M$ ) antenna elements are located at the receiver. Let  $y_m(k)$  be the received discrete-time signal, sampled at the symbol-rate, from the  $m$ th receive antenna and define  $\mathbf{y}(k) := [y_1(k), y_2(k), \dots, y_M(k)]^T \in \mathbb{C}^M$ . Collecting  $\mathbf{y}(k)$  over  $K$  successive symbol periods, we have the ST signal model (2.72). The following assumptions are made in the sequel.

- (a1) The symbol streams  $s_q(k)$ ,  $q = 1, 2, \dots, Q$ , are i.i.d. with zero-mean and unit-variance.
- (a2) Each entry of the MIMO channel matrix  $\mathbf{H}_q$ ,  $q = 1, 2, \dots, Q$ , is i.i.d. complex Gaussian random variable with zero-mean and unit-variance, and assumed to be static during the  $K$  signaling periods.
- (a3) The noise  $\mathbf{V}(k)$  is spatially and temporally white, each entry being with zero-mean and variance  $\sigma_v^2$ .
- (a4) We assume that at least one user signals the data in the STBC mode, hence  $Q_D \geq 1$ .
- (a5) We consider the case  $N \leq 4$  and hence, according to [47], the symbol block length  $P \in \{2, 4\}$ . The proposed approach is exclusively applicable to this scenario.
- (a6) For  $3 \leq N \leq 4$  with complex-valued constellations, the half rate codes [47] are used.
- (a7) The number of receive antennas is chosen so that  $M \geq Q_D + NQ_M$ .

## 4.2.2 Vectorized Signal Model

To facilitate the detection and analysis, we consider the equivalent vectorized signal model (2.77) as described in Section 2.4.1. Without loss of generality we assume that, for each  $q \in \mathcal{S}_M$ , the  $NK$  symbols  $s_{q,l}(k)$ 's are renumbered so that the  $n$ th group of  $K$  symbols, namely,  $s_{q,l}(k)$  for  $l = (n-1)K+1, (n-1)K+2, \dots, nK$ , are precisely those sent via the  $n$ th transmit antenna ( $n = 1, 2, \dots, N$ ). Through linearly combining the received signal  $\mathbf{y}_c(k)$  with  $\mathbf{H}_c$ , we can obtain the MF signal vector (2.80), and we will thus detect the transmitted data streams based on the MF model (2.80). To better manifest the core ideas, throughout the context we will focus on the real-valued constellation case, and hence  $K = P$  so that  $L_T := PQ_D + PNQ_M$ . There are essentially the same results (see Appendices B and D) for our reports whenever complex-valued constellations are used.

## 4.3 Matched-Filtered Channel Matrix

For the particular MU STBC system, it can be easily shown that all the  $P \times P$  block submatrices of MFCM  $\mathbf{F}$  are orthogonal designs [47]. For the considered dual-signaling platform, in which the SM signaling could induce severe coupling effects against the O-STBC signals, the structure of the resultant  $\mathbf{F}$  could largely deviate from that of the MU STBC system. As we will see in what follows, the matrix  $\mathbf{F}$  in the dual-signaling environment, however, does preserve the appealing block orthogonal structure. This fact is primarily the guts for developing a group-wise OSIC detector.

To characterize  $\mathbf{F}$ , we should note that its diagonal submatrices (of appropriate dimensions) are basically the effective MF signal components of the  $Q$  users' streams, whereas the off diagonal submatrices account for the inter-user signal interference. In view of this observation, one can thus classify the block submatrices of  $\mathbf{F}$  based on these signal and interference "signatures". As such, the linear matrix modulation representation of the codeword matrices (4.2) will allow a systematic way of computing these signature matrices and, based

on which, the structure of  $\mathbf{F}$  can be readily determined. Since each user sends data via either the SM or the O-STBC mode, there are essentially *two* types of signal signatures, one associated with a signaling scheme. Also, among all the interference signatures there are only *three* distinct canonical building blocks needed to be identified: two of which reflect the interference between each pair of distinct users adopting the same signaling strategy; the other is thus for the different-signaling interference. To further specify these signatures, we shall first determine the respective dimensions. Recall that during consecutive  $K$  time slots ( $K = P$  for unity code rate), the numbers of symbols sent from an O-STBC and an SM terminal are, respectively,  $P$  and  $NP$ . As a result, if we denote  $\mathbf{F}_{p,q}$  the submatrix of  $\mathbf{F}$  representing the interference signature between the  $p$ th and the  $q$ th users' streams, we then have  $\mathbf{F}_{p,q} \in \mathbb{R}^{P \times P}$  for  $p, q \in \mathcal{S}_D$ ,  $\mathbf{F}_{p,q} \in \mathbb{R}^{NP \times NP}$  for  $p, q \in \mathcal{S}_M$ , and  $\mathbf{F}_{p,q} \in \mathbb{R}^{P \times NP}$  for  $p \in \mathcal{S}_D$  and  $q \in \mathcal{S}_M$ . All such three  $\mathbf{F}_{p,q}$ 's, together with the signal signature  $\mathbf{F}_{q,q}$  for either  $q \in \mathcal{S}_D$  or  $q \in \mathcal{S}_M$ , are described in the next lemma.

In the sequel, we denote by  $\mathcal{O}(P)$  the set of all  $P \times P$  real orthogonal designs with constant diagonal entries as specified in [47].

**Lemma 4.3.1.** *Let  $\mathbf{F}_{p,q}$  be the submatrix of  $\mathbf{F}$  describing the mutual coupling between the  $p$ th and the  $q$ th users. Then we have the following results.*

- (1) *If  $p, q \in \mathcal{S}_D$ , then  $\mathbf{F}_{p,q} \in \mathcal{O}(P)$ . In particular, we have  $\mathbf{F}_{q,q} = \alpha_q \mathbf{I}_P$  for some scalar  $\alpha_q$ .*
- (2) *If  $p, q \in \mathcal{S}_M$ , then each  $P \times P$  submatrix of  $\mathbf{F}_{p,q} \in \mathbb{R}^{NP \times NP}$  is a scalar multiple of  $\mathbf{I}_P$ .*
- (3) *If  $p \in \mathcal{S}_D$  and  $q \in \mathcal{S}_M$ , then each  $P \times P$  submatrix of  $\mathbf{F}_{p,q} \in \mathbb{R}^{P \times NP}$  belongs to  $\mathcal{O}(P)$ .*

■

*Proof:* See Appendix A. □

Part (1) of Lemma 4.3.1 is known from [47] and can be exploited for developing a user-wise group OSIC detector for the MU STBC systems. The significance of Lemma 4.3.1 lies in (2) and (3), which are more relevant to a dual-signaling scenario. For  $p, q \in \mathcal{S}_M$ , it is easy

to see that the  $(i, j)$ th  $P \times P$  submatrix of  $\mathbf{F}_{p,q}$ ,  $1 \leq i, j \leq N$ , characterizes the coupling effect between the data streams transmitted from the  $i$ th antenna of the  $p$ th user and from the  $j$ th antenna of the  $q$ th user; for  $p = q$  and  $i = j$ , this is precisely the single-antenna SM signal signature. Since spatial multiplexing does not impose any spatial and temporal coding structure among the transmitted data, the interference between any pair of SM streams sent from two different antennas, and the respective signal components, would appear to be spatially and temporally decoupled. Hence, as evidenced by (2), the resultant signatures are diagonal matrices; the diagonal entries are all equal since the propagation channels are assumed to be static during  $K$  signaling instants. The independently-distributed SM streams, on the other hand, might interfere against the O-STBC signals to induce a coupling matrix that is no longer orthogonal. Part (3) of Lemma 4.3.1 shows that the resultant coupling signature is nonetheless block-wise an orthogonal design. To interpret this result, we first note that a single-antenna SM stream may only temporally interfere with an O-STBC codeword. The temporally-decoupled nature of SM data is likely to render the temporal correlation of O-STBC streams unchanged, resulting in an orthogonal type signature. The above discussions show that the symbol stream from a single SM antenna will introduce a set of diagonal blocks (the coupling among the same SM type streams) and a set of orthogonal design blocks (the coupling against the O-STBC signals) in the MFCM  $\mathbf{F}$ . This result relies solely on the multiplexing nature among all the  $NQ_M$  signals, *irrespective of the number of transmit antennas placed on each SM terminal*. In light of this observation, the asserted structure of the matrix  $\mathbf{F}$  will be preserved particularly when single-antenna cell users are present, as long as each one transmits independent symbols along his own antenna.

Since a matrix being a scalar multiple of  $\mathbf{I}_P$  is essentially a  $P \times P$  orthogonal design, Lemma 4.3.1 asserts that in the dual-signaling case, the MFCM  $\mathbf{F}$  does consist of orthogonal design based block submatrices. The presence of SM terminals thus substantially preserves the block orthogonal structure of  $\mathbf{F}$ . In the next section this fact will be exploited for developing a group-wise OSIC detector for the considered MU dual-signaling system.

**Remarks:**

(R1) As we will see in the next section, the proposed group-wise detection property benefits uniquely from the distinctive structures of  $\mathbf{F}$  specified as in Prop. 3.1. This attractive property thus also holds whenever single-input terminals exist (since the inherent structure of  $\mathbf{F}$  is preserved).

(R2) For complex constellations, there are analogue results as in Lemma 4.3.1, with possible modifications of the matrix dimensions; these are included in Appendices B and D.

## 4.4 Group-Wise OSIC Detection

For an MU STBC system, it has been shown in the following that the OSIC detector can per stage jointly detect a group of  $P$  symbols associated with a particular user. By exploiting the distinctive structure of the matrix  $\mathbf{F}$  shown in Lemma 4.3.1, this section proposes a group-wise OSIC detection scheme for the considered dual-signaling system. As we will see, the OSIC detector can per stage jointly detect a group of  $P$  symbols, transmitted either from an O-STBC terminal or from a single antenna of an SM station. This implies that only  $Q_D + NQ_M$  processing layers are required for separating the  $P(Q_D + NQ_M)$  transmitted dual-mode symbol streams. As a result, in a dual-signaling case, the “user-wise” group detection property of the O-STBC signals is preserved, and the “antenna-wise” detection for SM streams comes out as a nice byproduct. The proposed group detection capability can prevent significant computational overload due to the signal model expansion for processing the dual-mode signals.

### 4.4.1 OSIC Ordering

The OSIC algorithm resorts to certain ordering strategy, depending on the criterion for signal recovery, for deciding the best reliable symbol to be detected in each processing stage

[56]. Based on Lemma 4.3.1, in what follows we will show that the OSIC ordering in each processing layer sorts the symbol streams to be detected into a group-wise basis, which in turn results in a group-wise detector realization.

**1) Zero-Forcing (ZF) Criterion:** In the ZF OSIC detection, the optimal detection order at each step is determined by the index of the symbol decision statistics yielding maximal post-detection SNR [56]. Based on the MF signal model (2.80), the ZF decision vector in the initial stage is

$$\mathbf{s}_d(k) := \mathbf{F}^{-1}\mathbf{z}(k) = \mathbf{s}_c(k) + \mathbf{F}^{-1}\mathbf{v}(k). \quad (4.4)$$

Equation (4.4) shows that, for  $l = 1, 2, \dots, L_T$ , the  $l$ th symbol decision statistics, that is, the  $l$ th component of  $\mathbf{F}^{-1}\mathbf{z}(k)$ , is simply the desired symbol contaminated by the additive noise  $\mathbf{e}_l^T \mathbf{F}^{-1}\mathbf{v}(k)$ , where  $\mathbf{e}_l$  is the  $l$ th unit standard vector in  $\mathbb{R}^{L_T}$ . It is straightforward to compute the noise power as

$$\sigma_{0,l}^2 := E \left\{ \left| \mathbf{e}_l^T \mathbf{F}^{-1}\mathbf{v}(k) \right|^2 \right\} = \frac{\sigma_v^2}{2} \mathbf{e}_l^T \mathbf{F}^{-1} \mathbf{e}_l. \quad (4.5)$$

Since all the transmitted symbols are of equal variance, (4.4) and (4.5) imply that the (average) SNR in the  $l$ th decision statistics is completely determined by the  $l$ th diagonal entry of the noise covariance  $\mathbf{F}^{-1}$ . In particular, a small  $[\mathbf{F}^{-1}]_{l,l}$  (the  $l$ th diagonal entry of  $\mathbf{F}^{-1}$ ) implies a large SNR, and hence better detection accuracy attained by the  $l$ th branch. As a result, the optimal detection order at the initial stage, which specifies the symbol with slightest noise corruption, is obtained by searching for the index  $l = 1, 2, \dots, L_T$  at which  $[\mathbf{F}^{-1}]_{l,l}$  is minimal. As a result, the optimal index can be found as long as one can explicitly know the diagonal entries of the inverse matrix  $\mathbf{F}^{-1}$ . In the next theorem we will see that the matrix  $\mathbf{F}^{-1}$  “inherits” the key features of  $\mathbf{F}$  as established in Lemma 4.3.1. This result directly alleviates the efforts to search for the optimal index, and allows for a group-wise detection strategy. Also, this will lead to a very efficient procedure for computing the weighting matrices for recovering the symbol groups.

We need the following notation. For a fixed symbol block length  $P$  and a positive integer  $L$ , let us define  $\mathcal{F}(L)$  to be the set of all invertible real symmetric  $PL \times PL$  matrices such



that, for  $\mathbf{X} \in \mathcal{F}(L)$ , with  $\mathbf{X}_{i,j}$  being the  $(i, j)$ th  $P \times P$  block submatrix, we have  $\mathbf{X}_{i,i} = \gamma_i \mathbf{I}_P$  for some scalar  $\gamma_i$ , and  $\mathbf{X}_{i,j} \in \mathcal{O}(P)$ , for  $i \neq j$ , the set of  $P \times P$  real orthogonal design with equal diagonal entries.

**Theorem 4.4.1.** *Let  $\mathbf{F}$  be the MFCM as defined in (2.80). Then the inverse matrix of  $\mathbf{F}$  belongs to the set  $\mathcal{F}(L)$ , where  $L := Q_D + NQ_M$ . ■*

*Proof:* Lemma 4.3.1 shows that each  $P \times P$  block off-diagonal submatrix of  $\mathbf{F}$  belongs to  $\mathcal{O}(P)$ , and hence  $\mathbf{F} \in \mathcal{F}(Q_D + NQ_M)$ . The following lemma, which characterizes the inverse of the set of matrices in  $\mathcal{F}(L)$ , is used for proving Theorem 4.4.1.

**Lemma 4.4.1.** *If  $\mathbf{X} \in \mathcal{F}(L)$ , then so is  $\mathbf{X}^{-1}$ . ■*

*Proof:* See Appendix C. □

Since  $\mathbf{F} \in \mathcal{F}(Q_D + NQ_M)$ , the result then follows immediately from Lemma 4.4.1. □

Theorem 4.4.1 asserts that the  $PL$  diagonal entries of  $\mathbf{F}^{-1}$  assume  $L$  distinct levels only. It suffices to search among the  $L$  values, one associated with a symbol group transmitted from either an O-STBC user or from a single antenna of an SM terminal, for the optimal detection order. At the initial stage, the ZF OSIC ordering thus sorts the symbol to be detected into a group-wise basis; all the  $P$  symbols within one group are of equal detection priority. The OSIC detector can then jointly detect a group of  $P$  symbols, either of a particular O-STBC stream or of a single-antenna SM stream. The optimal group detection index is

$$\bar{l}_0 = \arg \min_l \beta_{0,l}, \quad (4.6)$$

where  $\beta_{0,l}$  is the  $((l - 1)P + 1)$ th diagonal entry of  $\mathbf{F}^{-1}$ ; the ZF weighting matrices are determined from the corresponding indexed columns of  $\mathbf{F}^{-1}$ .

The detected user's signal is cancelled from the received signal (2.77), yielding a reduced-size data model containing the yet-to-be-detected signals. With such a detect-and-cancel procedure followed by an associated linear combining of the resultant signal as in (2.80), it

can be directly verified that, at the  $i$ th stage, where  $i = 1, 2, \dots, L - 1$ , the noise covariance matrix associated with ZF decision statistics vector is

$$\mathbf{F}_i^{-1} := (\mathbf{H}_{c,i}^T \mathbf{H}_{c,i})^{-1} \in \mathbb{R}^{(L_T - iP) \times (L_T - iP)}, \quad (4.7)$$

where  $\mathbf{H}_{c,i}$  is obtained by deleting  $i$  block(s) of  $P$  columns (corresponding to the previously detected signals) from  $\mathbf{H}_c$ . Since  $\mathbf{F}_i = \mathbf{H}_{c,i}^T \mathbf{H}_{c,i} \in \mathbb{R}^{(L_T - iP) \times (L_T - iP)}$  is simply obtained by deleting the associated  $i$  block(s) of  $P$  columns and rows from  $\mathbf{F}$ , the matrix  $\mathbf{F}_i$  exhibits the same algebraic structure as  $\mathbf{F}$ . More precisely, we have  $\mathbf{F}_i \in \mathcal{F}(L - i)$ , and so is  $\mathbf{F}_i^{-1}$  by Lemma 4.4.1. This shows that the  $P(L - i)$  diagonal entries of  $\mathbf{F}_i^{-1}$  take on only  $(L - i)$  different levels and, by following the previous analysis, group-wise detection can thus be done at each processing step.

**2) Minimum Mean Square Error (MMSE) Criterion:** The MMSE OSIC ordering at each layer picks up the symbol attaining the minimal mean square error for detection. At the initial stage, the joint MMSE weight that minimizes the metric

$$\varepsilon_0 := E \left\{ \left\| \mathbf{s}_c(k) - \mathbf{W}_0^T \mathbf{z}(k) \right\|_2^2 \right\}, \quad (4.8)$$

is obtained as

$$\mathbf{W}_0 = \left[ \mathbf{F} + \frac{\sigma_v^2}{2} \mathbf{I}_{L_T} \right]^{-1}. \quad (4.9)$$

It is easy to compute the  $l$ th symbol mean square error, i.e.,

$$\varepsilon_{0,l} := E \left\{ \left| \mathbf{e}_l^T [\mathbf{s}_c(k) - \mathbf{W}_0^T \mathbf{z}(k)] \right|^2 \right\} = \mathbf{e}_l^T \left[ \left( \frac{2}{\sigma_v^2} \right) \mathbf{F} + \mathbf{I}_{L_T} \right]^{-1} \mathbf{e}_l. \quad (4.10)$$

Equation (4.10) shows that the optimal MMSE OSIC ordering is determined by the index of the minimal diagonal entry of  $[(2/\sigma_v^2) \mathbf{F} + \mathbf{I}_{L_T}]^{-1}$ . Since  $\mathbf{F} \in \mathcal{F}(L)$  and adding diagonal perturbation  $\mathbf{I}_{L_T}$  to a scaled  $\mathbf{F}$  essentially preserves the block orthogonal structure, it follows immediately that  $[(2/\sigma_v^2) \mathbf{F} + \mathbf{I}_{L_T}] \in \mathcal{F}(L)$  and so is  $[(2/\sigma_v^2) \mathbf{F} + \mathbf{I}_{L_T}]^{-1}$  by Lemma 4.4.1. The  $PL$  symbol mean square errors (diagonal entries of  $[(2/\sigma_v^2) \mathbf{F} + \mathbf{I}_{L_T}]^{-1}$ ) can thus be categorized into  $L$  groups of constant elements, one associated with a symbol group transmitted

from either an O-STBC user or from a single antenna of an SM terminal (as in the ZF case). This thus warrants the group-wise MMSE detection in the initial layer. Through the group detect-and-cancel process, it can be checked that, at the  $i$ th stage ( $i = 1, 2, \dots, L - 1$ ), the symbol mean square errors are computed as the diagonal entries of  $[(2/\sigma_v^2) \mathbf{F}_i + \mathbf{I}_{P(L-i)}]^{-1}$ , where  $\mathbf{F}_i = \mathbf{H}_{c,i}^T \mathbf{H}_{c,i}$ . Since  $[(2/\sigma_v^2) \mathbf{F}_i + \mathbf{I}_{P(L-i)}]^{-1} \in \mathcal{F}(L-i)$ , so is the inverse matrix (again by Lemma 1). This shows that mean square errors in the  $i$ th layer are sorted into the same group-wise manner, hence allowing for a group-wise MMSE detection.

#### 4.4.2 Algorithm Outline and Related Discussions

The proposed group-wise OSIC algorithm is outlined in Table 4.1 (in Table 4.1,  $\bar{\mathbf{H}}_{c,\bar{l}_i}$  is the channel matrix obtained from  $\mathbf{H}_c$  corresponding to the  $\bar{l}$ th group of data stream in the  $i$ th stage, and  $Q(\cdot)$  is the slicing operation associated with the adopted symbol constellation). Several discussions regarding the proposed method are given as follows.

(D1) The group-wise detection property benefits uniquely from the use of the orthogonal codes. When non-orthogonal codes are used, the  $PL$  diagonal entries of  $\mathbf{F}^{-1}$  in general will take on  $PL$  different levels: one has to resort to a symbol-wise based algorithm realization. Therefore,  $PL$  stages are needed for separating the  $PL$  dual-mode signals; the resultant algorithm complexity, however, could be large.

(D2) It is noted that, even if orthogonal codes are used, the appealing group-wise detection property does not hold if the number of the transmit antennas of each user is greater than four (for  $N > 4$ , the matrix  $\mathbf{F}$  is observed to lose the special structure as specified in Lemma 4.3.1). The assumption  $N \leq 4$  is thus necessary regarding the feasibility of the group-wise detection. This requirement can usually be met in practice since, to reduce the implementation cost and physical size, it is undesirable to place too many antenna elements on the user handsets.

(D3) In principle, the ZF metric aims for complete nulling of the interference from other

users but is subject to possible noise enhancement, whereas the MMSE criterion focuses on joint suppression of interference and noise. Although the two design metrics resort to different strategies for symbol recovery, in the considered scenario they both lead to the appealing group-wise detection property. This is because the respective optimal detection orders in each processing layer, as shown in the above discussions, are determined by the diagonal entries of certain structured matrices belonging to the family  $\mathcal{F}(L)$  (this is also a unique feature pertaining to O-STBC).

(D4) Another dual-signaling environment is seen in the mono-link systems recently considered in [107], in which a subset of antenna elements are selected for transmitting the Alamouti coded streams, while the others are left for spatial multiplexing. It is noted that, in this single-user scenario, the (antenna-wise) symbol synchronization assumption is typically satisfied, and the proposed group-wise OSIC detector can be used for separating the multi-antenna symbol streams.

#### 4.4.3 Conservation of Spatial Resource: CDMA Based Implementation

In the current framework, the assumption on the number of receive antennas  $M \geq Q_D + NQ_M$  is needed since only the spatial resource is employed for removing the multi-access interference (MAI). This requirement seems critical in practice because  $M$  could be prohibitively large in a user-dense environment. A typical approach to conserving the spatial resource is to alternatively adopt the multi-access techniques, e.g., CDMA, for MAI mitigation [14]. Basically, the MAI can be effectively suppressed through chip despreading, as long as all the cell user are assigned with distinct spreading (signature) codes; in this case, only  $M \geq N$  receive antennas are required in order to separate the symbol streams for each SM user. However, since the code resource could usually be limited, especially for the high-speed demand in which small spreading gains are preferred, some users may

have to share the same code, such that the antenna resource is still necessary for further MAI rejection. Hence, a conceivable implementation allowing for a moderate spatial cost is to incorporate CDMA, leverage the code resource to mitigate MAI from the distinct-code users, and reserve the spatial resource to tackle MAI among the remaining same-code users. The assumption  $M \geq Q_D + NQ_M$ , as a result, would not be too severe since  $Q_D$  and  $Q_M$  merely account for the numbers of the same-code O-STBC and SM terminals. The proposed group-wise detection property remains true when separation of the same-code user's signals is considered (see Appendix E).

**Remark:** It should be noted that, in a CDMA based implementation, the cell-wide synchronization is no longer necessary since the MAI among distinct-code users can be rejected through despreading. As a result, only the data streams transmitted from the same-code users need to be aligned for further signal separation: symbol synchronization is required merely within a user subset, namely, the same-code user group, but not for all the user terminals.



## 4.5 Low-Complexity Algorithm Implementation

By further exploiting the embedded structure of the MFCM  $\mathbf{F}$  and its inverse, this section derives a low-complexity detector realization. Since the ZF and MMSE weighting matrices exhibit essentially the same algebraic structure (namely, both fall within the class  $\mathcal{F}(L)$  for some  $L$ ), the discussions will focus on the ZF case for notational simplicity. In what follows it will be shown that the computation of  $\mathbf{F}^{-1}$ , which would often dominate the cost, boils down to solving a set of linear equations of relatively small dimensions. Moreover, inverting the “big”  $\mathbf{F}$  in the initial stage turns out to be the only direct matrix inversion to be performed; the inverse matrix  $\mathbf{F}_i^{-1}$  required at each subsequent stage can be recursively computed based on the parameters available in the previous stage. Flop count analysis is also provided for complexity comparison with other competitive methods.

### 4.5.1 Computation of $\mathbf{F}^{-1}$

Recall from Theorem 4.4.1 that *every*  $P \times P$  block off-diagonal submatrix of  $\mathbf{F}^{-1}$  is a  $P \times P$  orthogonal design, and each diagonal block is sparse (it is a scalar multiple of  $\mathbf{I}_P$ ). This imposes certain structural redundancy in  $\mathbf{F}^{-1}$  that should be carefully tackled for avoiding the computation of duplicate parameters. Indeed, since a  $P \times P$  orthogonal design is completely characterized by  $P$  independent variables [47], it suffices to determine one column, say, the last one, for each off-diagonal block submatrix; the rest columns can simply be obtained from the last one through some known linear transformations [47]. For each diagonal block, in particular, only one unknown needs to be found. The aforementioned *a priori* structural information shows that, to completely specify  $\mathbf{F}^{-1}$ , we only need to find its  $(jP)$ th columns for  $1 \leq j \leq L$ : this amounts to solving the linear equations of reduced dimensions

$$\mathbf{F}\mathbf{G} = \mathbf{E}, \tag{4.11}$$

in which  $\mathbf{G}$  and  $\mathbf{E}$  are  $L_T \times L$  matrices whose  $l$ th columns are, respectively, the  $(jP)$ th columns of  $\mathbf{F}^{-1}$  and the identity matrix  $\mathbf{I}_{L_T}$ . To solve for the unknown  $\mathbf{G}$  based on (4.11), one can further take into account the sparse nature of  $\mathbf{G}$ . Specifically, for the  $j$ th column  $\mathbf{g}_j$ , we *must* have  $g_{i,j} = 0$  for  $(j-1)P + 1 \leq i \leq jP - 1$ ; the imbedded  $P - 1$  consecutive zero entries in  $\mathbf{g}_j$  come from the last column of the  $j$ th  $P \times P$  diagonal block of  $\mathbf{F}^{-1}$ . As a result, only the nonzero entries are to be determined. Moreover, since  $\mathbf{F}^{-1}$  is Hermitian, in each  $\mathbf{g}_j$ , we only have to compute the entries *lying below*  $g_{jP-1,j}(= 0)$ . In summary, for the  $j$ th column  $\mathbf{g}_j$ , only the last  $P(L - j) + 1$  entries are to be determined. It is noted that the number of unknowns is decreased by an amount of  $P$  as the column index  $j$  increases to  $j + 1$  (for the last column  $\mathbf{g}_{jP-1}$ , only one unknown is yet to be computed).

To incorporate the above structural information for solving (4.11), let  $\mathbf{F} = \mathbf{L}\mathbf{L}^T$ , where  $\mathbf{L}$  is an  $L_T \times L_T$  lower triangular matrix, be a Cholesky factorization [97] of the matrix  $\mathbf{F}$ ; such a factorization is typically required for inverting a nonsingular square real symmetric

matrix [97]. In terms of columns of  $\mathbf{G}$  and  $\mathbf{E}$ , (4.11) can thus be equivalently rewritten as

$$\mathbf{L}\mathbf{L}^T\mathbf{g}_j = \mathbf{e}_j, \quad 1 \leq j \leq L. \quad (4.12)$$

Since  $\mathbf{L}$  is lower triangular and hence  $\mathbf{L}^T$  is upper triangular, a standard approach to solve for the unknown column vector  $\mathbf{g}_j$  in (4.12) is the forward and back substitutions [97]: for each  $j$ , it first solves  $\mathbf{L}\mathbf{u}_j = \mathbf{e}_j$ , where  $\mathbf{u}_j := \mathbf{L}^T\mathbf{g}_j$ , by forward substitutions for the intermediate vector  $\mathbf{u}_j$  and then backward solves  $\mathbf{L}^T\mathbf{g}_j = \mathbf{u}_j$  for the desired unknown  $\mathbf{g}_j$ . As long as the intermediate vector  $\mathbf{u}_j$  is obtained, the back substitution process successively computes the elements in  $\mathbf{g}_j$  one after another, starting from the *last* entry (since  $\mathbf{L}^T$  is upper triangular). Since the unknowns to be determined in each  $\mathbf{g}_j$  all lie below the entry  $g_{jP-1,j}(=0)$ , the back substitution procedure simply terminates as long as  $g_{jP,j}$  is computed; the remaining entries on top of  $g_{jP-1,j}$  are redundant since  $\mathbf{F}^{-1}$  is Hermitian.

**Remark:** In the MMSE OSIC case, an alternative for computing the initial MMSE weight  $[(2/\sigma_v^2)\mathbf{F} + \mathbf{I}_{L_T}]^{-1}$  is to decompose  $\mathbf{F} = \mathbf{H}_c^T\mathbf{H}_c$  into a sum of  $L_T$  rank-one matrices, each being an outer-product of a row of the channel matrix  $\mathbf{H}_c$ , and then uses the Sherman-Morrison formula to recursively obtain the solution [108]. Such a recursive procedure does not seem to be a good choice for the considered structured inverse computation. This is because the recursive formulation, each time incorporating a “piece” of the channel matrix component, renders it difficult to exploit the structural information (seen based on the “whole” channel matrix) for discarding the redundant coefficients for computational reduction. In the proposed algorithm [108] (see (28) in [108]), the adopted recursive computation of  $\mathbf{F}^{-1}$  at each step needs to perform the  $PM$  dimensional matrix and vector operations. After performing  $PL$  steps, the total number of flop counts is thus

$$C_{Benesty} = \frac{7}{2}P^3L^2M + \frac{5}{2}P^2LM, \quad (4.13)$$

where  $M$  is the number of receive antennas with  $M \geq L$ . For the proposed method, according to [97], the number of flop counts<sup>1</sup> of performing the Cholesky factorization of  $\mathbf{F}$  is

$$\begin{aligned} C_{Cholesky} &= \frac{1}{3}N^3Q_M^3 + N^2P^2Q_DQ_M^2 + \frac{1}{2}N^2Q_M^2 + NP^2Q_D^2Q_M - 2NP^2Q_DQ_M \\ &\quad + 3NPQ_DQ_M + \frac{1}{3}P^2Q_D^3. \end{aligned} \quad (4.14)$$

The number of flop counts of the forward substitution for solving  $\mathbf{u}_j$ ,  $1 \leq j \leq L$ , is

$$\begin{aligned} C_{Forward} &= \frac{1}{3}N^3P^2Q_M^3 + \frac{1}{2}N^2P^2Q_DQ_M^2 - N^2PQ_D^2Q_M + \frac{1}{3}NP^2Q_D^3 \\ &\quad + \frac{3}{2}NP^2Q_D^2Q_M - \frac{1}{2}NP^2Q_DQ_M^2 - 4NPQ_DQ_M. \end{aligned} \quad (4.15)$$

To solve  $\mathbf{g}_j$ ,  $1 \leq j \leq L$ , by the backward substitution, we will need

$$\begin{aligned} C_{Backward} &= \frac{1}{3}N^3P^2Q_M^3 + \frac{3}{2}N^2P^2Q_M^2 - 2N^2PQ_D^2 + \frac{1}{2}NP^2Q_D^2Q_M \\ &\quad - 2NP^2Q_DQ_M + NP^2Q_D^3 - \frac{1}{2}P^2Q_D^2 \end{aligned} \quad (4.16)$$

flop counts. As a result, the total number of flop counts for solving  $\mathbf{F}^{-1}$  is

$$\begin{aligned} C_{initial} &= \frac{2}{3}N^3P^2Q_M^3 + \frac{1}{3}N^3Q_M^3 + \frac{3}{2}N^2P^2Q_DQ_M^2 + \frac{3}{2}N^2P^2Q_M^2 - N^2PQ_D^2Q_M \\ &\quad - 2N^2PQ_D^2 + \frac{1}{2}N^2Q_M^2 + \frac{1}{3}NP^2Q_D^3 + \frac{3}{2}NP^2Q_D^2Q_M - 4NP^2Q_DQ_M \\ &\quad - NPQ_DQ_M + NP^2Q_D^3 + \frac{3}{2}NP^2Q_D^2Q_M - \frac{1}{2}NP^2Q_DQ_M^2 + \frac{1}{3}P^2Q_D^3 \\ &\quad - \frac{1}{2}P^2Q_D^2. \end{aligned} \quad (4.17)$$

It can be seen that the proposed method requires less computation.

## 4.5.2 Recursive Computation of $\mathbf{F}_i^{-1}$

Recall from Section 4.4 that, at the  $i$ th stage, the inverse matrix  $\mathbf{F}_i^{-1} := (\mathbf{H}_{c,i}^T \mathbf{H}_{c,i})^{-1}$ , where  $\mathbf{H}_{c,i}$  is obtained by deleting  $i$  block(s) of  $P$  columns from  $\mathbf{H}_c$ , is required for determining the optimal detection order and the associated weighting matrix. With  $\mathbf{F}^{-1}$  obtained

---

<sup>1</sup>The low-order terms which are insignificant to the total count are neglected.



in the initial stage, in what follows we will show how  $\mathbf{F}_i^{-1}$  at each stage can be recursively computed based on  $\mathbf{F}_{i-1}$  and  $\mathbf{F}_{i-1}^{-1}$ .

It is noted again that, at the  $i$ th processing stage,  $i = 1, 2, \dots, L - 1$ , the matrix  $\mathbf{F}_i = \mathbf{H}_{c,i}^T \mathbf{H}_{c,i}$  is simply obtained from  $\mathbf{F}_{i-1}$  ( $= \mathbf{H}_{c,i-1}^T \mathbf{H}_{c,i-1}$ ) by deleting one block of  $P$  columns and the corresponding indexed block of  $P$  rows. Without loss of generality, we may assume that the last column and row blocks of  $\mathbf{F}_{i-1}$  are to be deleted; otherwise we can simply permute those to be discarded to the right and bottom ends of  $\mathbf{F}_{i-1}$  to fit the prescribed form. As a result, we can partition  $\mathbf{F}_{i-1}$  as

$$\mathbf{F}_{i-1} = \left[ \begin{array}{c|c} \mathbf{F}_i & \mathbf{B}_{i-1} \\ \hline \mathbf{B}_{i-1}^T & \mathbf{D}_{i-1} \end{array} \right], \quad (4.18)$$

where  $\mathbf{B}_{i-1} \in \mathbb{R}^{(L_T - iP) \times P}$  and  $\mathbf{D}_{i-1} = d_{i-1} \mathbf{I}_P$  for some scalar  $d_{i-1}$  are to be deleted. Denote by  $\bar{\mathbf{F}}_{i-1}$  the  $(L_T - iP) \times (L_T - iP)$  principle submatrix of  $\mathbf{F}_{i-1}^{-1}$  obtained by deleting its last  $iP$  columns and last  $iP$  rows; the matrix  $\bar{\mathbf{F}}_{i-1}$  is thus available from the  $(i - 1)$ th stage. From (4.18) and by using the inversion lemma for block matrix,  $\bar{\mathbf{F}}_{i-1}$  can be expressed in terms of  $\mathbf{F}_i$ ,  $\mathbf{B}_{i-1}$ , and  $\mathbf{D}_{i-1}$  as

$$\bar{\mathbf{F}}_{i-1} = (\mathbf{F}_i - \mathbf{B}_{i-1} \mathbf{D}_{i-1}^{-1} \mathbf{B}_{i-1}^T)^{-1} = (\mathbf{F}_i - d_{i-1}^{-1} \mathbf{B}_{i-1} \mathbf{B}_{i-1}^T)^{-1}, \quad (4.19)$$

where the second equality in (4.19) follows since  $\mathbf{D}_{i-1} = d_{i-1} \mathbf{I}_P$ . Equation (4.19) links the matrix  $\mathbf{F}_i$ , which is to be inverted at the  $i$ th step, to the elements of  $\mathbf{F}_{i-1}$  and  $\mathbf{F}_{i-1}^{-1}$ , which are available from the previous stage. In particular, it follows immediately from (4.19) that  $\mathbf{F}_i = \bar{\mathbf{F}}_{i-1}^{-1} + d_{i-1}^{-1} \mathbf{B}_{i-1} \mathbf{B}_{i-1}^T$ , and we can use the matrix inversion lemma [4] to obtain

$$\begin{aligned} \mathbf{F}_i^{-1} &= (\bar{\mathbf{F}}_{i-1}^{-1} + d_{i-1}^{-1} \mathbf{B}_{i-1} \mathbf{B}_{i-1}^T)^{-1} \\ &= \bar{\mathbf{F}}_{i-1} - \bar{\mathbf{F}}_{i-1} \mathbf{B}_{i-1} (\mathbf{B}_{i-1}^T \bar{\mathbf{F}}_{i-1} \mathbf{B}_{i-1} + d_{i-1} \mathbf{I}_P)^{-1} \mathbf{B}_{i-1}^T \bar{\mathbf{F}}_{i-1}. \end{aligned} \quad (4.20)$$

From (4.20), we can see that the computation of the  $(L_T - iP) \times (L_T - iP)$  inverse matrix  $\mathbf{F}_i^{-1}$  is relieved into inverting the  $P \times P$  matrix  $\mathbf{B}_{i-1}^T \bar{\mathbf{F}}_{i-1} \mathbf{B}_{i-1} + d_{i-1} \mathbf{I}_P$ , which is of a lower

dimension. In fact, the efforts to invert this  $P \times P$  matrix can be reduced even further. To see this, we need the next result.

**Theorem 4.5.1.** *Let  $\mathbf{B}_{i-1}$  and  $\bar{\mathbf{F}}_{i-1}$  be defined in (4.18) and (4.19), respectively. Then it follows that  $\mathbf{B}_{i-1}^T \bar{\mathbf{F}}_{i-1} \mathbf{B}_{i-1} = \lambda_{i-1} \mathbf{I}_P$  for some scalar  $\lambda_{i-1}$ .  $\blacksquare$*

*Proof:* For a fixed  $i$ , let us define  $J := L - i$ . For  $1 \leq k, l \leq J$ , denote by  $\mathbf{U}_{k,l}$  the  $(k, l)$ th  $P \times P$  block submatrix of  $\bar{\mathbf{F}}_{i-1}$ . We drop the index indicating the dependency of  $J$  and  $\mathbf{U}_{k,l}$  on the number of stage  $i - 1$  to simplify notation. Let us write  $\mathbf{B}_{i-1} = [\mathbf{B}_1^T, \mathbf{B}_1^T, \dots, \mathbf{B}_J^T]^T$ , where  $\mathbf{B}_k \in \mathcal{O}(P)$ ; then it follows immediately that

$$\mathbf{B}_{i-1}^T \bar{\mathbf{F}}_{i-1} \mathbf{B}_{i-1} = \sum_{k,l=1}^J \mathbf{B}_k^T \mathbf{U}_{k,l} \mathbf{B}_l = \sum_{k=1}^J \mathbf{B}_k^T \mathbf{U}_{k,k} \mathbf{B}_k + \sum_{k,l=1, k \neq l}^J \mathbf{B}_k^T \mathbf{U}_{k,l} \mathbf{B}_l. \quad (4.21)$$

Since  $\bar{\mathbf{F}}_{i-1} \in \mathcal{F}(J)$ , we have by definition  $\mathbf{U}_{k,k} = \eta_k \mathbf{I}_k$  for some scalar  $\eta_k$ : the first summation on the right-hand-side of the second equality in (4.21) thus simplifies as  $\sum_{k=1}^J \mathbf{B}_k^T \mathbf{U}_{k,k} \mathbf{B}_k = \sum_{k=1}^J \eta_k \mathbf{B}_k^T \mathbf{B}_k = \eta \mathbf{I}_P$  for some scalar  $\eta$ . On the other hand, it can be shown that  $\mathbf{B}_k^T \mathbf{U}_{k,l} \mathbf{B}_k \in \mathcal{O}(P)$  [47], and this implies  $\mathbf{B}_k^T \mathbf{U}_{k,k} \mathbf{B}_l + \mathbf{B}_l^T \mathbf{U}_{l,k} \mathbf{B}_k = \alpha_{k,l} \mathbf{I}_P$  for some scalar  $\alpha_{k,l}$ . As a result, we have  $\sum_{k,l=1, k \neq l}^J \mathbf{B}_k^T \mathbf{U}_{k,l} \mathbf{B}_l = \tilde{\eta} \mathbf{I}_P$  for some scalar  $\tilde{\eta}$ , and the assertion follows.  $\square$

Theorem 4.5.1 implies

$$\mathbf{B}_{i-1}^T \bar{\mathbf{F}}_{i-1} \mathbf{B}_{i-1} + d_{i-1} \mathbf{I}_P = c_{i-1} \mathbf{I}_P, \quad (4.22)$$

and, from (4.20), we reach the following key equation for inverting the matrix  $\mathbf{F}_i^{-1}$

$$\mathbf{F}_i^{-1} = \bar{\mathbf{F}}_{i-1} - c_{i-1}^{-1} \bar{\mathbf{F}}_{i-1} \mathbf{B}_{i-1} \mathbf{B}_{i-1}^T \bar{\mathbf{F}}_{i-1}. \quad (4.23)$$

Given  $\mathbf{F}_{i-1}$  and  $\mathbf{F}_{i-1}^{-1}$ , equation (4.23) provides a simple recursive formula for computing  $\mathbf{F}_i^{-1}$  without any direct matrix inversion operations. The proposed recursive approach for computing  $\mathbf{F}_i^{-1}$  is basically a block based implementation of the method in [108] introduced for the conventional symbol-wise OSIC algorithm. A distinctive feature of our scheme, nonetheless, is the attractive simplification of (4.20) to (4.23), with which the computation of the  $P \times P$  inverse matrix  $(\mathbf{B}_{i-1}^T \bar{\mathbf{F}}_{i-1} \mathbf{B}_{i-1} + d_{i-1} \mathbf{I}_P)^{-1}$  in (4.20) boils down to finding the

scalar parameter  $c_{i-1}^{-1}$  (this benefits from the usage of orthogonal codes). To roughly assess the associated saving in flop cost, it is noted from (4.22) that the scalar parameter  $c_{i-1}$  is completely determined by the (constant) diagonal entries of the matrix  $\mathbf{B}_{i-1}^T \bar{\mathbf{F}}_{i-1} \mathbf{B}_{i-1}$ . This implies that the computation of  $c_{i-1}$  amounts to evaluating a quadratic form  $\mathbf{b}_{i-1}^T \bar{\mathbf{F}}_{i-1} \mathbf{b}_{i-1}$ , where  $\mathbf{b}_{i-1}$  denotes an arbitrary column of  $\mathbf{B}_{i-1}$ . The required number of flop counts is no more than  $2P^2 + P - 1$ , which is substantially small than that required for inverting a  $P \times P$  matrix.

### 4.5.3 Complexity Comparisons with Other Multiuser Detection Schemes

This subsection compares the algorithm complexity of the proposed group-wise OSIC detector with two typical signal detection schemes for MU ST coded wireless systems, namely, the Naguib's PIC scheme [78] and the Stamoulis's decoupled-based method [79].

It should be noted that the two comparable methods, originally tailored for the MU STBC environment, rely on the orthogonality property specific to the associated MU channel matrix. In the considered dual-signaling case, this structural requirement is not seen in the dual-mode MU channel matrix  $\mathbf{H}_c$  (owing to the presence of high-rate SM streams) but can be "restored" through ST matched filtering (cf. Lemma 4.3.1). As a result, the two alternative schemes can fit the considered dual-signaling systems based on the MF signal model (2.80). To evaluate the flops, one should note that, for a dual-signaling system with  $Q_M$  SM terminals, there are totally  $(NQ_M)^2$  signature blocks, each being a scalar multiple of  $\mathbf{I}_P$ , imbedded in the MFCM  $\mathbf{F}$ . These diagonal block submatrices will impose certain sparse structure distributed over  $\mathbf{F}$ , making it difficult to compute the accurate flop counts. To tackle this situation, we assume without loss of generality that the symbol groups of the  $Q_M$  SM users are permuted to the top end of the MU symbol vector  $\mathbf{s}_c(k)$ . As such, all these sparse blocks will cluster in the upper left corner of  $\mathbf{F}$  (each  $P \times P$  block of the first  $PNQ_M \times PNQ_M$  principle submatrix of  $\mathbf{F}$  is a scalar multiple of  $\mathbf{I}_P$ ). The "centralized" sparse structure of

$\mathbf{F}$  can further simplify the process of flop evaluations. It is also noted that, for a system with  $Q_M$  SM users and  $Q_D$  O-STBC users, there are totally  $(Q_D + NQ_M)!/[(Q_D)!(NQ_M)!]$  group OSIC orderings. Due to the imbedded sparse nature of  $\mathbf{F}$ , the required flop counts will be different for distinct sorting sequences. A reasonable complexity measure of the OSIC detector, therefore, would be the mean flop counts, averaged over all the possible orderings, but this turns out to be highly intractable. A sensible approximation to the exact mean flop counts is the average of the minimal and maximal costs. The detection orders allowing for the least computational effort must entail an utmost benefit from the sparse structure in per layer processing. The solutions are therefore the sorting sequences in which exactly all the  $Q_D$  O-STBC streams are to be detected in the initial  $Q_D$  layers; as such, all the dense blocks in  $\mathbf{F}$  resulting from the  $Q_D$  diversity users will be removed after the first  $Q_D$  stages and, meanwhile, the sparse structure is retained as much as possible in each processing layer. The detection orders incurring the highest complexity demand, on the other hand, will be the particular choices which decide to recover all the  $NQ_M$  SM signals in the initial  $NQ_M$  stages. This will leave as many as possible the dense blocks in each  $\mathbf{F}_i$  for  $i > 1$ , hence the smallest possible sparse region to be exploited for computational reduction. The average flop cost of two extreme cases is listed in Table 4.2 (the flop counts of the Naguib's and Stamoulis's methods are also obtained in essentially the same manner). The computed flop costs of the three methods are listed in Table 4.2 (see the first three rows).

**Example 4.5.1:** Considering the QPSK modulation (i.e.,  $D = 2$ ) and choosing  $N = 2$  (thus  $P = K = 2$ ),  $Q_D = Q_M = 2$ ,  $L = 6$ , we have the result:  $C_{Naguib} \approx 4336$ ,  $C_{Stamoulis} \approx 6448$  and  $C_{Group} \approx 1083$ , and this yields the approximate ratio of complexity of 4 : 6 : 1 for Naguib's 2-step method, Stamoulis's method and proposed group-wise OSIC method. As we can see, the proposed solution requires less computation. ■

## 4.6 Two-Stage Processing of Dual-Mode Signals

Let us consider a dual-signaling platform with  $Q$  users, each equipped with  $N = 2$  transmit antennas (Alamouti's code for diversity). In case that all the  $Q$  cell users are in the SM mode, there will be totally  $NQ = 2Q$  transmitted symbols during one signaling period, and one can use the conventional symbol-wise OSIC detector to separate the  $2Q$  coupled symbol streams. Assume that there are  $1 \leq Q_D \leq Q$  users otherwise choosing the O-STBC mode. To realize a two-fold diversity gain for the  $Q_D$  O-STBC links, the receiver has to spend two time periods for data buffering, during which there are totally  $4(Q - Q_D) + 2Q_D$  independent symbols sent from all the users:  $4(Q - Q_D)$  are from the SM users and  $2Q_D$  are from O-STBC users. Since  $4(Q - Q_D) + 2Q_D > 2Q$  whenever  $1 \leq Q_D \leq Q$ , the presence of  $Q_D$  users switching to the O-STBC mode does augment the data processing dimension (to an excess of  $2(Q - Q_D)$  over the full high-rate case). For  $Q = 16$ , Figure 4.2 shows the required flop counts of the group-wise OSIC detector as  $Q_D$  increases from 0 to 16. The  $Q_D = 0$  case, with the most compact signal model, serves as the inherent benchmark cost. As the figure shows, the proposed group-wise OSIC scheme tends to prevent significant excessive flop counts over the  $Q_D = 0$  case, and there is even a save in the counts for  $Q_D \geq 3$ . It is noted that the count reaches the peak when  $Q_D = 1$ , and monotonically decreases with  $Q_D$ . This is not unexpected, and is indeed true in general, since the excess data processing dimension over the benchmark case is  $2(Q - Q_D)$ , which attains the maximal when  $Q_D = 1$ . For the full diversity case ( $Q = Q_D = 16$ ), in which the number of symbols to be detected is the same as the full high-rate case ( $= 2Q$ ), the proposed method achieves largest flop count reduction. Based on these observations, the "joint" processing of the dual-mode signal could entail more excess flops over the benchmark performance when a few O-STBC users are present. In such a case, a plausible approach for complexity reduction is to first detect the O-STBC streams, since they may potentially be more robust. By removing the contributions of the detected O-STBC symbols from the signal model, one can resort to a symbol-wise OSIC algorithm to recover the remaining SM streams over a relatively small signal model

dimension. Since the detection order in this way may violate the actual optimal sorting, such a “two-stage” processing strategy can reduce computation at the expense of a possible performance drop. The computational cost of such an approach is also included in Table 4.2, based on which the amount of flop reduction with respect to the original method can be found as

$$\begin{aligned}
C_{\Delta} &:= (\text{flop counts of original approach}) - (\text{flop counts of two-stage approach}) \\
&= 2N^3P^2Q_M^3 + \frac{1}{6}N^3PQ_M^3 + \frac{1}{6}N^2P^2Q_DQ_M^2 + N^2P^2Q_M^2 - N^2PQ_D^2Q_M \\
&\quad - 2N^2PQ_D^2 + \frac{1}{2}N^2PQ_DQ_M^2 + \frac{3}{2}N^2PQ_M^2 - \frac{7}{2}N^2Q_M^3 + \frac{4}{3}NP^2Q_D^3 \\
&\quad + \frac{5}{2}NP^2Q_DQ_M - \frac{1}{2}NP^2Q_DQ_M^2 - 6NP^2Q_DQ_M - \frac{1}{6}NPQ_D^2Q_M \\
&\quad + \frac{1}{3}P^2Q_D^3. \tag{4.24}
\end{aligned}$$

Given the system parameters considered in Example 4.5.1, the two-stage approach reduces about a 47% computational complexity associated with the original method with optimal ordering.



## 4.7 Simulation Results

In this section we use several numerical simulations to illustrate the performance of the proposed group-wise OSIC detector. Each user’s channel is quasi-static: it remains constant over each packet of 100 symbol blocks and independently varies between packets. Also, perfect channel knowledge at the receiver is assumed. In all simulations, the transmit power of all users are set to be equal (i.e.,  $P_1 = P_2 = \dots = P_Q = P_T$ ) and define  $\text{SNR} := P_T/\sigma_v^2$  (as defined in [10], [48], [54], [62], [65], [68]); the number of receiver antennas  $M$  is set to meet the minimal requirement, i.e.,  $M = L = Q_D + NQ_M$ .

### A. MU STBC Systems with Alamouti’s Code

This simulation considers the special MU STBC case (with Alamouti’s code) and evaluates the performances of the proposed method with the Stamoulis’s method [79] and the

Naguib's method [78], both being tailored for the MU STBC systems. The ML decoding is also included for comparison and a single-user bound is given for a benchmark. Figure 4.4 compares the detection performances of the three families of methods in a four-user system over i.i.d. Rayleigh fading channels (with 8-PSK modulation) in terms of the average bit error rates (BERs) (averaged over the four detected streams). As we can see that the ML decoding achieves the best performance but needs a large decoding complexity for an exhaustive search. The results also show that the group-wise MMSE OSIC attains a better performance. The Naguib's two-step PIC method [78] yields a comparable performance when SNR is low but it degrades in the medium-to-high SNR regime. It is noted that, in the Naguib's two-step method, the detection accuracy in the second stage hinges entirely on the reliability of all the initial signal estimates. Accordingly, each user's symbol stream, detected via the PIC based mechanism, would be subject to an essentially equal risk of error propagation resulting from the incorrect decisions in the initial stage. The OSIC solution, on the other hand, can provide a layer-wise increase in receive diversity to limit the effect of possible decision error leakage: this would account for the superiority average performance over the Naguib's approach. The Stamoulis's method [79], with or without ordering, gives a relatively poor performance among the three families; this is because, as compared with the other two alternatives, the decoupled-based formulation does not induce an increase in receive diversity as the stage goes on.

### ***B. Symbol Detection in Dual-Signaling Systems***

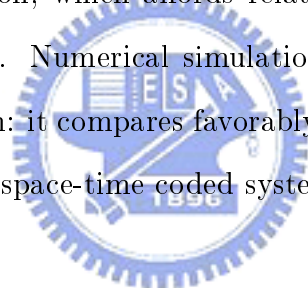
We consider a system with four users, two experiencing correlated channels described by the Ricean model [12] (or see (2.12) in Section 2.2.2) and the other two being over i.i.d. Rayleigh fading channels (two transmit antennas are placed at each user terminal). The Alamouti and SM schemes, respectively, are used for data transmission over Ricean and Rayleigh channels; the symbol constellations used are QPSK for SM terminals and 16-QAM for O-STBC terminals so that the bit data rates are the same [68]. The first

experiment compares the performances of the above three detection schemes in the dual-signaling environment. Figure 4.5 (a) (b), respectively, show the average BER of the two detected O-STBC users (the  $\mathcal{K}$ -factors in the two Ricean channels are both set to be  $\mathcal{K} = 10$ , which corresponds to a medium eigenvalue spread = 5.3) and the two SM users. Compared with Figure 4.4, we can see that the BER curves in the dual-singling case exhibit similar tendency as in the MU STBC systems; the proposed MMSE group-wise OSIC achieves the best performance as long as SNR is above 10 dB. It is noted that the performance of the proposed two-stage processing scheme (for further computational reduction) is comparable to that of the Naguib's two-step method; however, it incurs a 3 dB loss in SNR at BER =  $10^{-3}$  for O-STBC users and 1.5 ~ 2 dB for SM users as compared with the original method (with optimal ordering). The second experiment simulates the BER performances of three representative detection schemes (the ordered Stamoulis's method, the Naguib's two-step method, and the proposed group-wise MMSE OSIC) at different channel correlation tendencies. For the two Ricean channels, we consider five different Ricean  $\mathcal{K}$ -factors: 0, 1, 10, 30, and 100 (large  $\mathcal{K}$  implies severe correlations; the extreme selections  $\mathcal{K} = 0$  and  $\mathcal{K} = 100$ , respectively, render the channel to be independent fading and almost light-of-sight). Figures 4.6 (a) (b) show the average BER of the two classes of detected streams for different  $\mathcal{K}$  factors. It can be seen that the performances in all cases deteriorate as  $\mathcal{K}$  increases. This is not unexpected since the O-STBC scheme may lose the diversity gain over the correlated channels, and large  $\mathcal{K}$  factor thus incurs large BER degradation. The performance drop of the SM scheme may result from the increased amount of error propagation due to the poorly detected O-STBC streams caused by the loss in diversity gain over low-rank channels. The figure also shows that, for a fixed SNR, the proposed group-wise MMSE OSIC seems to incur less BER spread as  $\mathcal{K}$  increases. This could benefit from the OSIC mechanism, in which the detect-and-cancel process induces more receive diversity and improves detection accuracy in each layer, leading to better average performance against severe spatial correlation.



## 4.8 Summary

Co-channel interference mitigation in multiuser space-time wireless systems is of great importance for maintaining a good link quality. The originality of the presented study is the investigation of the impact of orthogonal ST block codes on the OSIC based detection in a multiuser dual-signaling environment. The proposed group-wise detection property, based on exploiting the block-orthogonal structure imbedded in the matched-filtered channel matrix, potentially reduces computations and the overall decoding load. Our flop count analysis shows that, with a medium number of O-STBC users in the cell, the complexity of the proposed solution is comparable to that of the conventional symbol-wise OSIC algorithm in a pure SM signaling environment: our solution is thus an attractive receiver candidate for a dual-signaling platform. The distinctive structure of the channel matrix also leads to a low-complexity detector realization, which affords relatively low computational cost when compared with existing methods. Numerical simulations demonstrate the effectiveness of the proposed OSIC based solution: it compares favorably with existing reported interference mitigation schemes for multiuser space-time coded systems.



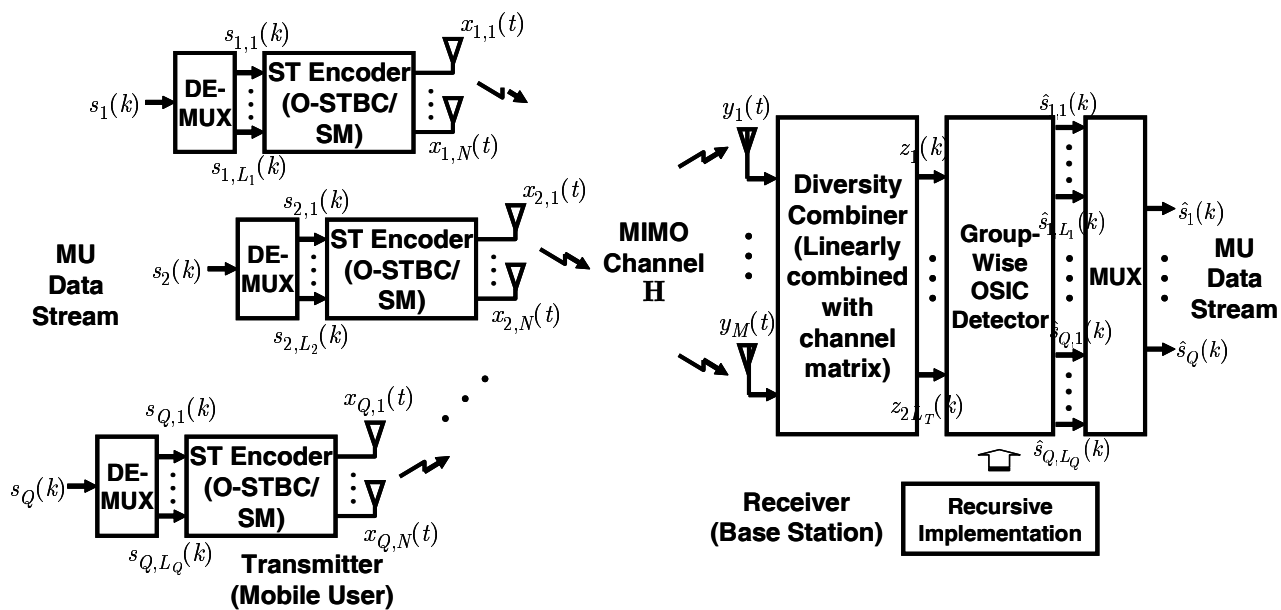


Figure 4.1: The schematic diagram of the transceiver.

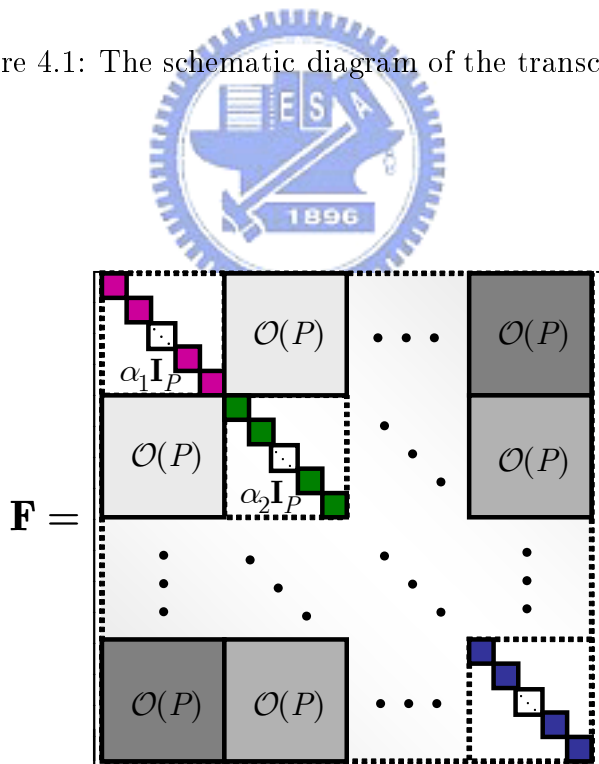


Figure 4.2: Structure of MFCM  $\mathbf{F}$ .

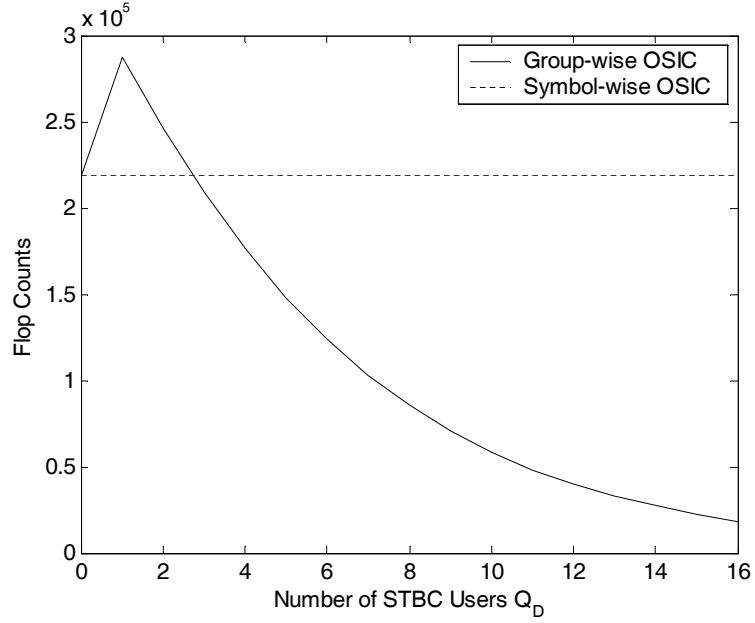


Figure 4.3: Flop counts of the proposed group-wise OSIC detection as a function of  $Q_D$  for an MU dual-signaling system, with  $Q = 16$ ,  $Q_M = Q - Q_D$  and  $N = 2$ .

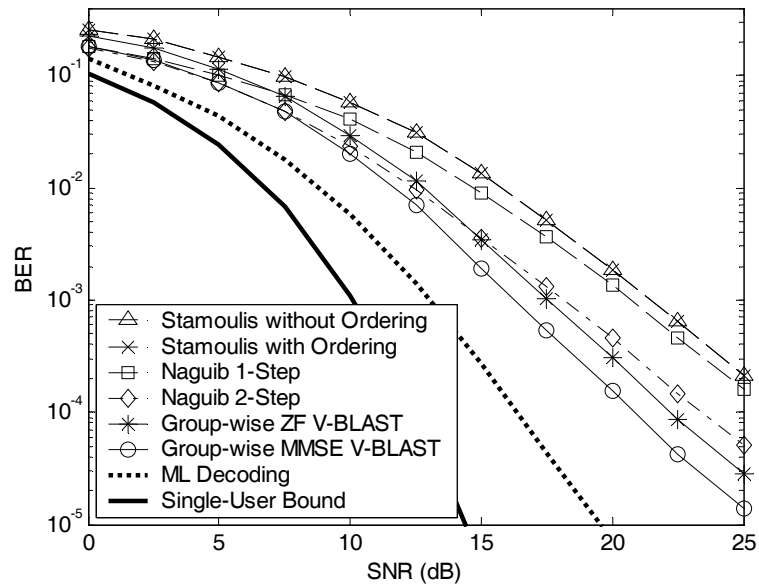


Figure 4.4: Average BER performances of various detection schemes as a function of SNR for a four-user MU STBC system, with  $N = 2$  and  $M = 4$ . The Alamouti's code with 8-PSK modulation is used for each user.

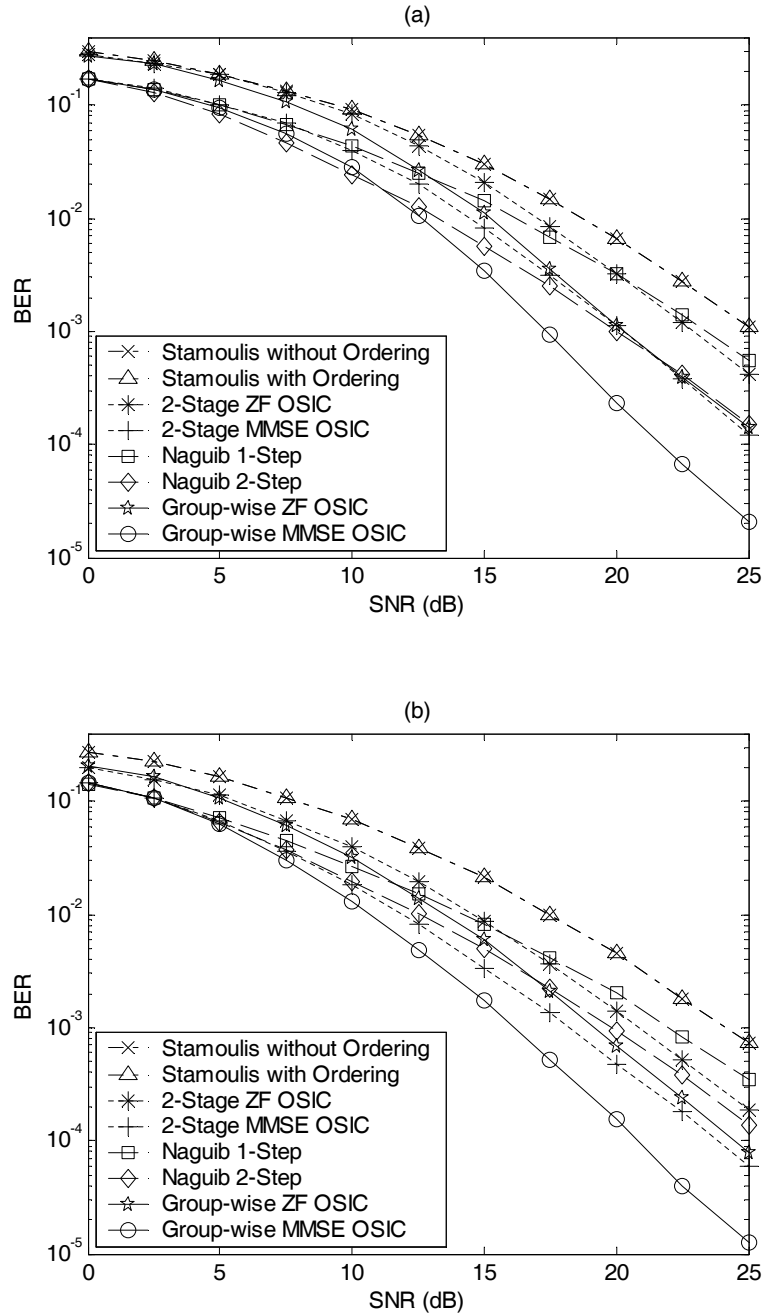


Figure 4.5: BER performance of various detection schemes as a function of SNR for a four-user dual-signaling system, with  $Q_D = Q_M = 2$ ,  $N = 2$ ,  $M = 6$  and  $\mathcal{K} = 10$ . 16-QAM and QPSK modulations are used for O-STBC signaling and SM signaling, respectively. (a) Average BER of the two detected O-STBC users. (b) Average BER of the two detected SM users.

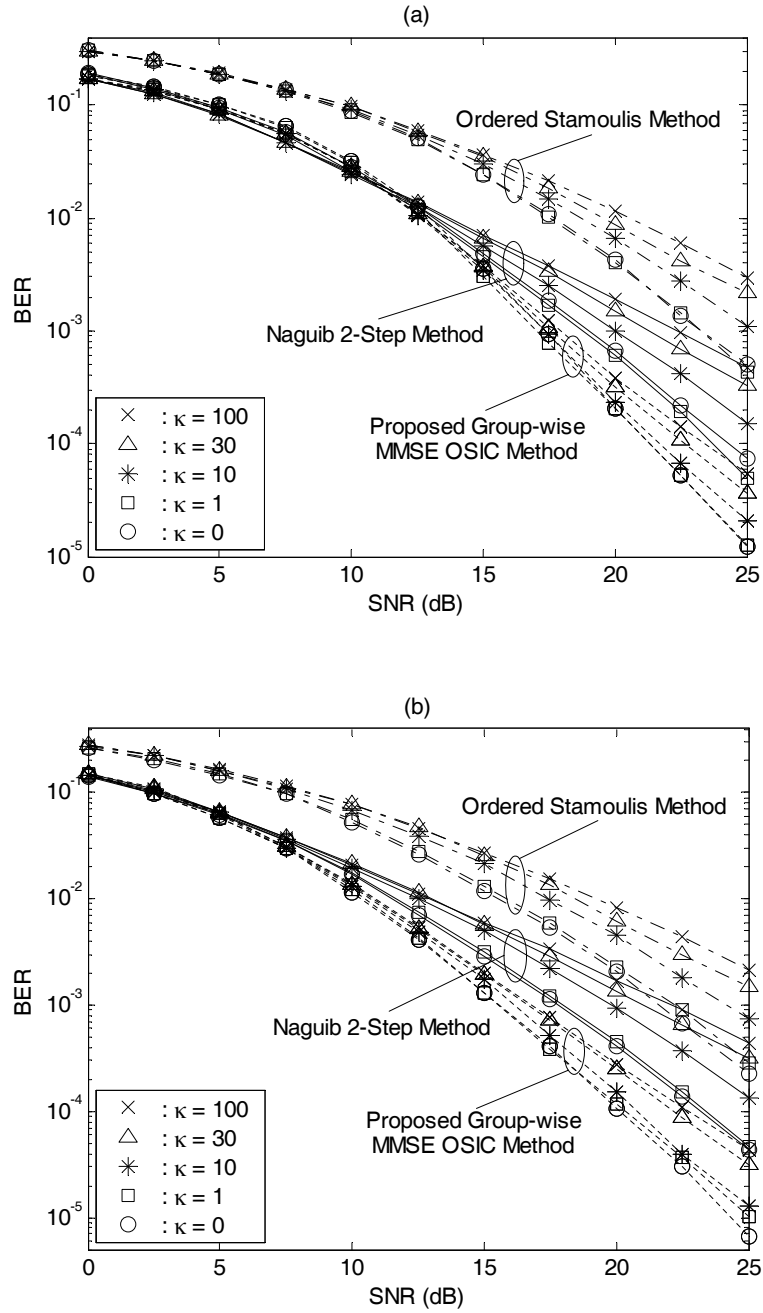


Figure 4.6: BER performance of three detection schemes in a four-user dual-signaling system for different Ricean  $\mathcal{K}$ -factors, with  $Q_D = Q_M = 2$ ,  $N = 2$  and  $M = 6$ . 16-QAM and QPSK modulations are used for O-STBC signaling and SM signaling, respectively. (a) Average BER of the two detected O-STBC users. (b) Average BER of the two detected SM users.

Table 4.1: Algorithm summary of the proposed group-wise OSIC detector.

---



---

**Initialization :**

$$\mathbf{H}_{c,0} = \mathbf{H}_c; \mathbf{F}_0 = \mathbf{F} = \mathbf{H}_c^T \mathbf{H}_c;$$

$$\mathbf{y}_{c,0}(k) = \mathbf{y}_c(k); \mathbf{z}_0(k) = \mathbf{z}(k) = \mathbf{H}_c^T \mathbf{y}_c(k);$$

**Recursion :** For  $0 \leq i \leq Q_D + NQ_M - 1$

1.  $\mathbf{Q}_i = \begin{cases} \mathbf{F}_i^{-1} & \text{for ZF Criterion} \\ \left[ (2/\sigma_v^2) \mathbf{F}_i + \mathbf{I}_{(L_T - iP)} \right]^{-1} & \text{for MMSE Criterion} \end{cases}$
  2.  $\bar{l}_i = \arg \min_{1 \leq l_i \leq Q_D + NQ_M - i} \beta_{l_i}$ , where  $\beta_{l_i}$  is the  $((l_i - 1)P + 1)$ th diagonal entry of  $\mathbf{Q}_i$
  3.  $\mathbf{G}_i = \begin{cases} \mathbf{F}_i^{-1} & \text{for ZF Criterion} \\ \left[ \mathbf{F}_i + (\sigma_v^2/2) \mathbf{I}_{(L_T - iP)} \right]^{-1} & \text{for MMSE Criterion} \end{cases}$
  4.  $\mathbf{W}_i = \mathbf{G}_i \begin{bmatrix} \mathbf{e}_{(\bar{l}_i - 1)P + 1} & \cdots & \mathbf{e}_{(\bar{l}_i - 1)P + P} \end{bmatrix}$
  5.  $\hat{\mathbf{s}}_{c,\bar{l}_i}(k) = \mathcal{Q}(\mathbf{W}_i^T \mathbf{z}_i(k))$
  6.  $\mathbf{y}_{c,i+1}(k) = \mathbf{y}_{c,i}(k) - \bar{\mathbf{H}}_{c,\bar{l}_i} \hat{\mathbf{s}}_{c,\bar{l}_i}(k)$
  7.  $\bar{\mathbf{H}}_{c,\bar{l}_i}$  is obtained from  $\mathbf{H}_c$  corresponding to  $\mathbf{s}_{c,\bar{l}_i}(k)$
  8.  $\mathbf{z}_{i+1}(k) = \mathbf{H}_{c,i+1}^T \mathbf{y}_{c,i+1}(k)$
  9.  $\mathbf{F}_{i+1} = \mathbf{H}_{c,i+1}^T \mathbf{H}_{c,i+1}$
  10.  $\mathbf{H}_{c,i}$  is obtained by deleting  $i$  block(s) of  $P$  columns from  $\mathbf{H}_c$
-

Table 4.2: Flop counts of different detection methods ( $D$ : constellation size).

Method	Flop Counts
Group-wise OSIC	$2N^3P^2Q_M^3 + \frac{1}{6}N^3PQ_M^3 + \frac{1}{3}N^3Q_M^3 + \frac{19}{6}N^2P^2Q_DQ_M^2 + N^2P^2Q_M^2 - N^2PQ_D^2Q_M$ $-2N^2PQ_D^2 + N^2PQ_DQ_M^2 + \frac{3}{2}N^2PQ_M^2 + \frac{4}{3}NP^2Q_D^3 + \frac{11}{2}NP^2Q_D^2Q_M - \frac{1}{2}NP^2Q_DQ_M^2$ $-12NP^2Q_DQ_M + \frac{1}{3}NPQ_D^2Q_M + \frac{4}{3}P^2Q_D^3$
Stamoulis's Method	$\frac{25}{12}N^4P^2Q_M^4 + \frac{23}{3}N^3P^2Q_DQ_M^3 - \frac{19}{6}N^3P^2Q_M^3 + \frac{25}{2}N^2P^2Q_D^2Q_M^2 - \frac{23}{2}N^2P^2Q_DQ_M^2$ $- \frac{5}{4}N^2P^2Q_M^2 + \frac{7}{4}N^2PQ_M^2 + \frac{25}{6}NP^2Q_D^3Q_M - \frac{23}{2}NP^2Q_D^2Q_M - \frac{7}{2}NP^2Q_DQ_M$ $+ \frac{25}{12}P^2Q_D^4 - \frac{23}{6}P^2Q_D^3$
Naguib's 2-Step Method	$2(2^D)N^2P^2Q_M^2 + 2(2^D)N^2PQ_M^2 + 4(2^D)NP^2Q_DQ_M + 5(2^D)NPQ_DQ_M + 2(2^D)P^2Q_D^2$ $+ 5N^3P^2Q_M^3 - 2N^3PQ_M^3 + 12N^2P^2Q_DQ_M^2 - 5N^2P^2Q_M^2 - 3N^2PQ_DQ_M^2 + \frac{9}{2}N^2PQ_M^2$ $+ 11NP^2Q_D^2Q_M - 10NP^2Q_DQ_M - 3NPQ_D^2Q_M + 4P^2Q_D^3$
Two-Stage OSIC	$3N^2P^2Q_DQ_M^2 + \frac{1}{2}N^2PQ_DQ_M^2 + \frac{7}{2}N^2Q_M^3 + 3NP^2Q_D^2Q_M - 6NP^2Q_DQ_M$ $+ \frac{1}{2}NPQ_D^2Q_M + P^2Q_D^3$

Table 4.3: Summary of structures of the MFCM  $\mathbf{F}_{p,q}$  for complex-valued constellations.

<b>Complex-Valued Constellation</b>		
	$N = 2$ ( $K = 2$ )	$N = 3$ or $4$ ( $K = 8$ )
$p, q \in \mathcal{S}_D$	$p = q : \mathbf{F}_{q,q} = \alpha_q \mathbf{I}_4$ $p \neq q : \mathbf{F}_{p,q} \in \mathcal{O}(4)$	$p = q : \mathbf{F}_{q,q} = \alpha_q \mathbf{I}_8$ $p \neq q : \mathbf{F}_{p,q} \in \mathcal{U}(8)$ where $\mathcal{U}^{(1,1)}(8) = \mathcal{U}^{(2,2)}(8) \in \mathcal{O}(4)$ $\mathcal{U}^{(1,2)}(8) = \mathcal{U}^{(2,1)}(8) = \mathbf{O}_4$
$p, q \in \mathcal{S}_M$	$p = q : \mathbf{F}_{q,q} \in \mathbb{R}^{8 \times 8}$ $\mathbf{F}_{q,q}^{(n,n)} = \alpha_{q,n} \mathbf{I}_4$ $\mathbf{F}_{q,q}^{(n,d)} \in \mathcal{V}(4), 1 \leq n, d \leq 2$ $p \neq q : \mathbf{F}_{p,q} \in \mathbb{R}^{8 \times 8}$ $\mathbf{F}_{p,q}^{(n,d)} \in \mathcal{V}(4), 1 \leq n, d \leq 2$ where $\mathcal{V}^{(1,1)}(4) = \mathcal{V}^{(2,2)}(4) = c_1 \mathbf{I}_2$ $\mathcal{V}^{(1,2)}(4) = -\mathcal{V}^{(2,1)}(4) = c_2 \mathbf{I}_2$	$p = q : \mathbf{F}_{q,q} \in \mathbb{R}^{16N \times 16N}$ $\mathbf{F}_{q,q}^{(n,n)} = \alpha_{q,n} \mathbf{I}_{16}$ $\mathbf{F}_{q,q}^{(n,d)} \in \mathcal{V}(16), 1 \leq n, d \leq N$ $p \neq q : \mathbf{F}_{p,q} \in \mathbb{R}^{16N \times 16N}$ $\mathbf{F}_{p,q}^{(n,d)} \in \mathcal{V}(16), 1 \leq n, d \leq N$ where $\mathcal{V}^{(1,1)}(16) = \mathcal{V}^{(2,2)}(16) = c_1 \mathbf{I}_8$ $\mathcal{V}^{(1,2)}(16) = -\mathcal{V}^{(2,1)}(16) = c_2 \mathbf{I}_8$
$p \in \mathcal{S}_D$ $q \in \mathcal{S}_M$	$\mathbf{F}_{p,q} \in \mathbb{R}^{4 \times 8}$ $\mathbf{F}_{p,q}^{(1,n)} \in \mathcal{O}(4), 1 \leq n \leq 2$	$\mathbf{F}_{p,q} \in \mathbb{R}^{8 \times 16N}$ $\mathbf{F}_{p,q}^{(1,n)} \in \mathcal{D}(8,16), 1 \leq n \leq N$ , where $\mathcal{D}^{(1,1)}(8,16) = \mathcal{D}^{(1,2)}(8,16) = \mathcal{D}^{(2,3)}(8,16)$ $= -\mathcal{D}^{(2,4)}(8,16) \in \mathcal{O}(4)$ $-\mathcal{D}^{(2,1)}(8,16) = \mathcal{D}^{(2,2)}(8,16) = \mathcal{D}^{(1,3)}(8,16)$ $= \mathcal{D}^{(1,4)}(8,16) \in \mathcal{O}(4)$



# Chapter 5

## Efficient Transmitter and Receiver

## Design for Grouped Space-Time

## Block Coded Systems with Feedback

## Information



### 5.1 Introduction

In this chapter, a flexible grouped STBC (G-STBC) with arbitrary number of total transmit antennas is presented for the downlink over the Rayleigh flat-fading channels. By treating each antenna group as an independent data stream unit, the signal detection/interference suppression becomes a detrimental factor dominating the link performance in such the systems. As known, to detect the transmitted symbols, the optimal solution is ML detection [4], [14]. However, it is usually prohibitive for use due to its high computational complexity. Recently, there are various associated interference mitigation schemes reported in the literature [78]-[81]. It was suggested in [80], [81] to tackle this problem through an MU detection framework, and demonstrated that if all users use the O-STBC scheme for transmission

under the same number of transmit antennas, the OSIC detector allows a “user-wise” joint detection property. By borrowing from this detection framework, it is shown in this chapter that an “antenna group-wise” detection property can be applied to the real-valued constellations in the proposed G-STBC system. However, for the complex-valued constellations, it is shown that the per-antenna group detection property will fail leading to an increase in computational complexity. To remedy this, we then propose an appropriate OSIC detector to guarantee the antenna group-wise detection property for the possible codeword structures of G-STBCs. Moreover, a computationally efficient recursion based implementation associated with such an OSIC detector is then developed based on the distinctive structure embedded in the MFCM to further alleviate the detection computational load. Finally, we study the codeword structures and propose an optimal codeword selection criterion based on the minimum BER performance under the fixed total transmit power and total SE. Numerical examples are used to illustrate the performance of the proposed G-STBCs and corresponding OSIC detector.

The rest of the chapter is organized as follows. Section 5.2 describes the system model and some basic assumptions for G-STBC system. Section 5.3 investigates the embedded structures of MFCM and develops an antenna group-wise OSIC detection scheme based on the distinctive structures of MFCM for real-valued constellations. On the contrast, Section 5.4 gives a development of a particular semi-antenna group-wise OSIC detection algorithm for complex-valued constellations. The implementation issues for complex-valued constellations including the antenna group-wise OSIC solution, two-stage detection strategy and computationally efficient recursion based realization are then presented in Section 5.5. In Section 5.6, the codeword structures, properties and selection criterion of G-STBCs are studied. Finally, Section 5.7 shows the simulation examples, and Section 5.8 concludes the chapter. Most of the mathematical details required in our discussions are relegated to the appendix.

## 5.2 System Model

### 5.2.1 System Description and Basic Assumptions

Consider the G-STBC system over the Rayleigh flat-fading channels as illustrated in Figure 5.1, in which  $N$  antennas are placed at the transmitter and  $M$  antennas are located at the receiver. The  $N$  transmit antenna elements are partitioned into  $Q$  antenna groups with each comprising  $2 \leq N_q \leq 4$  ( $\leq N$ ) antennas<sup>1</sup> so that  $N_1 + N_2 + \dots + N_Q = N$ . In particular, for the  $q$ th group, consecutive  $B_q$  symbols of the data stream are spatially and temporally encoded according to [47], and are then transmitted across  $N_q$  antennas over  $K_q$  symbol periods. Assume that the unit-rate codes for real-valued ( $2 \leq N_q \leq 4$ ) and complex-valued constellations (i.e.,  $N_q = 2$ ) and half-rate codes for complex-valued constellations (i.e.,  $3 \leq N_q \leq 4$ ) [47] are applied to each antenna group. If  $K := \max\{K_1, K_2, \dots, K_Q\}$ , then according to [47],  $K$  will thus be a multiple of  $K_q$ , that is,  $K = \kappa_q K_q$  with a positive integer  $\kappa_q := K/K_q$ . During the  $K$  symbol periods, each antenna group then sends  $L_q := \kappa_q B_q$  independent symbols, and there are thus in total

$$L_T := \sum_{q=1}^Q L_q = K \sum_{q=1}^Q \frac{B_q}{K_q} \quad (5.1)$$

data symbols transmitted from the  $Q$  antenna groups every  $K$  symbol periods. Each antenna group's code, called the *group code*, can also be completely described by the associated  $N_q \times K$  ST codeword matrix  $\mathbf{X}_q(k) \in \mathbb{C}^{N_q \times K}$ ,  $q = 1, 2, \dots, Q$ , as defined in (4.2), where  $\mathbf{A}_{q,l} \in \mathbb{C}^{N_q \times K}$  is the ST modulation matrix. Denote that each  $N_q \times K$  matrix  $\mathbf{A}_{q,l}$  has the following properties [62] (c.f. (4.3))

$$\begin{cases} \mathbf{A}_{q,k} \mathbf{A}_{q,l}^H = \frac{K_q}{B_q} \mathbf{I}_{N_q} & k = l, \\ \mathbf{A}_{q,k} \mathbf{A}_{q,l}^H + \mathbf{A}_{q,l} \mathbf{A}_{q,k}^H = \mathbf{O}_{N_q} & k \neq l. \end{cases} \quad (5.2)$$

---

<sup>1</sup>It is known by [47] that the O-STBCs exist for  $2 \leq N_q \leq 4$  when complex-valued constellations are used, and  $2 \leq N_q \leq 8$  for real-valued constellations. Here we only consider the case  $2 \leq N_q \leq 4$ . This is because that the capability of the appealing group-wise detection property in OSIC algorithm will fail if  $5 \leq N_q \leq 8$  (see Section 4.1).

even if  $K > K_q$ . Moreover, splitting the source symbols into the real and imaginary parts will also unify both the problem formulation and the underlying analysis, *regardless of the number of antennas of each group  $N_q$  and symbol constellations*.

Collecting received signal vector  $\mathbf{y}(k) := [y_1(k), y_2(k), \dots, y_M(k)]^T \in \mathbb{C}^M$  over  $K$  successive symbol periods, we have the  $M \times K$  ST signal model (2.72) with  $N$  being replaced by  $N_q$  (assuming that the  $Q$  antenna groups are symbol synchronized). Note that in (2.72)  $P_q$  is the transmit power of the  $q$ th antenna group so that  $P_1 + P_2 + \dots + P_Q = P_T$ , with  $P_T$  being the total transmit power,  $\mathbf{H}_q$  is an  $M \times N_q$  MIMO matrix channel from the  $q$ th antenna group to the receiver, and  $\mathbf{V}(k) \in \mathbb{C}^{M \times K}$  is the channel noise. The following assumptions are also made in the sequel.

- (a1) The symbol streams  $s_q(k)$ ,  $q = 1, 2, \dots, Q$ , are i.i.d. with zero-mean and unit-variance.
- (a2) Each entry of the MIMO matrix channel  $\mathbf{H}_q$ ,  $q = 1, 2, \dots, Q$ , is an i.i.d. complex Gaussian random variable with zero-mean and unit-variance, and assumed to be static during the  $K$  signaling periods.
- (a3) The noise  $\mathbf{V}(k)$  is spatially and temporally white, each entry being with zero-mean and variance  $\sigma_v^2$ .
- (a4) Equal power allocation for all groups is assumed, i.e.,  $P_1 = P_2 = \dots = P_Q = \frac{P_T}{Q}$ .
- (a5) Assume that  $2 \leq N_q \leq 4$  and hence, according to [47], the symbol block length  $B_q \in \{2, 4\}$ . The proposed approach is exclusively applicable to this scenario.
- (a6) For  $3 \leq N_q \leq 4$  with complex-valued constellations, the half rate codes [47] are used.
- (a7) The number of receive antennas is chosen so that  $M \geq Q$ .

### 5.2.2 Real-Valued Vectorized Signal Model

To facilitate the detection and analysis, we again consider the equivalent (real-valued) vectorized signal model built in Section 2.4.1. Since the number of transmit antennas is

different at different antenna groups, we will use the vectorized signal model built in Section 2.4.1 with  $N$  being replaced by  $N_q$ . Based on the MF signal  $\mathbf{z}(k)$  (c.f. (2.80)) we can detect the unknown symbols over an observation space of a relatively small dimension. We will hereafter rely on the filtered model (2.80) for detection.

### 5.3 OSIC Detection: Real-Valued Constellations

For MU STBC systems [78], [79], [94] with the same number of antennas placed at each user terminal, it has been shown in Chapter 4 that the MFCM  $\mathbf{F}$  will exhibit the appealing block orthogonal structures to allow a “user-wise” OSIC detection property. Such a system architecture can be regarded as a special case of the G-STBC systems in which  $N_1 = N_2 = \dots = N_Q$ , by merging all users’ ST codewords into a “big” one and treating each user as a particular antenna group. However, for the general G-STBC systems, due to that the number of antennas placed at each antenna group could be different, the structure of the resultant MFCM  $\mathbf{F}$  might largely deviate from that considered in MU STBC systems in Chapter 4. As we will see in what follows, the matrix  $\mathbf{F}$  in the G-STBC systems will reveal another appealing block orthogonal structures. This fact is primarily the gut for developing an antenna group-wise OSIC detector.

To detect the transmitted symbols in the G-STBC systems, we again propose to adopt the OSIC algorithm [56] since it yields reasonable trade-off between performance and computational complexity with respect to the optimal ML decoding [6], [68]. For the MU STBC systems with the same number of antennas at each mobile user, it has been shown in Chapter 4 that the OSIC detector can per stage jointly detect a block of multiple symbols associated with a particular user. In this section, by using the distinctive structures of the MFCM  $\mathbf{F}$  shown in the sequel, we will see that the OSIC detector can per stage jointly detect a block of  $K$  symbols associated with a particular antenna group in the considered G-STBC systems, called the “antenna group-wise” OSIC detection scheme (as presented in Chapter

4), for *real-valued* symbol constellations.

### 5.3.1 Matched-Filtered Channel Matrix

Denote that  $\mathbf{F}_{q,q}$  and  $\mathbf{F}_{p,q}$  are the signal signature of the  $q$ th antenna group and the inter-group interference between the  $p$ th and the  $q$ th antenna groups, respectively. To characterize the structures of  $\mathbf{F}_{q,q}$  and  $\mathbf{F}_{p,q}$ , or equivalently  $\mathbf{F}$ , we might have to gather each piece of entry and put them altogether to examine how  $\mathbf{F}_{q,q}$  and  $\mathbf{F}_{p,q}$  are actually like. This can be done through the following lemma. In the sequel, we denote by  $\mathcal{O}(K)$  the set of all  $K \times K$  real orthogonal designs with  $K$  independent values as specified in [47]. Also, we denote by  $\mathcal{O}(K, L)$  the set of all  $K \times K$  real orthogonal designs with  $L$  independent values.

**Lemma 5.3.1.** *Consider the real-valued constellations with  $2 \leq N_p, N_q \leq 4$ . According to [47], we get  $K \in \{2, 4\}$ . Let  $\mathbf{F}_{p,q}$  be the  $(p, q)$ th  $L_p \times L_q$  block submatrix of  $\mathbf{F}$ , where  $\mathbf{F}$  is defined in (2.81). Then we have  $\mathbf{F}_{q,q} = \alpha_q \mathbf{I}_K$  and  $\mathbf{F}_{p,q} \in \mathcal{O}(K)$  whenever  $p \neq q$ . ■*

*Proof:* See Appendix F. □

Precisely, Lemma 5.3.1 specifies that for  $p \neq q$ :

- (p1) When  $K = 2$ , it turns out  $N_1 = N_2 = \dots = N_Q = 2$ . Then we have  $\mathbf{F}_{p,q} \in \mathcal{O}(2)$ .
- (p2) When  $K = 4$  and  $N_p = N_q = 2$ , then each  $2 \times 2$  block diagonal submatrix of  $\mathbf{F}_{p,q} \in \mathbb{R}^{4 \times 4}$  belongs to an orthogonal design and each  $2 \times 2$  block off-diagonal submatrix of  $\mathbf{F}_{p,q}$  is a zero matrix. As a result, we have  $\mathbf{F}_{p,q} \in \mathcal{O}(4, 2)$ .
- (p3) When  $K = 4$  and  $2 \leq N_p, N_q \leq 4$  but  $N_p \neq N_q \neq 2$ , then we have  $\mathbf{F}_{p,q} \in \mathcal{O}(4)$ .

The results of Lemma 5.3.1 are summarized in Table 5.1. Part (p1) of Lemma 5.3.1 is known from [47] and is exploited in Chapter 4 for developing a user-wise OSIC detector in the MU STBC systems. The significance of Lemma 5.3.1 lies in Part (p2) and Part (p3), which are more relevant to the G-STBC systems. In particular, Part (p2) and Part (p3)

show that as  $K = 4$  (i.e., at least one of  $Q$  antenna groups places more than two transmit antennas), the cross-coupling matrix  $\mathbf{F}_{p,q}$  describing the interference between the  $p$ th and the  $q$ th antenna groups turns out to be a  $4 \times 4$  orthogonal design. Since a matrix being a scalar multiple of  $\mathbf{I}_K$  is essentially a  $K \times K$  orthogonal design  $\mathcal{O}(K, 1)$ , Lemma 5.3.1 asserts that whenever the number of transmit antennas ( $2 \leq N_q \leq 4$ ) at each group is, the MFCM  $\mathbf{F}$  does consist of orthogonal design based block submatrices. The case of each antenna group with different number of antennas thus substantially preserves the block orthogonal structures of  $\mathbf{F}$  as described in Chapter 4 and allows an “antenna group-wise” OSIC detection.

### 5.3.2 Antenna Group-Wise OSIC Detection

For real-valued constellations, the unit-rate codes [47] are applied to each antenna group to form the group codes. In this scenario, we have  $B_q = K_q$ . In what follows, we will consider the ZF and MMSE criteria for developing OSIC based detection.

Consider the ZF OSIC detection, in which the optimal detection order at each stage is based on the maximal post-detection SNR criterion [56]. Through the same procedures (4.4)-(4.5) as what we have done in Section 4.4.1, the optimal detection order at the initial stage can be obtained by searching for the index  $l = 1, 2, \dots, L_T$  at which  $[\mathbf{F}^{-1}]_{l,l}$  is minimal. In the following theorem, we will see that  $\mathbf{F}^{-1}$ , loosely stated, “inherits” the key features of  $\mathbf{F}$  established in Lemma 5.3.1.

**Theorem 5.3.1.** *Consider the real-valued constellations with  $2 \leq N_p, N_q \leq 4$  and hence  $K \in \{2, 4\}$ . Let  $\mathbf{F} \in \mathbb{R}^{L_T \times L_T}$  be the MFCM as defined in (2.81). Then each  $K \times K$  block diagonal submatrix of  $\mathbf{F}^{-1}$  is a scalar multiple of  $\mathbf{I}_K$  and each  $K \times K$  block off-diagonal submatrix of  $\mathbf{F}^{-1}$  belongs to  $\mathcal{O}(K)$ . ■*

*Proof:* Let us first define  $\mathcal{F}_{KL}(L)$  to be the set of all invertible real symmetric  $KL \times KL$  matrices, where  $K$  and  $L$  are two positive integers, so that, for  $\mathbf{X} \in \mathcal{F}_{KL}(L)$ , with  $\mathbf{X}_{k,l}$  being the  $(k, l)$ th  $K \times K$  submatrix of  $\mathbf{X}$ , we have  $\mathbf{X}_{l,l} = \beta_l \mathbf{I}_K$  for some scalar  $\beta_l$ , and  $\mathbf{X}_{k,l} \in \mathcal{O}(K)$

for  $k \neq l$ . Therefore, Theorem 5.3.1 is in fact an immediate consequence of the following result by setting  $L = Q$ .  $\square$

**Lemma 5.3.2.** *If  $\mathbf{F} \in \mathcal{F}_{KL}(L)$ , then so is  $\mathbf{F}^{-1}$ .*  $\blacksquare$

*Proof:* Also see Appendix A.  $\square$

Theorem 5.3.1 shows that the total  $KL$  diagonal entries of  $\mathbf{F}^{-1}$  assume  $L = Q$  distinct levels  $\beta_{0,l}$ ,  $l = 1, 2, \dots, L$ , that is

$$\text{diag}(\mathbf{F}^{-1}) = \underbrace{\{\beta_{0,1}, \dots, \beta_{0,1}\}}_{K \text{ entries}} \underbrace{\{\beta_{0,2}, \dots, \beta_{0,2}\}}_{K \text{ entries}} \dots \underbrace{\{\beta_{0,L}, \dots, \beta_{0,L}\}}_{K \text{ entries}}. \quad (5.3)$$

From (5.3), we can see that it suffices to search among the  $L$  values, one associated with a particular “antenna group” (or say the *layer* in the standard V-BLAST detection), for the optimal detection order. Therefore, we can simultaneously detect a block of  $K$  symbols at the initial stage, with the optimal detection order being given by (4.6), and the ZF weighting matrix can be computed from the corresponding indexed columns of  $\mathbf{F}^{-1}$  as

$$\mathbf{W}_0 = \mathbf{F}^{-1} [\mathbf{e}_{K(\bar{l}_0-1)+1} \cdots \mathbf{e}_{K(\bar{l}_0-1)+K}] \in \mathbb{R}^{LK \times K}. \quad (5.4)$$

The detected signal is then cancelled from the received signal (2.77), yielding a “modified” signal model for detection at the next stage.

With such a detect-and-cancel procedure followed by an associated linear combining of the resultant signal (2.80), it can be directly verified that, at the  $i$ th stage,  $i = 1, 2, \dots, L-1$ , the noise covariance matrix is of the form  $\mathbf{F}_i^{-1}$ . From Section 4.4.1, we can see that  $\mathbf{F}_i \in \mathcal{F}_{KL}(L-i)$ , and using Lemma 5.3.2, it can be immediately shown that  $\mathbf{F}_i^{-1} \in \mathcal{F}_{KL}(L-i)$ , which implies that

$$\text{diag}(\mathbf{F}_i^{-1}) = \underbrace{\{\beta_{i,1}, \dots, \beta_{i,1}\}}_{K \text{ entries}} \underbrace{\{\beta_{i,2}, \dots, \beta_{i,2}\}}_{K \text{ entries}} \dots \underbrace{\{\beta_{i,L-i}, \dots, \beta_{i,L-i}\}}_{K \text{ entries}}, \quad (5.5)$$

where  $\beta_{i,l}$  is the  $l$ th distinct value distributed on the diagonal of  $\mathbf{F}_i^{-1}$ . As a result, a block of  $K$  symbols transmitted from a particular antenna group can be jointly detected at each stage building to an antenna group-wise OSIC detection property.



**Remark:** The joint detection of a block of  $K$  symbols per stage benefits uniquely from the use of orthogonal codes. However, even if the orthogonal codes are used, the appealing group-wise detection property does not hold for  $N_q > 4$ . This is because that  $\mathbf{F}$  is observed to lose the special form as specified in Lemma 5.3.1 and, as a consequence, the assertion on  $\mathbf{F}^{-1}$  in Theorem 5.3.1 may not be true. This confirms the assumption (a5) mentioned in Section 5.2.1.

**Remark:** The MMSE OSIC detector is also capable of per stage jointly detecting a block of  $K$  symbols in essentially the same manner as in the ZF case. From Section 4.4.1, it is shown that the MMSE OSIC detector can be implemented in the same per antenna group-wise detection manner.

## 5.4 OSIC Detection: Complex-Valued Constellations

So far we have developed an antenna group-wise OSIC detection algorithm for real-valued constellations. In what follows, by using the distinctive structures of MFCM  $\mathbf{F}$  again shown in the sequel for complex symbol case, we will develop a particular semi-antenna group-wise OSIC detection scheme for the considered G-STBC systems: only a half of a block of  $2L_q$  real-valued symbols, (i.e., a block of  $L_q$  real-valued symbols either from the real part or imaginary part of the complex-valued symbols associated with an antenna group) may be per stage jointly detected in OSIC based processing.

### 5.4.1 Matched-Filtered Channel Matrix

For complex-valued constellations, by regarding the real part and imaginary part of a complex symbol as two independent real-valued symbols, there are some relevant results (see following lemma) essentially different to those in Lemma 5.3.1. These results will significantly affect the detection framework in OSIC based processing. In the sequel, we denote by  $\mathbf{F}_{p,q}^{(s,t)}$  the  $(s, t)$ th block submatrix of  $\mathbf{F}_{p,q}$  with a proper dimension.

**Lemma 5.4.1.** Consider the complex-valued constellations with  $2 \leq N_p, N_q \leq 4$ . According to [47], we get  $K \in \{2, 8\}$ . Let  $\mathbf{F}_{p,q}$  be the  $(p, q)$ th  $2L_p \times 2L_q$  block submatrix of  $\mathbf{F}$ , where  $\mathbf{F}$  is defined in (2.81). Then the following results hold.

(p1) When  $K = 2$ , it turns out  $N_1 = N_2 = \dots = N_Q = 2$ . Then we have  $\mathbf{F}_{q,q} = \alpha_q \mathbf{I}_4$  and  $\mathbf{F}_{p,q} \in \mathcal{O}(4)$  whenever  $p \neq q$ .

(p2) When  $K = 8$  and  $N_p = N_q = 2$ , then  $\mathbf{F}_{q,q} = \alpha_q \mathbf{I}_{16}$  and  $\mathbf{F}_{p,q} \in \mathbb{R}^{16 \times 16}$  with  $\mathbf{F}_{p,q}^{(s,t)} \in \mathcal{O}(8, 2)$ ,  $s, t = 1, 2$ , whenever  $p \neq q$ . Moreover, we have  $\mathbf{F}_{p,q}^{(1,1)} = \mathbf{F}_{p,q}^{(2,2)}$  and  $\mathbf{F}_{p,q}^{(1,2)} = -\mathbf{F}_{p,q}^{(2,1)}$ .

(p3) When  $K = 8$  and  $N_p = 2$ ,  $3 \leq N_q \leq 4$ , then  $\mathbf{F}_{q,q} = \alpha_q \mathbf{I}_{2L_q}$  and  $\mathbf{F}_{p,q} \in \mathbb{R}^{16 \times 8}$  with  $\mathbf{F}_{p,q}^{(s,t)} \in \mathcal{O}(4)$ ,  $s = 1, \dots, 4$ ,  $t = 1, 2$ , whenever  $p \neq q$ . Moreover, we have  $\mathbf{F}_{p,q}^{(1,1)} = \mathbf{F}_{p,q}^{(2,1)}$ ,  $\mathbf{F}_{p,q}^{(3,1)} = \mathbf{F}_{p,q}^{(4,1)}$ ,  $\mathbf{F}_{p,q}^{(1,2)} = -\mathbf{F}_{p,q}^{(2,2)}$  and  $\mathbf{F}_{p,q}^{(3,2)} = -\mathbf{F}_{p,q}^{(4,2)}$ .

(p4) When  $K = 8$  and  $3 \leq N_p, N_q \leq 4$ , then  $\mathbf{F}_{q,q} = \alpha_q \mathbf{I}_8$  and  $\mathbf{F}_{p,q} \in \mathbb{R}^{8 \times 8}$  with  $\mathbf{F}_{p,q}^{(1,1)} = \mathbf{F}_{p,q}^{(2,2)} \in \mathcal{O}(4)$  and  $\mathbf{F}_{p,q}^{(1,2)} = \mathbf{F}_{p,q}^{(2,1)} = \mathbf{O}_4$ , whenever  $p \neq q$ . In this case,  $\mathbf{F}_{p,q} \in \mathcal{O}(8, 4)$ . ■

*Proof:* See Appendix G. □

Based on Lemma 5.4.1, following facts are asserted.

**Fact 5.4.1.** From Lemma 5.4.1, we have

(f1) If  $K = 8$  and  $N_p = N_q = 2$ , then  $\mathbf{F}_{p,q}^T \mathbf{F}_{p,q} = \mathbf{F}_{p,q} \mathbf{F}_{p,q}^T = c \mathbf{I}_{16}$  for some scalar  $c$ .

(f2) If  $K = 8$  and  $N_p = 2$ ,  $3 \leq N_q \leq 4$ , then  $\mathbf{F}_{p,q}^T \mathbf{F}_{p,q} = \begin{bmatrix} c_1 \mathbf{I}_4 & \mathbf{O}_4 \\ \mathbf{O}_4 & c_2 \mathbf{I}_4 \end{bmatrix}$  for some scalars  $c_1$  and  $c_2$ . ■

The results of Lemma 5.4.1 are summarized in Table 5.2. From Lemma 5.4.1, it is shown that each “ $4 \times 4$ ” (minimum size) submatrix of  $\mathbf{F}$  belongs to an orthogonal design. It is worth to note that, from Lemma 5.3.1 and Lemma 5.4.1,  $\mathbf{F}_{p,q}$  will be a square matrix

except for the case of complex-valued constellations with  $K = 8$  and  $N_p = 2$ ,  $3 \leq N_q \leq 4$ . This is because that, in this case, two different code rates (unit-rate and half-rate) [47] are used simultaneously. This special structure will no longer allow the “antenna group-wise” OSIC detection framework as described in the real-valued constellations case, but instead of a “semi-antenna group-wise” OSIC detection strategy (see the next section for further explanation).

## 5.4.2 Semi-Antenna Group-Wise OSIC Detection

Observing from Lemma 5.4.1 (or Table 5.2) that  $\mathbf{F}$  consists of the orthogonal type block submatrices, it seems intuitively that the antenna group-wise OSIC detection algorithm for complex-valued constellations can also be allowed. However, due to the presence of different code rates (unit-rate and half-rate) among the antenna groups in G-STBC systems, the structures of  $\mathbf{F}^{-1}$  and  $\mathbf{F}_i^{-1}$  may lose some appealing properties. Some results must hence need to be re-examined and re-investigated. Specifically, property (p1) of Lemma 5.4.1 has been discussed in Chapter 4 and shown that it can per stage detect a block of  $2K$  real symbols for a particular antenna group and thus guarantee the antenna group-wise OSIC detection property. By going through essentially the same arguments as what have done in Chapter 4, it can be easily verified that property (p4) of Lemma 5.4.1 also promises the appealing antenna group-wise OSIC detection as mentioned above. For complex-valued constellations, we will thus only focus on cases (p2) and (p3) of Lemma 5.4.1 to develop an appropriate ZF/MMSE OSIC detector. To compute the optimal indexes and corresponding weights (either for ZF criterion or for MMSE criterion) required in OSIC based detection, we need to see the explicit knowledge of diagonal entries of  $\mathbf{F}_i^{-1}$ . In the following theorem, we will see that  $\mathbf{F}_i^{-1}$  no longer inherits the essential features of  $\mathbf{F}_i$ .

Before investigating the feature of  $\mathbf{F}_i^{-1}$ , we need the following some definitions. Define a *decision group*  $\mathcal{G}_{i,g}$ ,  $g = 1, \dots, G_i$ , where  $G_i$  is the total number of decision groups at the  $i$ th stage, that has a half of real-valued symbols of an antenna group at the  $i$ th detection

stage. One antenna group thus includes two decision groups by assumption, each of which has  $L_q$  real-valued symbols. Let  $\mathcal{I}_{i,1}$  and  $\mathcal{I}_{i,1/2}$  be the respective index sets of decision group for unit-rate codes and half-rate codes, with  $G_{i,1} := |\mathcal{I}_{i,1}|$  and  $G_{i,2} := |\mathcal{I}_{i,1/2}|$  denoting the respective cardinalities. Also, let  $\mathcal{I}_i := \mathcal{I}_{i,1} \cup \mathcal{I}_{i,1/2}$  be the index set of total decision groups, with  $G_i := |\mathcal{I}_i|$  denoting the corresponding cardinality. Then we have the facts

$$\mathcal{I}_i = \begin{cases} \mathcal{I}_{i,1} & \text{if } \mathcal{I}_i \cap \mathcal{I}_{i,1/2} = \emptyset, \\ \mathcal{I}_{i,1/2} & \text{if } \mathcal{I}_i \cap \mathcal{I}_{i,1} = \emptyset. \end{cases} \quad (5.6)$$

On the other hand, let us to partition the diagonal entries of  $\mathbf{F}_i$  into  $G_i$  decision groups, each of which has the same (nonzero) value, namely

$$\begin{aligned} \text{diag}(\mathbf{F}_i) &= \underbrace{\{\alpha_{i,1}, \dots, \alpha_{i,1}\}}_{1^{\text{st}} \text{ group: } \mathcal{G}_{i,1}}, \underbrace{\{\alpha_{i,2}, \dots, \alpha_{i,2}\}}_{2^{\text{nd}} \text{ group: } \mathcal{G}_{i,2}}, \dots, \underbrace{\{\alpha_{i,G}, \dots, \alpha_{i,G}\}}_{G_i^{\text{th}} \text{ group: } \mathcal{G}_{i,G_i}} \\ &:= \{\mathcal{G}_{i,1}, \mathcal{G}_{i,2}, \dots, \mathcal{G}_{i,G_i}\}. \end{aligned} \quad (5.7)$$

Assume that  $\{\alpha_{i,g}\}_{g=1}^{G_i}$  exhibit  $D_i(G_i)$  different levels with

$$\lceil G_i/2 \rceil \leq D_i(G_i) \leq G_i, \quad (5.8)$$

where  $D_i$  is a function of  $G_i$ . This is because that when the diagonal entries of  $\mathbf{F}_i$  have  $G_i$  decision groups, there will exist  $G_i - \lceil G_i/2 \rceil + 1$  possible outcomes that have different number of levels presenting on the diagonal of  $\mathbf{F}_i$ . Hence,  $D_i(G_i)$  will also has  $G_i - \lceil G_i/2 \rceil + 1$  possible different values, depending on which outcome of  $G_i$  decision groups occurs. For a concise notation presentation, in the following, we drop the dependence  $G_i$  of  $D_i(G_i)$ .

Next, let us define  $\tilde{\mathcal{F}}_J(G, D)$  to be the set of all invertible real symmetric  $J \times J$  matrices, where  $J, G, D$  are the positive integers, so that, for  $\mathbf{X} \in \tilde{\mathcal{F}}_J(G, D)$ , we have (1) each block diagonal submatrix of  $\mathbf{X}$  is a (nonzero) scaled identity matrix  $\alpha_g \mathbf{I}_{M_g}$ ,  $g = 1, \dots, G$ , with  $M_g \in \{2, 4, 8\}$ , (2)  $\{\alpha_g\}_{g=1}^G$  exhibit  $D$  different values, with  $\lceil G/2 \rceil \leq D \leq G$ , (3) for  $i, j = 1, \dots, G$ ,  $i \neq j$ , each  $4 \times 4$  block submatrix of  $M_i \times M_j$  block off-diagonal submatrix of  $\mathbf{X}$  belongs to  $\mathcal{O}(4)$  or is a zero matrix. Moreover, if  $D = G$ , then  $\tilde{\mathcal{F}}_J(G, D = G)$  will be simplified as  $\tilde{\mathcal{F}}_J(G)$ .

**Theorem 5.4.1.** Consider the complex-valued constellations. Assume that unit-rate and half-rate orthogonal codes [47] exist simultaneously at the  $i$ th detection stage, i.e.,  $\mathcal{I}_i \cap \mathcal{I}_{i,1} \neq \emptyset$  and  $\mathcal{I}_i \cap \mathcal{I}_{i,1/2} \neq \emptyset$ . Let  $\mathcal{I}_i(g)$ ,  $g = 1, \dots, G_i$  be the  $g$ th entry of the set  $\mathcal{I}_i$  and  $\mathbf{F}_i \in \mathbb{R}^{J_i \times J_i}$  the MFCM as defined in (2.81), where

$$J_i := \sum_{j \in \mathcal{I}_i} L_{\lceil j/2 \rceil} = \sum_{g=1}^{G_i} L_{\lceil \mathcal{I}_i(g)/2 \rceil}, \quad (5.9)$$

with  $L_q \in \{2, 4, 8\}$  for all  $q$ . If  $\mathbf{F}_i \in \tilde{\mathcal{F}}_{J_i}(G_i, D_i)$ , then  $\mathbf{F}_i^{-1} \in \tilde{\mathcal{F}}_{J_i}(G_i)$ . ■

*Proof:* See Appendix H. □

Theorem 5.4.1 shows that  $J_i$  diagonal entries of  $\mathbf{F}_i^{-1}$  will assume  $G_i \geq D_i$  distinct levels  $\{\beta_{i,g}\}_{g=1}^{G_i}$  (where  $\mathbf{F}_i$  only has  $D_i$  distinct levels), that is

$$\begin{aligned} \text{diag}(\mathbf{F}_i^{-1}) &= \underbrace{\{\beta_{i,1}, \dots, \beta_{i,1}\}}_{1^{\text{st}} \text{ group: } \mathcal{G}_{i,1}} \underbrace{\{\beta_{i,2}, \dots, \beta_{i,2}\}}_{2^{\text{nd}} \text{ group: } \mathcal{G}_{i,2}} \dots \underbrace{\{\beta_{i,G_i}, \dots, \beta_{i,G_i}\}}_{G_i^{\text{th}} \text{ group: } \mathcal{G}_{i,G_i}} \\ &:= \{\mathcal{G}_{i,1}, \mathcal{G}_{i,2}, \dots, \mathcal{G}_{i,G_i}\}. \end{aligned} \quad (5.10)$$

From (5.10), we can see that it suffices to search among the  $G_i$  values, one associated with a particular block of  $L_q$  real-valued symbols (say the *layer*), that is, a half of real-valued symbols from the  $q$ th antenna group, for the optimal detection order. Based on the same procedures of the antenna group-wise OSIC algorithm (ZF or MMSE criterion) developed for the real-valued constellations, we thus can simultaneously detect a block of  $L_q$  real-valued symbols from a particular antenna group rather than  $2L_q$  real-valued symbols at the  $i$ th stage. We call such a detection strategy as the “semi-antenna group-wise” detection. The same detection manner holds at the latter stages if the unit-rate and half-rate codes still exist simultaneously in those yet-to-be-detected antenna groups. However, when the code rates of the yet-to-be-detected antenna groups are the same, which means that (5.6) holds, it can be shown by applying Theorem 5.3.1 that the detection property will be simplified to the antenna group-wise detection manner, that is, it will per stage jointly detect either a block of  $L_q$  or a block of  $2L_q$  real-valued symbols depending on the number of symbols remained

in the corresponding yet-to-be-detected antenna group. As a result, to completely detect the  $2L_q$  real-valued symbols associated with a particular antenna group, such a detection manner might double the computational load compared to the antenna group-wise detection property, so that the overall detection complexity is at most the double of the antenna group-wise detection property.

For example, partitioning the  $N = 8$  transmit antennas into three groups which are allocated with 2, 2 and 4 antennas, respectively, and the corresponding code rates are 1, 1 and 1/2 leads to the required number of stages  $L$  for optimal ordering performed in the OSIC based detection mentioned above will be bounded by  $4 \leq L \leq 6$ . On the contrary, if we perform the antenna group-wise OSIC detection, only three stages may be sufficient to detect all the transmitted symbols.

**Remark:** For complex-valued constellations with  $3 \leq N_q \leq 4$ , the more spectral efficient orthogonal codes (or called the delay optimal codes) are the 3/4-rate codes [47], [94]. It is known in the literatures that these codes provide the highest code rate. However, with such the codes used, by going through essentially the same procedures as what we have done in the proof of Theorem 5.4.1, it can be shown that all the diagonal entries of  $\mathbf{F}_i^{-1}$  will result in different values from each other. This will lose the capability of the appealing group-wise detection property and thus induce a relatively large detection computational load. From this observation and based on the tradeoff between the performance and computational load, we hence do not consider such the codes.

**Remark:** The Naguib's [78] and Stamoulis's [79] methods are two popular interference suppression/signal detection algorithms for the MU STBC systems. Based on the block orthogonal structure embedded in  $\mathbf{F}$  as specified in Lemma 5.3.1 and 5.4.1, the two methods can also be realized in the aforementioned system. In the numerical results, we will consider the two methods to evaluate the detection performance of the proposed OSIC based detector.

## 5.5 Implementation Issues of OSIC Detection

In this section, some implementation issues of the OSIC based detection for complex-valued constellations including the antenna group-wise detection strategy, two-stage detection strategy and a computationally efficient recursion based realization are presented to further reduce the receiver complexity.

### 5.5.1 Antenna Group-Wise Detection Strategy

It is shown in Section 5.3.2 and 5.4.2, the antenna group-wise detection property can only be done for the real-valued constellations. However, for the complex-valued constellations, such a detection property will be fail, leading to an increase in computational complexity. To reduce the receiver complexity for the considered system without a critical performance degradation, a simple antenna group-wise OSIC detector is proposed, in which a block of  $2L_q$  real-valued symbols associated with a particular antenna group is jointly detected per stage. It is noticed from Theorem 5.4.1 that the  $2L_{q_i}$  entries distributed on the diagonal of  $\mathbf{F}_i^{-1}$  within an antenna group will response to two levels as  $\beta_{L_{q_i},1}$  and  $\beta_{L_{q_i},2}$ .

To carry out the *antenna group-wise* detection, an intuitive approach is to “directly search” the group index of the diagonal entries of  $\mathbf{F}_i^{-1}$  at which antenna group is minimal. This is the simplest method, but however it may also induce a large detection error (see the computer simulations). To tackle this problem, we propose to “average” the two-level values  $\beta_{L_{q_i},1}$  and  $\beta_{L_{q_i},2}$  within an antenna group as follows

$$\beta_{i,q} := \frac{\beta_{L_{q_i},1} + \beta_{L_{q_i},2}}{2}, \quad i = 1, \dots, Q-1, \quad q = 1, \dots, Q-i, \quad (5.11)$$

and rewrite the  $\sum_{q=1}^{Q-i} 2L_q$  diagonal entries of  $\mathbf{F}_i^{-1}$  as

$$\text{diag}(\mathbf{F}_i^{-1}) = \underbrace{[\beta_{i,1}, \dots, \beta_{i,1}]}_{2L_1 \text{ entries}} \underbrace{[\beta_{i,2}, \dots, \beta_{i,2}]}_{2L_2 \text{ entries}} \dots \underbrace{[\beta_{i,Q-i}, \dots, \beta_{i,Q-i}]}_{2L_{Q-i} \text{ entries}}^T. \quad (5.12)$$

Based on  $\beta_{i,1}, \beta_{i,2}, \dots, \beta_{i,Q-i}$ , we can thus search the corresponding indices at which antenna group is minimal. Since the detection order under these ways may violate the actual optimal

sorting, such a simple processing strategy can reduce computation at the expense of a possible performance drop. However, as we will see in the simulation results, the performance drop is not critical. Note that this type of processing strategy is unique through the use of real-valued representation of signal model shown in Section 5.2.2.

### 5.5.2 Two-Stage Detection Strategy

As mentioned in Section 5.4.2, if the group code rates among the yet-to-be-detected antenna groups are different, the antenna group-wise detection property will be fail and thus may increase the detection complexity. However, as the group code rates are the same, it will reduce to the antenna group-wise OSIC detection. An appropriate solution to solve this problem can be done based on the following two-stage processing. (1) We first categorize the antenna groups into two classes based on code rate: one class for high-rate (unit-rate) code (i.e.,  $N_q = 2$ ) and another for low-rate (half-rate) code (i.e.,  $N_q = 3$  or  $N_q = 4$ ). (2) Detect the symbols based on class-by-class manner. To this end, we must explicitly know which class should be detected first. Fortunately, since all the  $N$  transmit antennas are partitioned into several small groups, each of which places two, three or four antennas and is ST encoded based on O-STBC, the transmit diversity advantages obtained from these groups may be different leading to different BER performances among these groups. This fact will consequentially dominate the detection order in the proposed OSIC biased detection. Theoretically, the antenna group that has the higher diversity advantage (i.e., larger  $N_q$ ) is robust against the channel impairments and can thus be detected first. From this point of view, we propose a “two-stage” detection strategy, in which the low-rate antenna groups ( $N_q = 3$  or  $N_q = 4$ ) are detected first through the OSIC detection algorithm and then for low-rate ones ( $N_q = 2$ ), to further reduce the detection computational complexity. Likewise, due to the non-optimal detection ordering, such a detection strategy may also cause a possible performance loss, but this performance loss is slight and within an acceptable regain (see the simulation results for illustration). Note that in the first processing stage, since the different



code rates still exist, the semi-antenna group-wise detection may be done, but this can be solved by the proposed “average” or “direct” method described in previous section.

For the G-STBC system, since some antenna groups may be allocated more antenna elements (e.g., three and four elements), the receiver will suffer from a certain time latency for data detection to exploit the diversity benefit for such the antenna groups. For example, if three or four antennas are used for a particular antenna group,  $K = 8$  symbol periods are the temporal latent cost for collecting a diversity gain of order three or four. The inherent time latency produces link robustness for those antenna groups with larger antenna elements at the expense of a reduced data processing efficiency. This is because that during the processing time for larger diversity advantage, the receiver will receive extra independent source symbols from other high-rate antenna groups (i.e.,  $N_q = 2$ ). This will enlarge the overall data processing dimension. As a consequence, there will be an unavoidable increase in the detector complexity. Fortunately, the two-stage detection strategy can alleviate the increase of such the detector complexity. Since as the low-rate antenna groups detected and cancelled from the signal  $\mathbf{y}_c(k)$  leaving the high-rate antenna groups, the time latency can thus be vanished and the detection property can turn back to the pure high-rate detection case where only two symbol periods are sufficient for data detection.

### 5.5.3 Recursive Implementation

To alleviate the detection complexity, by using the embedded structures of  $\mathbf{F}$  and  $\mathbf{F}^{-1}$ , a recursive algorithm is then developed to implement the OSIC based detection. In the proposed OSIC based detection algorithms (either for ZF or MMSE criterion), it needs the information of detection order and corresponding weights. In particular, the computations of detection order and weights require the explicit knowledge of the inverses of MFCM<sup>2</sup>  $\mathbf{F}^{-1}$  at initial stage and  $\mathbf{F}_i^{-1}$  at the  $i$ th stage. As a result, the main computational burden of the OSIC algorithm lies in the successive matrix inversions throughout all stages. However, it

---

<sup>2</sup>For notation simplicity, we only focus on the ZF criterion.

will be shown in what follows how the knowledge of the embedded structures of  $\mathbf{F}$ , and its inverse  $\mathbf{F}^{-1}$ , can further help to alleviate the computations.

Specifically, with the spatial structure of  $\mathbf{F}$  given, there is an efficient way of finding  $\mathbf{F}^{-1}$  by solving a set of linear equations of relatively small dimensions based on the Cholesky factorization [97]. Moreover, the inverse matrix required at each stage could be recursively computed based on the parameters available in the previous stage. This is because that the computation of  $\mathbf{F}_i^{-1}$  can be directly and completely obtained from the information of  $\mathbf{F}_{i-1}^{-1}$  and  $\mathbf{F}_{i-1}$  (see Section 4.5.1).

In the proof of Theorem 5.4.1, it is shown that the minimum dimension that can form an orthogonal matrix in  $\mathbf{F}_{p,q}^{-1}$  is four, where  $\mathbf{F}_{p,q}^{-1} \in \mathbb{R}^{2L_p \times 2L_q}$  is the  $(p, q)$ th block submatrix of  $\mathbf{F}^{-1}$ . Since the recursion based implementation can only tackle a block orthogonal matrix once at a time, as the matrix dimension of  $\mathbf{F}$  is large, directly implement the recursion based processing for the semi-antenna group-wise OSIC detection described in Section 5.4 may need more stages. Fortunately, the two-stage detection strategy, which detects the low rate codes first and then for high rate codes, can help to reduce the required number of stages. As a result, in the following we will develop the recursive implementation based on the two-stage detection strategy. To this end, we assume that: (1) there are two levels on the diagonal entries of  $\mathbf{F}_i^{-1}$  within an antenna group at each stage, (2) the last column and row blocks of  $\mathbf{F}_i = \mathbf{H}_{c,i}^T \mathbf{H}_{c,i}$  corresponding to the desired signature of an antenna group are to be deleted (i.e., to be detected) at the  $i$ th stage, and (3) the antenna groups with three or four antennas are first detected. With  $\mathbf{F}_0^{-1} := \mathbf{F}^{-1}$  obtained at the initial stage, in what follows we will show how  $\mathbf{F}_i^{-1}$  at each stage can be recursively computed based on  $\mathbf{F}_{i-1}$  and  $\mathbf{F}_{i-1}^{-1}$ . Denote by  $\mathbf{F}_i \in \mathbb{R}^{2(L_T - \sum_{j=1}^i L_{q_j}) \times 2(L_T - \sum_{j=1}^i L_{q_j})}$  the MFCM at the  $i$ th stage, where  $L_{q_i}$  is the symbol block length of the  $q$ th group to be deleted at the  $i$ th stage. Then  $\mathbf{F}_{i-1}$  can

be partitioned as

$$\mathbf{F}_{i-1} := \left[ \begin{array}{c|c} & \\ \hline \mathbf{F}_i & \mathbf{B}_{i-1} \\ \hline \mathbf{B}_{i-1}^T & \mathbf{D}_{i-1} \\ \hline \end{array} \right] \in \mathbb{R}^{2(L_T - \sum_{j=1}^{i-1} L_{q_j}) \times 2(L_T - \sum_{j=1}^{i-1} L_{q_j})}, \quad (5.13)$$

where  $\mathbf{B}_{i-1} \in \mathbb{R}^{2(L_T - \sum_{j=1}^{i-1} L_{q_j}) \times 2L_{q_{i-1}}}$ , and  $\mathbf{D}_{i-1} = d_{i-1} \mathbf{I}_{2L_{q_{i-1}}}$  for some scalar  $d_{i-1}$ . Denote by  $\bar{\mathbf{F}}_{i-1}$  the  $2(L_T - \sum_{j=1}^i L_{q_j}) \times 2(L_T - \sum_{j=1}^i L_{q_j})$  principle submatrix of  $\mathbf{F}_{i-1}^{-1}$ . From (5.13) and using the inversion lemma for block matrix (see Appendix C),  $\bar{\mathbf{F}}_{i-1}$  can be expressed as

$$\bar{\mathbf{F}}_{i-1} = (\mathbf{F}_i - \mathbf{B}_{i-1} \mathbf{D}_{i-1}^{-1} \mathbf{B}_{i-1}^T)^{-1}. \quad (5.14)$$

In particular, it follows from (5.14) that

$$\mathbf{F}_i = \bar{\mathbf{F}}_{i-1}^{-1} + \mathbf{B}_{i-1} \mathbf{D}_{i-1}^{-1} \mathbf{B}_{i-1}^T, \quad (5.15)$$

and then using the matrix inversion lemma [4], we have

$$\begin{aligned} \mathbf{F}_i^{-1} &= (\bar{\mathbf{F}}_{i-1}^{-1} + \mathbf{B}_{i-1} \mathbf{D}_{i-1}^{-1} \mathbf{B}_{i-1}^T)^{-1} \\ &= \bar{\mathbf{F}}_{i-1} - \bar{\mathbf{F}}_{i-1} \mathbf{B}_{i-1} (\mathbf{B}_{i-1}^T \bar{\mathbf{F}}_{i-1} \mathbf{B}_{i-1} + \mathbf{D}_{i-1})^{-1} \mathbf{B}_{i-1}^T \bar{\mathbf{F}}_{i-1} \\ &= \bar{\mathbf{F}}_{i-1} - \mathbf{E}_{i-1} \mathbf{C}_{i-1}^{-1} \mathbf{E}_{i-1}^T, \end{aligned} \quad (5.16)$$

where  $\mathbf{E}_{i-1} := \bar{\mathbf{F}}_{i-1} \mathbf{B}_{i-1} \in \mathbb{R}^{2(L_T - \sum_{j=1}^i L_{q_j}) \times 2L_{q_{i-1}}}$ , and

$$\mathbf{C}_{i-1} := \mathbf{B}_{i-1}^T \bar{\mathbf{F}}_{i-1} \mathbf{B}_{i-1} + \mathbf{D}_{i-1} = \begin{bmatrix} c_{1,i-1} \mathbf{I}_{L_{q_{i-1}}} & \mathbf{O}_{L_{q_{i-1}}} \\ \mathbf{O}_{L_{q_{i-1}}} & c_{2,i-1} \mathbf{I}_{L_{q_{i-1}}} \end{bmatrix}, \quad (5.17)$$

for some scalars  $c_{j,i-1}$ ,  $j = 1, 2$ . In (5.17), we have used the fact that  $\mathbf{B}_{i-1}^T \bar{\mathbf{F}}_{i-1} \mathbf{B}_{i-1}$  possesses exactly the same structure as that of  $\mathbf{C}_{i-1}$ , which benefits from the usage of the orthogonal codes, and this fact can be shown immediately from the proof of Theorem 5.4.1 and the Fact 5.4.1. The simplification in (5.16) implies that  $\mathbf{F}_i^{-1}$  at each stage can be recursively computed based on  $\mathbf{F}_{i-1}$  and  $\mathbf{F}_{i-1}^{-1}$ . This provides a simple recursive formula for computing  $\mathbf{F}_i^{-1}$  based on  $\mathbf{F}_{i-1}$  and  $\mathbf{F}_{i-1}^{-1}$  without any ‘‘direct’’ matrix inversion operations and hence

reduces the detection computational load. Note that the good property described in (5.17) is unique for the two-stage detection. If we detect the symbols without the use of two-stage strategy, the result of  $\mathbf{B}_{i-1}^T \bar{\mathbf{F}}_{i-1} \mathbf{B}_{i-1}$  is no longer a diagonal matrix, and we will thus need some matrix inversions or more stages for symbol detection leading to an additional increase in computational complexity. It is also noticed that as the antenna groups placed three or four antennas detected, based on the two-stage detection property we have  $c_{1,i} = c_{2,i}$  in equation (5.17). The proposed recursive algorithm for antenna group-wise OSIC detection is basically a block based realization of the method [108] applied to the conventional symbol-wise OSIC detection. A distinctive feature proposed here is the key result (5.17) so that the inverse of  $\mathbf{B}_{i-1}^T \bar{\mathbf{F}}_{i-1} \mathbf{B}_{i-1} + \mathbf{D}_{i-1}$  in the computation of  $\mathbf{F}_i^{-1}$  can be completely avoided.

## 5.6 Grouped Space-Time Block Codes

In G-STBC systems, with the antenna partition done, the code rate  $R_q$  associated with an antenna group will thus be defined depending on the number of antennas  $N_q$ . Specifically, combining the antenna group codewords into a “big” ST codeword induces the G-STBC. To fulfil the block orthogonal matrix property for allowing a low-complexity group-wise OSIC detection as described in Section 5.3 and 5.4, in what follows, we will develop a computationally efficient G-STBCs regardless of the number of total transmit antennas  $N$ . Based on the designed codewords, we then provide a code selection criterion to appropriately choose the codewords in accordance with the link performance under the constraints of total transmit power and SE.

### 5.6.1 Codeword Construction and Property

Since  $L_q$  symbols are transmitted from the  $q$ th antenna group over  $K$  symbol periods, or in other words, there are in total  $L_T$  data symbols are transmitted from  $N$  antennas over  $K$

symbol periods, the code rate of a G-STBC can be given by

$$R^N := \frac{L_T}{K} = \sum_{q=1}^Q \underbrace{\frac{L_q}{K}}_{:=R_q^N} = \sum_{q=1}^Q \frac{\kappa B_q}{K} = \sum_{q=1}^Q \underbrace{\frac{B_q}{K_q}}_{\bar{R}_q^N}, \quad (5.18)$$

where  $\kappa_q := K/K_q = L_q/B_q$  is the number of regular O-STBCs, called the *elementary codes*, in the  $q$ th antenna group over  $K$  symbol periods, and  $R_q^N := L_q/K$  and  $\bar{R}_q^N := B_q/K_q$  are the code rates of the  $q$ th antenna group code and elementary code, respectively. Note that in such a G-STBC system,  $R_q^N = \bar{R}_q^N$ . From (5.18), we can see that the overall code rate of G-STBC is just the sum of the code rates of  $Q$  group codes. As a result, the total ST area [86]  $NK$ , occupied by the grouped ST codeword will satisfy

$$\sum_{q=1}^Q \left( \frac{L_q}{B_q} \right) N_q K_q = \sum_{q=1}^Q \kappa_q N_q K_q = NK. \quad (5.19)$$

For the fixed  $N$  and  $Q$ , let us define the array antenna architecture as  $(N_1, N_2, \dots, N_Q)$  with  $2 \leq N_q \leq 4$  and  $N_1 + N_2 + \dots + N_Q = N$ . Let  $\mathcal{S}^N$  be the set of all possible antenna architectures over  $N$  transmit antennas and define  $J^N := |\mathcal{S}^N|$  be the respective cardinality, which is the number of all possible sets for constructing an  $N \times K$  G-STBC. Note that during each symbol block  $K$ , different antenna configuration (code construction) can be used for transmission based on the system requirements and/or channel conditions. Moreover, if we define  $Q_j^N$  to be the number of antenna groups of the  $j$ th possible set for  $N$  transmit antennas, then we have

$$\mathcal{S}^N = \left\{ \left( N_1, \dots, N_{Q_j^N} \right) \right\}, \quad j = 1, \dots, J^N, \quad (5.20)$$

so that  $Q_{\min}^N \leq Q_j^N \leq Q_{\max}^N$ , where

$$Q_{\min}^N := \lceil N/4 \rceil \quad (5.21)$$

and

$$Q_{\max}^N := \lfloor N/2 \rfloor \quad (5.22)$$

are the respective minimum and maximum numbers of antenna groups over  $\mathcal{S}^N$ .

**Example 5.6.1:** When  $N = 10$ , there are  $J^N = 5$  possible antenna configuration sets:

$$\mathcal{S}^N = \{ \underbrace{(3, 3, 4)}_{\mathcal{S}_1^N: Q_1^N=3}, \underbrace{(2, 4, 4)}_{\mathcal{S}_2^N: Q_2^N=3}, \underbrace{(2, 2, 3, 3)}_{\mathcal{S}_3^N: Q_3^N=4}, \underbrace{(2, 2, 2, 4)}_{\mathcal{S}_4^N: Q_4^N=4}, \underbrace{(2, 2, 2, 2, 2)}_{\mathcal{S}_5^N: Q_5^N=5} \}, \quad (5.23)$$

and  $Q_{\min}^N = \lceil N/4 \rceil = 3$ ,  $Q_{\max}^N = \lfloor N/2 \rfloor = 5$ . The corresponding code structures are shown in Figure 5.2. With above example, some interpretations and discussions regarding the code properties are as follows.

- (a) **Code Rate:** As we can see from (5.23) that,  $\mathcal{S}_1^N$  and  $\mathcal{S}_2^N$  have the same number of antenna groups, i.e.,  $Q_1^N = Q_2^N = 3$ , but different antenna configurations (3,3,4) and (2,4,4). This is also observed from  $\mathcal{S}_3^N$  and  $\mathcal{S}_4^N$ . Specifically, according to (5.18),  $\mathcal{S}_1^N$  provides a code rate of 1.5 but  $\mathcal{S}_2^N$  provides a code rate of 2, and 3, 3.5 and 5 for  $\mathcal{S}_3^N$ ,  $\mathcal{S}_4^N$  and  $\mathcal{S}_5^N$ , respectively, which means that, for a fixed  $N$ , different antenna configurations may provide different code rates even under the same number of antenna groups.
- (b) **Diversity advantages:** Different transmit diversity gains are provided by different antenna configurations leading to different BER performances.
- (c) **Computational complexity:** Based on the OSIC based detection described in Section 5.3 and 5.4, the maximum required number of stages  $\bar{L}^N$  for data detection are respective 3, 6, 8, 8 and 5, showing that different antenna configurations will also cause different computational loads at the receiver.

As a result, for a fixed  $N$ , the code characteristics including the code rate, BER performance and receiver computational complexity will be significantly affected by the antenna configuration. In general, for a fixed  $N$ , an antenna configuration with more antenna groups will provide higher code rate, but lower diversity advantage. However, for a fixed  $N$  and a fixed  $Q$ , an antenna configuration with lower code rate does not necessarily provide a higher diversity advantage, and the antenna configuration with larger difference among  $N_q$ 's may not perform worse than that with small difference among  $N_q$ 's (see the computer simulations). To evaluate the codeword performance, it should jointly consider the corresponding

required detection computational complexity to achieve a fair comparison. Based on above discussions, we can conclude that an optimal selection of the antenna configuration, namely the code selection, that can achieve the best system performance should jointly consider the code rate, BER performance and receiver computational complexity. Table 5.3 shows the all possible antenna configurations, the corresponding code rate  $R^N$  and maximum required number of stages  $\bar{L}^N$  for OSIC based with the number of total transmit antennas from  $N = 2$  to  $N = 16$ .

### 5.6.2 Codeword Selection Criterion

As mentioned above, the code selection is a very critical factor to the overall system performance. The code rate, modulation type, diversity advantage and detection complexity should be jointly considered at the receiver to efficiently choose an optimal codeword (antenna configuration), to feed back to the transmitter. We refer to a combination of specific codeword and modulation as a *mode*. This is similar to the definition named in [109]. Denote by  $\mathcal{M}_j^N$  the  $j$ th mode of all the possible mode candidates over  $N$  transmit antennas, and  $\eta(\mathcal{M}_j^N)$  the corresponding SE. Here we consider the  $\bar{M}$ -ary PSK and  $\bar{M}$ -ary QAM modulations. As a result, the SE of the  $j$ th mode can be represented as

$$\eta(\mathcal{M}_j^N) = R^N(j) \times R_b(j) \quad (\text{bits/sec/Hz}), \quad (5.24)$$

where  $R^N(j)$  is the code rate of the  $j$ th mode according to the antenna configuration and  $R_b(j)$  is the transmission bit rate of the  $j$ th mode according to the modulation type. This shows that the SE  $\eta(\mathcal{M}_j^N)$  varies with the code rate  $R^N$  and transmission bit rate  $R_b$ , and we can appropriately adjust the two parameters to achieve the desired SE. Equivalently, specify the codeword and modulation type will thus define the overall SE. Note that we do not consider the transmit power allocation strategy even an efficient method applied to pure SM systems has been derived in [110] and can be incorporated in the proposed systems.

Since the antenna group-wise detection strategy can reduce the detection complexity significantly with an acceptable performance drop, in the following, we will design the code

selection criterion under this detection strategy. Also, by using the recursion based processing for realizing the antenna group-wise detection, we will neglect the receiver computational load for deriving the code selection criterion (note that different detection algorithm may select different codeword). Then the optimal mode selection (i.e., code selection) criterion under the given SNR constraint and SE  $\eta(\mathcal{M}_j^N)$  can thus be found by searching the index of candidate modes whose has the minimum BER performance

$$j = \arg \min_{\forall j} P_e(\mathcal{M}_j^N | \{\text{SNR}, \eta(\mathcal{M}_j^N)\}). \quad (5.25)$$

Since SE is a function of code rate  $R^N$  and transmission bit rate  $R_b$ , for a fixed SE, specifying  $R_b$  (i.e., modulation type) will specify  $R^N$  or the codeword. Then the codeword is preferred if

$$j = \arg \min_{\forall j} P_e(\mathcal{S}_j^N | \{P_T, R_b\}). \quad (5.26)$$

This shows that the optimal codeword is chosen based on the candidate at which the antenna configuration set  $\mathcal{S}_j^N$  can achieve the minimum BER performance under the constraints of total transmit power  $P_T$  and transmission bit rate  $R_b$ .

Since the transmitted symbols of a particular antenna group are independent of those of another group, the overall BER  $P_e$  can be calculated by averaging the BERs of all groups

$$P_e = \frac{1}{Q} \sum_{q=1}^Q P_{e,q}, \quad (5.27)$$

where  $P_{e,q}$  is the BER of the  $q$ th antenna group. By ignoring error propagation effects in all interactions of OSIC detection [110], the BER of the  $q$ th antenna group can be approximated as a function of the post-detection SINR  $\gamma_q$  depending on the adopted detection criterion and transmission bit rate  $R_{b,q}$

$$P_{e,q} \approx g_{\gamma, R_b}(\gamma_q, R_{b,q}), \quad (5.28)$$

with [14]

$$\gamma_q = \begin{cases} 1/\sigma_{v,q}^2 & \text{for ZF criterion} \\ (1 - \varepsilon_q)/\varepsilon_q & \text{for MMSE criterion} \end{cases} \quad (5.29)$$



where  $\sigma_{v,q}^2$  and  $\varepsilon_q$  are the output noise power and symbol MSE of  $q$ th antenna group as defined in (4.5) and (4.10), respectively. From (5.28) and (5.29), we can see that the BER performance is greatly depends on the detection metric  $\gamma_q$  and  $R_{b,q}$ . When uncoded  $\bar{M}$ -ary QAM modulation is used for all transmitted symbols, the BER of the  $q$ th antenna group can be tightly approximated as [111]

$$\begin{aligned}
g_{\gamma, R_b}(\gamma_q, R_b) &\approx \frac{2}{R_{b,q}} \left(1 - \frac{1}{\sqrt{2^{R_{b,q}}}}\right) \operatorname{erfc} \left( \sqrt{\frac{1.5\gamma_q}{2^{R_{b,q}} - 1}} \right) \\
&= \begin{cases} \frac{2}{R_{b,q}} \left(1 - \frac{1}{\sqrt{2^{R_{b,q}}}}\right) \operatorname{erfc} \left( \sqrt{\frac{1.5}{(2^{R_{b,q}} - 1)\sigma_{v,q}^2}} \right) & \text{for ZF criterion} \\ \frac{2}{R_{b,q}} \left(1 - \frac{1}{\sqrt{2^{R_{b,q}}}}\right) \operatorname{erfc} \left( \sqrt{\frac{1.5(1-\varepsilon_q)}{(2^{R_{b,q}} - 1)\varepsilon_q}} \right) & \text{for MMSE criterion} \end{cases} \quad (5.30)
\end{aligned}$$

where  $2^{R_{b,q}} = \bar{M}$  and  $\operatorname{erfc}(\cdot)$  is the complementary error function.

Based on the above mathematical analysis, the optimal codeword selection algorithm in minimum BER sense under the constraints of total transmit power and required SE is summarized as follows.

- Choose the number of total transmit antennas  $N$ , and give the total transmit power  $P_T$  and required SE  $\eta$ .
- For the fixed  $N$ , choose the proper codeword candidates according the the Table 5.3 under the constraints of total transmit power  $P_T$  and required SE  $\eta$ .
- For different SNR values, select the optimal ST codeword of candidates based on the minimum BER performance through the analysis results (5.27)-(5.30).

## 5.7 Computer Simulations

Several computer simulations are conducted in this section to evaluate the performance of the proposed OSIC based detector in a packet data system. The fading channels between the transmitter and receiver are assumed to be quasi-static, which remain constant over each packet of 100 symbol blocks and independently vary between packets. Perfect channel

information is assumed to be available at the receiver but not at the transmitter. In all simulations, unless otherwise mentioned, QPSK modulation is used. Finally, we assume that the antenna groups are equal power and define  $\text{SNR} := P_T/\sigma_v^2$  (as defined in [10], [48], [54], [62], [65], [68]).

The first simulation evaluates the performance of the proposed OSIC based detection and compares with the Naguib's method [78] and Stamoulis's method [79], which are the two popular interference suppression/signal detection algorithms adopted in the MU STBC systems. In this simulation,  $Q = 3$  antenna groups are assumed at the transmitter and  $M = 3$  antenna elements are placed at the receiver. Figure 5.3 plots the BER performances of the three detection schemes as a function of SNR. In Figure 5.3(a), total  $N = 6$  transmit antennas are used with the antenna configuration being  $\mathcal{S}^N = (2, 2, 2)$  ( $\bar{L}^N = 3$ ), but in Figure 5.3(b),  $N = 7$  with  $\mathcal{S}^N = (2, 2, 3)$  are considered ( $\bar{L}^N = 6$ ). As shown in Figures 5.3(a) and (b), the performances of all methods can be roughly separated into two groups. The Stamoulis's method achieves the worst performance since it is a pure decouple based algorithm and cannot enjoy the increased receive diversity gain as the algorithm goes on, even it is combined with the power ordering strategy. The similar performance is also confirmed by the Naguib's one-step method. For the better performance group, on the contrary, the Naguib's two-step method provides a considerable performance at lower SNR cases but it suffers from a performance degradation in the medium-to-high SNR cases due to the PIC detection mechanism. The results also show that, in most SNR regions, the proposed method can successfully suppress the interference and obtain the large diversity gain through the SIC mechanism. To investigate the performance of the proposed OSIC based detection algorithm for G-STBCs, in the rest of simulations, only the ZF OSIC detection is considered for simplicity.

In the second simulation, the effects on the proposed detection strategies described in Section 5.5.1 and 5.5.2 are evaluated for  $N = 8$ ,  $M = 3$ ,  $Q = 3$  and  $\mathcal{S}^N = (2, 2, 4)$ . Both the actual and maximum ( $\bar{L}^N = 6$ ) required numbers of stages performed in OSIC

based detection are included and compared. Note that in this simulation, there are two different levels distributed on the diagonal of  $\mathbf{F}^{-1}$  within an antenna group leading to an semi-antenna group-wise OSIC detection since the different code rates exist. We adopt the average and direct methods described in Section 5.5.1 for realizing the antenna group-wise detection. In addition, we consider the two-stage detection strategy described in Section 5.5.2 combined with above average method. In this simulation, the minimum and maximum required numbers of stages are four and six, respectively, but the numbers of stages for antenna group-wise and two-stage detection strategies are three. The BER performance results plotted in Figure 5.4 show that the two-stage and antenna group-wise detection strategies suffer from a slight performance degradation compared with the proposed OSIC based method with maximum number of stages (about 1.5 dB for two-stage scheme and 0.5  $\sim$  1 dB for antenna group-wise scheme at  $10^{-5}$  BER performance) due to the insufficient stages and non-optimal detection ordering. Also as expected, the performance of average method is superior to that of direct selection method. Moreover, with an appropriate number of stages ( $4 \leq L \leq 6$ ), the proposed recursive OSIC based solution will perform exactly the same as that of the case with maximum number of stages. For simplicity, in the following simulations, we will only consider the two-stage with average antenna group-wise detection strategy.

The third simulation investigates the flexibility of the proposed ST codewords and compares it with two existing extreme transmission techniques for  $N = M = 4$ : pure SM technique with ZF OSIC detection [56] and pure O-STBC technique with ML decoding [47]. In this simulation, the total SE is constrained<sup>3</sup> to be  $\eta = 4$  (bits/sec/Hz). As a result, BPSK modulation and 256-QAM modulation are used for the pure SM and STBC techniques, respectively. On the other hand, for the proposed G-STBCs,  $\mathcal{S}^N = (2, 2)$  ( $Q = 2$ ) with QPSK is considered. The BER performances of the three different transmission techniques as a

---

<sup>3</sup>To fairly evaluate the performance of the different transmission techniques, the most used approach is to examine the BER performance under a given SE constraint (also see [3], [68], [82])

function of SNR are plotted in Figure 5.5. As we can see from this figure, the pure O-STBC technique has a performance limit in lower SNR regions due to the use of high order QAM modulation. The pure SM technique also achieve a poor BER performance especially in media-to-high SNR regions due to the small degrees-of-freedom for interference suppression and the lower diversity advantages for mitigating the channel variation (no TD gain). However, the proposed technique provides a very excellent performance in all SNR cases. This is because that the proposed technique in fact appropriately combines these two extreme techniques and use a moderate modulation order (through (5.24)) to provide a better diversity advantage under the required SE. The results also show the flexibility provided by the proposed technique through simply selecting the ST codeword and modulation type to achieve a better performance.

Finally, we examine and compare the performance of the proposed ST codewords for a fixed  $N$ . In this simulation, we also evaluate the BER performance using the mathematical analysis through (5.27)-(5.30). In the first experiment,  $N = 6$  transmit antennas and  $M = 3$  receive antennas are used. As a result, according to Table 5.3, we have three possible antenna configuration sets (i.e., ST codewords), and they are:  $\mathcal{S}_1^N = (3, 3)$  ( $Q = 2$ ),  $\mathcal{S}_2^N = (2, 4)$  ( $Q = 2$ ) and  $\mathcal{S}_3^N = (2, 2, 2)$  ( $Q = 3$ ) with the corresponding code rates being  $R^N = 1, 1.5$  and 3, respectively. We assume that the total SE is constrained to be  $\eta = 6$  (bits/sec/Hz). To meet the SE constraint, 64-QAM, 16-QAM and QPSK modulations are respectively used for the above three antenna configuration sets. As observed in Figure 5.6(a), the curves of mathematical analysis for all codeword cases are nearly the same as those of simulation results. Figure 5.6(a) also shows that,  $\mathcal{S}_2^N = (2, 4)$  achieves the best BER performance in medial-to-high SNRs. However, for lower SNR cases,  $\mathcal{S}^N = (2, 2, 2)$  may be the best candidate. In the second experiment,  $N = 8$  and  $M = 4$  are assumed and the results are plotted in Figure 5.6(b). In this scenario, we assume that  $\eta = 4$  (bits/sec/Hz). From Table 5.3 and under the total SE constraint, we thus adopt the following three antenna configuration sets for comparison:  $\mathcal{S}_1^N = (4, 4)$  ( $Q = 2$ ),  $\mathcal{S}_2^N = (2, 3, 3)$  ( $Q = 3$ ) and  $\mathcal{S}_3^N =$

$(2, 2, 2, 2)$  ( $Q = 4$ ), with the respective modulation types being 16-QAM, QPSK and BPSK. Again, the mathematical analysis is consistent with the simulation result. For large  $L$ , however, a slight performance difference between the analysis result and simulation one occurs. This may be due to the approximation in (5.30) and the assumption of ignoring the error propagation effects in OSIC detection algorithm for the analytic derivation. Based on the observations, the best codeword can thus be selected in accordance with the analytic BER performance as follows:  $\mathcal{S}_3^N = (2, 2, 2, 2)$  for low SNRs ( $\leq 2$  dB),  $\mathcal{S}_1^N = (2, 3, 3)$  for moderate SNRs ( $2 \sim 14$  dB) and  $\mathcal{S}_2^N = (4, 4)$  for high SNRs ( $\geq 14$  dB).

## 5.8 Summary

In this chapter, an efficient MIMO transceiver architecture with a small feedback information is proposed for the downlink over the Rayleigh flat-fading channels. In the transmitter, a grouped STBC with arbitrary number of transmit antennas is presented for achieving the high link quality and at the same time the high spectral efficiency. In particular, the total transmit antennas are partitioned into several small groups with each being individually encoded according to the orthogonal based STBC. The proposed encoding strategy reduces the number of antennas required at the receiver meeting the practical consideration in implementation cost and physical size. At the receiver, based on the distinctive structure of the matched-filtered channel matrix, it is shown that an appealing antenna group-wise OSIC detection property, in which a block of symbols associated with an antenna group can be jointly detected per stage, is allowed for real-valued symbols. This detection strategy, however, is then shown that it cannot be realized for complex-valued symbols leading to an increase in computational complexity. To tackle this problem, an average antenna group-wise detection approach and a two-stage scheme are then proposed to reduce the detection complexity at the expense of a small performance drop. These schemes are unique through the use of orthogonal STBCs under the real-valued signal model representation. Moreover,

to further alleviate the detection computational load, a recursive implementation of such a group-wise OSIC detector by using the algebraic properties of orthogonal codes is also developed. Next, based on the proposed OSIC detection property, we can find all the possible codewords of the grouped STBCs regardless of the number of transmit antennas. We then study the code properties and design a simple selection criterion for choosing the optimal ST codeword based on the minimum BER criterion when the total transmit power and data throughput are constrained. Finally, simulation results show that the proposed ST encoding technique can flexibly and judiciously select the ST codewords and modulation types to achieve the better performance than the pure spatial multiplexing and transmit diversity techniques, and the semi-antenna/antenna group-wise OSIC detection scheme can provide a computationally efficient solution for such the systems.



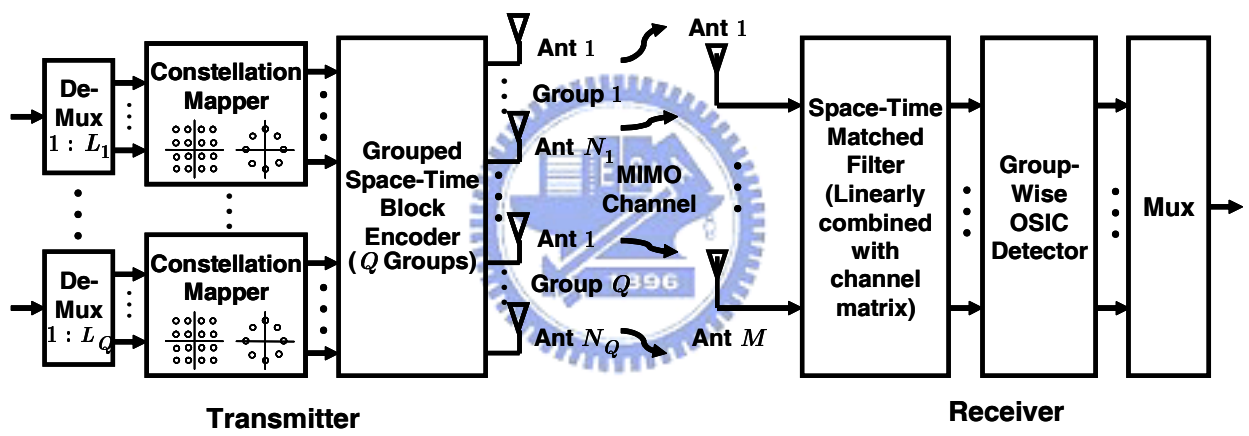


Figure 5.1: Proposed transmitter and receiver architectures for G-STBC system.

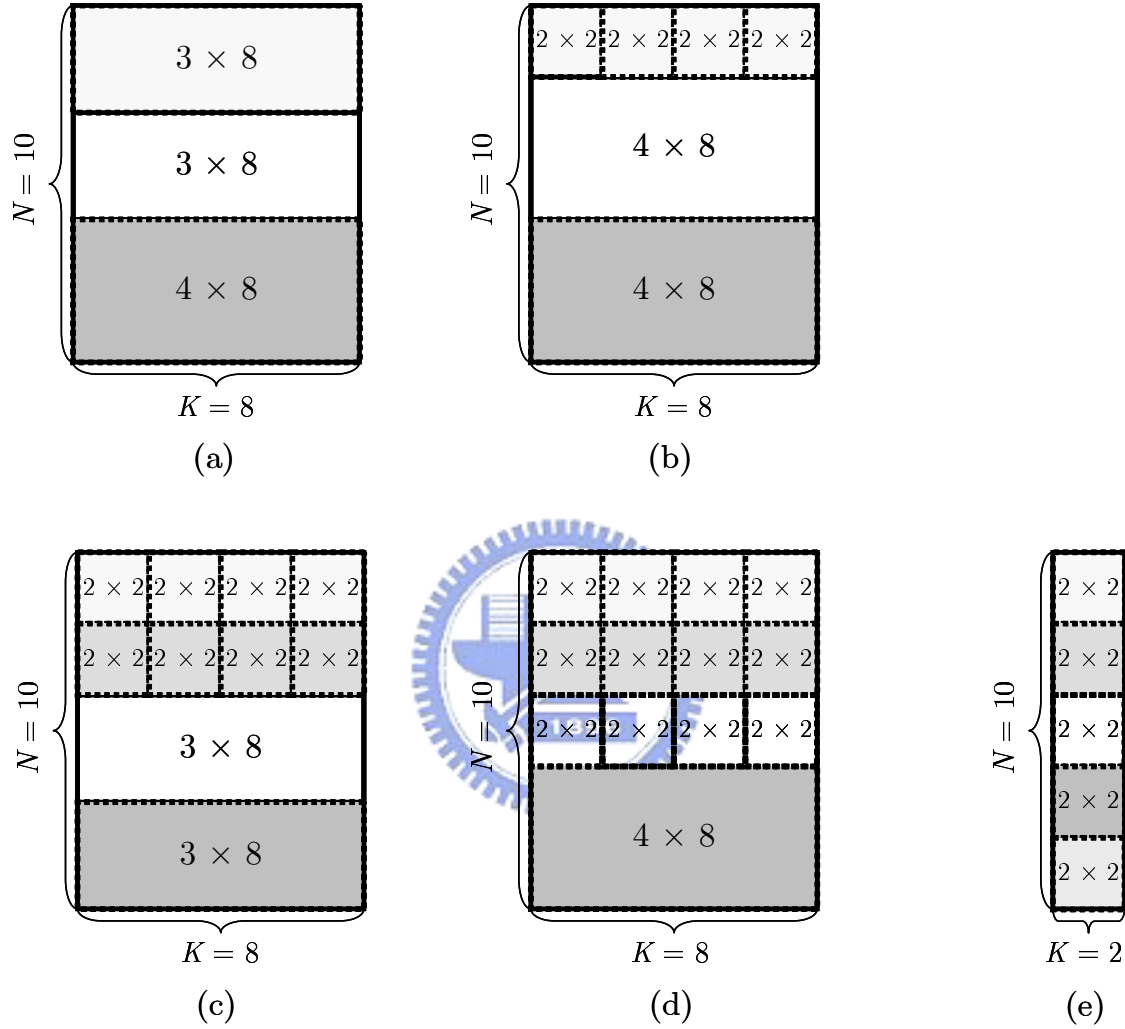


Figure 5.2: Five possible  $N \times K$  G-STBC structures with  $N = 10$ . (a)  $K = 8$ ,  $Q = 3$ ,  $\mathcal{S}^N = (3, 3, 4)$ ,  $R^N = 1.5$  and  $\bar{L}^N = 3$ . (b)  $K = 8$ ,  $Q = 3$ ,  $\mathcal{S}^N = (2, 4, 4)$ ,  $R^N = 2$  and  $\bar{L}^N = 6$ . (c)  $K = 8$ ,  $Q = 4$ ,  $\mathcal{S}^N = (2, 2, 3, 3)$ ,  $R^N = 3$  and  $\bar{L}^N = 8$ . (d)  $K = 8$ ,  $Q = 4$ ,  $\mathcal{S}^N = (2, 2, 2, 4)$ ,  $R^N = 3.5$  and  $\bar{L}^N = 8$ . (e)  $K = 2$ ,  $Q = 5$ ,  $\mathcal{S}^N = (2, 2, 2, 2, 2)$ ,  $R^N = 5$  and  $\bar{L}^N = 5$ .



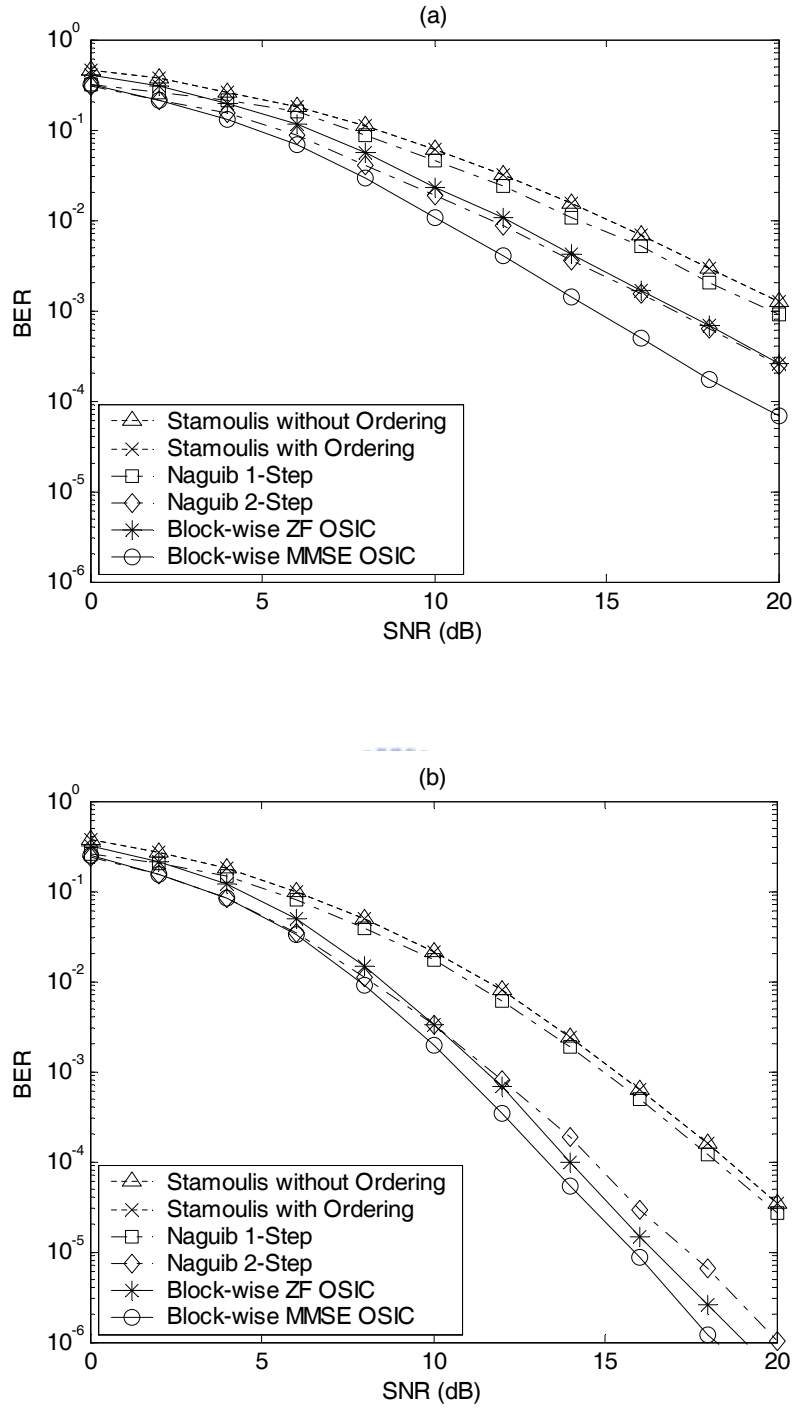


Figure 5.3: BER performance of different detection methods as a function of SNR with  $M = 3$  and  $Q = 3$ . (a)  $N = 6$  and  $\mathcal{S}^N = (2, 2, 2)$ . (b)  $N = 7$  and  $\mathcal{S}^N = (2, 2, 3)$ .

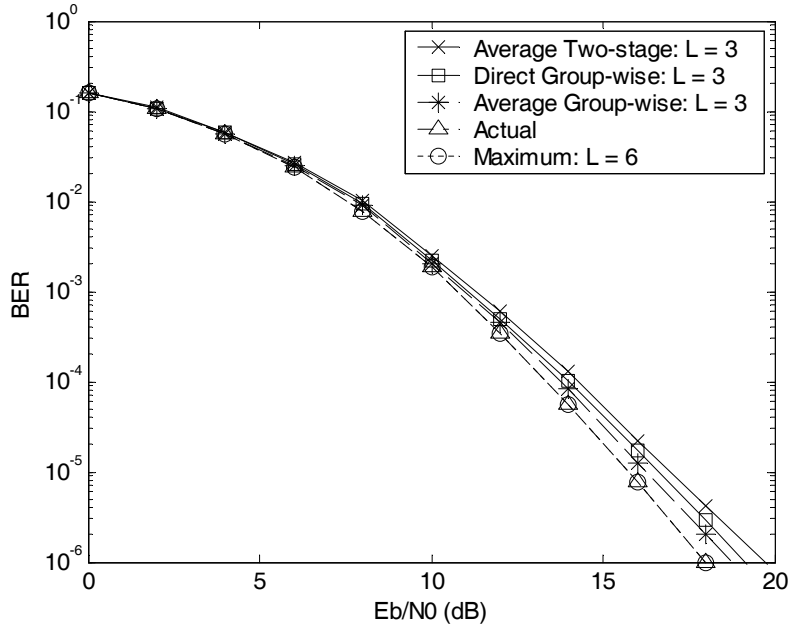


Figure 5.4: BER performance of different detection strategies of proposed OSIC detector as a function of SNR with  $N = 8$ ,  $M = 3$ ,  $Q = 3$  and  $\mathcal{S}^N = (2, 2, 4)$ .

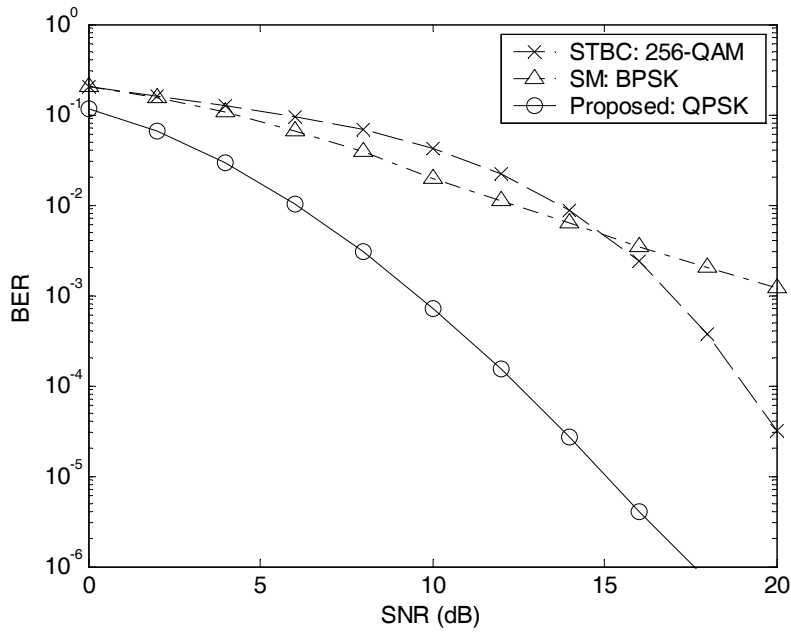


Figure 5.5: BER performance of different transmission techniques as a function of SNR with  $N = 4$  and  $M = 4$ .

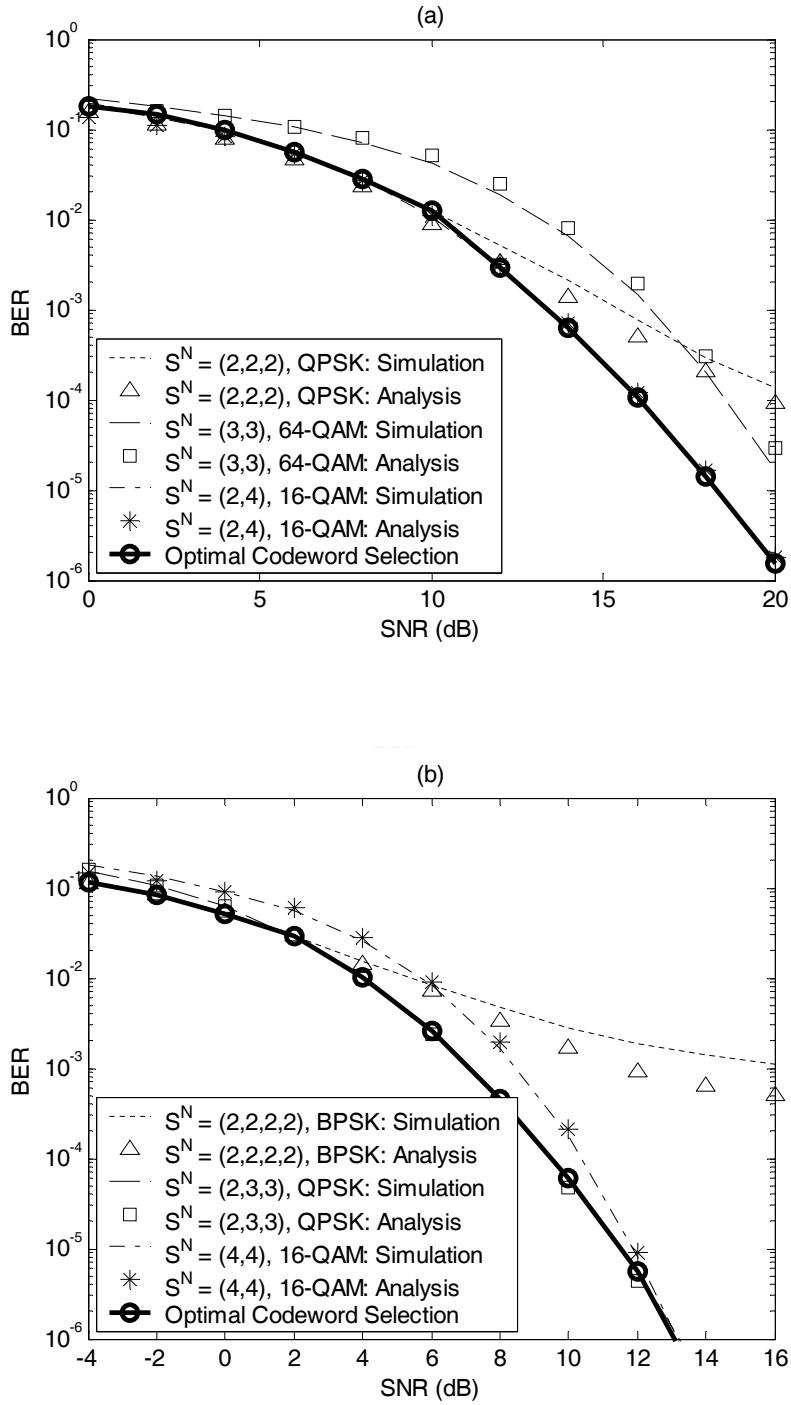


Figure 5.6: BER performance of different proposed ST codewords as a function of SNR. (a)  $N = 6$  and  $M = 3$ . (b)  $N = 8$  and  $M = 4$ .

Table 5.1: Summary of structures of the MFCM  $\mathbf{F}_{p,q}$  for real-valued constellations.

Rreal-Valued Constellations		
$K = 2$	$N_p = N_q = 2$	$p = q : \mathbf{F}_{q,q} = \alpha_q \mathbf{I}_2$ $p \neq q : \mathbf{F}_{p,q} \in \mathcal{O}(2)$
$K = 4$	$N_p = N_q = 2$	$p = q : \mathbf{F}_{q,q} = \alpha_q \mathbf{I}_4$ $p \neq q : \mathbf{F}_{p,q} \in \mathbf{R}^{4 \times 4}$ $\mathbf{F}_{p,q}^{(1,1)} = \mathbf{F}_{p,q}^{(2,2)} \in \mathcal{O}(2);$ $\mathbf{F}_{p,q}^{(1,2)} = \mathbf{F}_{p,q}^{(2,1)} = \mathbf{O}_2$
	$2 \leq N_p, N_q \leq 4$ $N_p \neq N_q \neq 2$	$p = q : \mathbf{F}_{q,q} = \alpha_q \mathbf{I}_4$ $p \neq q : \mathbf{F}_{p,q} \in \mathcal{O}(4)$

Table 5.2: Summary of structures of the MFCM  $\mathbf{F}_{p,q}$  for complex-valued constellations.

Complex-Valued Constellations		
$K = 2$	$N_p = N_q = 2$	$p = q : \mathbf{F}_{q,q} = \alpha_q \mathbf{I}_4$ $p \neq q : \mathbf{F}_{p,q} \in \mathcal{O}(4)$
$K = 8$	$N_p = N_q = 2$	$p = q : \mathbf{F}_{q,q} = \alpha_q \mathbf{I}_{16}$ $p \neq q : \mathbf{F}_{p,q} \in \mathbf{R}^{16 \times 16}$ $\mathbf{F}_{p,q}^{(s,t)} \in \mathcal{O}(8,2), \quad 1 \leq s, t \leq 2$ $\mathbf{F}_{p,q}^{(1,1)} = \mathbf{F}_{p,q}^{(2,2)}; \quad \mathbf{F}_{p,q}^{(1,2)} = -\mathbf{F}_{p,q}^{(2,1)}$
	$N_p = 2$ $3 \leq N_q \leq 4$	$p = q : \mathbf{F}_{q,q} = \alpha_q \mathbf{I}_{2L_q}$ $p \neq q : \mathbf{F}_{p,q} \in \mathbf{R}^{16 \times 8}$ $\mathbf{F}_{p,q}^{(s,t)} \in \mathcal{O}(4), \quad 1 \leq s \leq 4, \quad 1 \leq t \leq 2$ $\mathbf{F}_{p,q}^{(1,1)} = \mathbf{F}_{p,q}^{(2,1)}; \quad \mathbf{F}_{p,q}^{(3,1)} = \mathbf{F}_{p,q}^{(4,1)};$ $\mathbf{F}_{p,q}^{(1,2)} = -\mathbf{F}_{p,q}^{(2,2)}; \quad \mathbf{F}_{p,q}^{(3,2)} = -\mathbf{F}_{p,q}^{(4,2)}$
	$3 \leq N_p, N_q \leq 4$	$p = q : \mathbf{F}_{q,q} = \alpha_q \mathbf{I}_4$ $p \neq q : \mathbf{F}_{p,q} \in \mathbf{R}^{8 \times 8}$ $\mathbf{F}_{p,q}^{(1,1)} = \mathbf{F}_{p,q}^{(2,2)} \in \mathcal{O}(4); \quad \mathbf{F}_{p,q}^{(1,2)} = \mathbf{F}_{p,q}^{(2,1)} = \mathbf{O}_4$

Table 5.3: Possible sets of antenna configuration and corresponding code rate and maximum required number of stages for OSIC based detection.

$N$	$J^N$	Possible Sets of Antenna Configuration, $\mathcal{S}^N$	Coding Rates, $R^{N*}$	Max Number of Iterations, $\bar{L}^N *$
2	1	(2)	1	1
3	1	(3)	0.5	1
4	2	(4), (2,2)	0.5, 2	1, 2
5	1	(2,3)	1.5	4
6	3	(3,3), (2,4), (2,2,2)	1, 1.5, 3	2, 4, 3
7	2	(3,4), (2,2,3)	1, 2.5	2, 6
8	4	(4,4), (2,3,3), (2,2,4), (2,2,2,2)	1, 2, 2.5, 4	2, 6, 6, 4
9	3	(3,3,3), (2,3,4), (2,2,2,3)	1.5, 2, 3.5	6, 3, 8
10	5	(3,3,4), (2,4,4), (2,2,3,3), (2,2,2,4), (2,2,2,2,2)	1.5, 2, 3, 3.5, 5	3, 6, 8, 8, 5
11	4	(3,4,4), (2,3,3,3), (2,2,3,4), (2,2,2,2,4)	1.5, 2.5, 3, 4.5	3, 8, 8, 10
12	7	(4,4,4), (3,3,3,3), (2,3,3,4), (2,2,4,4), (2,2,2,3,3), (2,2,2,2,4), (2,2,2,2,2,2)	1.5, 2, 2.5, 3, 4, 4.5, 6	3, 4, 8, 8, 10, 10, 6
13	5	(3,3,3,4), (2,3,4,4), (2,2,3,3,3), (2,2,2,3,4), (2,2,2,2,2,3)	2, 2.5, 3.5, 4, 5.5	4, 8, 10, 10, 12
14	8	(3,3,4,4), (2,4,4,4), (2,3,3,3,3), (2,2,3,3,4), (2,2,2,4,4), (2,2,2,2,3,3), (2,2,2,2,2,4), (2,2,2,2,2,2,2)	2, 2.5, 3, 3.5, 4, 5, 5.5, 7	4, 8, 10, 10, 10, 12, 12, 7
15	7	(3,4,4,4), (3,3,3,3,3), (2,3,3,3,4), (2,2,3,4,4), (2,2,2,3,3,3), (2,2,2,2,3,4), (2,2,2,2,2,2,3)	2, 2.5, 3, 3.5, 4.5, 5, 6.5	4, 5, 10, 10, 12, 12, 14
16	10	(4,4,4,4), (3,3,3,3,4), (2,3,3,4,4), (2,2,4,4,4), (2,2,3,3,3,3), (2,2,2,3,3,4), (2,2,2,2,4,4), (2,2,2,2,2,3,3), (2,2,2,2,2,2,4), (2,2,2,2,2,2,2,2)	2, 2.5, 3, 3.5, 4, 4.5, 5, 6, 6.5, 8	4, 10, 10, 10, 12, 12, 12, 14, 14, 8

\* For complex-valued symbol constellations.

# Chapter 6

## Conclusions

### 6.1 Summary of Thesis

The use of multiple transmit antennas and multiple receive antennas in wireless communications has been considered in this thesis. Several ST processing techniques regarding the ST signaling and interference suppression for MIMO wireless communications have also been addressed and some new transmitter and receiver architectures have been proposed. The proposed ST transceivers have been shown through mathematical analysis and computer simulations to be (i) low-complexity implementation, (ii) smart and robust to the channel variation, and (iii) better matched to the channel condition and system requirement over the popular existing methods.

The introductory chapter included the background overview, literature review, motivations and contributions of the thesis related to the topics under consideration. In Chapter 2, we gave an overview of the MIMO wireless communications. The basic concepts including the ST system model, channel capacity and two popular ST techniques, namely the STBC and V-BLAST have been discussed.

In Chapter 3, an OSIC based MIMO equalizer has been proposed for the MIMO wireless systems over the frequency selective multipath channels. Such an MIMO equalizer was

developed as an reduced-rank (RR) realization of the conventional MMSE DFE. In particular, the FFF weights of the MMSE DFE at each stage of OSIC are determined in the RR form based on the GSC technique for reduced complexity implementation, but the FBF weights are the same as that of MMSE DFE. To further alleviate the computational load of the receiver, the RR realization of the FFF part of the DFE was derived by incorporating the CG algorithm. It has been shown that the proposed RR MIMO equalizer has a much faster convergence behavior and lower computational load while achieving nearly the same performance as that of optimum MMSE DFE, which often requires a higher complexity and overhead for pilot symbols.

In Chapter 4, a flexible MIMO transceiver has been proposed for the uplink in MU dual-signaling systems over the Rayleigh flat-fading channels. In such a system, each mobile terminal data stream can be either ST block encoded for transmit diversity or spatially multiplexed for achieving high data rate, across multiple antennas based on its channel condition. At the base station, the received signal is first linearly combined with the channel matrix followed by an OSIC algorithm to detect the transmitted symbols from each mobile terminal. By exploiting the distinctive structure of matched-filtered channel matrix (MFCM), resulting uniquely from the O-STBCs, it has been shown that the OSIC detection can be realized in a group-wise manner. Moreover, the imbedded structure of MFCM was also exploited for deriving a low-complexity recursive detector implementation. Flop count analysis has shown that the proposed method can indeed potentially reduce the computational load of the receiver, and numerical simulations have demonstrated the effectiveness of the proposed OSIC based solution which compares favorably with the existing interference mitigation schemes in MU ST coded systems.

In contrast to Chapter 4, an efficient transmitter and receiver design with a slight amount of feedback information in the downlink over a point-to-point G-STBC system has been studied in Chapter 5. Our emphasis is on the ST encoding and decoding schemes that can both efficiently provide the TD for high LQ and achieve the parallel transmission for

high SE. In particular, the transmit antenna array was decoupled into several sets with each being allocated two, three or four antennas, and being encoded based on O-STBCs. At the receiver, for low-complexity detector implementation, an antenna group-wise OSIC detection for real-valued constellations and a semi-antenna group-wise OSIC detection for complex-valued constellations have been developed similarly based on the approach derived in Chapter 4. To relieve the computational complexity of the receiver, several implementation issues have also been discussed. Next, based on the group-wise OSIC detection property, we have derived all possible ST codewords of the G-STBC regardless of the number of transmit antennas. According to the ST codewords, we have studied the codeword properties and designed a selection criterion for properly choosing the codeword based on the minimum BER performance subject to the total transmit power and required SE. Such an ST encoding strategy can potentially reduce the number of receiver antennas. Simulation study has shown that the proposed codeword selection scheme can flexibly and judiciously choose the optimal ST codeword over the conventional pure SM and TD techniques, and the OSIC based detection method can provide a reasonable solution for such a system.



## 6.2 Future Work

So far, the study presented in this thesis has thoroughly discussed the ST signal processing techniques for MIMO wireless communications. There are yet several other interesting related topics remaining to be addressed:

- **Advanced ST Codeword Design**

A future research topic related to our work is the ST codeword design. For an MU scenario, the joint signal can be viewed as an ST coded signal without a centralized control. MU interference presents a major impairment that limits the system capacity. To carry out a practical MIMO environment, on the other hand, in a multi-cell and MU scenario, the receiver will receive the CCI from other cells and thus also reduce the



system performance. A judicious signal design at each mobile user is thus important to effectively mitigate the interference. We may combine the STC scheme and interference resistant modulation to yield a new ST coding/modulation scheme with an additional gain when each user employs multiple antennas. Rank and determinant criteria would be two important issues for developing an optimal code, as far as the extension of our study is concerned.

- **Transmit Signal Processing**

In this thesis, we only considered the receiver based MU signal processing. However, in a wireless system using a central base station and several mobile terminals, only the uplink can be practically handled by the receiver based techniques because they require relatively intensive computation and associated power. The desire to keep mobile terminals simple and power efficient makes complex receiver algorithms unattractive for processing the downlink signal received at the user terminal. As a result, if the channel information is known to the transmitter (i.e., base station), an alternative to MU detection is to transfer the system complexity to the transmitter and precode the signal such that the interference is minimized at each of mobile terminals.

- **Adaptive Transmission Mode Selection**

The thesis considered only the ST transmission techniques. Depending on the channel conditions, the optimal transmission technique will be selected to combat the channel impairments. As a result, the case of switching mechanism among the transmission techniques, including STC, SM and beamforming, should be studied as well and an adaptive transceiver should dynamically adjust the transmission parameters such as the ST processing mode and modulation order, according to the instantaneous channel statistics, to meet the target error rate and data rate.

- **Link Adaptation**

Since wireless channels exhibit a time-varying response, adaptive transmission strate-

gies should be taken into account in our extension work to prevent insufficient utilization of the channel capacity. Therefore, the further research activity in link adaptation is aimed at selecting a transmission scheme making the best possible use of the resources available for transmission by adaptively adjusting the system parameters, e.g., transmit power level, bandwidth, modulation order (constellation size) and coding rate in order to achieve a required quality of service (QoS), in terms of the error probability, bandwidth efficiency, SNR and complexity. For an assigned QoS, the goal is to increase the average SE by taking advantage of the transmitter having knowledge of the channel information.

- **Cross-Layer Design**

Observing that the network performance in mobile wireless applications is determined significantly by a complex interaction among physical layer, link layer, medium access control (MAC) and transmission control protocol (TCP), a joint design of these layers becomes a trend of further research topics. The cross-layer design stack, including the adaptive resource management, dynamic management of the allocation spectrum, dynamic management of the multiple access schemes and dynamic soft channel management, may work toward an optimized interconnection among different layers so as to efficiently couple the physical layer and upper protocol layer design. Note that the AMC is essentially a powerful technique in physical layer for meeting the required QoS. In order to achieve the best performance demands, integration of AMC schemes and MAC protocol for different requirements will be a potential future work.

# Appendix A

## Proof of Lemma 4.3.1

Assume that real-valued constellations with unit-rate codes ( $K = P$ ) are used for STBC terminal.

*Proof of (1):* We first note from (2.72) and (2.73) that the effective signal component (priori to matched filtering) of the stream from the  $p$ th O-STBC user is  $\sqrt{\frac{P_p}{N}} \bar{\mathbf{H}}_p \bar{\mathbf{A}}_p$ , where  $\bar{\mathbf{H}}_p$  and  $\bar{\mathbf{A}}_p$  are defined in (2.73) and (2.76), respectively. Then it can be easily checked that the effective signal coupling matrix is  $\sqrt{\frac{P_p P_q}{N^2}} \bar{\mathbf{A}}_p^T \bar{\mathbf{H}}_p^T \bar{\mathbf{H}}_q \bar{\mathbf{A}}_q$ , with the  $(i, j)$ th entry,  $i, j = 1, 2, \dots, P$ , being computed as (c.f. (2.91))

$$f_{p,q}^{(i,j)} = \sqrt{\frac{P_p P_q}{N^2}} \sum_{k=1}^P \left( \tilde{\mathbf{a}}_{p,i}^{(k)} \right)^T \tilde{\mathbf{H}}_p^T \tilde{\mathbf{H}}_q \tilde{\mathbf{a}}_{q,j}^{(k)} = \text{Re} \left\{ \sqrt{\frac{P_p P_q}{N^2}} \sum_{m=1}^M \left( \mathbf{h}_p^{(m)} \right)^H \mathbf{A}_{p,i} \mathbf{A}_{q,j} \mathbf{h}_q^{(m)} \right\}, \quad (\text{A.1})$$

where  $\left( \mathbf{h}_p^{(m)} \right)^T$  is the  $m$ th row of  $\mathbf{H}_p$ . Note that since  $p, q \in \mathcal{S}_D$ ,  $\mathbf{A}_p = \mathbf{A}_q$  and thus  $\mathbf{A}_{p,i} = \mathbf{A}_{q,j}$ ,  $i, j = 1, 2, \dots, P$ . We also notice that the first constraint in (4.3) implies that  $f_{q,q}^{(i,i)} = \frac{P_q}{N} \sum_{m=1}^M \|\mathbf{h}_{q,m}\|^2$  for each  $q$ ; the second constraint in (4.3), namely, the matrix  $\mathbf{A}_{p,i} \mathbf{A}_{q,j}^H$  is skew-symmetric for  $i \neq j$ , guarantees that  $f_{q,q}^{(i,i)} = 0$ . Thus  $\mathbf{F}_{q,q}$  is always a scalar multiple of the identity matrix (of proper dimension).

To prove (1), it thus suffices to check that  $\mathbf{F}_{p,q} \in \mathcal{O}(P)$  whenever  $p \neq q$ . Since  $\mathbf{A}_{p,i} \in \mathbb{R}^{N \times K}$  is real, we write

$$f_{p,q}^{(i,j)} = \text{Re} \left\{ \sqrt{\frac{P_p P_q}{N^2}} \sum_{m=1}^M \left( \mathbf{h}_p^{(m)} \right)^H \mathbf{A}_{p,i} \mathbf{A}_{q,j} \mathbf{h}_q^{(m)} \right\}$$

$$\begin{aligned}
&= \sqrt{\frac{P_p P_q}{N^2}} \sum_{m=1}^M (\text{Re}\{\mathbf{h}_{p,m}\})^T \mathbf{A}_{p,i} \mathbf{A}_{q,j}^T \text{Re}\{\mathbf{h}_{q,m}\} \\
&\quad + (\text{Im}\{\mathbf{h}_{p,m}\})^T \mathbf{A}_{p,i} \mathbf{A}_{q,j}^T \text{Im}\{\mathbf{h}_{q,m}\},
\end{aligned} \tag{A.2}$$

where  $\mathbf{h}_{q,m} := \text{Re}\{\mathbf{h}_{q,m}\} + j\text{Im}\{\mathbf{h}_{q,m}\}$ . For  $N = 2$  (i.e.,  $P = 2$ ), we have

$$\mathbf{A}_{p,1} = \mathbf{A}_{q,1} = \mathbf{I}_2, \quad \mathbf{A}_{p,2} = \mathbf{A}_{q,2} = \begin{bmatrix} 0 & -1 \\ 1 & 0 \end{bmatrix}, \tag{A.3}$$

and it is easy to check with (A.2) that  $\mathbf{F}_{p,q} \in \mathcal{O}(2)$ . For  $N = 3$  or 4 (i.e.,  $P = 4$ ), it follows from [47] that

$$\begin{aligned}
\mathbf{A}_{p,1} = \mathbf{A}_{q,1} &= \mathbf{I}_4, \quad \mathbf{A}_{p,2} = \mathbf{A}_{q,2} = \begin{bmatrix} 1 & 0 \\ 0 & -1 \end{bmatrix} \otimes \begin{bmatrix} 0 & -1 \\ 1 & 0 \end{bmatrix}, \\
\mathbf{A}_{p,3} = \mathbf{A}_{q,3} &= \begin{bmatrix} 0 & -1 \\ 1 & 0 \end{bmatrix} \otimes \begin{bmatrix} 1 & 0 \\ 0 & 1 \end{bmatrix}, \quad \mathbf{A}_{p,4} = \mathbf{A}_{q,4} = \begin{bmatrix} 0 & 1 \\ 1 & 0 \end{bmatrix} \otimes \begin{bmatrix} 0 & -1 \\ 1 & 0 \end{bmatrix}.
\end{aligned} \tag{A.4}$$

It is easy to see that

$$\mathbf{A}_{p,i}^T = -\mathbf{A}_{p,i} \quad 2 \leq i \leq 4, \tag{A.5}$$

and

$$\mathbf{A}_{p,2} \mathbf{A}_{p,3}^T = \mathbf{A}_{p,4}, \quad \mathbf{A}_{p,2} \mathbf{A}_{p,4}^T = -\mathbf{A}_{p,3}, \quad \mathbf{A}_{p,3} \mathbf{A}_{p,4}^T = \mathbf{A}_{p,2}. \tag{A.6}$$

Based on (A.2), (A.5) and (A.6), it can be shown that  $\mathbf{F}_{p,q} \in \mathcal{O}(4)$  and this proves (1).  $\square$

*Proof of (2):* From (2.72) and (2.73) again, the effective signal component (priori to matched filtering) of the stream from the  $n$ th transmit antenna of the  $p$ th SM user is  $\sqrt{\frac{P_p}{N}} \bar{\mathbf{H}}_{p,n} \bar{\mathbf{A}}_p^{(n)}$ , where  $\bar{\mathbf{H}}_{p,n} \in \mathbb{R}^{2MP \times 2P}$  denotes the matrix consisting of the  $(2P(n-1)+l)$ th columns of  $\bar{\mathbf{H}}_p$  (see (2.73)), for  $1 \leq l \leq 2P$ ,  $\bar{\mathbf{A}}_p^{(n)} \in \mathbb{R}^{2P \times P}$  denotes the real-valued ST modulation matrix of the  $n$ th antenna at the  $p$ th SM user as defined in (2.73). Accordingly, the MF coupling signature between this stream and that from the  $d$ th antenna of the  $q$ th

SM user is  $\sqrt{\frac{P_q P_q}{N^2}} (\bar{\mathbf{A}}_p^{(n)})^T \bar{\mathbf{H}}_{p,n}^T \bar{\mathbf{H}}_{q,d} \bar{\mathbf{A}}_q^{(d)}$ , whose  $(i, j)$ th entry,  $i, j = 1, 2, \dots, P$ , is directly computed as

$$\begin{aligned} f_{p,q}^{(i,j)}(n, d) &= \sqrt{\frac{P_q P_q}{N^2}} \sum_{k=1}^P (\tilde{\mathbf{a}}_{p,i}^{(k)}(n))^T \tilde{\mathbf{H}}_{p,n}^T \tilde{\mathbf{H}}_{q,d} \tilde{\mathbf{a}}_{q,j}^{(k)}(d) \\ &= \sum_{k=1}^K \operatorname{Re} \left\{ \sqrt{\frac{P_q P_q}{N^2}} (a_{p,i}^{(k)}(n))^* \mathbf{h}_{p,n}^H \mathbf{h}_{q,d} a_{q,j}^{(k)}(d) \right\} \\ &= \operatorname{Re} \left\{ \sqrt{\frac{P_q P_q}{N^2}} \sum_{m=1}^M (h_{p,n}^{(m)})^* \mathbf{a}_{p,i}^H(n) \mathbf{a}_{q,j}(d) h_{q,d}^{(m)} \right\}, \end{aligned} \quad (\text{A.7})$$

where

$$\tilde{\mathbf{a}}_{p,i}^{(k)}(n) := \left[ \operatorname{Re} \{ a_{p,i}^{(k)}(n) \} \quad \operatorname{Im} \{ a_{p,i}^{(k)}(n) \} \right]^T \in \mathbb{R}^2, \quad (\text{A.8})$$

with  $a_{p,i}^{(k)}(n)$  being the  $n$ th entry of  $\mathbf{a}_{p,i}^{(k)}$ , (the  $k$ th column of the ST modulation matrix  $\mathbf{A}_{p,i}$ ),

$$\tilde{\mathbf{H}}_{p,n} := \begin{bmatrix} \operatorname{Re} \{ \mathbf{h}_{p,n} \} & -\operatorname{Im} \{ \mathbf{h}_{p,n} \} \\ \operatorname{Im} \{ \mathbf{h}_{p,n} \} & \operatorname{Re} \{ \mathbf{h}_{p,n} \} \end{bmatrix} \in \mathbb{R}^{2M \times 2}, \quad (\text{A.9})$$

with  $\mathbf{h}_{p,n} := [h_{p,n}^{(1)}, h_{p,n}^{(2)}, \dots, h_{p,n}^{(M)}]^T \in \mathbb{C}^M$  being the  $n$ th column of  $\mathbf{H}_p$ , and  $\mathbf{a}_{p,i}^T(n)$  is the  $n$ th row of  $\mathbf{A}_{p,i}$ . Recall that  $\mathbf{A}_{p,i}$  is simply a  $P \times P$  zero matrix except that the  $r$ th row is equal to  $\mathbf{e}_s^T$ , where  $i = (r-1)P + s$  with  $r = 1, 2, \dots, N$ ,  $s = 1, 2, \dots, P$ , and  $\mathbf{e}_s$  is the  $s$ th standard unit vector in  $\mathbb{R}^P$ . As a result, it is easy to check that for  $i, j = 1, 2, \dots, P$ ,  $\mathbf{a}_{p,i}^H(n) \mathbf{a}_{q,j}(d) = 1$  if  $i = j$ , but  $\mathbf{a}_{p,i}^H(n) \mathbf{a}_{q,j}(d) = 0$  whenever  $i \neq j$ . The above analysis thus shows that, for  $p, q \in \mathcal{S}_M$ , we always have

$$\sqrt{\frac{P_q P_q}{N^2}} (\bar{\mathbf{A}}_p^{(n)})^T \bar{\mathbf{H}}_{p,n}^T \bar{\mathbf{H}}_{q,d} \bar{\mathbf{A}}_q^{(d)} = \alpha \mathbf{I}_P \quad (\text{A.10})$$

for some scalar  $\alpha$ . □

*Proof of (3):* It suffices to verify that the MF coupling signature between the  $p$ th STBC stream and the SM stream transmitted from the  $n$ th antenna of the  $q$ th SM terminal is a  $P \times P$  orthogonal design. It is easy to see that the effective signal coupling matrix is  $\sqrt{\frac{P_q P_q}{N^2}} \bar{\mathbf{A}}_p^T \bar{\mathbf{H}}_p^T \bar{\mathbf{H}}_{q,n} \bar{\mathbf{A}}_q^{(n)}$ , where  $\tilde{\mathbf{A}}_p$  is the real-valued ST modulation matrix of the  $p$ th user,

with the  $(i, j)$ th entry,  $i, j = 1, 2, \dots, P$ , being computed as

$$\begin{aligned} f_{p,q}^{(i,j)}(n) &= \sqrt{\frac{P_q P_q}{N^2}} \sum_{k=1}^P \left( \tilde{\mathbf{a}}_{p,i}^{(k)} \right)^T \bar{\mathbf{H}}_p^T \bar{\mathbf{H}}_{q,n} \tilde{\mathbf{a}}_{q,j}^{(k)}(n) \\ &= \operatorname{Re} \left\{ \sqrt{\frac{P_q P_q}{N^2}} \sum_{m=1}^M \left( \mathbf{h}_p^{(m)} \right)^H \mathbf{A}_{p,i} \mathbf{a}_{q,j}(n) h_{q,n}^{(m)} \right\}, \end{aligned} \quad (\text{A.11})$$

In (A.11)  $\mathbf{a}_{q,j}^T(n)$  is the  $n$ th row of  $\mathbf{A}_{q,j}$ , whereas the O-STBC ST modulation matrix  $\mathbf{A}_{p,i}$  is directly determined by the construction of the orthogonal codewords (see [47]). For a fixed  $N \in \{2, 3, 4\}$ , we first find the  $\mathbf{A}_{p,i}$ 's matrices according to [47]. We then analytically compute all the  $P^2$  entries based on (A.11) and, for any  $1 \leq n \leq N$ , it can be checked that  $\sqrt{\frac{P_q P_q}{N^2}} \bar{\mathbf{A}}_p^T \bar{\mathbf{H}}_p^T \bar{\mathbf{H}}_{q,n} \bar{\mathbf{A}}_q^{(n)}$  is precisely a  $P \times P$  orthogonal design.

a) For  $N = 2$  ( $P = 2$ ), we have

$$\mathbf{A}_{p,1} = \mathbf{I}_2, \quad \mathbf{A}_{p,2} = \begin{bmatrix} 0 & -1 \\ 1 & 0 \end{bmatrix}, \quad (\text{A.12})$$

and

$$\mathbf{a}_{q,1}(n) = [1 \ 0]^T, \quad \mathbf{a}_{q,2}(n) = [0 \ 1]^T. \quad (\text{A.13})$$

Based on (A.12) and (A.13), it is easy to check with (A.11) that  $\sqrt{\frac{P_q P_q}{N^2}} \bar{\mathbf{A}}_p^T \bar{\mathbf{H}}_p^T \bar{\mathbf{H}}_{q,n} \bar{\mathbf{A}}_q^{(n)} \in \mathcal{O}(2)$ .

b) For  $N = 3$  or  $4$  ( $P = 4$ ), we have  $\mathbf{A}_{p,i}$  for  $1 \leq i \leq 4$  as defined in (A.4), and

$$\begin{aligned} \mathbf{a}_{q,1}(n) &= [1 \ 0 \ 0 \ 0]^T, \quad \mathbf{a}_{q,2}(n) = [0 \ 1 \ 0 \ 0]^T, \\ \mathbf{a}_{q,3}(n) &= [0 \ 0 \ 1 \ 0]^T, \quad \mathbf{a}_{q,4}(n) = [0 \ 0 \ 0 \ 1]^T. \end{aligned} \quad (\text{A.14})$$

It is easy to see that

$$\mathbf{A}_{p,i} \mathbf{a}_{q,k}(n) = \mathbf{a}_{p,i}^{(k)}, \quad (\text{A.15})$$

where  $\mathbf{a}_{p,i}^{(k)}$  is the  $k$ th column of  $\mathbf{A}_{p,i}$ . Substituting (A.15) into (A.11), we have

$$\begin{aligned} f_{p,q}^{(1,1)} &= \operatorname{Re} \left\{ \sqrt{\frac{P_q P_q}{N^2}} \sum_{m=1}^M \left( \mathbf{h}_p^{(m)} \right)^H \mathbf{a}_{p,1}^{(1)} h_{q,n}^{(m)} \right\} = \operatorname{Re} \left\{ \sqrt{\frac{P_q P_q}{N^2}} \sum_{m=1}^M \left( h_{p,1}^{(m)} \right)^* h_{q,n}^{(m)} \right\}, \\ f_{p,q}^{(1,2)} &= \operatorname{Re} \left\{ \sqrt{\frac{P_q P_q}{N^2}} \sum_{m=1}^M \left( \mathbf{h}_p^{(m)} \right)^H \mathbf{a}_{p,1}^{(2)} h_{q,n}^{(m)} \right\} = \operatorname{Re} \left\{ \sqrt{\frac{P_q P_q}{N^2}} \sum_{m=1}^M \left( h_{p,2}^{(m)} \right)^* h_{q,n}^{(m)} \right\}, \\ f_{p,q}^{(1,3)} &= \operatorname{Re} \left\{ \sqrt{\frac{P_q P_q}{N^2}} \sum_{m=1}^M \left( \mathbf{h}_p^{(m)} \right)^H \mathbf{a}_{p,1}^{(3)} h_{q,n}^{(m)} \right\} = \operatorname{Re} \left\{ \sqrt{\frac{P_q P_q}{N^2}} \sum_{m=1}^M \left( h_{p,3}^{(m)} \right)^* h_{q,n}^{(m)} \right\}, \\ f_{p,q}^{(1,4)} &= \operatorname{Re} \left\{ \sqrt{\frac{P_q P_q}{N^2}} \sum_{m=1}^M \left( \mathbf{h}_p^{(m)} \right)^H \mathbf{a}_{p,1}^{(4)} h_{q,n}^{(m)} \right\} = \operatorname{Re} \left\{ \sqrt{\frac{P_q P_q}{N^2}} \sum_{m=1}^M \left( h_{p,4}^{(m)} \right)^* h_{q,n}^{(m)} \right\}, \end{aligned} \quad (\text{A.16})$$

and similarly we can obtain

$$\begin{aligned} f_{p,q}^{(2,1)} &= f_{p,q}^{(1,2)}, & f_{p,q}^{(2,1)} &= f_{p,q}^{(1,3)}, & f_{p,q}^{(4,1)} &= f_{p,q}^{(1,4)}, \\ f_{p,q}^{(2,2)} &= -f_{p,q}^{(1,1)}, & f_{p,q}^{(3,2)} &= f_{p,q}^{(1,4)}, & f_{p,q}^{(4,2)} &= -f_{p,q}^{(1,3)}, \\ f_{p,q}^{(2,3)} &= -f_{p,q}^{(1,4)}, & f_{p,q}^{(3,3)} &= -f_{p,q}^{(1,1)}, & f_{p,q}^{(4,3)} &= f_{p,q}^{(1,2)}, \\ f_{p,q}^{(2,4)} &= f_{p,q}^{(1,3)}, & f_{p,q}^{(3,4)} &= -f_{p,q}^{(1,2)}, & f_{p,q}^{(4,4)} &= -f_{p,q}^{(1,1)}. \end{aligned} \quad (\text{A.17})$$

It can be checked that the effective signal coupling matrix  $\sqrt{\frac{P_q P_q}{N^2}} \bar{\mathbf{A}}_p^T \bar{\mathbf{H}}_p^T \bar{\mathbf{H}}_{q,n} \bar{\mathbf{A}}_p^{(n)}$  will be

$$\begin{aligned} \sqrt{\frac{P_q P_q}{N^2}} \bar{\mathbf{A}}_p^T \bar{\mathbf{H}}_p^T \bar{\mathbf{H}}_{q,n} \bar{\mathbf{A}}_p^{(n)} &:= \begin{bmatrix} f_{p,q}^{(1,1)} & f_{p,q}^{(1,2)} & f_{p,q}^{(1,3)} & f_{p,q}^{(1,4)} \\ f_{p,q}^{(2,1)} & f_{p,q}^{(2,2)} & f_{p,q}^{(2,3)} & f_{p,q}^{(2,4)} \\ f_{p,q}^{(3,1)} & f_{p,q}^{(3,2)} & f_{p,q}^{(3,3)} & f_{p,q}^{(3,4)} \\ f_{p,q}^{(4,1)} & f_{p,q}^{(4,2)} & f_{p,q}^{(4,3)} & f_{p,q}^{(4,4)} \end{bmatrix} \\ &= \begin{bmatrix} f_{p,q}^{(1,1)} & f_{p,q}^{(1,2)} & f_{p,q}^{(1,3)} & f_{p,q}^{(1,4)} \\ f_{p,q}^{(1,2)} & -f_{p,q}^{(1,1)} & -f_{p,q}^{(1,4)} & f_{p,q}^{(1,3)} \\ f_{p,q}^{(1,3)} & f_{p,q}^{(1,4)} & -f_{p,q}^{(1,1)} & -f_{p,q}^{(1,2)} \\ f_{p,q}^{(1,4)} & -f_{p,q}^{(1,3)} & f_{p,q}^{(1,2)} & -f_{p,q}^{(1,1)} \end{bmatrix} \in \mathcal{O}(4), \end{aligned} \quad (\text{A.18})$$

which in fact is a  $P \times P$  ( $P = 4$ ) orthogonal design, and this proves *b*).  $\square$

## Appendix B

# Matched-Filtered Channel Matrix: Complex-Valued Constellation Case

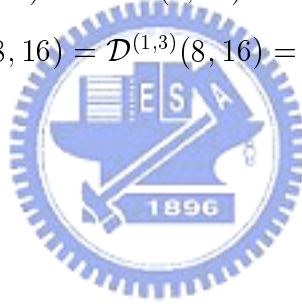
We present the analogue results of Lemma 4.3.1 when the complex-valued symbols are used. It is noted that, in this case, the available code rate depends on the number of transmit antennas  $N$  [47]: full-rate code for  $N = 2$  (hence  $K = P = 2$ ), and half-rate code for  $N = 3$  or 4 ( $K = 8, P = 4$ ). The derivations of the MFCM for complex-valued constellation case are to first identify in each case the ST modulation matrices; each signature matrix is then computed to verify the result. Since the derivations are basically the same as those in the real symbol case, we will not go them through but only present the results (see the following Lemma). The results are also summarized in Table 4.3. Note that in Table 4.3,  $\mathcal{A}^{(i,j)}$  is the  $(i, j)$ th block submatrix of  $\mathcal{A}$  with proper matrix dimension.

**Lemma B.0.1.** *Let  $\mathbf{F}_{p,q}$  be the submatrix of  $\mathbf{F}$  describing the mutual coupling between the  $p$ th and the  $q$ th user. Then the following results hold.*

- (1) *If  $p, q \in \mathcal{S}_D$ , for  $N = 2$ , then  $\mathbf{F}_{p,q} \in \mathcal{O}(4)$ . In particular, we have  $\mathbf{F}_{q,q} = \alpha_q \mathbf{I}_4$  for some scalar  $\alpha_q$ .*
- (2) *If  $p, q \in \mathcal{S}_D$ , for  $N = 3$  or 4, then  $\mathbf{F}_{p,q} \in \mathcal{U}(8)$ , where  $\mathcal{U}^{(1,1)}(8) = \mathcal{U}^{(2,2)}(8) \in \mathcal{O}(4)$  and  $\mathcal{U}^{(1,2)}(8) = \mathcal{U}^{(2,1)}(8) = \mathbf{O}_4$ . In particular, we have  $\mathbf{F}_{q,q} = \alpha_q \mathbf{I}_8$  for some scalar  $\alpha_q$ .*



- (3) If  $p, q \in \mathcal{S}_M$ , for  $N = 2$ , then  $\mathbf{F}_{p,q} \in R^{8 \times 8}$ , with  $\mathbf{F}_{p,q}^{(n,d)} \in \mathcal{V}(4)$ ,  $1 \leq n, d \leq 2$ , where  $\mathcal{V}^{(1,1)}(4) = \mathcal{V}^{(2,2)}(4) = c_1 \mathbf{I}_2$  and  $\mathcal{V}^{(1,2)}(4) = -\mathcal{V}^{(2,1)}(4) = c_2 \mathbf{I}_2$  for some scalars  $c_1$  and  $c_2$ . Also, we have  $\mathbf{F}_{q,q} \in R^{8 \times 8}$ , with  $\mathbf{F}_{q,q}^{(n,n)} = \alpha_{q,n} \mathbf{I}_4$  for some scalar  $\alpha_{q,n}$ , and  $\mathbf{F}_{q,q}^{(n,d)} \in \mathcal{V}(4)$ ,  $1 \leq n, d \leq 2$ .
- (4) If  $p, q \in \mathcal{S}_M$ , for  $N = 3$  or  $4$ , then  $\mathbf{F}_{p,q} \in R^{16N \times 16N}$ , with  $\mathbf{F}_{p,q}^{(n,d)} \in \mathcal{V}(16)$ ,  $1 \leq n, d \leq N$ , where  $\mathcal{V}^{(1,1)}(16) = \mathcal{V}^{(2,2)}(16) = c_1 \mathbf{I}_8$  and  $\mathcal{V}^{(1,2)}(16) = -\mathcal{V}^{(2,1)}(16) = c_2 \mathbf{I}_8$  for some scalars  $c_1$  and  $c_2$ . Also, we have  $\mathbf{F}_{q,q} \in R^{16N \times 16N}$ , with  $\mathbf{F}_{q,q}^{(n,n)} = \alpha_{q,n} \mathbf{I}_{16}$  for some scalar  $\alpha_{q,n}$ , and  $\mathbf{F}_{q,q}^{(n,d)} \in \mathcal{V}(16)$ ,  $1 \leq n, d \leq N$ .
- (5) If  $p \in \mathcal{S}_D$  and  $q \in \mathcal{S}_M$ , for  $N = 2$ , then  $\mathbf{F}_{p,q} \in R^{4 \times 8}$ , with  $\mathbf{F}_{p,q}^{(1,n)} \in \mathcal{O}(4)$ ,  $1 \leq n \leq 2$ .
- (6) If  $p \in \mathcal{S}_D$  and  $q \in \mathcal{S}_M$ , for  $N = 3$  or  $4$ , then  $\mathbf{F}_{p,q} \in R^{8 \times 16N}$ , with  $\mathbf{F}_{p,q}^{(1,n)} \in \mathcal{D}(8, 16)$ ,  $1 \leq n \leq N$ , where  $\mathcal{D}^{(1,1)}(8, 16) = \mathcal{D}^{(1,2)}(8, 16) = \mathcal{D}^{(2,3)}(8, 16) = -\mathcal{D}^{(2,4)}(8, 16) \in \mathcal{O}(4)$ , and  $-\mathcal{D}^{(2,1)}(8, 16) = \mathcal{D}^{(2,2)}(8, 16) = \mathcal{D}^{(1,3)}(8, 16) = \mathcal{D}^{(1,4)}(8, 16) \in \mathcal{O}(4)$ . ■



# Appendix C

## Proof of Lemma 4.4.1

The proof is based on a crucial fact about the orthogonal designs [47]. Specifically, it can be checked by analytic computations that, if  $\mathbf{M}_1, \mathbf{M}_2 \in \mathcal{O}(P)$ , then so are  $\mathbf{M}_1 + \mathbf{M}_2$  and  $\mathbf{M}_1\mathbf{M}_2$ , that is,

**Fact C.0.1.** *The set  $\mathcal{O}(P)$  is closed under addition and multiplication. Moreover, for any  $\mathbf{M}_1 \in \mathcal{O}(P)$ , it is easy to see that  $\mathbf{M}_1 + \mathbf{M}_1^T = \gamma\mathbf{I}_P$  for some  $\gamma$ . ■*

Based on Fact C.0.1, the result can be shown by induction on  $L$ .

For the  $L = 1$  case, the result is obvious since  $\mathbf{F} = \alpha\mathbf{I}_P$ . Assume that the result is true for an arbitrary  $L > 1$ , that is,  $\mathbf{F} \in \mathcal{F}(L)$  implies  $\mathbf{F}^{-1} \in \mathcal{F}(L)$  for such an  $L$ . We have to check that  $\mathbf{F}^{-1} \in \mathcal{F}(L+1)$  whenever  $\mathbf{F} \in \mathcal{F}(L+1)$ . To see this, let us partition an arbitrary  $\mathbf{F} \in \mathcal{F}(L+1)$  as

$$\mathbf{F} = \left[ \begin{array}{c|c} \mathbf{A} & \mathbf{B} \\ \hline \mathbf{B}^T & \mathbf{D} \end{array} \right], \quad (\text{C.1})$$

where  $\mathbf{A} \in \mathbb{R}^{PL \times PL}$ ,  $\mathbf{B} \in \mathbb{R}^{PL \times P}$ , and  $\mathbf{D} \in \mathbb{R}^{P \times P}$ . We note that, since  $\mathbf{F} \in \mathcal{F}(L+1)$ , we have (a)  $\mathbf{A} \in \mathcal{F}(L)$  and hence  $\mathbf{A}^{-1} \in \mathcal{F}(L)$  by assumption, (b)  $\mathbf{D} = c\mathbf{I}_P$  for some scalar  $c$ ,

and (c) if we write  $\mathbf{B} = [\mathbf{B}_1^T, \mathbf{B}_2^T, \dots, \mathbf{B}_L^T]^T$ , where  $\mathbf{B}_i \in \mathbb{R}^{P \times P}$ , then we have  $\mathbf{B}_i \in \mathcal{O}(P)$ .

Let us similarly write

$$\mathbf{F}^{-1} = \left[ \begin{array}{c|c} \bar{\mathbf{A}} & \bar{\mathbf{B}} \\ \hline \bar{\mathbf{B}}^T & \bar{\mathbf{D}} \end{array} \right], \quad (\text{C.2})$$

where  $\bar{\mathbf{A}} \in \mathbb{R}^{PL \times PL}$ ,  $\bar{\mathbf{B}} \in \mathbb{R}^{PL \times P}$ , and  $\bar{\mathbf{D}} \in \mathbb{R}^{P \times P}$ . To show that  $\mathbf{F}^{-1} \in \mathcal{F}(L+1)$ , it suffices to check that (1)  $\bar{\mathbf{A}} \in \mathcal{F}(L)$ , (2)  $\bar{\mathbf{B}} = [\bar{\mathbf{B}}_1^T, \bar{\mathbf{B}}_2^T, \dots, \bar{\mathbf{B}}_L^T]^T$ , where  $\bar{\mathbf{B}}_i \in \mathbb{R}^{P \times P}$ , is such that each  $\bar{\mathbf{B}}_i \in \mathcal{O}(P)$ , and (3)  $\bar{\mathbf{D}} = d\mathbf{I}_P$  for some scalar  $d$ . Properties (1)–(3) can be shown based on the inversion formula for block matrices

$$\begin{aligned} \mathbf{F}^{-1} &:= \left[ \begin{array}{c|c} \bar{\mathbf{A}} & \bar{\mathbf{B}} \\ \hline \bar{\mathbf{B}}^T & \bar{\mathbf{D}} \end{array} \right] \\ &= \left[ \begin{array}{c|c} (\mathbf{A} - \mathbf{B}\mathbf{D}^{-1}\mathbf{B}^T)^{-1} & -(\mathbf{A} - \mathbf{B}\mathbf{D}^{-1}\mathbf{B}^T)^{-1}\mathbf{B}\mathbf{D}^{-1} \\ \hline -(\mathbf{D} - \mathbf{B}^T\mathbf{A}^{-1}\mathbf{B})^{-1}\mathbf{C}\mathbf{A}^{-1} & (\mathbf{D} - \mathbf{B}^T\mathbf{A}^{-1}\mathbf{B})^{-1} \end{array} \right]. \quad (\text{C.3}) \end{aligned}$$

*Proof of (1):* From (C.3), we have  $\bar{\mathbf{A}} = (\mathbf{A} - \mathbf{B}\mathbf{D}^{-1}\mathbf{B}^T)^{-1} = (\mathbf{A} - c^{-1}\mathbf{B}\mathbf{B}^T)^{-1}$ , where the last equality follows since  $\mathbf{D} = c\mathbf{I}_P$ . Since each  $\mathbf{B}_i \in \mathcal{O}(P)$ , with direct block submatrix multiplication and using Fact C.0.1 it is easy to show that  $\mathbf{A} - c^{-1}\mathbf{B}\mathbf{B}^T \in \mathcal{F}(L)$ , and hence  $\bar{\mathbf{A}} \in \mathcal{F}(L)$  by assumption.  $\square$

*Proof of (2):* From (C.3), we have  $\bar{\mathbf{B}} = -\bar{\mathbf{A}}\mathbf{B}\mathbf{D}^{-1} = c^{-1}\bar{\mathbf{A}}\mathbf{B}$ . Since  $\bar{\mathbf{A}} \in \mathcal{F}(L)$  and each  $\mathbf{B}_i \in \mathcal{O}(P)$ , direct block submatrix multiplication together with Fact C.0.1 shows that each  $\bar{\mathbf{B}}_i \in \mathcal{O}(P)$ .  $\square$

*Proof of (3):* Since  $\bar{\mathbf{D}} = (\mathbf{D} - \mathbf{B}^T \mathbf{A}^{-1} \mathbf{B})^{-1}$  and  $\mathbf{D} = c \mathbf{I}_P$ , it suffices to check that  $\mathbf{B}^T \mathbf{A}^{-1} \mathbf{B} = c_1 \mathbf{I}_P$  for some scalar  $c_1$ . For  $k, l = 1, 2, \dots, L$ , denote by  $\mathbf{U}_{kl}$  the  $(k, l)$ th  $P \times P$  block submatrix of  $\mathbf{A}^{-1}$ . Since  $\mathbf{B} = [\mathbf{B}_1^T, \mathbf{B}_2^T, \dots, \mathbf{B}_L^T]^T$ , it is easy to verify that

$$\mathbf{B}^T \mathbf{A}^{-1} \mathbf{B} = \sum_{k,l=1}^L \mathbf{B}_k^T \mathbf{U}_{kl} \mathbf{B}_l = \sum_{k=1}^L \mathbf{B}_k^T \mathbf{U}_{kk} \mathbf{B}_k + \sum_{k,l=1, k \neq l}^L \mathbf{B}_k^T \mathbf{U}_{kl} \mathbf{B}_l. \quad (\text{C.4})$$

Since  $\mathbf{A}^{-1} \in \mathcal{F}(L)$ , we have by definition  $\mathbf{U}_{kk} = \eta_k \mathbf{I}_P$  for some scalar  $\eta_k$ . The first summation on the right-hand-side of the second equality in (C.4) thus simplifies as

$$\sum_{k=1}^L \mathbf{B}_k^T \mathbf{U}_{kk} \mathbf{B}_k = \sum_{k=1}^L \eta_k \mathbf{B}_k^T \mathbf{B}_k = \eta \mathbf{I}_P. \quad (\text{C.5})$$

On the other hand, since for  $k, l = 1, 2, \dots, L$ ,  $\mathbf{B}_k \in \mathcal{O}(P)$  and  $\mathbf{U}_{kl} \in \mathcal{O}(P)$  by assumption. Then we have each  $\mathbf{B}_k^T \mathbf{U}_{kl} \mathbf{B}_l \in \mathcal{O}(P)$ , and it follows that

$$\mathbf{B}_k^T \mathbf{U}_{kl} \mathbf{B}_l + \mathbf{B}_l^T \mathbf{U}_{lk} \mathbf{B}_k = \alpha_{kl} \mathbf{I}_P \quad (\text{C.6})$$

by Fact C.0.1. This shows that

$$\sum_{k,l=1, k \neq l}^L \mathbf{B}_k^T \mathbf{U}_{kl} \mathbf{B}_l = \tilde{\eta} \mathbf{I}_P. \quad (\text{C.7})$$

Lemma 4.4.1 thus follows. □



# Appendix D

## Group-Wise OSIC Detection: Complex-Valued Constellation Case

Let us first define  $\mathcal{G}(J_L)$  to be the set of all invertible real symmetric  $4J_L \times 4J_L$  matrices, where  $J_L := \frac{1}{2} \sum_{l=1}^L L_l$  with  $L_l = P$  if  $l \in \mathcal{S}_D$  and  $L_l = K$  if  $l \in \mathcal{S}_M$ , such that, for  $\mathbf{X} \in \mathcal{G}(J_L)$ , we have (i) each  $4 \times 4$  block diagonal submatrix of  $\mathbf{X}$  is a (nonzero) scalar multiple of  $\mathbf{I}_4$  (ii) each  $4 \times 4$  block off-diagonal submatrix of  $\mathbf{X}$  belongs to  $\mathcal{O}(4)$  or is a zero matrix  $\mathbf{O}_4$  (iii) the diagonal entries assume  $L$  levels.

**Lemma D.0.2.** *If  $\mathbf{F} \in \mathcal{G}(J_L)$ , then so is  $\mathbf{F}^{-1}$ .*

*Proof:* The group-wise OSIC detection for complex-valued constellation case can similarly be established if we observe from Table 4.3 that the MF channel matrix  $\mathbf{F}$  indeed consists of orthogonal design block submatrices. By going through essentially the same arguments as what we have done in the real symbol case, we can similarly derive a group-wise ZF/MMSE OSIC detector ( $2P$  real symbols are detected for an STBC user and  $2K$  real symbols for an antenna of an SM user per iteration).

The overall derivation for proving Lemma D.0.2 is based on the proof of Lemma 4.4.1. We will prove Lemma D.0.2 by induction. For the  $L = 1$  case, the result is obvious since  $\mathbf{F} = \alpha \mathbf{I}_P$ . Assume that the result is true for an arbitrary  $L > 1$ , that is,  $\mathbf{F} \in \mathcal{G}(J_L)$  implies  $\mathbf{F}^{-1} \in \mathcal{G}(J_L)$

for such an  $L$ . We have to check that  $\mathbf{F}^{-1} \in \mathcal{G}(J_{L+1})$ , where  $J_{L+1} := \frac{1}{2} \sum_{l=1}^{L+1} P_l$ , whenever  $\mathbf{F} \in \mathcal{G}(J_{L+1})$ . Let us partition an arbitrary  $\mathbf{F} \in \mathcal{G}(J_{L+1})$  as (C.1), where  $\mathbf{A} \in \mathbb{R}^{4J_L \times 4J_L}$ ,  $\mathbf{B} \in \mathbb{R}^{4J_L \times 2P_{L+1}}$ , and  $\mathbf{D} \in \mathbb{R}^{2P_{L+1} \times 2P_{L+1}}$ . We note that, since  $\mathbf{F} \in \mathcal{G}(J_{L+1})$ , we have (a)  $\mathbf{A} \in \mathcal{G}(J_L)$  and hence  $\mathbf{A}^{-1} \in \mathcal{G}(J_L)$  by assumption, (b) if we write  $\mathbf{B} = [\mathbf{B}_1^T, \mathbf{B}_2^T, \dots, \mathbf{B}_L^T]^T$ , where  $\mathbf{B}_l \in \mathbb{R}^{2P_l \times 2P_{L+1}}$ , then according to Table 4.3 we have that  $\mathbf{B}_l \in \{\mathcal{O}(4), \mathcal{V}(4)\}$  for  $N = 2$  or  $\mathbf{B}_l \in \{\mathcal{U}(8), \mathcal{V}(16), \mathcal{D}(8, 16), \mathcal{D}^T(8, 16)\}$  for  $N = 3$  or 4, and (c)  $\mathbf{D} = c\mathbf{I}$  for some scalar  $c$ . Also, let us similarly write  $\mathbf{F}^{-1}$  as (C.2), where  $\bar{\mathbf{A}} \in \mathbb{R}^{4J_L \times 4J_L}$ ,  $\bar{\mathbf{B}} \in \mathbb{R}^{4J_L \times 2P_{L+1}}$ , and  $\bar{\mathbf{D}} \in \mathbb{R}^{2P_{L+1} \times 2P_{L+1}}$ . To show that  $\mathbf{F}^{-1} \in \mathcal{G}(J_{L+1})$ , it suffices to check that (1)  $\bar{\mathbf{A}} \in \mathcal{G}(J_L)$ , (2) if we write  $\bar{\mathbf{B}} = [\bar{\mathbf{B}}_1^T, \bar{\mathbf{B}}_2^T, \dots, \bar{\mathbf{B}}_L^T]^T$ , where  $\bar{\mathbf{B}}_l \in \mathbb{R}^{2P_l \times 2P_{L+1}}$ , then each  $4 \times 4$  block submatrix of  $\bar{\mathbf{B}}_l$  is an orthogonal design, and (3)  $\bar{\mathbf{D}} \in \mathcal{G}(J_1)$  for  $N = 3$  or 4, and the  $(L+1)$ th signaling belonging to SM, or otherwise  $\bar{\mathbf{D}} = d\mathbf{I}_{2P_{L+1}}$ . Properties (1)-(3) can be shown based on the inversion formula for block matrices (see (C.3)).

*Proof of (1):* From (C.3), we have  $\bar{\mathbf{A}} = (\mathbf{A} - \mathbf{B}\mathbf{D}^{-1}\mathbf{B}^T)^{-1} = (\mathbf{A} - \frac{1}{c}\mathbf{B}\mathbf{B}^T)^{-1}$ , and it thus suffices to check that  $\mathbf{B}\mathbf{B}^T \in \mathcal{G}(J_L)$ . In particular,  $\mathbf{B}\mathbf{B}^T$  can be expressed as follows

$$\mathbf{B}\mathbf{B}^T = \begin{bmatrix} \mathbf{B}_1 \\ \mathbf{B}_2 \\ \vdots \\ \mathbf{B}_L \end{bmatrix} \begin{bmatrix} \mathbf{B}_1^T & \mathbf{B}_2^T & \cdots & \mathbf{B}_L^T \end{bmatrix} = \begin{bmatrix} \mathbf{B}_1\mathbf{B}_1^T & \mathbf{B}_1\mathbf{B}_2^T & \cdots & \mathbf{B}_1\mathbf{B}_L^T \\ \mathbf{B}_2\mathbf{B}_1^T & \mathbf{B}_2\mathbf{B}_2^T & \cdots & \mathbf{B}_2\mathbf{B}_L^T \\ \vdots & \vdots & \ddots & \vdots \\ \mathbf{B}_L\mathbf{B}_1^T & \mathbf{B}_L\mathbf{B}_2^T & \cdots & \mathbf{B}_L\mathbf{B}_L^T \end{bmatrix}, \quad (\text{D.1})$$

and each  $\mathbf{B}_k\mathbf{B}_l^T$ ,  $1 \leq k, l \leq L$ , has the following special structures. a) If  $N = 2$ ,  $\mathbf{B}_l \in \{\mathcal{O}(4), \mathcal{V}(4)\}$ , then we can easily obtain  $\mathbf{B}_l\mathbf{B}_l^T = \alpha\mathbf{I}_P$  for some  $\alpha$ . b) If  $N = 3$  or 4,  $\mathbf{B}_l \in \{\mathcal{U}(8), \mathcal{V}(16), \mathcal{D}(8, 16), \mathcal{D}^T(8, 16)\}$ , then based on fact C.0.1, it can be checked that (i) each  $4 \times 4$  block diagonal submatrix of  $\mathbf{B}_l\mathbf{B}_l^T$  is a diagonal matrix with a constant value, (ii) each  $4 \times 4$  block off-diagonal submatrix of  $\mathbf{B}_l\mathbf{B}_l^T$  belongs to an orthogonal design, and (iii) the diagonal entries of  $\mathbf{B}_l\mathbf{B}_l^T$  are the same. c) Similar to b), it is easy to check that each  $4 \times 4$  block submatrix of  $\mathbf{B}_k\mathbf{B}_l^T$  belongs to an orthogonal design. As a result, we indeed have  $\mathbf{B}\mathbf{B}^T \in \mathcal{G}(J_L)$ , and this proves the property (1).  $\square$

*Proof of (2):* From (C.3), we have  $\bar{\mathbf{B}} = -\bar{\mathbf{A}}\mathbf{B}\mathbf{D}^{-1} = \frac{1}{c}\bar{\mathbf{A}}\mathbf{B}$ , and it thus suffices to check the structure of  $\bar{\mathbf{A}}\mathbf{B}$ . From the proof of (1), we can see that each  $4 \times 4$  block submatrix of  $\bar{\mathbf{A}}$  or  $\mathbf{B}$  belongs to an orthogonal design or a zero matrix. Based on Fact C.0.1 again and through the same procedures as what we have done in the proof of (1), it can thus be verified that each  $4 \times 4$  block submatrix of  $\bar{\mathbf{A}}\mathbf{B}$  will also belong to an orthogonal design.  $\square$

*Proof of (3):* Since  $\bar{\mathbf{D}} = (\mathbf{D} - \mathbf{B}^T\mathbf{A}^{-1}\mathbf{B})^{-1}$  and  $\mathbf{D} = c\mathbf{I}_{2P_{L+1}}$ , it suffices to check that  $\mathbf{B}^T\mathbf{A}^{-1}\mathbf{B}$  is a diagonal matrix with a constant value. To this end, for  $1 \leq k, l \leq L$ , we denote by  $\mathbf{U}_{kl}$  the  $(k, l)$ th  $2P_k \times 2P_l$  block submatrix of  $\mathbf{A}^{-1}$ . Since  $\mathbf{B} = [\mathbf{B}_1^T, \mathbf{B}_2^T, \dots, \mathbf{B}_L^T]^T$ , we can obtain equation (C.4). Since  $\mathbf{A}^{-1} \in \mathcal{G}(J_L)$ , we have by definition  $\mathbf{U}_{kk} = \eta_k \mathbf{I}_{2P_k}$  for some scalar  $\eta_k$ . The first summation on the right-hand-side of the second equality in (C.4) thus simplifies as

$$\sum_{k=1}^L \mathbf{B}_k^T \mathbf{U}_{kk} \mathbf{B}_k = \sum_{k=1}^L \eta_k \mathbf{B}_k^T \mathbf{B}_k \in \mathcal{G}(J_1). \quad (\text{D.2})$$

for  $N = 3$  or  $4$ , and the  $(L + 1)$ th user terminal signals the data in the SM mode, or

$$\sum_{k=1}^L \mathbf{B}_k^T \mathbf{U}_{kk} \mathbf{B}_k = \sum_{k=1}^L \eta_k \mathbf{B}_k^T \mathbf{B}_k = \eta \mathbf{I}_{2P_{L+1}}. \quad (\text{D.3})$$

otherwise. On the other hand, since for  $k, l = 1, 2, \dots, L$ , each  $4 \times 4$  block submatrix of  $\mathbf{U}_{kl}$  or  $\mathbf{B}_k$  belongs to an orthogonal design or a zero matrix by assumption, then we have that each  $4 \times 4$  block submatrix of  $\mathbf{B}_k^T \mathbf{U}_{kl} \mathbf{B}_l$  also belongs to an orthogonal design or a zero matrix, and by Fact C.0.1 it follows that

$$\mathbf{B}_k^T \mathbf{U}_{kl} \mathbf{B}_l + \mathbf{B}_l^T \mathbf{U}_{lk} \mathbf{B}_k \in \mathcal{G}(J_1), \quad (\text{D.4})$$

for  $N = 3$  or  $4$ , and the  $(L + 1)$ th user terminal signals the data in the SM mode, or

$$\mathbf{B}_k^T \mathbf{U}_{kl} \mathbf{B}_l + \mathbf{B}_l^T \mathbf{U}_{lk} \mathbf{B}_k = \alpha_{kl} \mathbf{I}_{2P_{L+1}}, \quad (\text{D.5})$$

otherwise. This shows that

$$\sum_{k, l=1, k \neq l}^L \mathbf{B}_k^T \mathbf{U}_{kl} \mathbf{B}_l \in \mathcal{G}(J_1), \quad (\text{D.6})$$

for  $N = 3$  or  $4$ , and the  $(L + 1)$ th user terminal signals the data in the SM mode, or

$$\sum_{k,l=1, k \neq l}^L \mathbf{B}_k^T \mathbf{U}_{kl} \mathbf{B}_l = \tilde{\eta} \mathbf{I}_{2P_{L+1}}. \quad (\text{D.7})$$

otherwise, and this proves property (3).  $\square$

Based on above discussions, Lemma D.0.2 thus follows.  $\square$





# Appendix E

## Group-Wise OSIC Detection in CDMA Based Implementation

In the rest of this section, we will show that the proposed group-wise detection property remains true in the aforementioned CDMA based implementation. To see this, it suffices to check that resultant MF channel matrix still possesses the structures as specified in Lemma 4.3.1. Assume that all the  $Q$  users' symbol streams are spread by the same code  $\mathbf{c} \in \mathbb{R}^G$ , where  $G$  is the spreading gain. Collecting the  $G$  received discrete-time signal, sampled at the chip-rate, from the  $m$ th antenna over the  $k$ th symbol period, we have

$$\mathbf{y}_m(k) = \sum_{q=1}^Q \check{\mathbf{H}}_q^{(m)} \mathbf{x}_q(k) + \mathbf{i}_m(k) + \mathbf{v}_m(k), \quad (\text{E.1})$$

where  $\mathbf{x}_q(k) := [x_{q,1}(k), x_{q,2}(k), \dots, x_{q,N}(k)]^T \in \mathbb{C}^N$ ,  $\check{\mathbf{H}}_q^{(m)} := [\check{\mathbf{h}}_{q,1}^{(m)}, \check{\mathbf{h}}_{q,1}^{(m)}, \dots, \check{\mathbf{h}}_{q,N}^{(m)}] \in \mathbb{C}^{G \times N}$  with

$$\check{\mathbf{h}}_{q,n}^{(m)} := g_{q,n}^{(m)} \mathbf{c} \in \mathbb{C}^G, \quad (\text{E.2})$$

being the composite channel vector between the  $n$ th antenna of the  $q$ th mobile user and the  $m$ th base station antenna, which includes the effect of spreading code  $\mathbf{c}$  and channel propagation gain  $g_{q,n}^{(m)}$ , and  $\mathbf{i}_m(k) \in \mathbb{C}^G$  and  $\mathbf{v}_m \in \mathbb{C}^G$  are respectively the corresponding

MAI and noise vectors. Stacking  $\mathbf{y}_m(k)$  over  $M$  receive antennas yields an  $MG \times 1$  received signal vector

$$\mathbf{y}(k) := [\mathbf{y}_1^T(k), \mathbf{y}_2^T(k), \dots, \mathbf{y}_M^T(k)]^T = \sum_{q=1}^Q \check{\mathbf{H}}_q \mathbf{x}_q(k) + \mathbf{i}(k) + \mathbf{v}(k), \quad (\text{E.3})$$

where

$$\check{\mathbf{H}}_q := \begin{bmatrix} \check{\mathbf{h}}_{q,1}^{(1)} & \check{\mathbf{h}}_{q,2}^{(1)} & \cdots & \check{\mathbf{h}}_{q,N}^{(1)} \\ \check{\mathbf{h}}_{q,1}^{(2)} & \check{\mathbf{h}}_{q,2}^{(2)} & \cdots & \check{\mathbf{h}}_{q,N}^{(2)} \\ \vdots & \ddots & \vdots & \\ \check{\mathbf{h}}_{q,1}^{(M)} & \check{\mathbf{h}}_{q,2}^{(M)} & \cdots & \check{\mathbf{h}}_{q,N}^{(M)} \end{bmatrix} \in \mathbb{C}^{MG \times N}, \quad (\text{E.4})$$

is the channel matrix from the  $q$ th mobile user to the receiver, and  $\mathbf{i}(k) \in \mathbb{C}^{MG}$  and  $\mathbf{v}(k) \in \mathbb{C}^{MG}$  are respectively the MAI and noise terms. Following essentially the same procedures as what we have done in Section 2.4.1 (through (2.74)-(2.80)), we can obtain the MF signal vector (2.80), where the MAI term  $\mathbf{i}(k)$  has been perfectly removed due to use of the (orthogonal) spreading codes,  $\check{\mathbf{H}}_c = [\check{\mathbf{H}}_1 \bar{\mathbf{A}}_1, \check{\mathbf{H}}_2 \bar{\mathbf{A}}_2, \dots, \check{\mathbf{H}}_Q \bar{\mathbf{A}}_Q] \in \mathbb{R}^{2KM \times 2LT}$  with  $\check{\mathbf{H}}_q$  and  $\bar{\mathbf{A}}_q$  being respectively defined as in (2.74) and (2.76), and the MF channel matrix  $\check{\mathbf{F}} = \check{\mathbf{H}}_c^T \check{\mathbf{H}}_c \in \mathbb{R}^{2LT \times 2LT}$  is defined as in (2.81).

To see the proposed group-wise detection property remains true in the CDMA based implementation, we only need to check the entries of matrix  $\check{\mathbf{H}}_p^T \check{\mathbf{H}}_q \in \mathbb{R}^{2KN \times 2KN}$ . According to (2.74) and using the property  $(\mathbf{A} \otimes \mathbf{B})^T = (\mathbf{A}^T \otimes \mathbf{B}^T)$ , after some manipulations, we have

$$\check{\mathbf{H}}_p^T \check{\mathbf{H}}_q = \mathbf{I}_K \otimes \begin{bmatrix} \text{Re} \{ \check{\mathbf{H}}_p^H \check{\mathbf{H}}_q \} & -\text{Im} \{ \check{\mathbf{H}}_p^H \check{\mathbf{H}}_q \} \\ \text{Im} \{ \check{\mathbf{H}}_p^H \check{\mathbf{H}}_q \} & \text{Re} \{ \check{\mathbf{H}}_p^H \check{\mathbf{H}}_q \} \end{bmatrix}, \quad (\text{E.5})$$

with the  $(i, j)$ th entry of  $\check{\mathbf{H}}_p^H \check{\mathbf{H}}_q$  being given by

$$\begin{aligned} [\check{\mathbf{H}}_p^H \check{\mathbf{H}}_q]_{i,j} &= \left( \check{\mathbf{h}}_{p,i}^{(1)} \right)^H \check{\mathbf{h}}_{q,j}^{(1)} + \left( \check{\mathbf{h}}_{p,i}^{(2)} \right)^H \check{\mathbf{h}}_{q,j}^{(2)} + \cdots + \left( \check{\mathbf{h}}_{p,i}^{(M)} \right)^H \check{\mathbf{h}}_{q,j}^{(M)} \\ &= \left( g_{p,i}^{(1)} \right)^* g_{q,j}^{(1)} + \left( g_{p,i}^{(2)} \right)^* g_{q,j}^{(2)} + \cdots + \left( g_{p,i}^{(M)} \right)^* g_{q,j}^{(M)} \\ &= [\mathbf{H}_p^H \mathbf{H}_q]_{i,j}, \quad 1 \leq i, j \leq N. \end{aligned} \quad (\text{E.6})$$

Note that the second equality of (E.6) holds since  $\tilde{\mathbf{h}}_{q,n}^{(m)} = g_{q,n}^{(m)} \mathbf{c}$  and  $\mathbf{c}^T \mathbf{c} = 1$ . From (E.6), we can see that  $\tilde{\mathbf{H}}_p^T \tilde{\mathbf{H}}_q = \bar{\mathbf{H}}_p^T \bar{\mathbf{H}}_q$ , which confirms the capability of the proposed group-wise detection in CDMA based implementation.



# Appendix F

## Proof of Lemma 5.3.1

Part (p1) of Lemma 5.3.1 has been shown in Appendix C. It only needs to prove Parts (p2)-(p3).

*Proof of (p2):* We first note from (2.72)-(2.76) that the effective signal component (priori to matched filtering) of the  $q$ th antenna group is  $\bar{\mathbf{H}}_q \bar{\mathbf{A}}_q$ . Accordingly, the MFCM coupling signature between the  $p$ th and the  $q$ th antenna groups is  $\bar{\mathbf{A}}_p^T \bar{\mathbf{H}}_p^T \bar{\mathbf{H}}_q \bar{\mathbf{A}}_q$ , whose  $(i, j)$ th entry,  $i, j = 1, 2, \dots, L_q$ , is directly computed as

$$f_{p,q}^{(i,j)} = \sqrt{\frac{P_p P_q}{N_p N_q}} \sum_{k=1}^K \left( \tilde{\mathbf{a}}_{p,i}^{(k)} \right)^T \tilde{\mathbf{H}}_p^T \tilde{\mathbf{H}}_q \tilde{\mathbf{a}}_{q,j}^{(k)} = \text{Re} \left\{ \sqrt{\frac{P_p P_q}{N_p N_q}} \sum_{m=1}^M \mathbf{h}_{p,m}^H \mathbf{A}_{p,i} \mathbf{A}_{q,j}^H \mathbf{h}_{q,m} \right\}, \quad (\text{F.1})$$

where  $\mathbf{h}_{q,m}^T$  is the  $m$ th row of  $\mathbf{H}_q$ . Equation (F.1) gives an important observation that the  $(i, j)$ th element of  $\mathbf{F}_{p,q}$  fully describing the structure of  $\mathbf{F}_{p,q}$  is completely characterized by  $\mathbf{A}_{p,i}$  and  $\mathbf{A}_{q,j}$  or simply just the result of  $\mathbf{A}_{p,i} \mathbf{A}_{q,j}^H$ . As a result, to see the particular structures of  $\mathbf{F}_{p,q}$ , we need to first compute  $\mathbf{A}_{p,i} \mathbf{A}_{q,j}^H$ . For  $N_p = N_q = 2$ , and according to [47], we thus have

$$\begin{aligned} \mathbf{A}_{p,1} = \mathbf{A}_{q,1} &= \begin{bmatrix} 1 & 0 & 0 & 0 \\ 0 & 1 & 0 & 0 \end{bmatrix}, & \mathbf{A}_{p,2} = \mathbf{A}_{q,2} &= \begin{bmatrix} 0 & -1 & 0 & 0 \\ 1 & 0 & 0 & 0 \end{bmatrix}, \\ \mathbf{A}_{p,3} = \mathbf{A}_{q,3} &= \begin{bmatrix} 0 & 0 & 1 & 0 \\ 0 & 0 & 0 & 1 \end{bmatrix}, & \mathbf{A}_{p,4} = \mathbf{A}_{q,4} &= \begin{bmatrix} 0 & 0 & 0 & -1 \\ 0 & 0 & 1 & 0 \end{bmatrix}. \end{aligned} \quad (\text{F.2})$$

From (F.1) and (F.2) and using the property given in (5.2), it can be easily checked that the  $(i, j)$ th entry of  $\mathbf{F}_{p,q}$  will be zero except for the following entries

$$\begin{cases} f_{p,q}^{(1,1)} = f_{p,q}^{(2,2)}, & f_{p,q}^{(1,2)} = -f_{p,q}^{(2,1)}, \\ f_{p,q}^{(3,3)} = f_{p,q}^{(4,4)}, & f_{p,q}^{(3,4)} = -f_{p,q}^{(4,3)}, \\ f_{p,q}^{(1,1)} = f_{p,q}^{(3,3)}, & f_{p,q}^{(2,2)} = f_{p,q}^{(4,4)}. \end{cases} \quad (\text{F.3})$$

Likewise, for  $i, j = 1, 2, 3, 4$ , we can also obtain  $f_{q,q}^{(i,i)} = \alpha_q$  and  $f_{q,q}^{(i,j)} = 0$  whenever  $i \neq j$ . Based on the above results, Part (p2) is asserted.  $\square$

*Proof of (p3):* For  $N_p = N_q = 3$  and  $N_p = N_q = 4$  cases, the assertions have been proved in [80]. The cases need to be proved are those ones for (a)  $N_p = 2, 3 \leq N_q \leq 4$  and (b)  $N_p = 3, N_q = 4$ . Now, we first consider case (a). In particular, for  $N_q = 4$ , we have

$$\begin{aligned} \mathbf{A}_{q,1} &= \mathbf{I}_4, & \mathbf{A}_{q,2} &= \begin{bmatrix} 0 & -1 & 0 & 0 \\ 1 & 0 & 0 & 0 \\ 0 & 0 & 0 & 1 \\ 0 & 0 & -1 & 0 \\ 0 & 0 & 0 & -1 \\ 0 & 0 & 1 & 0 \\ 0 & -1 & 0 & 0 \\ 1 & 0 & 0 & 0 \end{bmatrix}, \\ \mathbf{A}_{q,3} &= \begin{bmatrix} 0 & 0 & -1 & 0 \\ 0 & 0 & 0 & -1 \\ 1 & 0 & 0 & 0 \\ 0 & 1 & 0 & 0 \end{bmatrix}, & \mathbf{A}_{q,4} &= \begin{bmatrix} 0 & -1 & 0 & 0 \\ 1 & 0 & 0 & 0 \end{bmatrix}. \end{aligned} \quad (\text{F.4})$$

To efficiently prove it, let's define a crucially intermediary matrix

$$\bar{\mathbf{A}}_{p,q} := \mathbf{A}_p \mathbf{A}_q^H \in \mathbb{C}^{N_p L_p \times N_q L_q}, \quad (\text{F.5})$$

where

$$\begin{aligned} \mathbf{A}_p &:= \left[ \mathbf{A}_{p,1}^T, \mathbf{A}_{p,2}^T, \dots, \mathbf{A}_{p,L_p}^T \right]^T \in \mathbb{C}^{N_p L_p \times K}, \\ \mathbf{A}_q &:= \left[ \mathbf{A}_{q,1}^T, \mathbf{A}_{q,2}^T, \dots, \mathbf{A}_{q,L_q}^T \right]^T \in \mathbb{C}^{N_q L_q \times K}. \end{aligned} \quad (\text{F.6})$$

It is noticed that the  $(i, j)$ th  $N_p \times N_q$  block submatrix of  $\bar{\mathbf{A}}_{p,q}$ , for  $i = 1, 2, \dots, L_p$  and  $j = 1, 2, \dots, L_q$ , is just  $\mathbf{A}_{p,i} \mathbf{A}_{q,j}^H$ . In particular, for case (a),  $\mathbf{A}_{p,i}$  and  $\mathbf{A}_{q,j}$ , for  $i, j = 1, 2, 3, 4$ ,

is given in (F.2) and (F.4), respectively, then it can be shown, after some manipulations, that

$$\bar{\mathbf{A}}_{p,q} = \begin{bmatrix} \mathbf{A}_{p,1} & -\mathbf{A}_{p,2} & \mathbf{A}_{p,3} & -\mathbf{A}_{p,4} \\ \mathbf{A}_{p,2} & \mathbf{A}_{p,1} & \mathbf{A}_{p,4} & \mathbf{A}_{p,3} \\ \mathbf{A}_{p,3} & -\mathbf{A}_{p,4} & -\mathbf{A}_{p,1} & -\mathbf{A}_{p,2} \\ \mathbf{A}_{p,4} & -\mathbf{A}_{p,3} & -\mathbf{A}_{p,2} & \mathbf{A}_{p,1} \end{bmatrix}. \quad (\text{F.7})$$

Observing from (F.7), with  $\mathbf{A}_{p,i}$  regarded as a particular variable, then we can find that the matrix  $\bar{\mathbf{A}}_{p,q}$  belongs to a (super) orthogonal design. With above discussions, we can conclude that the resultant structure of  $\bar{\mathbf{A}}_{p,q}$  can completely and directly reflect on that of  $\mathbf{F}_{p,q}$ . This means that to see the structure of  $\mathbf{F}_{p,q}$  we only to check the structure of  $\bar{\mathbf{A}}_{p,q}$ .

For  $N_q = 3$  case,  $\mathbf{A}_{q,j}$ ,  $j = 1, 2, \dots, L_q$  can be easily obtained as that shown in (F.4) by deleting the last row of it. Also, it can be shown that  $\bar{\mathbf{A}}_{p,q}$  has exactly the same structure as that given by (F.7). Similarly, for  $i, j = 1, 2, 3, 4$ , we can also obtain  $f_{q,q}^{(i,i)} = \alpha_q$  and  $f_{q,q}^{(i,j)} = 0$  whenever  $i \neq j$ . Based on the above results, case (a) of Part (p3) is thus proved.

For the case (b) of Part (p3), the results can be shown by first identifying the matrix  $\bar{\mathbf{A}}_{p,q}$  and by following the same procedures, in which

$$\bar{\mathbf{A}}_{p,q} = \begin{bmatrix} \mathbf{A}_{p,1} & -\mathbf{A}_{p,2} & -\mathbf{A}_{p,3} & -\mathbf{A}_{p,4} \\ \mathbf{A}_{p,2} & \mathbf{A}_{p,1} & \mathbf{A}_{p,4} & -\mathbf{A}_{p,3} \\ \mathbf{A}_{p,3} & -\mathbf{A}_{p,4} & \mathbf{A}_{p,1} & \mathbf{A}_{p,2} \\ \mathbf{A}_{p,4} & \mathbf{A}_{p,3} & -\mathbf{A}_{p,2} & \mathbf{A}_{p,1} \end{bmatrix}. \quad (\text{F.8})$$

□

# Appendix G

## Proof of Lemma 5.4.1

Parts (p1) and (p4) of Lemma 5.4.1 have been shown in Appendix D. It only needs to prove Parts (p2)-(p3). For Parts (p2) and (p3), the structure of  $\mathbf{F}_{q,q}$  is easily derived, and we thus omit it.

*Proof of (p2):* Noticed that for real-valued constellations, the distinct structure of  $\mathbf{F}_{p,q}$  is completely and directly identified by that of  $\bar{\mathbf{A}}_{p,q}$ . However, in complex-valued constellations, the resultant structure of  $\bar{\mathbf{A}}_{p,q}$  cannot directly and previously determine that of  $\mathbf{F}_{p,q}$ . To effectively identify the structure of  $\mathbf{F}_{p,q}$ , let's introduce the following four basic matrices:

$$\mathcal{A}_1 := \begin{bmatrix} 1 & 0 \\ 0 & 1 \end{bmatrix}, \quad \mathcal{A}_2 := \begin{bmatrix} 0 & -1 \\ 1 & 0 \end{bmatrix}, \quad \mathcal{A}_3 := \begin{bmatrix} 1 & 0 \\ 0 & -1 \end{bmatrix}, \quad \mathcal{A}_4 := \begin{bmatrix} 0 & 1 \\ 1 & 0 \end{bmatrix}. \quad (\text{G.1})$$

Also defining  $\mathcal{A} := [\mathcal{A}_1^T \ \mathcal{A}_2^T \ \mathcal{A}_3^T \ \mathcal{A}_4^T]^T$ , we obtain the fact

$$\mathcal{A}\mathcal{A}^T = \begin{bmatrix} \mathcal{A}_1 & -\mathcal{A}_2 & \mathcal{A}_3 & \mathcal{A}_4 \\ \mathcal{A}_2 & \mathcal{A}_1 & \mathcal{A}_4 & -\mathcal{A}_3 \\ \mathcal{A}_3 & \mathcal{A}_4 & \mathcal{A}_1 & -\mathcal{A}_2 \\ \mathcal{A}_4 & -\mathcal{A}_3 & \mathcal{A}_2 & \mathcal{A}_1 \end{bmatrix}, \quad (\text{G.2})$$

For  $K = 8$ , and  $N_p = N_q = 2$ ,  $k = l$ , we have

$$\mathbf{A}_{p,k} = \mathbf{A}_{q,l} = \begin{cases} \mathbf{e}_{\lceil (k/2) \rceil}^T \otimes \mathcal{A}_1 & \text{if } k \text{ is odd} \\ \mathbf{e}_{\lceil (k/2) \rceil}^T \otimes \mathcal{A}_2 & \text{if } k \text{ is even} \end{cases} \quad k = 1, 2, \dots, 8,$$

$$\mathbf{A}_{p,k} = \mathbf{A}_{q,l} = \begin{cases} j \cdot \mathbf{e}_{[(k-8)/2]}^T \otimes \mathcal{A}_3 & \text{if } k \text{ is odd} \\ j \cdot \mathbf{e}_{[(k-8)/2]}^T \otimes \mathcal{A}_4 & \text{if } k \text{ is even} \end{cases} \quad k = 9, 10, \dots, 16, \quad (\text{G.3})$$

where  $\mathbf{e}_i$  is the  $i$ th unit standard vector in  $\mathbb{R}^4$ . Based on (G.3) and using the fact (G.2) and the following properties

$$(\mathbf{A} \otimes \mathbf{B})^H = \mathbf{A}^H \otimes \mathbf{B}^H, \quad (\mathbf{A} \otimes \mathbf{B})(\mathbf{C} \otimes \mathbf{D}) = (\mathbf{A}\mathbf{C} \otimes \mathbf{B}\mathbf{D}), \quad (\text{G.4})$$

it can be checked with (F.1) that each  $2 \times 2$  block diagonal matrix of  $\mathbf{F}_{p,q}^{(s,t)} \in \mathbb{R}^{8 \times 8}$ ,  $s, t = 1, 2$ , belongs to an orthogonal design and thus  $\mathbf{F}_{p,q}^{(s,t)} \in \mathcal{O}(8)$  with 2 inputs. Also, we can find that  $\mathbf{F}_{p,q}^{(1,1)} = \mathbf{F}_{p,q}^{(2,2)}$  and  $\mathbf{F}_{p,q}^{(1,2)} = -\mathbf{F}_{p,q}^{(2,1)}$ .  $\square$

*Proof of (p3):* Similarly, to identify the structure of  $\mathbf{F}_{p,q}$ , let's first define the following augmented matrices:

$$\mathcal{B}_1 := \mathcal{A}_1 \otimes \mathcal{A}_1, \quad \mathcal{B}_2 := \mathcal{A}_3 \otimes \mathcal{A}_2, \quad \mathcal{B}_3 := \mathcal{A}_2 \otimes \mathcal{A}_1, \quad \mathcal{B}_4 := \mathcal{A}_4 \otimes \mathcal{A}_2, \quad (\text{G.5})$$

where  $\mathcal{A}_i$ ,  $i = 1, 2, 3, 4$ , are defined in (G.1). For  $N_q \in \{3, 4\}$ ,  $\mathbf{A}_{q,l}$ , can be obtained as the direct augmentation of two  $\mathcal{B}_i$  matrices, that is [47]

$$\mathbf{A}_{q,l} = \begin{bmatrix} j^{[(l-1)/4]} \mathcal{B}_{\text{mod}(l,4)} & (-j)^{[(l-1)/4]} \mathcal{B}_{\text{mod}(l,4)} \end{bmatrix}, \quad l = 1, 2, \dots, 8, \quad (\text{G.6})$$

where  $\text{mod}(x, y)$  denotes the remainder after  $y$  dividing  $x$ , and  $\mathcal{B}_0 := \mathcal{B}_4$ . Based on (G.3) and (G.6), we first compute  $\mathbf{A}_{p,i} \mathbf{A}_{q,j}^H$  and substitute it into (F.1). Then gathering each piece of  $f_{p,q}^{(i,j)}$  and putting them altogether to examine  $\mathbf{F}_{p,q}$ , it can be shown that, after some manipulations,  $\mathbf{F}_{p,q}$  indeed has the desired properties.  $\square$



# Appendix H

## Proof of Theorem 5.4.1

Similarly, we will prove Theorem 5.4.1 by induction. When  $G_i = 1$ , the result is obvious since  $\mathbf{F}_i = \alpha_{i,1} \mathbf{I}_{M_1}$ , with  $M_1 \in \{2, 4, 8\}$ . Assume that the result is true for an arbitrary  $G_i > 1$ , i.e.,  $\mathbf{F}_i \in \tilde{\mathcal{F}}_{J_i}(G_i, D_i)$  implies  $\mathbf{F}_i^{-1} \in \tilde{\mathcal{F}}_{J_i}(G_i)$  for such a  $G_i$ . We thus have to check that  $\mathbf{F}_{i-1}^{-1} \in \tilde{\mathcal{F}}_{J_{i-1}}(G_i + 1)$  (since  $G_i + 1 \equiv G_{i-1}$ ), whenever  $\mathbf{F}_{i-1} \in \tilde{\mathcal{F}}_{J_{i-1}}(G_i + 1, D_{i-1})$ . Let us partition an arbitrary  $\mathbf{F}_{i-1} \in \tilde{\mathcal{F}}_{J_{i-1}}(G_i + 1, D_{i-1})$  as

$$\mathbf{F}_{i-1} := \left[ \begin{array}{c|c} \mathbf{A} & \mathbf{B} \\ \hline \mathbf{B}^T & \mathbf{D} \end{array} \right] \in \mathbb{R}^{J_{i-1} \times J_{i-1}}, \quad (\text{H.1})$$

where  $\mathbf{A} \in \mathbb{R}^{J_i \times J_i}$ ,  $\mathbf{B} \in \mathbb{R}^{J_i \times L_{\lceil \mathcal{I}_{i-1}(G_i+1)/2 \rceil}}$ , and  $\mathbf{D} \in \mathbb{R}^{L_{\lceil \mathcal{I}_{i-1}(G_i+1)/2 \rceil} \times L_{\lceil \mathcal{I}_{i-1}(G_i+1)/2 \rceil}}$ . We note that, since  $\mathbf{F}_{i-1} \in \tilde{\mathcal{F}}_{J_{i-1}}(G_i + 1, D_{i-1})$ , we have (a)  $\mathbf{A} \in \tilde{\mathcal{F}}_{J_i}(G_i, D_i)$  and hence  $\mathbf{A}^{-1} \in \tilde{\mathcal{F}}_{J_i}(G_i)$  by assumption (b) if we write  $\mathbf{B} := [\mathbf{B}_1^T, \mathbf{B}_2^T, \dots, \mathbf{B}_{G_i}^T]^T$ , where  $\mathbf{B}_l \in \mathbb{R}^{L_{\lceil \mathcal{I}_i(l)/2 \rceil} \times L_{\lceil \mathcal{I}_{i-1}(G_i+1)/2 \rceil}}$ ,  $l = 1, 2, \dots, G_i$ , whose matrix structure has been established in Lemma 5.4.1 (or Table 2)

(c)  $\mathbf{D} = c\mathbf{I}_{L_{[\mathcal{I}_{i-1}(G_i+1)/2]}}$ . Also, let us similarly write

$$\mathbf{F}_i^{-1} := \left[ \begin{array}{c|c} & \\ \hline \bar{\mathbf{A}} & \bar{\mathbf{B}} \\ \hline \bar{\mathbf{B}}^T & \bar{\mathbf{D}} \\ \hline \end{array} \right] \in \mathbb{R}^{J_{i-1} \times J_{i-1}}, \quad (\text{H.2})$$

where  $\bar{\mathbf{A}} \in \mathbb{R}^{J_i \times J_i}$ ,  $\bar{\mathbf{B}} \in \mathbb{R}^{J_i \times L_{[\mathcal{I}_{i-1}(G_i+1)/2]}}$ , and  $\bar{\mathbf{D}} \in \mathbb{R}^{L_{[\mathcal{I}_{i-1}(G_i+1)/2]} \times L_{[\mathcal{I}_{i-1}(G_i+1)/2]}}$ . To show that  $\mathbf{F}_{i-1}^{-1} \in \tilde{\mathcal{F}}_{J_{i-1}}(G_i + 1)$ , it suffices to check that (i)  $\bar{\mathbf{A}} \in \tilde{\mathcal{F}}_{J_i}(G_i)$  (ii) if we write  $\bar{\mathbf{B}} := [\bar{\mathbf{B}}_1^T \dots \bar{\mathbf{B}}_{G_i}^T]^T$ , where  $\bar{\mathbf{B}}_l \in \mathbb{R}^{L_{[\mathcal{I}_i(l)/2]} \times L_{[\mathcal{I}_{i-1}(G_i+1)/2]}}$ ,  $l = 1, \dots, G_i$ , then each  $4 \times 4$  block off-diagonal submatrix of  $\bar{\mathbf{B}}_l$  belongs to  $\mathcal{O}(4)$  or is a zero matrix  $\mathbf{O}_4$  (iii)  $\bar{\mathbf{D}} = d\mathbf{I}_{L_{[\mathcal{I}_{i-1}(G_i+1)/2]}}$ . Properties (i)-(iii) can be shown based on the inversion formula for block matrices

$$\begin{aligned} \mathbf{F}_i^{-1} &= \left[ \begin{array}{c|c} & \\ \hline \bar{\mathbf{A}} & \bar{\mathbf{B}} \\ \hline \bar{\mathbf{B}}^T & \bar{\mathbf{D}} \\ \hline \end{array} \right] \\ &= \left[ \begin{array}{c|c} & \\ \hline (\mathbf{A} - \mathbf{B}\mathbf{D}^{-1}\mathbf{B}^T)^{-1} & -(\mathbf{A} - \mathbf{B}\mathbf{D}^{-1}\mathbf{B}^T)^{-1}\mathbf{B}\mathbf{D}^{-1} \\ \hline -(\mathbf{D} - \mathbf{B}^T\mathbf{A}^{-1}\mathbf{B})^{-1}\mathbf{C}\mathbf{A}^{-1} & (\mathbf{D} - \mathbf{B}^T\mathbf{A}^{-1}\mathbf{B})^{-1} \\ \hline \end{array} \right]. \end{aligned} \quad (\text{H.3})$$

*Proof of (i):* From (H.3), we have  $\bar{\mathbf{A}} = (\mathbf{A} - \mathbf{B}\mathbf{D}^{-1}\mathbf{B}^T)^{-1} = (\mathbf{A} - \frac{1}{c}\mathbf{B}\mathbf{B}^T)^{-1}$ . Since  $\mathbf{A} \in \tilde{\mathcal{F}}_{J_i}(G_i, D_i)$ , to prove  $\bar{\mathbf{A}} \in \tilde{\mathcal{F}}_{J_i}(G_i)$ , it suffices to check the structure of  $\mathbf{B}\mathbf{B}^T$ . In particular,  $\mathbf{B}\mathbf{B}^T$  can be expressed as given in (D.1), where  $\mathbf{B}_k\mathbf{B}_l^T$ ,  $k, l = 1, 2, \dots, G_i$ , have the following structures. a) If  $N_{[\mathcal{I}_i(l)/2]} = N_{[\mathcal{I}_{i-1}(G_i+1)/2]} = 2$ , then according to (p2) of Lemma 5.4.1  $\mathbf{B}_l \in \mathcal{O}(8, 2)$  or  $\mathbf{B}_l = \mathbf{O}_8$ . Therefore, we have  $\mathbf{B}_l\mathbf{B}_l^T = c_l\mathbf{I}_8$  or  $\mathbf{B}_l\mathbf{B}_l^T = \mathbf{O}_8$ . b) If  $N_{[\mathcal{I}_i(l)/2]} = 3$  or  $4$ ,  $N_{[\mathcal{I}_{i-1}(G_i+1)/2]} = 2$ , then according to (p3) of Lemma 5.4.1 each  $4 \times 4$  submatrix of  $\mathbf{B}_l \in \mathbb{R}^{4 \times 8}$  belongs to orthogonal design. It can be easily checked that  $\mathbf{B}_l\mathbf{B}_l^T = c_l\mathbf{I}_4$ . c) If  $N_{[\mathcal{I}_i(l)/2]} = 2$ ,  $N_{[\mathcal{I}_{i-1}(G_i+1)/2]} = 3$  or  $4$ , then according to (p3) of Lemma

5.4.1 each  $4 \times 4$  submatrix of  $\mathbf{B}_l \in \mathbb{R}^{8 \times 4}$  belongs to orthogonal design. It can be verified that

$$\mathbf{B}_l \mathbf{B}_l^T = \begin{bmatrix} c_l \mathbf{I}_4 & -c_l \mathbf{I}_4 \\ -c_l \mathbf{I}_4 & c_l \mathbf{I}_4 \end{bmatrix}. \quad (\text{H.4})$$

d) If  $N_{[\mathcal{I}_i(l)/2]} = N_{[\mathcal{I}_{i-1}(G_i+1)/2]} = 3$  or  $4$ , then according to (p4) of Lemma 5.4.1  $\mathbf{B}_l \in \mathcal{O}(4)$  or  $\mathbf{B}_l = \mathbf{O}_4$ , and we thus have  $\mathbf{B}_l \mathbf{B}_l^T = c_l \mathbf{I}_4$  or  $\mathbf{B}_l \mathbf{B}_l^T = \mathbf{O}_4$ . Based on the results a)-d), we can see that the diagonal entries of  $\mathbf{B}_l \mathbf{B}_l^T$  are the same. (e) To check the structure of  $\mathbf{B}_k \mathbf{B}_l^T$ , whenever  $k \neq l$ , we first identify the families of  $\mathbf{B}_k$ 's and  $\mathbf{B}_l$ 's according to Lemma 5.4.1, and then compute  $\mathbf{B}_k \mathbf{B}_l^T$  using Fact C.0.1. Using the same procedures as done in a)-d) above, we indeed can find that each  $4 \times 4$  block submatrix of  $\mathbf{B}_k \mathbf{B}_l^T$  belongs to an orthogonal design, or is a scaled identity matrix or zero matrix. Based on above results, we have  $\mathbf{B} \mathbf{B}^T \in \tilde{\mathcal{F}}_{J_i}(G'_i, D'_i)$ , where  $G'_i = G_i$  and  $D_i \leq D'_i \leq G_i$ . This leads to  $(\mathbf{A} - \frac{1}{c} \mathbf{B} \mathbf{B}^T) \in \tilde{\mathcal{F}}_{J_i}(G'_i, D'_i)$  since  $\mathbf{A} \subset \mathbf{B} \mathbf{B}^T$ . As a result, we can obtain  $\bar{\mathbf{A}} = (\mathbf{A} - \frac{1}{c} \mathbf{B} \mathbf{B}^T)^{-1} \in \tilde{\mathcal{F}}_{J_i}(G'_i)$  by assumption. This proves property (i).  $\square$

*Proof of (ii):* From (H.3), we have  $\bar{\mathbf{B}} = -\bar{\mathbf{A}} \mathbf{B} \mathbf{D}^{-1} = \frac{1}{c} \bar{\mathbf{A}} \mathbf{B}$ , and it thus suffices to check the structure of  $\bar{\mathbf{A}} \mathbf{B}$ . From the proof of (i), we can see that each  $4 \times 4$  block submatrix of  $\bar{\mathbf{A}}$  or  $\mathbf{B}$  belongs to an orthogonal design or is a zero matrix. By using Fact 5.4.1 and C.0.1, it can thus be verified that each  $4 \times 4$  block submatrix of  $\bar{\mathbf{A}} \mathbf{B}$  will also belong to an orthogonal design or be a zero matrix, which follows property (ii).  $\square$

*Proof of (iii):* Since  $\bar{\mathbf{D}} = (\mathbf{D} - \mathbf{B}^T \mathbf{A}^{-1} \mathbf{B})^{-1}$  and  $\mathbf{D} = c \mathbf{I}_{L_{[\mathcal{I}_{i-1}(G_i+1)/2]}}$ , to prove property (iii), it suffices to check that  $\mathbf{B}^T \mathbf{A}^{-1} \mathbf{B}$  is a scalar multiple of  $\mathbf{I}_{L_{[\mathcal{I}_{i-1}(G_i+1)/2]}}$ . To this end, for  $k, l = 1, \dots, G_i$ , we denote by  $\mathbf{U}_{k,l}$  the  $(k, l)$ th  $L_{[\mathcal{I}_{i-1}(k)/2]} \times L_{[\mathcal{I}_{i-1}(l)/2]}$  block submatrix of  $\mathbf{A}^{-1}$ . Since  $\mathbf{B} = [\mathbf{B}_1^T, \mathbf{B}_2^T, \dots, \mathbf{B}_{G_i}^T]^T$ , it is easy to check that

$$\begin{aligned} \mathbf{B}^T \mathbf{A}^{-1} \mathbf{B} &= \sum_{k,l=1}^{G_i} \mathbf{B}_k^T \mathbf{U}_{k,l} \mathbf{B}_l \\ &= \sum_{k=1}^L \mathbf{B}_k^T \mathbf{U}_{k,k} \mathbf{B}_k + \sum_{k,l=1, k \neq l}^{G_i} \mathbf{B}_k^T \mathbf{U}_{k,l} \mathbf{B}_l. \end{aligned} \quad (\text{H.5})$$

Since  $\mathbf{A}^{-1} \in \tilde{\mathcal{F}}_{J_i}(G_i)$ , we have by definition  $\mathbf{U}_{k,k} = \eta_k \mathbf{I}_{L_{\lceil \mathcal{I}_{i-1}(k)/2 \rceil}}$  for some scalar  $\eta_k$ . Using Fact 5.4.1, the first summation on the right-hand-side of the second equality in (H.5) can thus be simplified as

$$\begin{aligned} \sum_{k=1}^{G_i} \mathbf{B}_k^T \mathbf{U}_{k,k} \mathbf{B}_k &= \sum_{k=1}^{G_i} \eta_k \mathbf{B}_k^T \mathbf{B}_k \\ &= \begin{cases} \alpha_k \mathbf{I}_{L_{\lceil \mathcal{I}_{i-1}(G_i+1)/2 \rceil}} & \text{if } N_{\lceil \mathcal{I}_i(k)/2 \rceil}, N_{\lceil \mathcal{I}_{i-1}(G_i+1)/2 \rceil} = 2, \\ a_k \mathbf{I}_4 & \text{if } N_{\lceil \mathcal{I}_i(k)/2 \rceil} = 2, N_{\lceil \mathcal{I}_{i-1}(G_i+1)/2 \rceil} \in \{3, 4\}. \end{cases} \end{aligned} \quad (\text{H.6})$$

On the other hand, since  $k, l = 1, 2, \dots, G_i$ , each  $4 \times 4$  block submatrix of  $\mathbf{U}_{k,l}$  or  $\mathbf{B}_k$  belongs to an orthogonal design or is a zero matrix by assumption, then we have that each  $4 \times 4$  block submatrix of  $\mathbf{B}_k^T \mathbf{U}_{k,l} \mathbf{B}_l$  also belongs to an orthogonal design or is a zero matrix. Therefore, by using Fact C.0.1 it follows that

$$\begin{aligned} \mathbf{B}_k^T \mathbf{U}_{k,l} \mathbf{B}_l + \mathbf{B}_l^T \mathbf{U}_{l,k} \mathbf{B}_k &= \begin{cases} \mu_k \mathbf{I}_{L_{\lceil \mathcal{I}_{i-1}(G_i+1)/2 \rceil}} & \text{if } N_{\lceil \mathcal{I}_i(k)/2 \rceil}, N_{\lceil \mathcal{I}_{i-1}(G_i+1)/2 \rceil} = 2, \\ \delta_k \mathbf{I}_4 & \text{if } N_{\lceil \mathcal{I}_i(k)/2 \rceil} = 2, N_{\lceil \mathcal{I}_{i-1}(G_i+1)/2 \rceil} \in \{3, 4\}. \end{cases} \end{aligned} \quad (\text{H.7})$$

From (H.7), it can be verified that

$$\sum_{k,l=1, k \neq l}^L \mathbf{B}_k^T \mathbf{U}_{k,l} \mathbf{B}_l = \begin{cases} \beta_k \mathbf{I}_{L_{\lceil \mathcal{I}_{i-1}(G_i+1)/2 \rceil}} & \text{if } N_{\lceil \mathcal{I}_i(k)/2 \rceil}, N_{\lceil \mathcal{I}_{i-1}(G_i+1)/2 \rceil} = 2, \\ b_k \mathbf{I}_4 & \text{if } N_{\lceil \mathcal{I}_i(k)/2 \rceil} = 2, N_{\lceil \mathcal{I}_{i-1}(G_i+1)/2 \rceil} \in \{3, 4\}. \end{cases} \quad (\text{H.8})$$

Theorem 5.4.1 thus asserts. □

# Bibliography

- [1] J. G. Proakis, *Digital Communications*, 4th edition, The McGraw-Hill Companies, Inc., 2001.
- [2] T. S. Rappaport, *Wireless Communications: Principles and Practice*, Prentice Hall, 1996.
- [3] B. Vucetic and J. Yuan, *Space-Time Coding*, John Wiley & Sons Ltd, England, 2003.
- [4] E. G. Larsson and P. Stoica, *Space-Time Block Coding for Wireless Communications*, Cambridge University Press, 2003.
- [5] H. Bölcskei and A. J. Paulraj, "Multiple-input multiple-output (MIMO) wireless systems," in *The Communications Handbook*, J. Gibson, Ed., pp. 90.1-90.14, CRC Press, 2nd edition, 2001.
- [6] A. J. Paulraj, D. A. Gore, R. U. Nabar and H. Bölcskei, "An overview of MIMO communications-A key to gigabit wireless," *Proc. IEEE*, vol. 92, no. 2, pp. 198-218, Feb. 2004.
- [7] A. F. Naguib, N. Seshadri and A. R. Calderbank, "Increasing data rate over wireless channels: Space-time coding and signal processing for high data rate wireless communications," *IEEE Signal Processing Mag.*, vol. 17, no. 3, pp. 76-92, May 2000.
- [8] A. F. Naguib and A. R. Calderbank, "Space-time coding and signal processing for high data rate wireless communications," *Wireless Commun. and Mobile Comput.*, vol. 1, pp. 13-43, 2001.
- [9] E. Telatar, "Capacity of multiantenna Gaussian channels," AT&T Bell Laboratories, Tech. Memo., June 1995.
- [10] G. J. Foschini and M. J. Gans, "On limits of wireless communications in a fading environment when using multiple antennas," *Wireless Pers. Commun.*, vol. 6, no. 3, pp. 311-335, March 1998.

- [11] G. J. Foschini, D. Chizhik, M. J. Gans, C. Papadias and R. A. Valenzuela, "Analysis and performance of some basic space-time architectures," *IEEE J. Select. Areas Commun.*, vol. 21, no. 3, pp. 303-320, March 2003.
- [12] F. R. Farrokhi, G. J. Foschini, A. Lozano and R. A. Valenzuela, "Link-optimal space-time processing with multiple transmit and receive antennas," *IEEE Commun. Lett.*, vol. 5, no. 3, pp. 85-87, March 2001.
- [13] D. Gesbert, H. Bolcskei, D. Gore and A. J. Paulraj, "Outdoor MIMO wireless channels: Models and performance prediction," *IEEE Trans. Commun.*, vol. 50, no. 12, pp. 1926-1934, Dec. 2002.
- [14] A. J. Paulraj, R. Nabar and D. Gore, *Introduction to space-time wireless communications*, Cambridge University Press, 2003.
- [15] A. J. Paulraj and C. B. Papadias, "Space-time processing for wireless communications," *IEEE Signal Processing Mag.*, vol. 14, no. 6, pp. 49-83, Nov. 1997.
- [16] R. Kohno, "Spatial and temporal communication theory using adaptive antenna array," *IEEE Pers. Commun.*, vol. 5, no. 1, pp. 28-35, Feb. 1998.
- [17] G. J. Foschini, G. D. Golden, R. A. Valenzuela and P. W. Wolnianski, "Simplified processing for high spectral efficiency wireless communication employing multi-element arrays," *IEEE J. Select. Areas Commun.*, vol. 17, no. 11, pp. 1841-1852, Nov. 1999.
- [18] A. F. Naguib, A. Paulraj and T. Kailath, "Capacity improvement with base-station antenna arrays in cellular CDMA," *IEEE Trans. Veh. Technol.*, vol. 43, no. 3, pp. 691-698, Aug. 1994.
- [19] K. Sheikh, D. Gesbert, D. Gore and A. Paulraj, "Smart antenna for broadband wireless access networks," *IEEE Pers. Commun.*, vol. 37, no. 11, pp. 100-105, Nov. 1999.
- [20] L. Zheng and D. N. C. Tse, "Diversity and multiplexing: A fundamental tradeoff in multiple-antenna channels," *IEEE Trans. Inform. Theory*, vol. 49, no. 5, pp. 1073-1096, May 2003.
- [21] B. D. Van Veen and K. M. Buckley, "Beamforming: A versatile approach to spatial filtering," *IEEE ASSP Mag.*, vol. 5, pp. 4-24, April 1988.

- [22] L. C. Godara, "Applications of antenna arrays to mobile communications, Part I: Performance improvement, feasibility, and system considerations," *Proc. IEEE*, vol. 85, no. 7, pp. 1031-1060, July 1997.
- [23] D. H. Johnson and D. E. Dudgeon, *Array Signal Processing: Concepts and Techniques*, Englewood Cliffs, NJ: Prentice-Hall, 1993.
- [24] H. L. Van Trees, *Part IV of detection, estimation, and modulation theory: Optimum array processing*, John Wiley and Sons, Inc., New York, 2002.
- [25] G. V. Tsoulos, "Smart antennas for mobile communication systems," *Electron. Commun. Eng. J.*, vol. 11, no. 2, pp. 84-94, April 1999.
- [26] P. H. Lehne and M. Pettersen, "An overview of smart antennas technology for mobile communication systems," *IEEE Commun. Surveys*, vol. 2, no. 4, pp. 2-13, 4th Quarter 1999.
- [27] D. H. Tuan and P. Russer, "Signal processing for wideband smart antenna array applications," *IEEE Microwave Mag.*, vol. 5, no. 1, pp. 57-67, March 2004.
- [28] P. Balaban and J. Salz, "Optimum diversity combining and equalization in digital data transmission with applications to cellular mobile radio-Part I: Theoretical considerations," *IEEE Trans. Commun.*, vol. 40, no. 5, pp. 885-894, May 1992.
- [29] J. W. Liang and A. Paulraj, "A two-stage hybrid approach for CCI/ISI reduction with space-time processing," *IEEE Commun. Lett.*, vol. 1, no. 6, pp. 163-165, Nov. 1997.
- [30] D. Gerlach and A. J. Paulraj, "Base station transmitting antenna arrays for multipath environments," *Signal Processing*, vol. 54, pp. 59-73, 1996.
- [31] F. R. Farrokhi, K. J. R. Liu and L. Tasiulas, "Transmit beamforming and power control for cellular wireless systems," *IEEE J. Select. Areas Commun.*, vol. 16, no. 8, pp. 1437-1450, Oct. 1998.
- [32] H. Liu and G. Xu, "Multiuser blind channel estimation and spatial channel pre-equalization," in *Proc. IEEE ICASSP-95.*, vol. 3, pp. 1756-1759, 1995.
- [33] W. Jakes, *Microwave Mobile Communications*, Wiley, New York, 1974.

- [34] A. Wittneben, "Basestation modulation diversity for digital SIMULCAST," in *Proc. IEEE VTC'91*, vol. 1, pp. 848-853, May 1991.
- [35] A. Hiroike, F. Adachi and N. Nakajima, "Combined effects of phase sweeping transmitter diversity and channel coding," *IEEE Trans. Veh. Technol.*, vol. 41, no. 2, pp. 170-176, May 1992.
- [36] A. Wittneben, "A new bandwidth efficient transmit antenna modulation diversity scheme for linear digital modulation," in *Proc. IEEE ICC'93*, vol. 3, pp. 1630-1634, May 1993.
- [37] N. Seshadri and J. H. Winters, "Two schemes for improving the performance of frequency-division duplex (FDD) transmission systems using transmitter antenna diversity," *Int. J. of Wireless Inform. Networks*, vol. 1, pp. 49-60, 1994.
- [38] J. C. Guey, M. P. Fitz, M. R. Bell and W. Y. Kuo, "Signal design for transmitter diversity wireless communication systems over Rayleigh fading channels," in *Proc. IEEE VTC'96*, vol. 1, pp. 136-140, 1996.
- [39] J. H. Winters, "Diversity gain of transmit diversity in wireless systems with Rayleigh fading," *IEEE Trans. Veh. Technol.*, vol. 47, no. 1, pp. 119-123, Feb. 1998.
- [40] V. Weerackody, "Diversity for the direct-sequence spread spectrum system using multiple transmit antennas," in *Proc. IEEE ICC'93*, vol. 3, pp. 1503-1506, 1993.
- [41] TIA/EIA IS-2000 Physical layer specification of CDMA spread spectrum communications system, June 2000.
- [42] B. Hochwald, T. L. Marzetta and C. B. Papadias, "A transmitter diversity scheme for wide-band CDMA systems based on space-time spreading," *IEEE J. Select. Areas Commun.*, vol. 19, no. 1, pp. 48-60, Jan. 2001.
- [43] L. M. A. Jalloul, K. Rohani, K. Kuchi and J. Chen, "Performance analysis of CDMA transmit diversity methods," in *Proc. IEEE Globecom'98*, vol. 1, pp. 968-973, Nov. 1998.
- [44] Y. Li, N. Seshadri and S. Ariyavisitakul, "Transmit diversity for OFDM systems with mobile wireless channels," in *Proc. IEEE VTC99-Fall*, vol. 3, pp. 1326-1330, 1999.



- [45] Y. Li, J. C. Chuang and N. R. Sollenberger, "Transmit diversity for OFDM systems and its impact on high-rate data wireless networks," *IEEE J. Select. Areas Commun.*, vol. 17, no. 7, pp. 1233-1243, July 1999.
- [46] S. Alamouti, "A simple transmit diversity scheme for wireless communications," *IEEE J. Select. Areas in Commun.*, vol. 16, no. 8, pp. 1451-1458, Oct. 1998.
- [47] V. Tarokh, H. Jafarkhani and A. R. Calderbank, "Space-time block codes from orthogonal designs," *IEEE Trans. Inform. Theory*, vol. 45, no. 7, pp. 1456-1467, July 1999.
- [48] V. Tarokh, H. Jafarkhani and A. R. Calderbank, "Space-time block coding for wireless communications: Performance results," *IEEE J. Select. Areas Commun.*, vol. 17, no. 3, pp. 451-460, March 1999.
- [49] V. Tarokh, N. Seshadri and A. R. Calderbank, "Space-time codes for high data rate wireless communication: Performance criterion and code construction," *IEEE Trans. Inform. Theory*, vol. 44, no. 2, pp. 744-765, March 1998.
- [50] H. Jafarkhani, "A quasi-orthogonal space-time block code," *IEEE Trans. Commun.*, vol. 49, no. 1, pp. 1-4, Jan. 2001.
- [51] O. Tirkkonen, A. Boariu and A. Hottinen, "Minimal non-orthogonal rate 1 space-time block code for 3+ Tx antennas," in *Proc. IEEE ISSSTA2000*, vol. 2, pp. 429-432, Sept. 2000.
- [52] J. H. Winters, "On the capacity of radio communication systems with diversity in a Rayleigh fading environment," *IEEE J. Select. Areas Commun.*, vol. 5, no. 6, pp. 871-878, June 1987.
- [53] A. J. Paulraj and T. Kailath, "Increasing capacity in wireless broadcast systems using distributed transmission/directional reception (DTDR)," U.S. Patent #5 345 599, Sept. 1994.
- [54] G. J. Foschini, "Layered space-time architecture for wireless communication in a fading environment when using multi-element antennas," *Bell Labs Tech. J.*, pp. 45-49, 1996.
- [55] P. W. Wolniansky, G. J. Foschini, G. D. Golden and R. A. Valenzuela, "V-BLAST: An architecture for realizing very high data rates over the rich-scattering wireless channel," in *Proc. URSI ISSSE-98*, pp. 295-300, 1998.

- [56] G. D. Golden, G. J. Foschini, R. A. Valenzuela and P. W. Wolniansky, "Detection algorithm and initial laboratory results using V-BLAST space-time communication structure," *Electronic Lett.*, vol. 35, no. 1, pp. 14-16, Jan. 1999.
- [57] M. O. Damen, A. Chkeif and J. C. Belfiore, "Lattice codes decoder for space-time codes," *IEEE Commun. Lett.*, vol. 5, no. 7, pp. 304-306, July 2001.
- [58] D. Shiu, "Wireless communication using dual antenna arrays," *Electronic Lett.*, ser. International Series in Engineering and Computer Science, Norwell, MA: Kluwer, 1999.
- [59] A. Lozano and C. Papadias, "Layered space-time receivers for frequency-selective wireless channels," *IEEE Trans. Commun.*, vol. 50, no. 1, pp. 65-73, Jan. 2002.
- [60] X. Zhu and R. D. Murch, "MIMO-DFE based BLAST over frequency selective channels," in *Proc. IEEE Globecom'2001*, San Antonio, Texas, pp. 499-503, Nov. 2001.
- [61] H. Huang and H. Viswanathan and G. J. Foschini, "Multiple antennas in cellular CDMA systems: Transmission, detection, and spectral efficiency," *IEEE Trans. Wireless Commun.*, vol. 1, no. 3, pp. 383-392, July 2002.
- [62] B. Hassibi and B. M. Hochwald, "High-rate codes that are linear in space and time," *IEEE Trans. Inform. Theory*, vol. 48, no. 7, pp. 1804-1824, July 2002.
- [63] R. W. Heath, Jr. and A. J. Paulraj, "Linear dispersion codes for MIMO systems based on frame theory," *IEEE Trans. Signal Processing*, vol. 50, no. 10, pp. 2429-2441, Oct. 2002.
- [64] N. Onggosanusi, A. G. Dabak and T. M. Schmidl, "High rate space-time block coded scheme: Performance and improvement in correlated fading channels," in *Proc. IEEE WCNC'02*, pp. 194-199, 2002.
- [65] S. Sandhu and A. J. Paulraj, "Unified design of linear space-time block codes," in *Proc. IEEE Globecom'01*, vol. 2, pp. 1073-1077, 2001.
- [66] R. W. Heath Jr. and A. Paulraj, "Switching between spatial multiplexing and transmit diversity based on constellation distance," in *Proc. Allerton Conf. on Commun., Control, and Computing*, Oct. 2000.
- [67] R. W. Heath Jr. H. Bölcskei and A. J. Paulraj, "Space-time signaling and frame theory," in *Proc. IEEE ICASSP01*, vol. 4, pp. 2445-2448, May 2001.

- [68] D. Gesbert, M. Shafi, D. Shiu, P. J. Smith and A. Naguib, "From theory to practice: An overview of MIMO space-time coded wireless systems," *IEEE J. Select. Areas in Commun.*, vol. 21, no. 3, pp. 281-302, April 2003.
- [69] S. N. Diggavi, N. Al-Dhahir, A. Stamoulis and A. R. Calderbank, "An Great expectations: The value of spatial diversity in wireless networks," *Proc. IEEE*, vol. 92, no. 2, pp. 219-270, Feb. 2004.
- [70] X. Wang and H. V. Poor, *Wireless Communication Systems: Advanced Techniques for Signal Reception*, Pearson Education Inc., 2004.
- [71] C. Tidestav, M. Sternad and A. Ahlén, "Reuse within a cell-interference rejection or multiuser detection?" *IEEE Trans. Commun.*, vol. 47, no. 10, pp. 1511-1522, Oct. 1999.
- [72] L. L. Scharf, "The SVD and reduced rank signal processing," *Signal Processing.*, vol. 25, no. 2, pp. 113-133, 1991.
- [73] J. S. Goldstein and I. S. Reed, "Subspace selection for partially adaptive sensor array processing," *IEEE Trans. Aerosp. Electron. Syst.*, vol. 33, no. 2, pp. 539-544, April 1997.
- [74] M. L. Honig and W. Xiao, "Performance of reduced-rank linear interference suppression," *IEEE Trans. Inform. Theory*, vol. 47, no. 5, pp. 1928-1946, July 2001.
- [75] D. A. Pados and S. N. Batalama, "Joint space-time auxiliary-vector filtering for DS/CDMA systems with antenna arrays," *IEEE Trans. Commun.*, vol. 47, no. 9, pp. 1406-1415, Sept. 1999.
- [76] D. A. Pados and G. N. Karystinos, "An iterative algorithm for the computation of the MVDR filter," *IEEE Trans. Signal Processing.*, vol. 49, no. 2, pp. 290-300, Feb. 2001.
- [77] C. L. Ho, T. S. Lee and C. C. Tan, "A low-complexity MIMO decision feedback equalizer with partially adaptive interference suppression," *ISCOM-2001*, Tainan, Taiwan, Nov. 2001.
- [78] A. F. Naguib, N. Seshadri and A. R. Calderbank, "Applications of space-time block codes and interference suppression for high capacity and high data rate wireless systems," in *Proc. IEEE 32th Asilomar Conf. Signals, Systems, and Computers*, vol. 2, pp. 1803-1810, Nov. 1998.

- [79] A. Stamoulis, N. Al-Dhahir and A. R. Calderbank, "Further results on interference cancellation and space-time block codes," in *Proc. IEEE 35th Asilomar Conf. Signals, Systems, and Computers*, vol. 1, pp. 257-261, Nov. 2001.
- [80] C. L. Ho, J. Y. Wu and T. S. Lee, "Block-based symbol detection for high rate space-time coded systems," in *Proc. IEEE VTC 2004-Spring*, May 2004.
- [81] J. Y. Wu, C. L. Ho and T. S. Lee, "User-wise group V-BLAST detection of multiuser space-time block coded systems," *IEEE Trans. Wireless Commun.*, May 2005, in revision.
- [82] V. Tarokh, A. Naguib, N. Seshadri and A. R. Calderbank, "Combined array processing and space-time coding," *IEEE Trans. Inform. Theory*, vol. 45, no. 4, pp. 1121-1128, May 1999.
- [83] Y. Dai, Z. Lei and S. Sun, "Ordered array processing for space-time coded systems," *IEEE Commun. Lett.*, vol. 8, no. 8, pp. 526-528, Aug. 2004.
- [84] M. Tao and R. S. Chen, "Generalized layered space-time codes for high data rate wireless communications," *IEEE Trans. Wireless Commun.*, vol. 3, no. 4, pp. 1067-1075, July 2004.
- [85] D. Gesbert, L. Haumonte, H. Bolcskei, R. Krishnamoorthy and A. J. Paulraj, "Technologies and performance for non-line-of-sight broadband wireless access network," *IEEE Commun. Mag.*, vol. 40, no. 4, pp. 86-95, April 2002.
- [86] I. M. Kim and V. Tarokh, "Variable-rate space-time block codes in  $M$ -ary PSK systems," *IEEE J. Select. Areas in Commun.*, vol. 21, no. 3, pp. 362-373, April 2003.
- [87] I. M. Kim, "Space-time power optimization of variable-rate space-time block codes based on successive interference cancellation," *IEEE Trans. Commun.*, vol. 52, no. 7, pp. 1204-1213, July 2004.
- [88] C. L. Ho and T. S. Lee, "An OSIC based reduced-rank MIMO equalizer using conjugate gradient algorithm," *IEICE Trans. Commun.*, vol. E86-B, no. 9, pp. 2656-2664, Sept. 2003.
- [89] C. L. Ho and T. S. Lee, "A flexible uplink CDMA space-time transceiver with reduced-complexity V-BLAST detection," Presented in *The 13th Annual Wireless & Optical Common. Conf. 2004*, March 2004.
- [90] C. L. Ho, J. Y. Wu and T. S. Lee, "Group-wise V-BLAST detection in multiuser space-time dual-signaling wireless systems," *IEEE Trans. Wireless Commun.*, March 2005, in revision.

- [91] C. L. Ho, J. Y. Wu and T. S. Lee, "Effective transmitter and receiver designs for grouped space-time block coded systems with feedback information," to be submitted to *IEEE Trans. Wireless Commun.*
- [92] C. Shannon, "A mathematical theory of communication," *Bell Labs Tech. J.*, vol. 27, pp. 379-423, 623-656, July and Oct. 1948.
- [93] T. M. Cover and J. A. Thomas, *Elements of Information Theory*, John Wiley & Sons, Inc., 1991.
- [94] G. Ganesan and P. Stoica, "Space-time block codes: A maximum SNR approach," *IEEE Trans. Inform. Theory*, vol. 47, no. 4, pp. 1650-1656, May 2001.
- [95] A. Benjebbour, H. Murata and S. Yoshida, "Comparison of ordered successive receivers for space-time transmission," *Proc. IEEE VTC 2001-Fall*, vol. 4, pp. 2053-2057, Oct. 2001.
- [96] A. Benjebbour and S. Yoshida, "On the relation between ordering metrics for ZF and MMSE successive detection in MIMO systems," *IEICE Trans. Commun.*, vol. E87-B, no. 7, pp. 2021-2027, July 2004.
- [97] G. H. Golub and C. F. Van Loan, *Matrix Computations*, 3rd edition, The Johns Hopkins University Press, 1996.
- [98] P. S. Chang and A. N. Willson, Jr., "Analysis of conjugate gradient algorithms for adaptive filtering," *IEEE Trans. Signal Processing*, vol. 48, no. 2, pp. 409-418, Feb. 2000.
- [99] P. A. Voois, I. Lee and J. M. Cioffi, "The effect of decision delay in finite length decision feedback equalization," *IEEE Trans. Inform. Theory*, vol. 42, no. 2, pp. 618-621, March 1996.
- [100] T. S. Lee and T. C. Tsai, "A beamspace-time interference cancelling CDMA receiver for sectored communications in a multipath environment," *IEEE J. Select. Areas Commun.*, vol. 19, no. 7, pp. 1374-1384, July 2001.
- [101] D. Reynolds and X. Wang, "Low complexity turbo-equalization for diversity channels," *Signal Processing*, vol. 81, no. 5, pp. 989-995, 2001.
- [102] X. Wang and H. V. Poor, "Iterative (turbo) soft interference cancellation and decoding for coded CDMA," *IEEE Trans. Commun.*, vol. 47, no. 7, pp. 1046-1061, July 1999.

- [103] T. Abe and T. Matsumoto, "Space-time turbo equalization in frequency-selective MIMO channels," *IEEE Trans. Veh. Technol.*, vol. 52, no. 3, pp. 469-475, May 2003.
- [104] S. Sfar, R. D. Murch and K. B. Letaief, "Layered space-time multiuser detection over wireless uplink systems," *IEEE Trans. Wireless Commun.*, vol. 2, no. 4, pp. 653-668, July 2003.
- [105] B. K. Ng and E. S. Sousa, "On bandwidth-efficient multiuser space-time signal design and detection," *IEEE J. Select. Areas in Commun.*, vol. 20, no. 2, pp. 320-329, Feb. 2002.
- [106] S. Shahbazpanahi, M. Beheshti, A. B. Gershman, M. Gharavi-Alkhansari, and K. M. Wong, "Minimum variance linear receivers for multi-access MIMO wireless systems with space-time block coding," *IEEE Trans. Signal Processing*, vol. 52, no. 12, pp. 3306-3312, Dec. 2004.
- [107] D. Gore and A. Paulraj, "Space-time block coding with optimal antenna selection," in *Proc. IEEE ICASSP '01*, vol. 4, pp. 2441-2444, May 2001.
- [108] J. Benesty, Y. Huang and J. Chen, "A fast recursive algorithm for optimal sequential signal detection in a V-BLAST system," *IEEE Trans. Signal Processing*, vol. 51, no. 7, pp. 1722-1730, July 2003.
- [109] S. Catreux, D. Gesbert and R. W. Heath, "Adaptive modulation and MIMO coding for broadband wireless data networks," *IEEE Commun. Mag.*, vol. 40, no. 6, pp. 108-115, June 2002.
- [110] S. H. Nam, O. S. Shin and K. B. Lee, "Transmit power allocation for a modified V-BLAST system," *IEEE Trans. Commun.*, vol. 52, no. 7, pp. 1074-1079, July 2004.
- [111] S. T. Chung and A. J. Goldsmith, "Degree of freedom in adaptive modulation: A unified view," *IEEE Trans. Commun.*, vol. 49, no. 9, pp. 1561-1571, Sept. 2001.
- [112] N. Prasad and M. K. Varanasi, "Analysis of decision feedback detection for MIMO Rayleigh-fading channels and the optimization of power and rate allocations," *IEEE Trans. Inform. Theory*, vol. 50, no. 6, pp. 1009-1025, June 2002.

## Vita

**Chung-Lien Ho** was born in Taoyuan, Taiwan, R.O.C., in June 1974. He received the B.S. degree in the Department of Electrical Engineering from Da Yeh University, Changhua, Taiwan, R.O.C., in 1996, the M.S. degree in the Department of Electrical and Computer Science Engineering from Yuan Ze University, Taoyuan, Taiwan, R.O.C., in 1998. He is currently completing the Ph.D. degree in the Department of Communication Engineering at National Chiao Tung University, Hsinchu, Taiwan, R.O.C.

His current research interests include the space-time, multi-input multi-output signal processing for wireless communications and statistical signal processing.



# Publication List

## A. Journal Papers

- 1 **C. L. Ho** and T. S. Lee, "Efficient transmitter and receiver designs for grouped space-time block coded systems with feedback information," to be submitted to *IEEE Trans. Wireles Commun.*, May 2005.
- 2 J. Y. Wu, **C. L. Ho** and T. S. Lee, "User-wise group V-BLAST detection of multiuser space-time block coded systems," *IEEE Trans. Wireles Commun.*, May 2005, in revision.
- 3 **C. L. Ho**, J. Y. Wu and T. S. Lee, "Group-wise V-BLAST detection in multiuser space-time dual-signaling wireless systems," *IEEE Trans. Wireles Commun.*, March 2005, in revision.
- 4 **C. L. Ho** and T. S. Lee, "An OSIC based reduced-rank MIMO equalizer using conjugate gradient algorithm," *IEICE Trans. Commun.*, vol. E86-B, no. 9, pp. 2610-2619, Sept. 2003.
- 5 **C. L. Ho** and T. S. Lee, "A low-complexity adaptive multi-beam receiver for CCI/ISI cancellation over frequency selective multipath channels," *Wireless Personal Commun.*, vol. 26, no. 2, pp. 137-161, May 2003.
- 6 **C. L. Ho** and T. S. Lee, "An beamspace-time approach to CCI/ISI cancellation for sectored wireless communications," *Journal of the Chinese Institute of Electrical Engineers.*, vol. 10, no. 1, pp. 33-45, Feb. 2003.

## B. Conference Papers

- 1 **C. L. Ho**, J. Y. Wu and T. S. Lee, "Block based symbol detection for high rate space-time coded systems," in Proc. *IEEE VTC 2004-Spring*, vol. 1, pp. 375-379, Genoa, Italy, May 2004.
- 2 **C. L. Ho** and T. S. Lee, "Unified space-time decoding approach for uplink CDMA systems," *WOCC-04*, Taipei, Taiwan, R.O.C., March 2004.



- 3 **C. L. Ho**, J. Y. Wu and T. S. Lee, "Path-time coding for downlink multiuser CDMA over multipath channels," in Proc. *IEEE VTC 2003-Spring*, vol. 3, pp. 1925-1929, Jeju, Korea, April 2003.
- 4 **C. L. Ho**, T. S. Lee and C. C. Tan, "A low-complexity MIMO decision feedback equalizer with partially adaptive interference suppression," *ISCOM-01*, Tainan, Taiwan, R.O.C., Nov. 2001.
- 5 **C. L. Ho** and T. S. Lee, "A blind space-time beamformer for sectored communications in a multipath environment," *ISCOM-00*, Taoyuan, Taiwan, R.O.C., Dec. 2000.

### C. Patents

- 1 **C. L. Ho**, J. Y. Wu and T. S. Lee, "A method of symbol detection for MIMO dual-signaling uplink CDMA systems," US Patent pending, 2004.



## 簡歷

姓 名：何從廉

性 別：男

出生年月日：民國 63 年 6 月 29 日

籍 貫：台灣省桃園縣

學 歷：私立明新科技大學電機系 (78 年 9 月~ 83 年 6 月)

私立大葉大學電機工程系畢業 (83 年 8 月~ 85 年 7 月)

私立元智大學電機與資訊工程研究所畢業 (85 年 8 月~ 87 年 7 月)

國立交通大學電信工程學系博士班 (87 年 8 月~)

經 歷：

論文題目：用於多輸入多輸出無線通訊系統之空-時信號處理：空-時信號  
模式與干擾抑制